Universidad de Oviedo

Programa de Doctorado en Ciencias de la Salud

Platelets as mirrors of the health status: a combined proteomics and cell biology approach

Las plaquetas como reflejo de la salud: una aproximación combinada de proteómica y biología celular

Tesis doctoral

Patricia Martínez Botía

Mayo de 2023

Universidad de Oviedo

RESUMEN DEL CONTENIDO DE TESIS DOCTORAL

1.- Título de la Tesis	
Español/Otro Idioma: **Las plaquetas como reflejo de la salud: una aproximación combinada de proteómica y biología celular**	Inglés: **Platelets as mirrors of the health status: a combined proteomics and cell biology approach**

2.- Autora	
Nombre: **Patricia Martínez Botía**	DNI/Pasaporte/NIE:
Programa de Doctorado: **Ciencias de la Salud**	
Órgano responsable: **Centro Internacional de Posgrado – Universidad de Oviedo**	

RESUMEN (en español)

Las plaquetas son los componentes anucleados de la sangre responsables de mantener la hemostasia del cuerpo. Las plaquetas forman coágulos (trombos) en el lugar donde se ha producido un daño endotelial, para prevenir una hemorragia, o sangrado. Lo hacen a través de la activación secuencial y a la acción sinérgica de sus receptores de superficie, que reconocen los diferentes ligandos y sustratos expuestos en el lugar del daño vascular. Sin embargo, en la última década se ha ido descubriendo un considerable número emergente de funciones no hemostáticas de las plaquetas, como pueden ser la inmunomodulación, la separación de vasos linfáticos y sanguíneos durante el desarrollo embrionario, o la metástasis en cáncer. De manera similar, las aplicaciones terapéuticas de las plaquetas se han expandido desde aquellas meramente hemostáticas hasta aquellas consideradas en medicina regenerativa.

Mientras que hasta ahora se consideraba de manera global que las plaquetas son un producto que guarda las mismas características tanto en salud como en enfermedad (excluyendo a las trombopatías en sí), las perspectivas actuales sugieren lo contrario: las plaquetas, y los megacariocitos de los que proceden, responden de manera distinta, y por tanto son producidos de forma distintiva en diferentes condiciones (pato)fisiológicas; y no solo eso, sino que las plaquetas también podrían ser sujetas a cambios en circulación, cuando se ven expuestas al ambiente.

Basándose en los resultados tanto de otros grupos como propios, se plantea la hipótesis de que las plaquetas son producidas con un perfil cualitativo y funcional distinto en diferentes condiciones patológicas o de estrés, especialmente llamativo cuando hay una inflamación subyacente. La cuestión que se plantea es entender estos cambios cualitativos y funcionales de las plaquetas, y comprender cómo los megacariocitos perciben ciertas condiciones patológicas o de estrés para producir unas plaquetas con una capacidad funcional específica, y que en el contexto particular de inflamación, se concibe como una funcionalidad limitada para no contribuir a una respuesta inmune exacerbada. Entender las muchas facetas de la megacariopoyesis y la función plaquetaria en pacientes afectados por condiciones hematológicas y no hematológicas contribuirá a una mejor caracterización de la patología específica subyacente, y contribuirá al desarrollo (u optimización) de los usos terapéuticos de las plaquetas y sus derivados, a través de una manipulación dirigida de los mismos; además de la potencial identificación de biomarcadores.

En este sentido, durante la presente Tesis Doctoral se ha llevado a cabo la caracterización de manera completa de la megacariopoyesis, y del proteoma, fenotipo y la función plaquetaria, tanto en salud (individuos sanos) como en enfermedad. Este último grupo incluye pacientes con patologías no hematológicas, pero que presentan una inflamación subclínica de bajo grado, a saber: diabetes tipo 1, psoriasis, dermatitis atópica, y depresión mayor con y sin tentativa suicida. Además, se ha hecho especial énfasis en la aplicabilidad de la proteómica para estudiar las características fenotípicas y funcionales de las plaquetas, que permitirían (como hipotetizamos) diferenciar entre salud y enfermedad, discerniendo entre diferentes estados patológicos, y en estudios en diferentes

especies animales. En referencia a este último punto, se ha estudiado las diferencias en el proteoma de dos modelos murinos de trombocitopenia inmune, y se ha comparado el proteoma plaquetario entre ratones y humanos. Así, aplicando tanto está ómica, como diversas aproximaciones celulares y funcionales, se ha generado una base de datos completa que añade al conocimiento actual en nuestro campo (*i.e.*, megacariopoyesis y plaquetas) y a su vez en el de las enfermedades estudiadas, proporcionando datos con potencial para el desarrollo de biomarcadores diagnósticos y pronósticos, o de respuesta a tratamiento.

RESUMEN (en Inglés)

Platelets are the enucleate components of the blood responsible for maintaining hemostasis. They form plugs (thrombi) at the site of endothelial damage to prevent blood loss, by means of the sequential activation and synergy of their surface receptors, which recognize the different exposed ligands and substrates. However, in the last decade, a number of non-hemostatic functions have been associated with platelets, such as immunomodulation, separation of the blood and lymphatic systems during development, and metastasis in cancer. Similarly, the therapeutic applications of platelets have been expanded to include those in regenerative medicine, besides the hemostatic ones.

Additionally, while platelets were historically considered as a product that remains static both in health and disease (excluding thrombopathies themselves), current perspectives point to the opposite: platelets and their megakaryocytic progenitors respond differently, and thus are produced distinctively in different physio(patho)logical conditions. Furthermore, platelets could also be subject to changes in the circulation, where they are directly exposed to the environment.

Based on the results from other groups and our own, we hypothesize that platelets are produced with a distinct qualitative and functional profile under different pathological conditions, notably when there is a subclinical inflammation. The question then revolves around not only understanding those changes in platelets, but also how megakaryocytes sense those pathological environments in order to produce platelets with a tailored function. Moreover, and in the particular context of inflammation, that fine-tuning is aimed at reducing their functionality as to hamper their contribution to the already-exacerbated immune response. Understanding the many faces of megakaryopoiesis and platelet function in patients with both hematological and non-hematological diseases will contribute to both the better characterization of the specific pathology and the development (or optimization) of the therapeutic uses of platelets and their products, through their targeted manipulation, as well as the identification of potential biomarkers.

In this regard, during the present PhD Thesis, we have conducted a thorough characterization of megakaryopoiesis, and the proteome, phenotype, and function of platelets, both in health and disease. This latter group includes patients with non-hematological pathologies, but presenting with a subclinical, low-grade inflammation, namely: type 1 diabetes, psoriasis, atopic dermatitis, and major depressive disorder concurrent with or without suicidal attempt. Furthermore, special emphasis has been placed in the applicability of proteomics to study the phenotypic and functional characteristics of platelets, which would allow (as we hypothesize) the distinction not only between health and disease, but also among pathological states, and animal species. Regarding this last point, we have studied the proteome of two different murine models of immune thrombocytopenia, and compared the platelet proteome between mice and humans. Thus, applying both this omic, as well as cellular and functional approaches, a comprehensive data source has been generated that expands our current knowledge of both the field (*i.e.*, megakaryopoiesis and platelets) and the other studied diseases, providing promising data for the development of diagnostic, prognostic, and response-to-treatment biomarkers.

SR. PRESIDENTE DE LA COMISIÓN ACADÉMICA DEL PROGRAMA DE DOCTORADO EN CIENCIAS DE LA SALUD

Table of contents

Abbreviations

AggA Aggretin A

A-ITP Active ITP model (chronic)

AUC Area under the curve

BP Biological process

CBC Complete blood count

CC Cellular component

CLEC2 C-type lectin-like receptor 2

CLP Common lymphoid progenitor

CMP Common myeloid progenitors

c-MPL Cellular-myeloproliferative leukaemia / TPO receptor

CVX Convulxin

DEP Differentially expressed protein

FcγR Immunoglobulin G Fc receptor

GMP Granulocyte-monocyte progenitor

GO Gene ontology

GP Glycoprotein

HSC Hematopoietic stem cell

IL Interleukin

ITP Immune thrombocytopenia

IVIg Intravenous γ-globulins

KEGG Kyoto Encyclopedia of Genes and Genomes

KSR1 Kinase suppressor of Ras 1

LAT Linker of activated T cells

LC-MS/MS Liquid chromatography with tandem mass spectrometry

MAR Maximum aggregation rate

MDD Major depressive disorder

ME Module eigenproteins

MEP Megakaryocyte-erythrocyte progenitor

MF Molecular function

MPP Multipotent progenitor

NET Neutrophil extracellular trap

PAR Protease-activated receptor

PBMC Peripheral blood mononucleate cell

PCA Principal component analysis

PECAM-1 Platelet endothelial cell adhesion molecule-1 (CD31)

PF4 Platelet factor 4

P-ITP Passive ITP model (acute)

PK Protein kinase

PLC Phospholipase C

PMA Phorbol 12-myristate 13-acetate

PRP Platelet-rich plasma

PS Phosphatidylserine

PTM Post-translational modification

SA Suicidal attempt

SDPR Serum deprivation response protein

SFK Src family kinase

TLR Toll-like receptor

TNF-α Tumor necrosis factor-α

TPO Thrombopoietin

TRALI Transfusion-related acute lung injury

TRAP6 Thrombin receptor-activating peptide-6

TxA_2 Thromboxane

vWF von Willebrand factor

WGCNA Weighted gene correlation network analysis

Introduction

The origins: The many faces of hematopoiesis

Hematopoiesis is the tightly regulated process by which hematopoietic stem cells (HSCs) differentiate towards the different cell types that compose the blood, and it is driven by key transcription factors and cytokines[1,2]. The classical model of hematopoiesis states the presence of two sub-populations of HSCs at the apex of the hierarchy, based on their CD34 expression: long-term (LT)-HSCs ($CD34^-$) and short-term (ST)-HSCs ($CD34^+$), which are both multipotent and able to self-renew[3]. LT-HSCs precede ST-HSCs, which in turn differentiate into multipotent progenitors (MPPs). The following steps entail the bifurcation into common myeloid progenitors (CMPs, with myeloid, erythroid, and megakaryocytic potential) and common lymphoid progenitors (CLPs, with only lymphoid potential). This constitutes the first branching of hematopoiesis, and subsequently CLPs directly differentiate into the mature cells: T, B, natural killer, and dendritic cells. A second bifurcation occurs at the CMP level, where they give rise to bipotent granulocyte-monocyte (GMPs) and megakaryocyte-erythrocyte progenitors (MEPs). The former further mature to granulocytes (basophils, neutrophils, and eosinophils), mast cells and monocytes (which can generate macrophages and monocyte-derived dendritic cells), while the latter differentiate into megakaryocytes (and finally into platelets), and erythrocytes[4] (Figure 1A).

However, numerous studies throughout the years have pointed to the shortcomings of this model, chiefly due to the fact that it is only based on studies in bulk cells, and thus many of the subtleties are lost, such as the complexity that is found at the stem and progenitor (HSPC) levels. On the one hand, recent single-cell RNA analysis of human bone marrow HSPCs have debunked the idea that hematopoiesis occurs in a step-wise manner, passing through several multi- and bi-potent progenitors, but rather that unilineage cells stem directly from a “continuum of low-primed undifferentiated HSPCs”[5,6] (Figure 1B). On the other hand, that complexity is particularly evident in the case of the megakaryocyte lineage, where a series of seminal studies found co-

expression of von Willebrand factor (vWF, a protein unique to these cells) and c-Kit (an HSC marker) in a sub-population of HSCs, pointing to a megakaryocyte bias within this compartment[7,8]. Furthermore, a posterior study confirmed this finding, and reported the finding of stem-like megakaryocyte-committed progenitors (SL-MkPs)[9]. This fact, along with other shared features between the two of them (*i.e.*, expression of thrombopoietin receptor [c-MPL], CXCR4, among others)[10,11], suggests firstly that megakaryocytes and HSCs are more alike than previously thought, and that the megakaryocyte differentiation, termed megakaryopoiesis, can potentially separate from the rest of the branches of the hematopoiesis tree earlier than the rest of lineages[12].

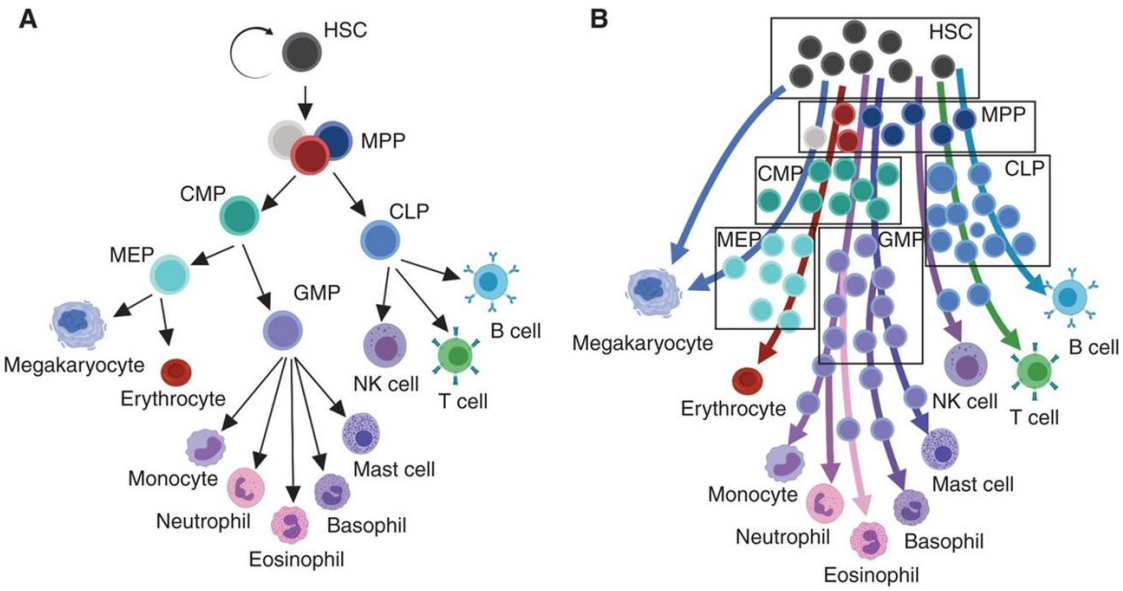

Figure 1. Models of hematopoiesis. (A) Classical step-wise, tree-like model of hematopoiesis, where the HSCs at the apex differentiate into multipotent progenitors, which in turn give rise to lineage-restricted progenitors. Ultimately, the different mature blood cells arise. (B) The continuous differentiation model (continuum), where the acquisition of the lineage-specific traits is gradual and occur at earlier stages in the differentiation process. CLP: common lymphoid progenitor, CMP: common myeloid progenitor, GMP: granulocyte-monocyte progenitor, HSC: hematopoietic stem cell, MEP: megakaryocyte-erythroid progenitor, MPP: multipotent progenitor, NK: natural killer cell. From Olson *et al.* 2020[1].

Zooming in: Megakaryopoiesis and thrombopoiesis

Megakaryopoiesis, that is, the process by which HSCs differentiate towards mature megakaryocytes within the bone marrow, entails a certain number of endomitotic cycles, where the DNA and thus the nucleus replicates (polyploidization, up to 64N in

human and 128N in mouse) without a subsequent cell division (cytokinesis)[13,14]. It also involves the formation of an extensive membrane system, termed the demarcation membrane system (DMS), originated at the plasma membrane[15]. As a consequence of these endomitotic cycles, there is an enormous growth of the cytoplasm, as it is packed with organelles, protein- and biomolecule-containing granules, and cytoskeletal proteins[16]. At the same time that this process occurs, the maturating megakaryocyte moves through the bone marrow osteoblastic (hypoxic) niche towards the sinusoidal blood vessels, by means of rearranging their membrane and cytoskeleton, following a gradient of chemotactic stromal cell-derived factor-1α (SDF-1α) and fibroblast growth factor-4, which is directed by dynamins and the expression of MYH9, among others[17,18]. Additionally, the sequential increase in the expression of certain integrins and receptors, such as GPVI[19], allow megakaryocytes to bind to elements of the extracellular bone marrow matrix, including fibronectins, collagens or laminins, which are richly expressed around the marrow sinusoids, and thus adding on the megakaryocyte cytoskeleton remodeling and migration[20]. The whole process culminates with the formation of platelets, a process termed thrombopoiesis.

At the molecular level, megakaryopoiesis is mainly driven by the hormone thrombopoietin (TPO)[21], which binds to its specific receptor MPL[22], eliciting a signaling cascade where Janus kinase 2 (JAK2), and the transcription factors signal transducers and activators of transcription 3 and 5 (STAT-3 and -5) translocate to the nucleus, triggering in turn the temporal transcription of other key transcription factors in megakaryopoiesis, such as RUNX1, GATA1/2, FLI1, GFI1B, MECOM, or ETV6[23]. However, as mentioned above, the exact differentiation path is still a matter of debate, since the notion of a hierarchical hematopoiesis is being displaced by findings that point to alternative routes, which do not necessarily require either TPO, or the differentiation through the bipotent progenitors[24]. For instance, it has been shown that platelets are still being produced, albeit at lower numbers (~10%), when the TPO signaling is abolished[25];

or that there are megakaryocyte-primed precursors at the apex of the hierarchy, and that under certain pathological circumstances (*i.e.*, inflammation), megakaryopoiesis bypasses the MEP[9,12,26] (Figure 2).

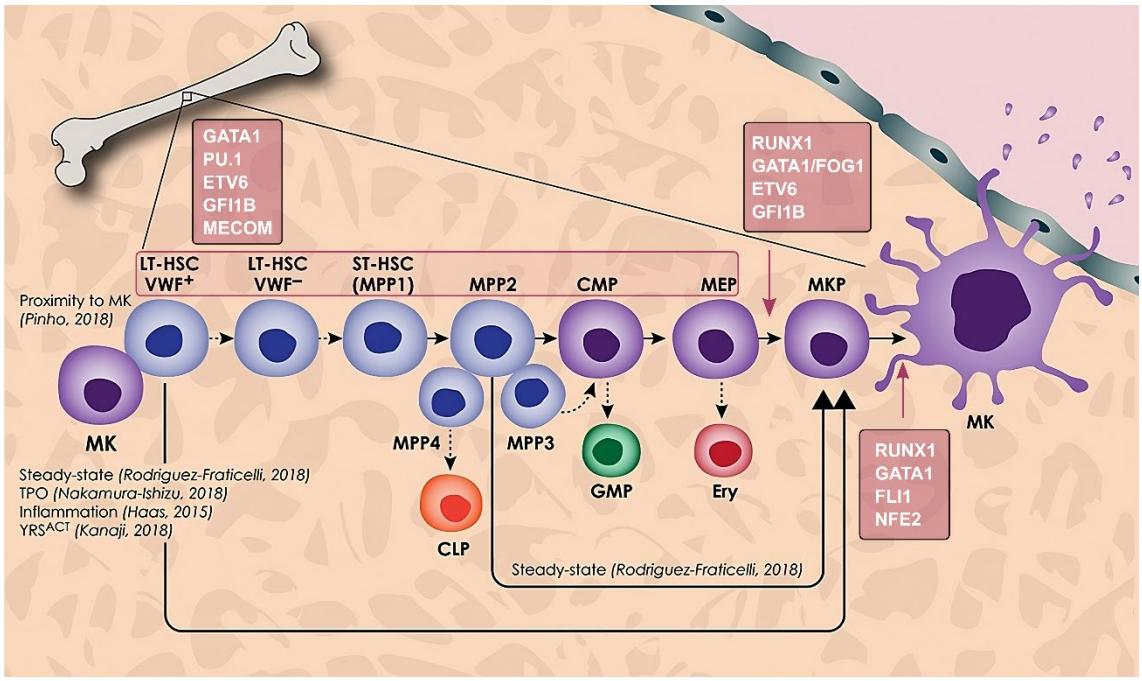

Figure 2. Overview of the megakaryopoiesis, encompassing canonical (main horizontal flow) and new models. The latter stemming from either the long-term hematopoietic stem cell (LT-HSC) vWF^{+} progenitor or the multipotent progenitor 2 (MPP2), towards the megakaryocyte progenitor (MKP), bypassing intermediate states. The major transcription factors governing the canonical model are indicated. CMP: common myeloid progenitor, CLP: common lymphoid progenitor, Ery: erythroblast, ETV6: ETS variant 6, FLI1: friend leukemia virus integration 1, FOG1: friend of GATA protein 1, GMP: granulocyte-monocyte progenitor, MECOM: MDS1 and EVI1 complex locus, MEP: megakaryocyte-erythroid progenitor, MK: megakaryocyte, NFE2: Nuclear factor erythroid 2, RUNX1: Runt-related transcription factor 1, ST-HSC: short-term hematopoietic stem cell, vWF: von Willebrand factor. Adapted from Noetzli *et al*. (2019).

However, it is still not clearly understood what signals the end of differentiation and the start of thrombopoiesis, that is, the biogenesis of platelets. What it is known is that mature megakaryocytes suffer a brutal conformational change where they extend cytoplasmic protrusions or elongations, called proplatelets[27], into the lumen of the blood vessel, which are adorned with small buddings, representing the nascent platelets. Here, the cytoskeleton not only plays a pivotal role in proplatelet formation, but also in the transport of both biomolecule-containing granules and organelles into the forming platelets[16,28]. Lastly, a combination of extracellular matrix degradation and the exposure

to the blood shear forces provokes the final rupture of the proplatelets[29], and frees the platelets into the circulation (Figure 3); while the remaining of the megakaryocyte extrudes its naked nuclei into the surrounding space[30]. Interestingly, in addition to the single platelet release by pro-platelets, an alternative mechanism of platelet generation has been proposed, where pro-platelets are fully dissociated from megakaryocytes, forming a sort of intermediate discoid-shaped platelet (termed pre-platelet), which finishes to mature in circulation[28]. Moreover, they have been described to be able to go back and forth between this state, and the detached, barbell-shaped pro-platelets.

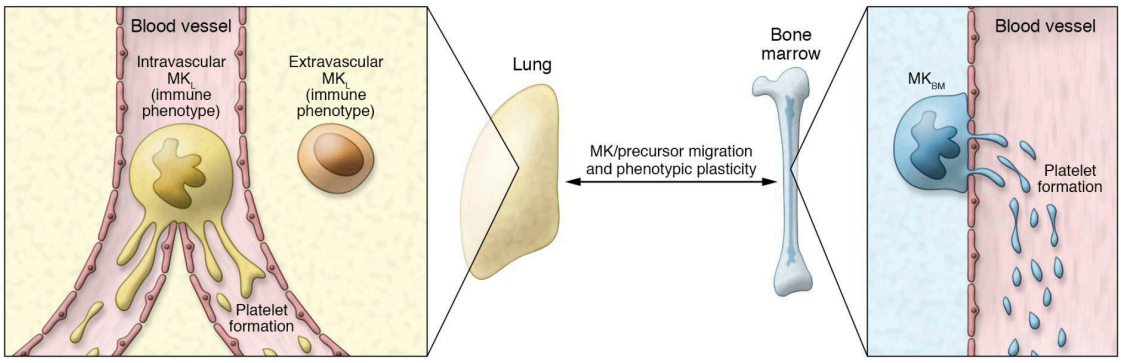

Figure 3. Models for megakaryocyte plasticity in regard to the site of thrombopoiesis. The lung harbors both intravascular and extravascular populations of megakaryocytes. The former are large, polyploid, and strategically positioned to release proplatelets, while the latter are diploid and smaller. The local environment modulates the phenotype of bone marrow and lung megakaryocytes. MK_{BM}: bone marrow megakaryocyte, MK_L: lung megakaryocyte. From Boillard and Machlus (2021).

The plasticity of megakaryopoiesis and thrombopoiesis

In mammals, during embryonic development, hematopoiesis first appears in the yolk sac, producing macrophages, erythroblasts, and megakaryocytes; followed by a migration of the process first to the aorta-gonad-mesonephros region and then to the fetal liver, where hematopoiesis becomes definitive, encompassing both the myeloid and lymphoid lineages[31,32]. It is during the last stages of gestation that hematopoiesis moves to its ultimate location, the bone marrow. However, it is also known that extramedullary hematopoiesis can occur in the sinusoidal blood vessels of the spleen and liver, under inflammatory conditions[33]. Additionally, although platelets are produced from their megakaryocytic progenitors mainly in the bone marrow, it can also take place in the

lungs, through megakaryocyte and megakaryocyte-primed hematopoietic progenitors that populate this tissue, taking advantage of the highly irrigated vasculature of this organ[34]. It is nevertheless still a matter of debate whether this reservoir of megakaryocytes can be considered as a prominent source of platelets, both in steady- and acute states (*i.e.*, thrombocytopenia); or rather they perform other roles, as it has been shown that lung-resident megakaryocytes display immunomodulatory features, most likely driven by their niche environment[35] (Figure 3).

It is well-known that hematopoiesis shifts its cellular balance to compensate for systemic changes, such as in infection and inflammation, in the overall ratio of the blood components (*i.e.*, cytopenias), but this primarily affects the final numbers that comprise each blood lineage[36]. In the end, the bone marrow constitutes an immune-privileged environment, due to both its physical characteristics and the cellular niche, which protects the HSCs from autoimmunity and excessive inflammation[37]. However, recent work shows that multiple exposure to inflammation throughout time can impact both HSCs and hematopoiesis beyond this balance, and in the long-term, promoting aged phenotypes and exhaustion of stem cells[38].

In the case of megakaryopoiesis this also stands. For instance, a study found that stress conditions triggered the rapid maturation of the aforementioned SL-MkPs directly to mature megakaryocytes, to replenish the platelet pool after inflammation-induced thrombocytopenia[9]. Additionally, another study found that elevated levels of the cytokine IL-1α triggered an alternative, TPO-independent pathway that caused the rapid production of platelets by means of megakaryocyte rupture, rather than by forming proplatelets[39]. Others pointed to deeper changes, where a reprogramming at the transcriptional level in megakaryocytes affected either by aging (*i.e.*, chronic low-grade inflammation caused by TNF-α), sepsis or the presence of a tumor, lead to hyperreactive platelets[40], increased ITGA2B expression[41], and megakaryocytes with a pro-inflammatory phenotype[42], respectively.

The main players: Platelets

Platelets are the small (2 to 4 μm in diameter) cytoplasmic fragments originated from megakaryocytes, which are responsible for the maintenance of the body hemostasis, and whom along with erythrocytes, conform the majority of the blood cell components[43]. One of their defining characteristics is the compartmentalized storage, in alpha and dense granules, and lysosomes, of a plethora of bioactive molecules capable of exerting a wide variety of functions[44,45]. They also display a complex cytoskeleton, a myriad of surface receptors and an accompanying signaling network, all of which allow them to undergo great and fast conformational changes in response to environmental cues[46] (Figure 4). Additionally, although they are essentially cytoplasmic fragments that lack a nucleus and, consequently, the apparatus to transcribe the information stored in the DNA, it has been described that platelets still retain, while still young, the sufficient amount of RNA and translation machinery to synthesize new proteins, albeit as a residual trait[47].

Platelet counts in blood results from a balance controlled by the rates at which they are produced and the kinetics of their clearing after showing signs of aging or dysfunction[48]. The lifespan of platelets is short, of approximately 7 to 10 days, and consequently they are also produced at a high rate (10^{11} a day) to compensate for this relatively fast turnover. Senescence is one of the key events that flags platelets to be removed, and it is orchestrated by an intrinsic apoptotic program that eventually trigger the cell surface changes (*i.e.*, phosphatidylserine exposure, or glycan desialylation) that are recognized by the professional phagocytes, macrophages and immature dendritic cells in the spleen and liver[49,50]. In line with all of this, platelet lifespan is also defined by the mitochondria[51]. This organelle, as in nucleated cells, is critical to the production of essential biomolecules by means of the aerobic respiration. However, it is also essential to the wellbeing and normal functioning of the platelets, as it has been observed that, when their mitochondria are damaged or dysfunctional, and thus the generation of

energy is compromised, it does not only affect their lifespan, but it also increases the risk of thrombotic events. Mitochondria, as well as other necessary organelles and the aforementioned granules, along with the cytoskeleton, and a dense tubular system (DTS), are inherited from their megakaryocytic progenitor (Figure 4).

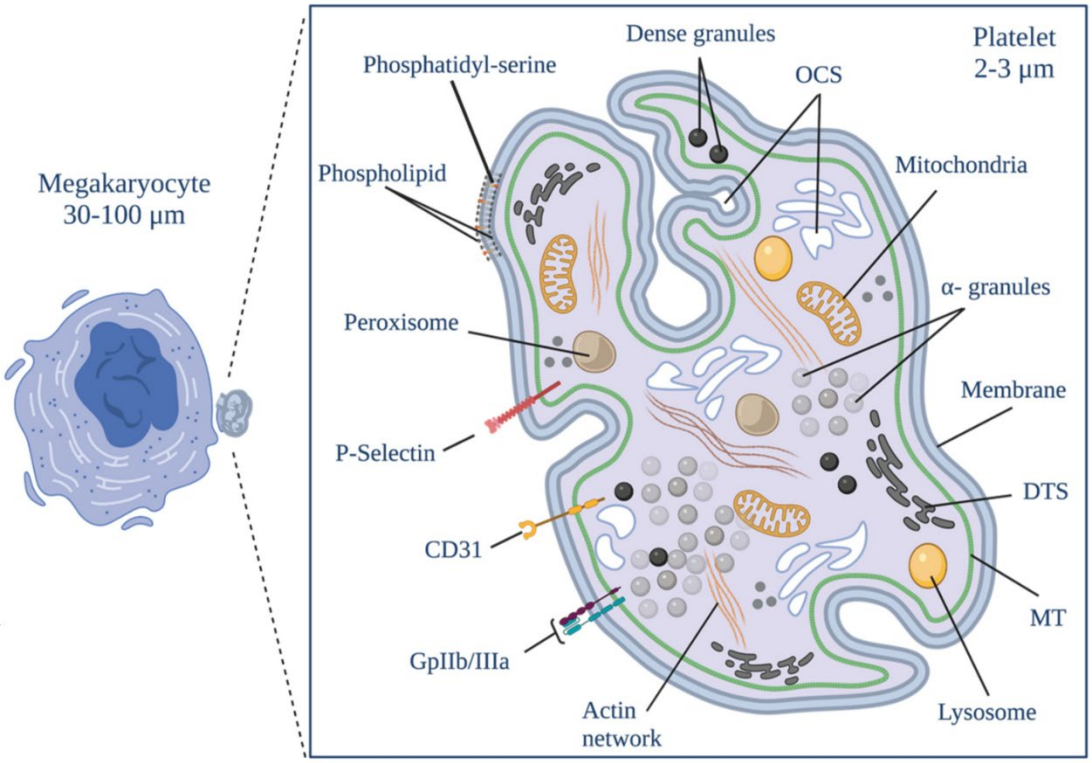

Figure 4. Morphology and main components of platelets. Platelets inherit their membrane and associated surface proteins, organelles (mitochondria), granules (alpha and dense granules, and lysosomes), and cytoskeleton from their megakaryocytic progenitor. DTS: dense tubular system, MT: microtubules, OCS: open canalicular system. Adapted from Durán-Saenz *et al*. (2022).

The major physiological role of platelets lies in preserving hemostasis, that is, in preventing blood loss and maintaining vascular integrity via the formation of clots at the site of injury. This function is tightly regulated, since the aberrant activation of platelets by inappropriate stimuli can lead to thrombosis (*i.e.*, the formation of thrombus), which in turn may trigger the onset of thrombotic events, such as stroke or myocardial infarction, among others. Thus, to keep platelets in that quiescent state, the healthy and intact vascular endothelial cells secrete inhibitory signals in the form of nitric oxide (NO) and prostacyclin (prostaglandin I2 [PGI2]), which activate the protein kinases G (PKG) and A (PKA) by means of regulating the intracellular levels of cyclic nucleotides[52], among others. The hemodynamic and rheologic characteristic of the blood flow force platelets

to circulate in close proximity to the vessel walls, which not only facilitates their inhibition in steady-state conditions, but also allows for the easier detection of hemostatically active components, such as tissue factor, collagen or vWF, which become exposed or attached after vascular injury (Figure 5).

The interaction of the receptors of the resting platelets with these molecules results in their adherence to the injury, followed by secretion of biomolecules to recruit a greater number of platelets, which then aggregate to form the thrombus. This whole process receives the name of platelet activation, and it is executed by a complex signaling network that can be divided into the following phases: 1) early receptor signaling triggered by soluble agonists, adhesion receptor ligands and inflammatory stimuli, 2) common signaling events and amplification, 3) inside-out signaling which activates the main adhesion receptor, the integrin $\alpha_{IIb}\beta_3$, and thus stabilizing the aggregation, and 4) outside-in integrin signaling that amplifies the whole process[53]. In summary, single receptor signaling pathways converge onto common signaling ones that greatly amplify the initial signals, ultimately eliciting robust platelet responses (Figure 5).

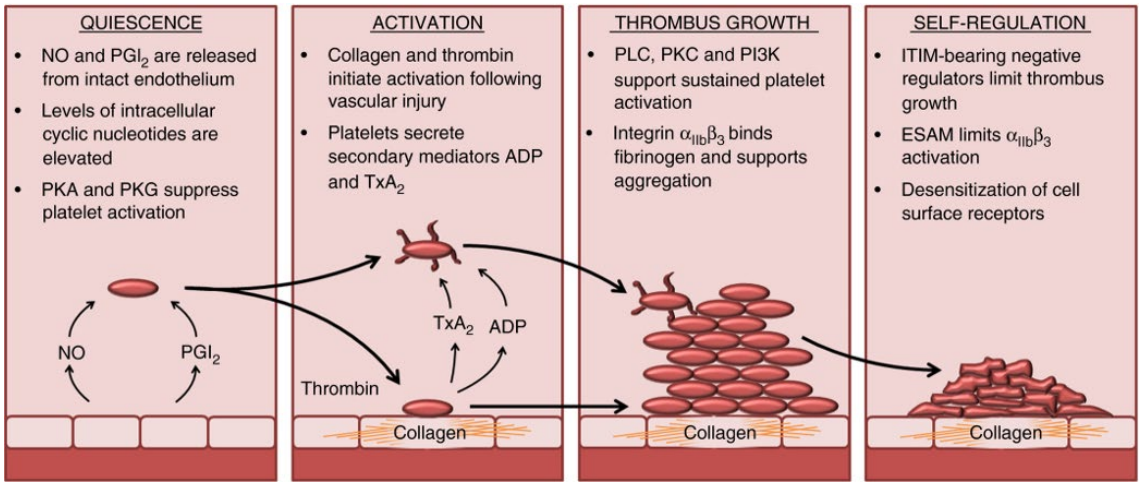

Figure 5. The different phases of platelet activation and thrombus formation. Initially, platelets are maintained in a resting (or quiescence) state, regulated by NO and PGI_2 through the protein kinases (PK) A and G. When there is a vascular injury, and collagen and other proteins are exposed, platelets activate and aggregate by triggering of several dedicated receptors, which sustains the secretion of secondary mediators (among other biomolecules) and elicits inside-out integrin signaling. Lastly, the mechanisms of self-regulation via negative feedback loops are initiated. ESAM: endothelial cell-selective adhesion molecule, NO: nitric oxide, PGI_2: prostaglandin, PI3K: phosphatidylinositide-3-kinase, PLC: phospholipase 2, TxA_2: thromboxane. From Bye *et al*. (2016)[53].

On the surface of the platelet membrane there are a plethora of receptors that can be classified depending on their common structure and subsequent signaling pathway, or their affinity to certain ligands[54]. For instance, the family of guanine nucleotide-binding-protein (G-protein) coupled transmembrane receptors (GPCR) encompass members of the purinergic, thromboxane and protease-activated (PAR) receptors[55]. The purinergic receptors P2Y1, P2Y12 and P2X1 are activated or inhibited upon ADP or ATP stimulation, and constitute one of the cornerstones of current antiplatelet therapies[56,57]. P2Y1 and P2Y12 are guanine nucleotide-binding-protein (G-protein) coupled receptors activated by ADP, but inhibited by ATP; whereas P2X1 is an ATP-gated cation channel receptor[58]. The first two signal through the activation of the β isoform of the platelet phospholipase C (PLC) and the inhibition of the platelet adenylyl cyclase (AC), respectively; while stimulation of P2X1 leads to a rapid calcium influx[56]. The thromboxane A_2 (TxA_2) receptor (TP), as well as the protease-activated receptors (PAR) 1 and 4, which activate when they are cleavage by the proteolytic enzyme thrombin – the main effector protease of the coagulation system –, share the same signaling through PLCβ as the purinergic receptors[59] (Figure 6). PLCβ mediates the positive feedback signaling and recruitment of platelets to the growing thrombi, as well as constituting the major route to the release of calcium.

For their part, the family of receptors containing the immunoreceptor tyrosine-based activation motif (ITAM) sequence (bearing the consensus sequence Yxx[L/I]x6–12Yxx[L/I]) is composed of the glycoprotein (GP) VI–FcRγ, FcγRIIA (not present in mouse), and C-type lectin receptor 2 (CLEC2, bearing a half-ITAM motif [hemITAM])[60]. Activation of these receptors by either collagen (GPVI) or podoplanin (CLEC2) triggers

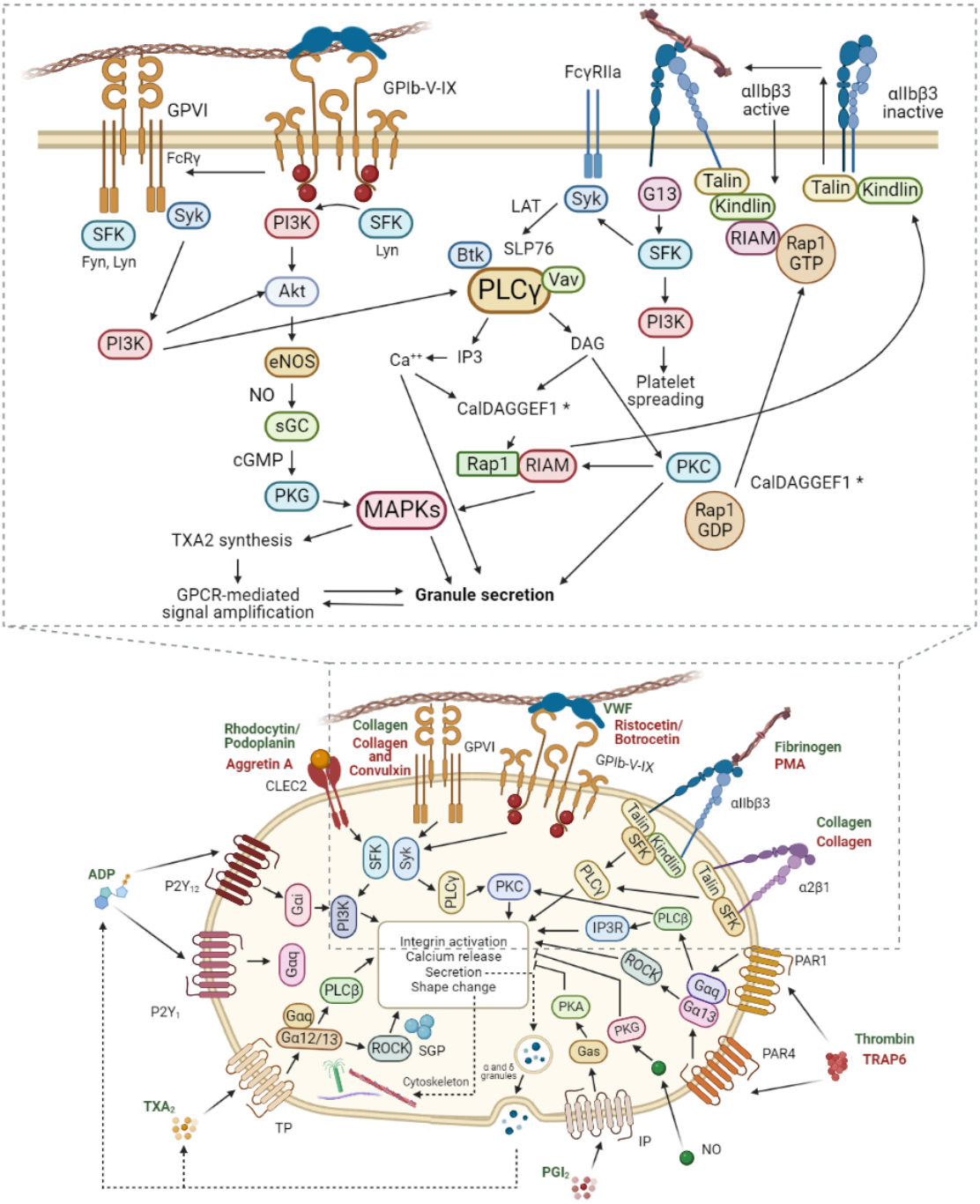

Figure 6. General overview of the main signaling pathways in platelets and the activation outcomes. The bottom figure shows the key platelet receptors and agonists, as well as the platelet-inhibiting prostacyclin I2 (PGI2) and nitric oxide (NO). Depicted are the proteinase-activated receptor (PAR)1 and PAR4, activated by thrombin; the thromboxane (TXA2) receptor (TP); the ADP (purinergic) receptors P2Y1 and P2Y12; the podoplanin and rhodocytin receptor C-type lectin receptor 2 (CLEC2), the collagen receptor glycoprotein (GP)VI; the vWF receptor GPIb-V-IX; and the integrins αIIbβ3 and αIIβ1 outside-in signaling. The outcomes of platelet activation are indicated in the box. The dashed arrows indicate secondary activation mediators (ADP and TXA2). The physiological ligands are colored in green, while the agonists are shown in red. The figure on top depicts the inside-out integrin signaling elicited by the ITAM receptors (GPVI, and also CLEC2), and GPIb-V-IX. Other abbreviations: Gα: heterotrimeric G proteins, GPCR: G protein-coupled receptor, MAPK: mitogen-activated protein kinase, PI3K: Phosphoinositide 3-kinase, PK: protein kinase, PLC: phospholipase C, SGP: small GTP-binding proteins, SFK: Src-family kinase. Adapted from Huang et al. (2021)[64] and Li et al. (2010). Created with BioRender.com.

the Src family kinase (SFK)-mediated activation of the ITAMs, which in turn

phosphorylates SYK, who mediates the recruitment of the phosphoinositide 3-kinase (PI3K), and proteins SLP-76 and GADS around the linker of activated T cells (LAT), and its subsequent phosphorylation[61] (Figure 6). The endpoint of this pathway is the activation of another isoform of PLC, PLCγ2, which also triggers the mobilization of intracellular calcium as well as the activation of the protein kinase C (PKC). Of note, ITAM-mediated activation plays a pivotal role in granule secretion and integrin outside-in signaling[62]. Additionally, and continuing with the trend of shared signaling molecules and synergic pathways, the vWF receptor GPIb-V-IX, and integrins $\alpha_{II}\beta_1$ and $\alpha_{IIb}\beta_3$, which bind to vWF, collagen and fibrinogen, respectively, also transduce their outside-in signal through the SFK–PI3K axis, towards PLCγ2 activation[63]. The integrin $\alpha_{IIb}\beta_3$ constitutes a bidirectional receptor, supporting both outside-in signaling, as mentioned above, and inside-out signaling, which is triggered by the myriad of the aforementioned agonists, but specially after GPVI and CLEC2 activation[64]. Thus, the inside-out signaling leads to the binding of the talin-1 and kindlin proteins to the integrin cytoplasmic tails, which in turn provokes its conformational change, switching from a low-affinity to a high-affinity state[64].

In recent years, the involvement of platelets in the functions of the immune system has led to the discovery of other receptors that were not traditionally found in platelets, namely, the toll-like receptors (TLRs)[65]. These TLRs are involved in the recognition of pathogen- and damage-associated molecular patterns (PAMPs and DAMPS, respectively), which in addition to contribute to the innate immunity and inflammation roles, they are likely to also activate platelets for thrombotic purposes, in response to microbial infection and tissue damage[66].

Platelet activation results in the transient elevation of intracellular calcium, leading to a dramatic reorganization of the actin-myosin cytoskeleton, which enables the adhesion, spreading and aggregation of platelets, as well as the formation of filopodia and lamellipodia[53]. Most importantly, these changes are necessary not only for the secretion of the secondary mediators that build the positive feedback, such as ADP and

TxA_2; but also for the degranulation response, which entails the fusion of the platelet granules with the plasma membrane, and the subsequent exocytosis of molecules stored in them (Figure 6). Platelets harbor three different types of these granules: α-granules, dense granules, and lysosomes. Dense granules contain a variety of small biomolecules, including catecholamines such as serotonin and histamine, ADP, ATP, and calcium; while lysosomes store acid hydrolases and glycosidases, among others[67].

Lastly, α-granules, the most abundant secretory organelles in platelets, are packed with a breadth of proteins that comprise hemostatically active molecules, such as vWF, fibrinogen, fibronectin, or thrombospondin[68]. Other proteins include growth factors, such as transforming growth factor-β (TGF-β), vascular endothelial growth factor (VEGF) or platelet-derived growth factor (PDGF); pro- and anti-angiogenic factors, such as angiogenin and angiostatin, respectively; and cytokines and chemokines, such as platelet factor 4 (PF4), interleukin-8 (IL-8), RANTES (CCL5), β-thromboglobulin (CXCL7), stromal cell-derived factor 1 (CXCL12) or growth-regulated alpha protein (CXCL1)[69]. Some of these are synthesized by megakaryocytes and packed into granules, while others are endocytosed from the plasma by circulating platelets.

The release of proteins from both dense and α-granules requires calmodulin[70], a calcium-sensing protein, to mediate the phosphorylation of myosin light chain, which interacts with the secretion complex containing soluble NSF-associated attachment protein receptor (SNARE) complex, composed of the vesicle-associated membrane proteins 3 and 8 (VAMP-3 and VAMP-8)[71], and SNARE regulators such as Munc13-4[72]. However, it is still not clear whether this secretion constitutes a stochastic event, or rather it is a controlled process, where proteins are either stored[73,74] or released differently[75].

Shifting the paradigm: beyond the hemostatic role of platelets

Since their discovery in the 1880s by Bizzozero[76], the classic paradigm stated that the role of platelets resided solely in the maintenance of the body hemostasis. When

platelets suffer some mechanical stress or when the vascular integrity is compromised, exposing collagen, and inducing the release of vWF by endothelial cells; they elicit a local thrombotic response. This entails the adhesion and recruitment of a great number of platelets to the site of injury that become activated and release a plethora of biomolecules, including chemokines and cytokines, as well as growth factors and other hemostatic factors, which aid to the tissue regeneration of the damaged vessel through the interaction with the coagulation system, and other blood counterparts[77].

However, evolutionary-wise, it is known that platelets do not always sport this role as their primary function. Furthermore, mammals are the only animals that present with megakaryocytes that ultimately give rise to around a thousand anucleate platelets each[78]. They evolved to what we know them today, as a response to a change in the circulatory system of mammals (*i.e.*, becoming more complex and harboring higher shear forces, and more capillaries), the development of the coagulation system[79], and the advent of the placenta, that is, to be able to support the hemochorial implantation of the embryo (*i.e.*, having the fetal epithelium bathed in maternal blood)[80]. In birds, amphibians, fish, and reptiles, platelets are called thrombocytes, they possess a nucleus (*i.e.*, one precursor gives rise to one thrombocyte), are able to phagocyte, and they participate mainly in immune responses, and thus are not as efficient in their hemostatic role as their mammalian counterparts[81]. It is then evident that platelets, from the evolutionary point of view, might have had another primary biological function, but shifted the spotlight to the hemostatic role out of necessity. Although the role of platelets (or thrombocytes) in other species were pointing toward additional roles other than thrombosis and hemostasis, it was not until relatively recently that studies showing proof of platelet involvement in other functions in mammals started to appear (Figure 7).

Newfound functions of platelets span from roles in embryonic and postnatal development, to tissue repair and regeneration, all processes closely related to each other, since one of the things that they have in common is the activation, adhesion (or

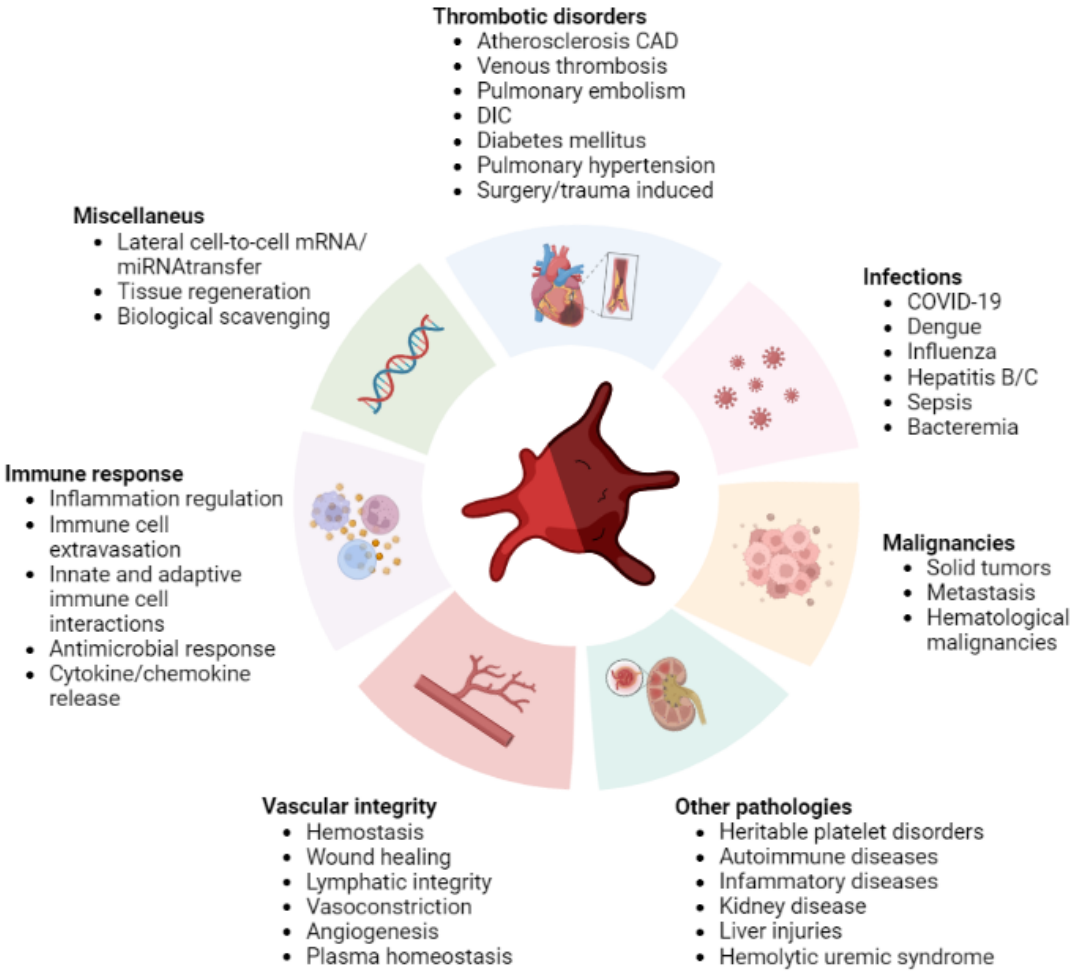

Figure 7. Summary of the classical and non-classical physiological and pathological roles of platelets. Beyond their established participation in maintaining the vascular integrity and preluding the onset of thrombotic disorders, platelets have also been found to engage in the immune and inflammatory responses, tissue regeneration, as well as in cancer and autoimmune diseases, with or without a hemostatic etiology. CAD: coronary artery disease, DIC: disseminated intravascular coagulation. Adapted from Tyagi *et al*. (2022). Created with BioRender.com.

cell-cell contact), and aggregation of platelets, followed by the release by platelets of a plethora of biologically active molecules (notably growth factors and chemokines, among others). Thus, platelets are involved in the separation of the lymphatic[82] and blood vasculatures[83] (vessel remodeling), as well as in the closure of the ductus arteriosus[84], although thus far both processes have only been shown in mice. Furthermore, they actively participate in the maintenance of the lymph nodes after birth, all via the CLEC2 receptor and its interaction with its natural ligand, podoplanin[85]. Additionally, this bioactive platelet cargo plays an invaluable role in tissue repair and regeneration,

orchestrating its different phases, including cellular recruitment and migration, proliferation of stem cells (*i.e.*, mesenchymal stem cells), and angiogenesis[86,87].

Another prominent and conserved role of platelets is their contribution to both the innate and adaptive immune responses[88]. Release of the aforementioned chemokines and other pro-inflammatory molecules attract leukocytes to sites of injury. Furthermore, the discovery of toll-like receptors (TLRs) on the platelet surface opened the door to the idea of platelets as circulating sentinels or surveyors, interacting either directly with pathogens, via recognition of both pathogen- and damage-associated molecular patterns (PAMPs and DAMPs)[89]; presenting them to other immune cells; releasing tumor necrosis factor-α (TNF-α) to promote inflammation, or interacting with activated neutrophils and triggering the release of extracellular traps (NETs), a process called NETosis, where they are able to physically catch pathogens[90]. Platelets also express the CD40 ligand (CD40L) upon activation, which not only elicits an inflammatory response when cleaved (soluble, sCD40L); but also triggers dendritic cell maturation, antibody class switching in mature B cells, and boosts $CD8^+$ T-cell responses, thus bridging the gap between innate and adaptive immunity[91].

The other face of the same coin of these tightly regulated processes that maintain the body hemostasis occurs when there is a platelet malfunction, either resulting in a lack of function from their part, or when their usual physiological roles get exacerbated. In recent years, platelets have been described as players in the onset and progression of some diseases, such autoimmune diseases. The ubiquitous, pathological relationship between platelets and immune cells, which receives the name of “immunothrombosis” or “thromboinflammation”[92], lies at the root of some immune-mediated inflammatory diseases, such as rheumatoid arthritis, systemic lupus erythematosus, psoriasis or viral infections (*i.e.*, COVID-19)[93]. Here, the platelet receptor GPVI takes on a greater role, with its involvement in the release of platelet microvesicles containing inflammatory cytokines, such as IL-1; and in the interplay between platelets and plasmacytoid dendritic

cells, to release interferon-α, or between platelets and neutrophils to trigger NETosis[94]. Exacerbated NETosis is also involved in thromboinflammation, leading to tissue injury, such as the one that occurs in atherosclerosis or sepsis. In the latter, infection-related exhaustion of platelets (thrombocytopenia) requires transfusion of platelets, which in turn can cause transfusion-related acute lung injury (TRALI) and liver injury, when they interact with neutrophils. This, in turn, promotes their massive extravasation to the affected tissue, releasing NETs that get trapped in the microvasculature, and ultimately causing destruction of the tissue[95].

Another prominent, pathological role of platelets concerns cancer. It has been shown that cancer cells can harness the many functions of platelets so that they play in their favor[96]. For instance, they are able to activate platelets by either secreting ADP and thrombin, or expressing podoplanin on their surface and thus binding to and activating the CLEC2 platelet receptor, to cause both deep venous thrombosis, and also the release of growth and pro-angiogenic factors that support tumor progression[97]. In order to survive their metastatic journey through the circulation, cancer cells interact with platelets via a variety of receptors and surface molecules (*i.e.*, P-selectin, CLEC2, integrins, leucine rich glycoproteins, among others), binding to them and forming aggregates that shield them from both the high shear forces of the blood and natural killer (NK) cells[98].

In addition, it has been noticed the uncanny resemblance that exists between platelets and neuronal cells, despite the fact that, in terms of morphology and function, they cannot seem more distinct. This similarity lies in their compartmentalized cytoplasm in the form of granules, their cargo (*i.e.*, platelets, as neurons, store several neurotransmitters, such as serotonin, glutamate and γ-aminobutyric acid, among others), and that its secretion results from drastic changes in the calcium dynamics[99]. Furthermore, platelets are involved in the antagonistic roles of maintaining brain homeostasis *(i.e.*, activated platelets promote neurogenesis and neuronal

differentiation)[100,101], and of being associated with a number of neurodegenerative diseases, such as multiple sclerosis, amyotrophic lateral sclerosis, Alzheimer's disease, or Parkinson's disease[102].

Lastly, although found in low numbers in circulation, megakaryocytes are also immune cells themselves[103], as it can be inferred from the fact that platelets inherit their phenotype from them. On their surface, they display those same receptors able to sense and react to inflammation, such as TLRs and IgG Fc receptors (FcγR), as well as CD40L and the major histocompatibility complex I (MHC I)[104], along with the corresponding machinery to perform antigen presentation. It has also been reported that megakaryocytes possess antiviral activity, by means of upregulation of the antiviral immune protein interferon-induced transmembrane protein 3 (IFITM3) during virus infections[105].

In summary, the different roles of platelets span across many physiological and pathological processes, although most (if not all) of the non-classic functions share the inflammation response as a common denominator. This fact positions platelets at a sort of crossroads, making them not only targets for the amelioration of a wide range of diseases, but also potential therapeutic assets, if we are able to harness and direct their many beneficial roles and qualities.

The crosstalk between platelets and the environment

The long-standing conception that platelets are necessary for performing exclusively one function, was accompanied by the even more stablished notion that megakaryocytes and platelets are generated similarly in both health and disease, that is, that they are static entities impervious to their surroundings. It was believed that the impact the environment, in this case an inflammation state, had on platelets lied exclusively in its interaction with the platelet receptors, and thus tuning the different aspects of their activation (*i.e.*, aggregation, degranulation, etc.). However, recent

studies point to the existence of a dialogue, where information flows in both directions: platelets are not only reacting to environmental cues (*i.e.*, cytokines, exposure of ligands), but also said cues are potentially inducing the generation of fine-tuned megakaryocytes and platelets, with different profiles than in health.

Hence, the study of the platelet phenotype under inflammation conditions hints to changes that profoundly affect platelet function. For instance, during acute infections and inflammation, like the one that occurs in sepsis, platelets are sometimes consumed in great quantities, resulting in a severe thrombocytopenia that increases the mortality risk[106]. However, regardless of the platelet count, the new batches of platelets produced under these conditions displayed increased levels of TLR4, CD62P, CD32 and PAR-1[107], while a study from our group showed a reduced response following podoplanin and collagen stimulation[108], pointing to their respective receptors CLEC2 and GPVI, the two receptors related to the thromboinflammation role of platelets, being specifically turned off, or subject to intense shedding[109]. However, activation through two of the classic hemostatic receptors, $\alpha_{IIb}\beta_3$ integrin and the vWF receptor, remained largely intact. Both platelets and their megakaryocytic progenitors, under these conditions, also displayed a completely different mRNA profile, and were able to induce lymphotoxicity via granzyme B[110]. Similarly, another study showed that blocking of GPVI reduced both the infarct size and the recruitment of inflammatory cells after myocardial ischemia-reperfusion injury, and reduced the neuronal damage caused by cerebral reperfusion after a stroke[111,112]. Contrariwise, the same strategy targeting the $\alpha_{IIb}\beta_3$ integrin, which is one of the main hemostatic receptors in platelets, resulted in a dramatic increase in intracranial hemorrhages and infarct growth[113].

The tailoring and tuning of platelets by inflammation extends not only to their receptors, but also to their protein cargo. Although platelets inherit said cargo from megakaryocytes, where the aforementioned transcriptional changes could further translate to certain protein profiles, it is also known that platelets directly endocytose

plasma components[114]. This means that, on top of being produced differently, if there are disease-induced systemic changes in the plasma, and given their surveillance-like role, then platelets can be considered as mirrors of the health status. One clear example of this is that of the neurodegenerative diseases. Although it has been demonstrated that platelets play a role in maintaining brain homeostasis, and thus any dysfunction from their part can negatively impact this environment, many studies that point to a role for platelets in the disease are also alluding to changes in their protein content. Examples of this are the increased levels of aspartate, glycine, and the mutant huntingtin (mHTT) protein found in platelets of patients diagnosed with Huntington's disease[115,116]; a decreased uptake in glutamate in Parkinson's disease[117]; or increased TDP-43 and decreased serotonin levels in amyotrophic lateral sclerosis[118,119].

However, although the causality between inflammation and altered megakaryo- and thrombopoiesis is stablished[9], the actual alterations and triggering mechanism *in vivo*, especially given the characteristics of the bone marrow, have yet to be fully elucidated. It is known that, in spite of the immune-privileged status of the bone marrow, inflammation has an impact on its microenvironment[120] and consequently on hematopoiesis[121], inducing the proliferation and differentiation of progenitors, as a response to inflammatory signals, such as cytokines (*i.e.*, interferons) and TLR ligands. Nevertheless, specific knowledge on the impact on the megakaryocytic lineage is lacking. Recently, a study pointed to the extracellular vesicles (EVs) derived from activated platelets as potential culprits[122]. These EVs were found to be able to enter the bone marrow niche and directly interact with HSCs and other progenitors, directing their inflammation-skewed differentiation towards megakaryocytes and platelets, and thus coming full circle in giving a possible and plausible explanation as to how inflammation is able to drive and modify megakaryocyte differentiation and platelet production. Although the cargo of these platelet EVs was not characterized, and consequently no individual protein or set of proteins could be associated to the transcriptional changes,

another study on rheumatoid arthritis highlighted the importance of platelet-derived, IL-1-containing EVs in driving inflammation and disease progression, and pointed to the activation of the GPVI receptor as the mechanism by which they were produced[123]. This sustains the idea that inflammatory cues in plasma, chiefly cytokines, are able to modulate the process.

Lastly, it cannot be ruled out the role of the lung and their resident, immune-primed megakaryocytes in the production of tailored platelets. It has been shown that certain pathologies display a notable increase in the number of lung and circulating MKs. For instance, this phenomenon has been described in humans with cardiovascular disease[124], inflammatory lung diseases[125] and, more recently, in COVID-19[126]; and in animal models after infection[127] or treatment with TNF-α[128]. This suggests that lung thrombopoiesis may be increased during lung infection and/or thromboinflammation.

Utilizing platelets as biosensors: the advent of platelet proteomics

Environmental cues are thus seemed to be able to shape megakaryopoiesis and generate a platelet produce tailored to the physiological needs of the organism. This positions platelets as mirrors of the health status, providing a wealth of knowledge on the different pathological processes. Specifically, the fact that they are able to stablish a bidirectional conversation with the environment, not only by inheritance from megakaryocytes, releasing bioactive molecules and modulating their receptor profile, but also, and most importantly, by incorporating them from the plasma to their cargo, makes them the perfect source of systemic biomarkers. Biomarkers are essential tools to establish, or even predict, the diagnosis and prognosis of diseases, as well as monitoring responses to treatments[129]. Many of the characteristics of platelets are currently being used as biomarkers, such as their count and other indices[130,131], the immature fraction[132] and its RNA content[133], and their activation status[134]. However, given the nature of platelets, which revolves around their lower level of complexity from the cytological point

of view, it is precisely their protein cargo the one feature that can be considered as the main source of platelet biomarkers. Consequently, among the different omics, proteomics[135], that is, the large-scale study of the structure, composition, function, and interactions of proteins; holds the most promise.

The advent of mass spectrometry-based (MS) proteomics along with the availability of the whole sequence of the human genome, opened the door to the deep analysis of the total content of proteins in a cell: the proteome. Although one step behind the more stablished omics (namely, genomics and transcriptomics), especially when it comes to its implementation in the clinic, proteomics has undergone a drastic improvement in the last decade, from sample preparation, peptide separation and MS-detection, to developing better tools for the data analysis, all resulting in a higher sample throughput, sensitivity, and reproducibility, shorter run times, and more reliable results[136,137]. As a result of this leap, >90% of proteins that compose the predicted proteome coded in the human genome (around 20,000 proteins), have now been reliably detected[138], there is a comprehensive proteome map by tissue[139]; and more recently, the deepest proteomics map collected to date was published, which sheds light on how variants and alternative splicing (isoforms) conform the proteome[140], also called the proteoform. All of this will most likely be further advanced in the near future, especially with the rapid development of single-cell proteomics[141].

Application of MS proteomics to the study of platelets started in the early 2000s[142], and has progressed hand in hand with its parent field, sharing the same advantages and limitations (*i.e.*, low membrane protein solubility, expensive and time-consuming, and not allowing high throughput without losing sensitivity and robustness)[143]. However, platelet proteomics also present with a number of inherent limitations, which have been the object of much debate throughout the years. Among said limitations, the one with less consensus corresponds to the sample extraction and preparation[144]. It is of vital importance that platelets are handled with care in every step

to avoid unwanted activation, which could potentially bias the results. This care must be ensured from the time of the extraction, taking into account potential comorbidities and drugs that could affect platelets, collecting the blood in anticoagulant-containing tubes (whether EDTA, sodium citrate or acid citrate dextrose, is still debated)[145], and maintaining them rotating at room temperature (similarly to what blood banks do with platelet concentrates)[146]. Afterward, a suitable amount of time between the moment of extraction and processing must be guaranteed, to avoid not only the small peak of activation due to the draw of blood, but also the activation due to long waiting times, even if the tubes are kept rotating. In regard to the sample preparation, it comprises the isolation from other blood components and the washing of platelets. These two steps entail several centrifugation and sample handling steps, which should be minimized as much as possible. Lastly, in addition to platelet activation, another key factor to control is the sample contamination with residual erythrocytes, leukocytes, and plasma elements, which could also confound the analysis[147]. However, it also has to be acknowledged that, due to the nature of platelets themselves *(i.e.*, the open canalicular system and their overall stickiness), it is not possible to avoid all contamination. Of note, the field is still studying the pool of platelets from a given sample, without information on platelet populations within that sample (*i.e.*, different age, reactivity).

Furthermore, the subsequent bioinformatics analysis, including the software and parameter selection, warrant special consideration, where data transformation, signal threshold attributions, and databases utilized can impact the final results. High rates of stochastic and nonrandom missing values, particularly in label-free quantitative proteomics, also thwart data analysis[148]. The normalization and imputation choices to tackle these issues are varied, and there are no unified criteria for the order in which they should be implemented[149].

Thus, since its beginnings, and despite its limitations and lack of consensus, platelet proteomics has been employed to the study of not only the whole proteome, but also a wide range of sub-proteomes, both in mouse and human, from the platelet cytoskeleton, the granule cargo[150,151], and membrane proteins[152], to specific signaling pathways (*i.e.*, through the focused analysis of post-translational modifications, PTMs)[153] and the content of granules released during activation (*i.e.*, releasate or secretome)[154] (Figure 8). This has allowed the comprehensive description of the platelet proteome, both in terms of identification and quantification[155]; and although it is estimated that it comprises around 15,000 proteins (based on platelet transcriptome information)[156], current studies report the identification of around a third of this number[157].

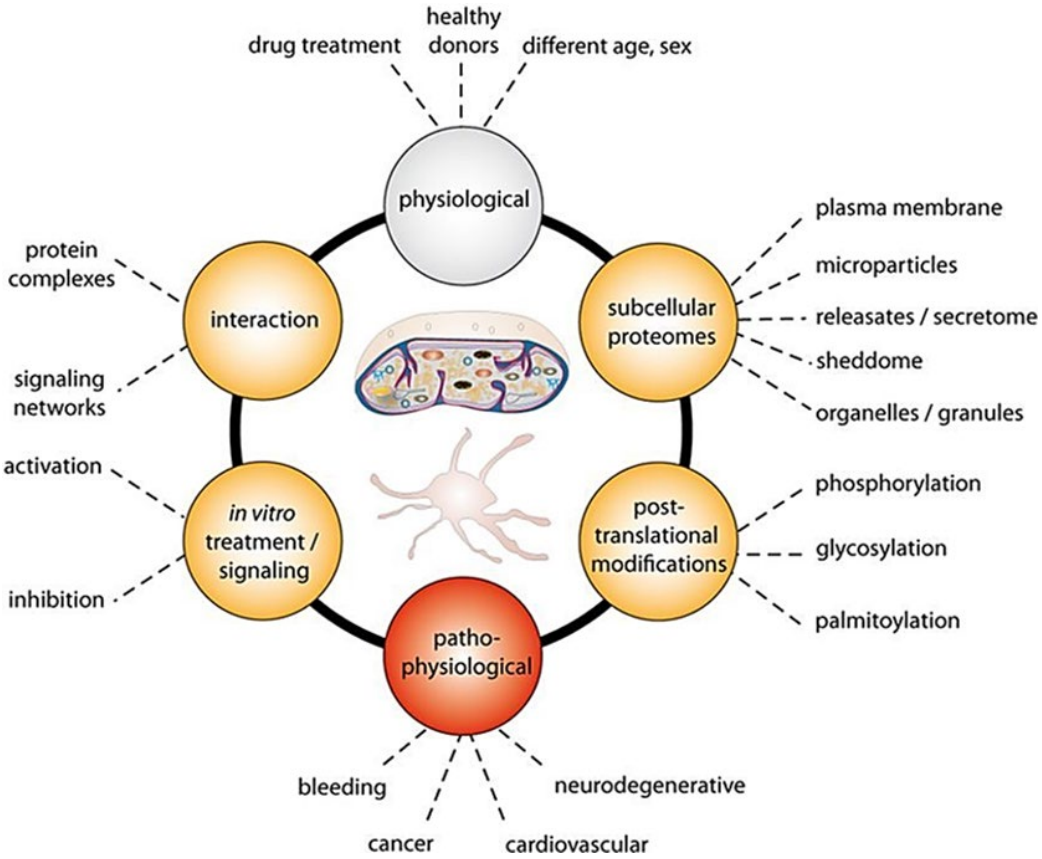

Figure 8. Overview of different applications of platelet proteomics. It has been implemented to study the platelet proteome both in health and disease, as well as to study its function, interactions, and signaling mechanism via post-translational modifications (PTM). Additionally, special attention has been put in the characterization of the different subcellular proteomes (membrane, releasate, cargo of the different granules, sheddome, or microparticles/microvesicles). From Burkhart *et al*. (2014)[155].

Much attention has thus been directed to the characterization of the steady-state, healthy platelet proteome and sub-proteomes, which has improved our understanding of the fundamental processes that regulate platelets, and also led to the acknowledgement that their proteome is fairly stable, showing little inter- and intra-donor variation[158]. This opened the door not only to the search of biomarkers, and novel therapeutic targets and interventions, but also to investigate if they are able to differentiate between health and disease, or between pathological states. For instance, there are proof-of-concept studies that point to its use in cancer, since it has been shown that changes in the platelet proteome already occur in early stages of the disease, preceding the metastasis process[159,160]. Furthermore, platelets proteomics has also been found useful in biomarker discovery of other disorders, such as neurodegenerative diseases, as noted in previous sections, or even to predict the response to antiplatelet drugs[157].

All in all, our understanding of how platelets are involved in maintaining not only the body hemostasis, but also homeostasis, and how that same environment is shaping and tailoring both the megakaryocyte differentiation and the production of platelets to suit it needs, has greatly advanced. Nonetheless, much of the attention has been directed towards studying the effect of acute inflammation or cardiovascular disease, but there is a lack of understanding of how low-grade, chronic inflammation impacts and shapes megakaryopoiesis, thrombopoiesis, and platelet phenotype and function. At the same time, given the nature of platelets, proteomics has positioned itself as one of the most promising tools to study the platelet phenotype and its disease-associated changes, which will greatly aid both in the discovery of new therapeutic targets and biomarkers, and in further advancing our knowledge in depicting the complex, pleiotropic roles that platelets play in disease.

Objectives

Platelets are the anucleate blood components responsible for maintaining the body hemostasis. However, in the last decade, they have been associated with a great number of non-hemostatic functions, such as cancer, tissue regeneration, or inflammation. Furthermore, the common understanding that platelets (and their progenitors, megakaryocytes) were produced equally both in health and disease, has progressively been debunked. Recent studies, both in mouse and human, of scenarios of acute inflammation, such as the one that occurs in sepsis, have revealed that megakaryocytes seem to originate following a non-canonical differentiation pathway, and that platelets are produced with a different phenotypic and functional profile, especially regarding the non-hemostatic receptors, GPVI and CLEC2. Whether these changes occur during their production, or as a result of their exposure to the environment in circulation, or a combination of the two, is still a matter of debate. Nonetheless, there is little understanding of how low-grade, chronic inflammation shapes megakaryopoiesis and thrombopoiesis, and the different aspects of the platelet produce, and how we can harness that knowledge to advance our understanding, prediction, and treatment of disease. Furthermore, the use of preclinical mouse models is still necessary to deepen into the pathophysiology of certain pathologies or conditions, prior to engaging in studies in human. It is of the utmost importance to understand how the results from the different studies can be extrapolated inter-species with the same objectives: understanding disease.

Thus, the specific objectives of this thesis are:

1. To determine if the platelet proteome is able to differentiate among healthy and pathological states, in murine preclinical models of immune thrombocytopenia, advancing our understanding of the disease.
2. To determine the applicability of platelet proteomics on mouse-human inter-species studies.

3. To thoroughly characterize human platelets in health, through functional and cellular assays, and proteomics, both in basal and activated states.

4. To understand how platelets and megakaryocytes are produced differently under subclinical, low-grade chronic inflammation in humans, by interrogating four different, non-hematological patient cohorts: type 1 diabetes, dermatitis, psoriasis, and major depressive disorder (concurrent with or without suicidal attempt), by combining a cell biology and proteomics approach.

Objetivos

Las plaquetas son los componentes enucleados de la sangre responsables de mantener la hemostasia corporal. Sin embargo, en la última década, se han asociado con un gran número de funciones no hemostáticas, como cáncer, regeneración tisular o inflamación. Por otro lado, el acuerdo tácito de que las plaquetas (y sus progenitores, los megacariocitos) eran producidos de igual forma en salud y enfermedad, ha sido desbancado de forma progresiva. Estudios recientes, tanto en ratón como en humano, en escenarios de inflamación aguda como el que ocurre en sepsis, han mostrado que los megacariocitos parecen originarse siguiendo una ruta de diferenciación distinta a la canónica. Además, las plaquetas producidas en estas circunstancias muestran un fenotipo y perfil funcional diferente, especialmente en relación con sus receptores no hemostáticos, GPVI y CLEC2. Sin embargo, aún no existe un consenso respecto a si estos cambios ocurren durante su producción, o como resultado de su exposición al ambiente en circulación, o por una combinación de los dos. A pesar de ello, se sabe muy poco de cómo la inflamación crónica de bajo grado es capaz de modular la megacariopoyesis y la trombopoyesis, así como los diferentes aspectos de las plaquetas, y cómo podemos aprovecharnos de ese conocimiento para mejorar en nuestro entendimiento, predicción y tratamiento de enfermedades. Por otro lado, el uso de modelos murinos preclínicos es todavía necesario para profundizar en la fisiopatología de ciertas enfermedades, previo a su estudio en humanos. Es de suma importancia entender cómo los resultados en diferentes especies pueden ser extrapolados a otros con los mismos objetivos: entender la enfermedad.

De este modo, los objetivos específicos de esta Tesis Doctoral son los siguientes:

1. Determinar si el proteoma de las plaquetas es capaz de diferenciar entre estados sanos y patológicos, usando modelos murinos preclínicos de trombocitopenia inmune, impulsando nuestro conocimiento de la enfermedad.
2. Determinar la aplicabilidad de la proteómica de plaquetas en estudios inter-especies ratón-humano.

3. Caracterizar de forma exhaustiva las plaquetas en salud, en humanos, a través de ensayos funcionales y celulares, y de proteómica, tanto en estado basal como tras activación.

4. Comprender, en humanos, cómo las plaquetas y los megacariocitos se producen de forma diferente bajo una inflamación crónica de bajo grado, interrogando cuatro cohortes de pacientes no hematológicos: diabetes tipo 1, dermatitis atópica, psoriasis, y depresión mayor presentando o no tentativa suicida, usando una aproximación combinada de proteómica y biología celular.

Experimental and bioinformatics procedures

Mouse studies

Study population

Mice were maintained in the animal care facilities of Lund University or the Netherlands Cancer Institute under specific-pathogen-free conditions. All animal experiments were approved by their respective animal ethics committees.

Passive immune thrombocytopenia (ITP) model

Mice were subject to intravenous (IV) injection in the tail vein of anti-GPIbα antibody (2μg/g bodyweight, Emfret Analytics). Blood samples were taken at 3 days (thrombocytopenic state, P-ITP D3 samples) and 7 days (platelet count recovery state, P-ITP D7 samples) after injection. The control group was mock-treated with the same volume of PBS (C samples). Each of the four groups were composed of three biological replicates.

Active ITP model

The active ITP mouse model was developed as previously described[161]. Briefly, BALB/c CD61 KO mice were immunized with weekly transfusions of 10^8 wildtype ($CD61^+$) platelets for 3 weeks. After immunization, mice were sacrificed, and after disaggregation of their spleen, $1.5x10^4$ splenocytes were transferred intravenously to mice with severe combined immunodeficiency (SCID), after which they develop ITP (A-ITP samples). A group of mice were injected intraperitoneally with intravenous γ-globulins (IVIg, 2 g/kg, Gamunex) 1 day before splenocyte transfer and twice a week afterwards (A-ITP IVIg samples). Blood samples from both groups (A-ITP and A-ITP IVIg) were collected 3 weeks after splenocyte transfer. Each group was composed of five mice.

Sample collection and processing

All blood samples were taken from the retro-orbital venous plexus or by cardiac puncture using ethylenediaminetetraacetic acid (EDTA)- or citrate/phosphate – dextrose – acetate buffer (CPDA)-coated tubes, and mixed gently afterwards. Mice were

anesthetized with isoflurane and euthanized by cervical dislocation after blood collection. Platelet-rich plasma (PRP) was separated by centrifuging the blood 15 min, at 50g, as described[162-164]. As a quality control step, the PRP was counted using a scil Vet abc Plus+ instrument (scil animal care company GmbH) or similar hematocounter, and thus ensuring that there were undetectable white or red blood cells. Platelets were further washed by centrifugation and snap-frozen in liquid nitrogen (LN_2) for proteomic analysis.

Flow cytometry–based aggregation assay (FCA)

Platelet aggregation was performed as described previously[162]. In short, CD9-APC (Abcam) and CD9-PE (Abcam) labeled platelets were mixed 1:1, and preincubated for 10 minutes (700 rpm, 37°C) in a heating and mixing block (ThermoCell Mixing and Heating, MB-102, Bioer), in the presence of 2% mouse plasma. As agonists, 100 ng/mL of phorbol 12-myristate 13-acetate (PMA, #P1585, Sigma-Aldrich), 10 µg/mL of Botrocetin (snake venom from *Bothrops jararaca*, #V5625, Sigma-Aldrich), 10 µg/mL of collagen (collagen solution from bovine skin, #C4243, Sigma-Aldrich), 0.5 µg/mL of convulxin (CVX, Santa Cruz) or 30 nM of Aggretin A (AggA, courtesy of Prof. Johannes Ebble) were used. Timed samples were fixed in 0.5% formaldehyde (FA)/PBS and measured on an LSRII + HTS or Canto flow cytometer, and analyzed for double-colored events by FACSDiva software (BD Biosciences).

Protein extraction and mass spectrometry (MS)

Platelet lysis and in-solution digestion of proteins, and mass spectrometry acquisition were performed as previously described[164,165]. Briefly, 10^9 platelets were lysed in 500 µL of 8M urea (ThermoFisher Scientific) and 100 mM tris(hydroxymethyl)aminomethane (TRIS)-HCl pH 8 (ThermoFisher Scientific). 5 µg protein was digested for 16 h at 37°C with MS-grade trypsin (Promega) in a ratio of 1:20 (trypsin:protein), after standard disulfide bond reduction and alkylation procedure. Tryptic peptides were separated by a nanoscale C18 reverse phase chromatographer coupled to an Orbitrap™ Fusion™ Tribrid™ mass spectrometer (ThermoFisher Scientific), via a

nanoelectrospray ion source (Nanospray Flex Ion Source; ThermoFisher Scientific), following standard procedures and settings. All data were acquired with Xcalibur software.

MS data analysis

The RAW mass spectrometry files were processed with the MaxQuant computational platform (version 1.6.17.0) running on Linux[166,167]. Searches were configured for label-free quantification (LFQ), with the options LFQ, match between runs and iBAQ, while the rest of the parameters were set to default. Peptides and proteins were identified using the Andromeda[168] search engine against the Mus musculus UniProt Swiss—Prot protein database (downloaded November 2020, 17,051 canonical entries). The 'proteinGroups.txt' output table was further analyzed within the R environment (version 4.0.3) (R Project for Statistical Computing)[169]. Proteins were filtered for potential contaminants, only identified by site and reverse hits, and iBAQ intensities were log2-transformed. We did not further consider biological replicates that did not pass quality control tests (namely > 35% of missing values). This resulted in the exclusion of some samples that would otherwise have confounded the results.

Protein hits were filtered in when they were present in all samples of at least one group. Intensities were quantile normalized, followed by imputation of missing data by the quantile regression imputation of left-censored data (QRILC) approach[170]. Next, we removed the batch effect created by the different mouse models using the conservative 'removeBatchEffect' function from the 'limma' package[171]. The resulting dataset was subsequently fed to a linear model combined with empirical Bayesian statistics implemented by this same package, for the differential expression analysis of proteins among every pairwise comparison. Differential expression of protein hits with adjusted p-values (Benjamini−Hochberg method) lower than 0.05 were considered significant, in any given comparison, and were used for further analysis.

Correlation-based network analysis

Weighted gene correlation network analysis (WGCNA) was performed on the differentially expressed proteins (DEPs) using the 'WGCNA' R package[172] and the tailored workflow designed by Wu *et al*. (2020) for proteomics data[173]. A 0.85 correlation coefficient threshold was chosen, while a soft threshold of 26 was selected for the construction of the weighted correlation and adjacency matrix by using the approximate scale-free network criteria. Of note, a signed network is constructed, so that only positively correlated proteins have a strong connection. Next, the topology overlap metrics (TOM) and its distances (1 – TOM) are calculated from the adjacency matrix in a step-wise fashion. The resulting protein sets are hierarchically clustered (average method) based on the TOM distance, and an optimal set of modules was determined by using a dynamic tree-cutting algorithm, with a minimum of 10 proteins in each module, followed by merging close clusters (cut height of 0.1). Additionally, module eigenproteins (ME) are generated by value decomposition of the first principal component and signed module memberships (kME) are obtained. Finally, module-trait (Pearson) correlations were calculated.

Annotation, and gene ontology (GO) and pathway enrichment

UniProt IDs were mapped to their respective Entrez Gene IDs, Symbols and Gene names using the 'AnnotationDbi'[174] (version 1.52.0) and 'org.Mm.eg.db'[175] (version 3.12.0) R packages. Gene Ontology (GO), Kyoto Encyclopedia of Genes and Genomes (KEGG), and Reactome enrichments on gene lists were obtained using the 'goseq'[176] (version 1.36.0), and the 'msigdbr'[177] (version 7.2.1) R packages. Intensity bias was taken into account, and the enrichment was calculated using the using the Wallenius approximation. The resulting P values were adjusted for multiple testing using the Benjamini and Hochberg correction, and an adjusted P value of <0.05 was considered significant. Figures were constructed with 'ggplot2'[178]. Additionally, protein–protein interaction graphics were obtained using the STRING app on Cytoscape[179] (version 3.7.2).

Data have been deposited to the ProteomeXchange Consortium[180] via the PRIDE partner repository with the dataset identifier PXD028814. The source code for the proteomics and subsequent WGCNA analyses is available on the GitHub repository: https://github.com/patmartinezb/ITP-mouse-proteomics.

Comparison of the human and mouse platelet proteomes

Database search of published platelet proteomics studies

We performed a search on Pubmed using the following keywords: platelet AND proteomics AND (lysate OR releasate OR secretome). After manually screening the abstract and method section, 30 studies of whole platelet lysate (27 in human, 3 in mouse)[145,157,158,165,181-206], and 5 studies of platelet releasate (4 in human, 1 in mouse) were selected[206-210]. The selection criteria took into account that the proteomics analysis was done using mass spectrometry, and that the protein digestion was performed in solution. Differences on the sample processing, mass spectrometer and search engine used were registered. In addition, these studies had to have a publicly available raw protein dataset (*i.e.*, datasets only showing differentially expressed proteins were not included), where healthy control samples had to be either clearly identified or easily deduced.

In addition, FASTA files of the human and mouse reference proteomes were downloaded from UniProt (November 2022). These included only reviewed, canonical proteins; with 20,385 and 17,127 entries, respectively.

Dataset cleaning, filtering, and analysis

All datasets were stored in a single Excel file (one dataset per sheet), and imported into RStudio[211]. For each dataset, the following cleaning and filtering was performed, when needed: protein and/or gene identifications (*i.e.*, UniProt IDs, gene names) were cleaned, so that only the leading identified, canonical protein/gene remained; additionally, a filtering step was performed to ensure that the working proteins

were expressed in at least two thirds of the controls. Moreover, and if it was specified in the dataset, contaminants and/or detected decoys were removed, as well as proteins with low-confidence detection. Lastly, to homogenize all datasets, protein/gene identifications were annotated so that they had an accompanying UniProt IDs, ENTREZID, SYMBOL and ENSEMBL ID.

In order to select a reliable set of proteins that composed the core of the platelet proteome/releasate, all identified proteins across any of the respective datasets (*i.e.*, 27 datasets for the human platelet lysate) were filtered so that only reviewed proteins were used, and the remaining were merged, and their occurrence counted. As a rule of thumb, those proteins that were detected in at least half of the datasets (*i.e.*, in 12 of the 27 datasets, for the human platelet lysate, so that it also reached a total count above 2,000) were considered as reliably expressed and part of the core proteome. In addition, orthologs were obtained in each case (both human to mouse, and mouse to human), as well as the overlap with the reference proteomes, all of it represented as Venn diagrams.

Those datasets that presented with clear, reliable relative quantification were used to study the protein distribution (x11 and x39 for the platelet lysate proteome, and s5 and s4 for the releasate proteome; for human and mouse, respectively). Thus, controls were selected, features were filtered based on missing values and the median expression of each protein was calculated. Based on this value, proteins were ranked for plotting, and the distribution was divided into three subsets, based on its quartiles (first quartile, inter-quartile, and third quartile). Each subset was further subject to a gene ontology enrichment analysis, plus an extra simplification step to remove redundancy of the resulting enriched GO terms, to determine which known biological functions were over-represented in each one of them.

Lastly, to study the overlap and correlation between platelet transcriptomics and proteomics, both in mouse and human, datasets from the study by Rowley *et al*. (2011) were used [212]. Transcripts were filtered based on their RPKM expression (RPKM > 0.3),

and the resulting datasets were overlapped with the respective proteomics data (core PLT proteome). Those common features further underwent a Pearson correlation analysis against the proteomics datasets (x11 and x39 for mouse and human, respectively), after log2-transformation of RPKM values.

All the data manipulation and analysis were conducted using R (R Core Team, version 4.0.3)[169]. Handling of the data was performed using the 'dplyr'[213] and 'stringr'[214] libraries, and plotting with the 'ggplot2'[178], 'ggpubr'[215] and 'eulerr'[216] libraries. The Bioconductor packages 'AnnotationDbi'[174], 'org.Hs.eg.db'[217] and 'org.Mm.eg.db'[175] were used to annotate the data, 'gprofiler2'[218] to extract the orthologs, and 'clusterProfiler'[219] to perform the enrichment analysis. The full reproducible code and datasets, as well as Table S1, are freely available at: https://github.com/PLT-lab/PLT-proteomics-review.

Human studies

Study population

The patient cohorts included in this study were selected based on the presence of subclinical, low-grade chronic inflammation. Thus, the subject population consisted of 34 patients recruited in the area of Oviedo, Spain, from November 2019 to November 2021, and diagnosed with any of the following diseases or disorders: type I diabetes (N = 10), major depression disorder concurrent with (N = 6) or without (N = 10) suicidal attempt, atopic dermatitis (N = 4), or psoriasis (N = 4); thus, conforming the five patient cohorts that comprise the study. Additionally, 20 sex- and age-matched adult, healthy volunteers were included. All samples were collected after written informed consent from all participants. The study was approved by the Ethical Committee for Medical Research of the Principality of Asturias (nº 205/18), and it was conducted following the principles of the Declaration of Helsinki.

General inclusion criteria

The general inclusion criteria encompassed unequivocal diagnosis by a physician, in the case of the patients, and age above 18 years old. On the other hand, individuals who had taken any anti-platelet medication less than a week before the recruitment, or that are treated regularly with any of these drugs, were excluded from the study, as well as patients treated with drugs that affect platelet function. Further exclusion criteria included current treatment with systemic anti-inflammatory or immunosuppressant drugs, presence of acute infection, smoking, obesity (BMI > 30 kg/m^2), pregnancy and lactation, autoimmune diseases other than the one being studied, history of chronic renal, hepatic, or cerebrovascular disease, acute coronary syndrome, and reported hematological disorders. In summary, as a rule, the recruitment was based on the absence of comorbidities, and the lack of medication. If medication was present, as required by the diagnosis (*i.e.*, insulin), it was previously searched in the literature that the drug had no impact on platelets or hematopoiesis in general.

Inclusion criteria per cohort

Major depression disorder (MDD) patients were diagnosed according to the Diagnostic and Statistical Manual of Mental Disorders (DSM-5), with a clinician-rated score ≥4 in the Clinical Global Impression-Severity (CGI-S) scale. Suicidal attempt (SA) was defined as a “self-initiated sequence of behaviors by an individual who, at the time of initiation, expected that the set of actions would lead to his or her own death” (American Psychiatric Association, 2013). MDD patients with SA were included within 7 days of the attempt.

Type 1 diabetes patients were included if they met the 2012 diagnosis standards of the American Diabetes Association (ADA), a blood test indicated the presence of at least one autoantibody to pancreatic islet β cells, had been diagnosed for more than 3 months, were free from symptoms of severe hypoglycemia or severe hyperglycemia, and had a stable daily insulin dose.

Atopic dermatitis and psoriasis patients were included if they have been diagnosed with an ICD-10 code of L20 or L40, and presented the “moderate” or “mild” stage of the disease, respectively. AD is considered “moderate” when presented with a score between 7.1 to 21 in the Eczema Area and Severity Index (EASI) or a score between 25–50 in the Scoring Atopic Dermatitis (SCORAD) scale; and psoriasis is considered “mild” when presented with scores <10 both in the Psoriasis Area and Severity Index (PASI) and in the Body Surface Area (BSA) score, and 2-3 in the static Physician Global Assessment (sPGA). In both cases, patients were prescribed with topical therapy or phototherapy, with no prescription of systemic therapies.

Sample collection and processing

Whole blood was drawn by venipuncture and collected into four tubes containing either buffered sodium citrate solution (NaCit, 0.129 M, 3.2%, 4.5 mL BD – 1x) or EDTA tripotassium dihydrate (K_3EDTA 9 mL, Greiner Bio-One – 3x), depending on whether the samples were meant for either the aggregation assay (citrate), or the cell culture, platelet immunophenotype, the degranulation assay and proteomic experiments (EDTA). Fasting before blood draw was not a requirement. Both types of anticoagulant tubes were gently mixed and kept rotating, at room temperature, before processing. Additionally, 500 µL of EDTA blood were set aside to perform a complete blood count (CBC) test right after collection, using a Sysmex XN-10/XN-20 hematology analyzer.

PRP was separated from the rest of the blood components by centrifuging the whole blood of the EDTA anticoagulated tubes (1000 rpm ─centrifugations were performed in a 5810 R Eppendorf centrifuge, with an A-4-62 rotor, unless otherwise specified─, 15 min, room temperature) without brake, to avoid the swirling of erythrocytes into the PRP fraction. The upper two-thirds of the PRP fraction were taken for further processing, in order to avoid leukocyte and erythrocyte contamination. As an extra quality control step, to measure the presence of these contaminating cells, and to take the required number of platelets for each subsequent procedure, the PRP was counted in

the same hematology analyzer as the one used for obtaining the CBC. The interphase was collected for the *in vitro* megakaryocyte culture, as explained below. A summary of the experimental procedure can be seen in Figure 1.

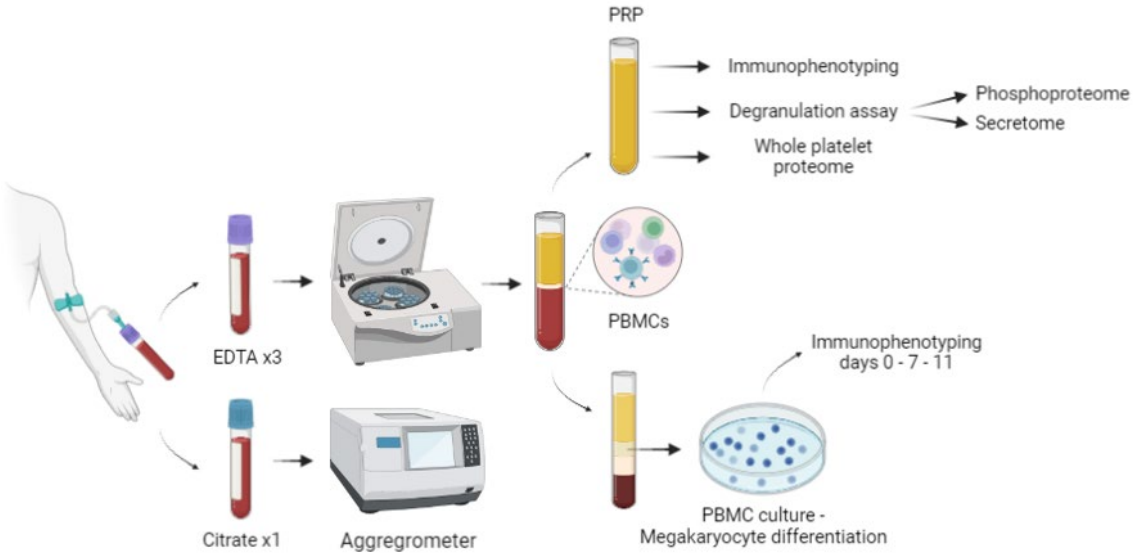

Figure 1. Schematic overview of the experimental workflow followed for all samples. The platelet rich plasma (PRP) was used for all platelet-related assays, except for the aggregation assay, which was performed on citrated whole blood. The interphase ring was transferred to another tube for a gradient separation step to isolate the peripheral blood mononuclear cell (PBMC) fraction, and further cultured. Created with BioRender.com.

In vitro megakaryocyte differentiation from human peripheral blood mononuclear cells

Culture of peripheral blood mononuclear cells (PBMCs) and subsequent megakaryocyte differentiation was performed as previously described[220,221]. Briefly, peripheral whole blood from EDTA tubes were centrifuged (1000 rpm, 15 min, no brake) and, after the PRP fraction was set aside, the interphase containing the PBMCs was diluted 1:1 in PBS. This dilution was carefully pipetted in a 5:1 ratio on top of a density gradient medium (Lymphoprep, 1.077 g/mL, STEMCELL Technologies), and centrifuged (2400 rpm, 20 min, no brake). The resulting PBMC ring was collected and washed twice (1500 rpm, 5 min), and the pellet was resuspended in 500 µL of PBS. Of these, 30 µL were set aside for immunophenotyping (PBMCs or megakaryocyte culture Day 0 samples). Subsequently, cells were counted using a Neubauer chamber (BRAND

counting chamber, BLAUBRAND), and seeded to a density of 1-1.5x10^6 cells/mL in 100 mm culture plates.

The basal culture medium (StemSpan™ Serum-Free Expansion Medium II, #09605, STEMCELL Technologies) was supplemented with 1% penicillin/streptomycin (P/S; 10,000 units penicillin and 10 mg streptomycin/mL, #P4333, Sigma-Aldrich), and 1:1000 of a lipid mix rich in cholesterol (Lipids Cholesterol Rich from adult bovine serum, #L4646, Sigma-Aldrich). To make the complete media, stem cell factor (SCF, see section below), N-plate® (thrombopoietin agonist Romiplostim) and erythropoietin (EPO, Binocrit 10.000 UI/1 mL, Sandoz) were added to the basal medium, in concentrations that depended on the phase of the culture, as shown in Figure 2.

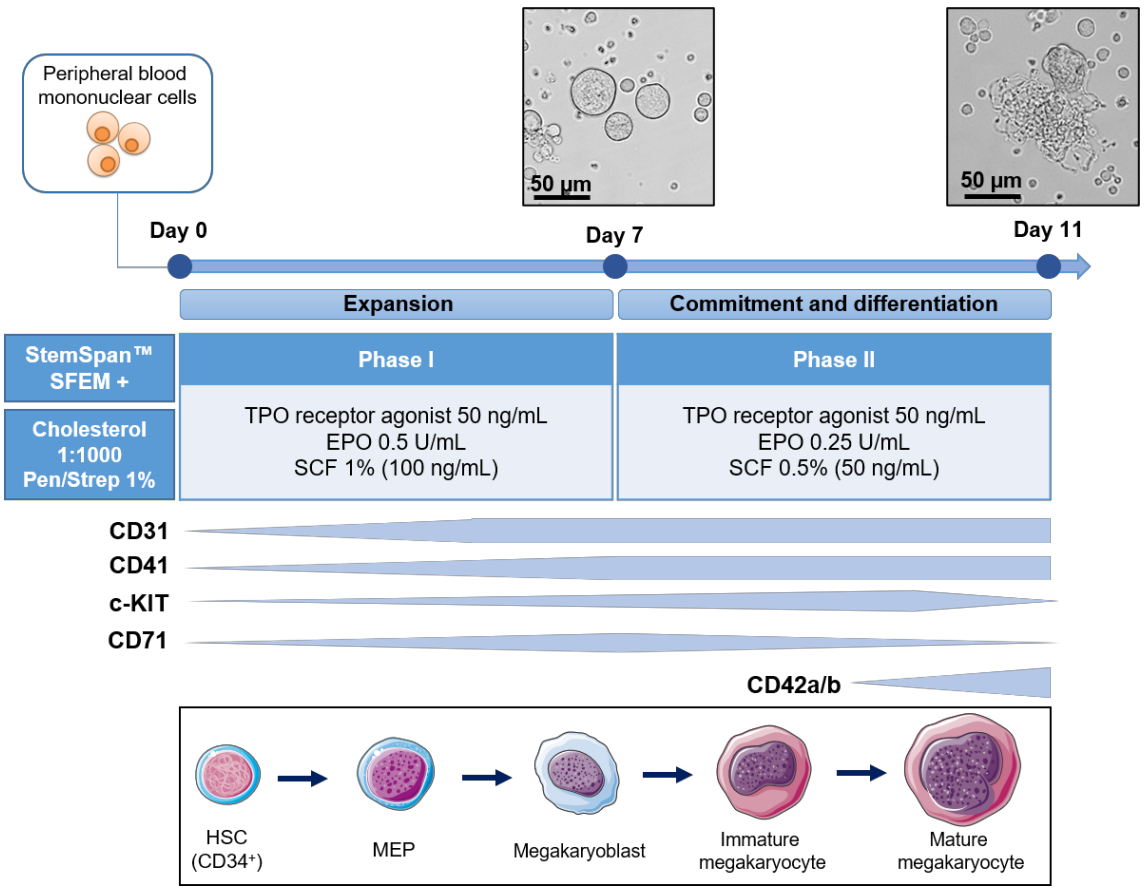

Figure 2. Schematic representation of the *in vitro* megakaryocyte differentiation from human peripheral blood mononuclear cells (PBMCs). PBMCs from patients and healthy donors were cultured following an adapted protocol from Salunkhe *et al*. (2015)[220]. It depicts the different stages of maturation, and the timing of marker acquisition (Panel 2). Pictures were taken with a 20X objective. Adapted from Acebes-Huerta *et al*. (2021). EPO: erythropoietin, HSC: hematopoietic stem cell, MEP: megakaryocyte–erythroid progenitor, SCF: stem cell factor, TPO: thrombopoietin.

During the first 7 days of culture, PBMCs were grown in Phase I culture medium (progenitor expansion phase, see Figure 2), which was refreshed after 3 days. Afterwards, to allow megakaryocyte differentiation, cells were centrifuged (700 rpm, 5min) and the culture medium was replaced to Phase II (see Table 3), while half of the cells were reserved for immunophenotyping. Lastly, at day 11 most of the megakaryocytes had reached a mature state, and started to form pro-platelets; thus, to avoid culture exhaustion, cells were harvested (700 rpm, 5min), and immunophenotyped.

SCF production from CHO–SCF transfected cells

Chinese hamster ovary (CHO) cells stably transfected with soluble human SCF were cultured in Iscove Modified Dulbecco's Medium (IMDM, with glucose, glutamine, HEPES, phenol red, and sodium pyruvate, #12440053, Gibco) with 10% of heat-inactivated (30 min, 56°C) fetal bovine serum (FBS, Gibco) and 1% P/S, in a T175 flask (VWR). When the cells reached an 80-90% of confluency, the medium was changed to IMDM with 1% BSA, with no antibiotics, and cells were grown for 2 days. Afterwards, the supernatant was collected, filtered and frozen at –20°C until use. An ELISA assay was performed to calculate SCF concentration in the supernatant (~10 µg/mL).

Phenotypic characterization of human megakaryocyte subpopulations

Cells from day 0 (PBMC fraction), and cultured cells harvested at day 7 and 11, were incubated with the corresponding megakaryocyte antibody panel (see Table 1 below), and additional aliquots were either stained with a cell viability marker, or left unstained as control. Thus, cultured cells were first washed with PBS (1000 [day 0] / 700 [days 7 and 11] rpm ─performed in a Mikro 185 Hettich centrifuge, with a 1226-A rotor─, 5 min) to remove the culture medium, and then were incubated in 100 µL of the antibody panel, for 20 min, in the dark. Afterwards, they were washed with 1 mL of PBS (700 / 1000 rpm, 5 min), and the pellet was resuspended in 300 µL of 1% PBS/BSA. The cell

pellets for the unstained and viability conditions were resuspended in 200 µL and 100µL of 1% PBS/BSA, respectively, and 10 min before the measurement, 20 µL of 7-Amino-actinomycin D (7-AAD, BD Via-Probe, BD Biosciences) were added to the latter. The final concentration of 7-AAD exceeds the one recommended by the manufacturing house, due to the fact that megakaryocytes reach higher ploidy levels than other cells. Lastly, the measurement was performed in a FACSAria II flow cytometer using FACSDiva software, or in a CytoFLEX S flow cytometer, immediately afterwards.

All antibodies from Table 1 were purchased from BD Biosciences; save for CD117, CD31, and CD71, which were purchased from BioLegend. The lineage cocktail 2 (lin 2) was composed of the following antibodies: CD3 (T3), CD14 (lipopolysaccharide receptor), CD19 (B4), CD20 (B1), and CD56 (neural cell adhesion molecule); which in combination, stain lymphocytes, monocytes, eosinophils, and neutrophils. The antibody cocktail was made in 1% PBS/BSA.

Table 1. Antibodies used in the phenotypic characterization of human megakaryocyte subpopulations. Inside the square brackets the alternative name (if required), and the working dilution are specified. GP: glycoprotein, MK: megakaryocyte, TFR: transferrin receptor.

Fluorochrome	**Panel MK**
FITC	lin 2 [1:200]
PE	CD42a [GPIX – 1:200]
PerCP	CD41 [GPIIb – 1:200]
PE-Cy7	CD117 [c-KIT – 1:400]
APC	CD31 [PECAM-1 – 1:200]
APC-Cy7	CD71 [TFR – 1:800]

Platelet aggregation assay

The aggregation capacity of human platelets was measured using a Platelet Function Analyzer (Aggrestar PL-12, SINNOWA Medical Science & Technology Co.). Briefly, 300 µL of citrated whole blood were loaded to the analyzer, and platelets were

stimulated with either 30 µg/mL of collagen, 100 µM of TRAP6 (PAR-1 agonist peptide, Abcam), 0.625 ng/mL of CVX, 100 ng/mL of PMA, 6.53 nM of AggA, 0.5 mg/mL of ristocetin (ristomycin monosulfate, #R7752, Sigma-Aldrich), or left unstimulated. Platelets were counted by the device at eight different time points, one minute apart, before (2 measurements) and after the addition of the agonist (6 measurements). The aggregation rate was thus calculated by comparing the number of platelets before and after said activation.

Platelet immunophenotyping

The PRP volume corresponding to 10^6 human platelets was added to 100 µL of four different antibody panels (see Table 2, Panels I to IV). Additionally, an unstained condition, with the same volume of 1% PBS/BSA, was included. Thus, platelets were incubated in their corresponding antibody panel for 10 min, at room temperature and in darkness. Similarly, an aliquot of activated platelets to obtain the secretome/releasate and phosphoproteome fractions for mass spectrometry (see below), was incubated with the “Degranulation” panel in the same conditions. Afterwards, they were fixed in 0.5% of FA/PBS, and measured in a FACSAria II flow cytometer using FACSDiva software (BD Biosciences) or in a CytoFLEX S flow cytometer (Beckman Coulter).

All antibodies from Table 2 were purchased from BD Biosciences; save for CD42b, CD117, CD31, CLEC2, and CD71, which were purchased from BioLegend; and FB-AF488 (fibrinogen from human plasma, Alexa Fluor 488 conjugate), which was purchased from Invitrogen. Cocktails of Panel II and “Degranulation", as indicated in Table 1, were made in a solution of HEPES buffer (132 mM NaCl, 6 mM KCl, 1 mM $MgSO_4$, 1.2 mM $KH_2PO_4 \cdot 7H_2O$, 20 mM HEPES; all from Sigma-Aldrich, except for the HEPES, which was purchased from Gibco), with 2 mM $CaCl_2$ (#C5670, Sigma-Aldrich). Cockails for Panels I, II and IV, were prepared in PBS containing 1% of bovine serum albumin (BSA, Sigma-Aldrich).

Table 2. Antibodies used in platelet immunophenotyping (panels I to IV) and degranulation assay. Inside the square brackets the alternative name (if required), and the working dilution are specified. CLEC2: C-type lectin-like receptor, FB: fibrinogen, GP: glycoprotein, GPA: glycophorin A, HPCA1: hematopoietic progenitor cell antigen 1, c-Mpl: thrombopoietin receptor, TFR: transferrin receptor.

Fluorochrome	Panel I	Panel II	Panel III	Panel IV	Degranulation
FITC	CD61 [GPIIIa – 1:200]	CLEC2 [1:200]	CD34 [HPCA1 – 1:200]		FB-AF488 [0.225 mg/mL]
PE	GPVI [1:200]	CD49b [GPIa – 1:200]	CD235a [GPA – 1:200]	CD42a [GPIX – 1:200]	CD62p [P-selectin – 1:200]
PerCP	CD42b [GPIbα – 1:200]	Annexin V [1:200]	CD41 [GPIIb – 1:200]		Annexin V [1:200]
PE-Cy7				CD117 [c-KIT – 1:400]	CD63 [LIMP – 1:200]
APC	CD9 [1:200]	CD31 [PECAM-1 – 1:200]	CD110 [c-Mpl – 1:200]	CD36 [GPIV – 1:200]	CD9 [1:200]
APC-Cy7				CD71 [TFR – 1:800]	

Preparation of platelet fractions for MS analysis

Platelet proteome

From each sample, 1 mL of PRP was centrifuged (4000 rpm, 5 min), and the platelet pellet was snap-frozen in LN_2 for further processing and proteomics analysis.

Secretome and phosphoproteome of activated platelets

Activation reactions composed of 10^8 platelets were prepared in order to obtain the platelet lysates to analyze the phosphoproteome, as well as the secretomes. For this, the corresponding PRP volume was centrifuged (4000 rpm, 5 min) at room temperature. The resulting platelet pellet was resuspended in 500 µL of HEPES with 5 mM glucose (D-(+)-Glucose, Sigma-Aldrich) buffer, and left to rest for 15 min. Afterwards, platelets were activated with either 30 µg/mL of collagen, 100 µM of TRAP6, 6.25 ng/mL of CVX, 100 ng/mL of PMA, 6.53 nM of AggA, 0.5 mg/mL of ristocetin, or left unstimulated. Activation was performed under constant stirring (1000 rpm) for 5 min, at 37°C, using a heating and mixing block. An extra condition was included, where unstimulated platelets were kept on ice for the same period of time. Immediately afterwards, the supernatant

fraction containing the platelet releasate (secretome) and the remaining activated platelets were separated by centrifugation (4000 rpm ─Mikro 185 Hettich centrifuge─, 5 min). The resulting platelet pellet was snap-frozen in LN_2, and stored at –80°C for the phosphoproteomics analysis. The supernatant was further centrifuged (10,000 rpm ─Mikro 185 Hettich centrifuge─, 3 min) to remove any remaining cell debris, snap-frozen, and stored at –80°C for the secretome mass spectrometry analysis.

Quality control: flow cytometry and cytospins

To check the extent of the platelet activation in each condition during the degranulation assay, 10 µL ($2x10^6$ platelets) of each reaction, including the unstimulated and ice conditions, were added to 100 µL of a dedicated antibody cocktail (see Table 2, Degranulation). Activated platelets were incubated with the panel for 10 min (room temperature, darkness), fixed in 0.5% FA/PBS, and measured in a FACSAria II flow cytometer using FACSDiva software, or in a CytoFLEX S flow cytometer.

For cytospin preparation, $10x10^6$ platelets resulting from the degranulation assay were fixed with 0.5% FA/PBS, placed on a slide and centrifuged (500 rpm ─Cytospin 4 Cytocentrifuge, Thermo Scientific─, 5 min). Photos were taken on a Leica DM RXA2 microscope, at 40X, and processed with the Leica Application Suite X (LAS X) software (version 4.9).

Sample preparation for MS and liquid chromatography with tandem mass spectrometry (LC-MS/MS)

Platelet lysate proteomes, and secretomes

Frozen samples were heat-inactivated on a thermomixer (Eppendorf) for 5 min, at 95°C. Platelet pellets were lysed in 0.1 M triethylammonium bicarbonate buffer (TEAB, T704, Sigma) with 1% sodium dodecyl sulfate (SDS, Genomics Solutions, #80-0175). After cooling down on ice, they were briefly centrifuged to collect the condensates. A further centrifugation step was performed for the secretomes to remove remaining cell debris (10 min, 16,000 g). Afterwards, samples were sonicated (Bioruptor Pico,

Diagenode) at 4°C for 10 cycles (30 s on/off), and an aliquot was set aside for protein determination (BCA protein assay, #23225, Thermo Scientific). Subsequently, 300 µg (400 µg for TMT) of each sample was adjusted to a 100 µL volume with 0.1 M TEAB, and proteins were reduced with 5 mM dithiothreitol (DTT, #D9163, Sigma) at 50°C for 60 min. After cooling the sample to room temperature, 1/20 vol of 200mM 2-chloro-acetamide (CAA, #22788, Fluka) was added for alkylation of the cysteines, and samples were incubated at room temperature for 45 min.

In the case of secretomes, to optimize the pH for enzymatic digestion, 1/10 vol of 1M tris(hydroxymethyl)aminomethane (TRIS)-HCl (#T6066, Sigma) pH 8.5 was mixed with the samples, followed by trypsin addition (1:40 protein ratio, TPCK treated, #20233, Thermo Fisher Scientific). Digestion was conducted overnight at 30°C, on a thermomixer. Subsequently, samples were centrifuged (5 min, 16,000 g) and 20 µg of digested protein was adjusted to 150 µL.

For the lysates, firstly protein precipitation was performed by adding 1/20 vol of 1M NaCl (#S9888, Sigma) followed by 4 vol of acetone (Biosolve, #1030602), and mixed by vortexing. The samples were centrifuged (20 min, 16,000 g), and the pellet washed with 4 vol cold acetone. Afterwards, the supernatant was removed, and the protein pellet was air-dried briefly, resuspended with 0.1 M TEAB, and sonicated at 4°C for 10 cycles (30 s on/off). The enzymatic digestion was performed with a 1:50 enzyme-to-protein ratio of LysC (Lysyl Endopeptidase, Mass Spectrometry Grade, #129-02541, FUJIFILM Wako Pure Chemical Corporation) for 70 min, at 37°C and 1,200 RPM; followed by overnight 1:20 trypsin (Immobilized Trypsin, TPCK Treated [Agarose Resin], #20230, Thermo Scientific) digestion (1,200 rpm, 30°C). Subsequently, the peptide suspension was filtered in a glass fiber filter tip, filters were rinsed with 0.1M TEAB and volumes were adjusted to a final concentration of 2 mg/mL.

For the TMT proteomics experiment, digested peptides were labeled with TMTpro™ 16-plex reagents (Thermo Fisher Scientific), according to the instructions of

the manufacturer. Briefly, 25 µg of the sample digest was diluted in 50 µL 0.1 M TEAB. A reference was prepared by pooling 10 µg of peptides from each sample, and 85 µg was diluted in 100 µL 0.1 M TEAB. Each sample was mixed with a specific TMT reagent and following incubation at room temperature for 1 h, the reaction was quenched with 5 µL of 5% hydroxylamine in 0.1 M TEAB. TMT-labeled samples were pooled at a 1:1 ratio, according to the mixture.

For all experiments, trifluoroacetic acid (TFA, #299537, Sigma-Aldrich) was added to a final concentration of 0.5% to achieve pH < 3 for Empore C18 StageTip (Supelco, #66883-U) cleaning (desalting). Cleaned digests were dried in a SpeedVac (Thermo Scientific) and residues were redissolved by mixing and sonication in 40 µL (100 µL for TMT) of 2% acetonitrile (ACN, Biosolve, #1204101BS) - 0.5% formic acid (FA, Biosolve, #06914143).

For nanoflow LC-MS/MS, 0.5 µL (~400 ng) of samples were injected into an EASY-nLC™ 1200 System Liquid Chromatograph (Thermo Scientific) coupled to an Orbitrap Fusion™ Lumos™ Tribrid™ Mass Spectrometer (Thermo Scientific) operating in positive mode and equipped with a nanospray source. For the TMT experiment, 3 µL (~600 ng) of each mixture were injected into an Orbitrap Eclipse™ Tribrid™ Mass Spectrometer (Thermo Scientific). Peptide mixtures were trapped on an Acclaim™ PepMap™ C18 column (100 Å, 5 µm, 100µm x 2 cm, Thermo Scientific). Peptide separation was performed on a ReproSil Pur C18 reversed phase column (120 Å, 2.4 µm, 25 cm × 75 µm, packed in-house, Dr Maisch GmbH) using a linear gradient from 0 to 80% B (A = 0.1% formic acid; B = 80% [v/v] acetonitrile, 0.1% formic acid) in 180 min, and at a constant flow rate of 250 nL/min. Mass spectra were acquired in continuum mode, and fragmentation of the peptides was performed in a data-dependent mode, and using the multinotch SPS MS3 reporter ion-based quantification method for the TMT experiment.

Phosphoproteome

Platelet pellets were lysed in 100 mM TRIS-HCl pH 8.5, 4% sodium deoxycholate, and immediately heated to 95°C for 5 minutes, on a thermomixer. After cooling down on ice and being briefly centrifuged to collect the condensates, samples were sonicated in a Bioruptor Pico at 4°C for 10 cycles (30 s on/off). Samples were reduced with 100 mM tris(2-carboxyethyl)phosphine hydrochloride (TCEP, #C4706, Sigma) and alkylated with 400 mM CAA. Subsequently, 120 µg of protein was digested with 1:100 LysC and trypsin beads (TPCK Treated) for 16 hours, at 37°C. Phospho-enrichment was performed following the EasyPhos protocol [5]. The samples were run on a Orbitrap Eclipse™ Tribrid™ Mass Spectrometer operating in positive mode and equipped with a nanospray source. Peptide mixtures were trapped on an Acclaim™ PepMap™ C18 column (100 Å, 5 µm, 100 µm x 2 cm). Peptide separation was performed on a ReproSil Pur C18 reversed phase column (100 Å, 3µm, 25 cm × 75 µm, packed in-house) using a linear gradient from 0 to 80% B (A = 0.1% formic acid; B = 80% [v/v] acetonitrile, 0.1% formic acid) in 120 min, and at a constant flow rate of 250 nL/min. Mass spectra were acquired in continuum mode, and fragmentation of the peptides was performed in a data-dependent mode.

Data analysis

CBC analysis

A Chi-square and ANOVA tests were used to check if there were any differences among groups, in terms of sex and age, respectively. Imputation of missing values was performed by cohort, using the predictive mean matching method from the ‘mice’ R library[222]. Monocyte-to-lymphocyte (MLR), platelet-to-lymphocyte (PLR) and neutrophil-to-lymphocyte (NLR) ratios were calculated by dividing the indicated count parameters by the respective lymphocyte count; while the systemic immune-inflammation index (SII) was calculated as the ratio between the product of the platelet and the neutrophil counts, and the lymphocyte count. An analysis of covariance (ANCOVA) was implemented for

each continuous variable, controlling for the sex and age of the subjects, using the 'car' library[223]. Subsequently, specific pairwise comparisons were conducted using the Tukey Honest Significant Differences test, to control the overall type I error rate resulting from multiple testing, using the 'multcomp' library[224]. Statistical significance was considered *p* value (or *q* value in the case of multiple testing correction) < 0.05.

Aggregation analysis

Percentages of aggregation per time point were calculated as follows:

$$P_i = 100 - \frac{M_j \times 100}{(M_1 + M_2)/2}$$

Where P_i is the percentage of aggregation corresponding to the i-th time, i = 1, 2, …, 7; M_1 and M_2 represent the first two measurements, before the addition of the agonist; and M_j corresponds to the measurements made after said addition, j = 3, 4, …, 8. If a negative value was produced (*i.e.*, the platelet count after the addition of the agonist [M_j] was higher than the mean of the first two, unstimulated measurements [M_1, M_2]). The maximum aggregation rate (MAR) is defined as the highest (maximum) recorded aggregation percentage at any given time point.

The area under the curve (AUC), used to measure the dynamics of the aggregation, was calculated as follows:

$$AUC = \sum_{i=1}^{7} \frac{T_{i+1} - T_i}{(P_{i+1} + P_i) \times 2}$$

Where T_i is the point value corresponding to the i-th time, i = 1, 2, …, 7; and P_i is the percentage of aggregation corresponding to the i-th time.

An analysis of variance (ANOVA) was implemented for each agonist, and the subsequent specific pairwise comparisons were conducted using Tukey's test. Statistical significance was considered *p* value (or *q* value in the case of multiple testing correction) < 0.05.

Flow cytometry analysis

To analyze the raw .fcs files, the FlowJo software was employed (version 10.8.1). The gating strategy is described in the respective result sections, and mean fluorescence intensities (MFIs) and percentages of interest were exported to Excel files.

Due to unexpected circumstances, samples had to be measured in two different flow cytometers, for every analysis (platelet and cultured megakaryocyte immunophenotype, and degranulation assay). Additionally, within the healthy cohort, half of it (the one not used for proteomics) used a different batch of AggA for the degranulation assay, which was also controlled for. To check if any of this caused any intra- and inter-group variation, a PCA was performed in each case. MFIs were previously log2-transformed, except in the case of the degranulation assay, where the MFIs of the different agonists were first normalized to the unstimulated condition, and then log2-transformed. Percentages did not require any scaling. If any batch effect due to the flow cytometer or AggA batch was indeed detected, an ANCOVA test was implemented for each continuous variable, controlling for each batch-causing variable. Subsequently, specific pairwise comparisons were conducted using Tukey's test, and statistical significance was considered with a p value (or q value in the case of multiple testing correction) < 0.05.

For plotting purposes, the batch effects were removed from both percentages and log2-MFIs, using the removeBatchEffect function from the 'limma' R package[171].

MaxQuant and FragPipe processing of MS data

Label-free RAW data from whole and activated (phosphoproteomics) platelet lysates, and secretomes from healthy controls were processed with the MaxQuant computational platform[166] (version 2.2.0.0). Searches were configured for label-free quantification (LFQ), with the options LFQ, match between runs and iBAQ, trypsin as set as the digestion enzyme; and carbamidomethyl (C), and oxidation (M) and acetylation (N-term), as fixed and variable modifications, respectively. Additionally, the

phosphoproteomics search included the Lys-C enzyme, and phospho (STY) as variable modification. The rest of the parameters were set to default. Peptides and proteins were identified using the Andromeda search engine[168] against the *Homo sapiens* UniProt Swiss—Prot protein database (downloaded on January 2023, comprising 20,432 canonical entries).

In addition, the whole platelet lysates were also processed with FragPipe's search engine, MSFragger, with the aim of comparing it to MaxQuant. For this, RAW data was previously converted to open mzML files using the MSConvert program (version 3.0.22143), which is part of the ProteoWizard Toolkit software package[225]. The resulting spectra files were searched against the same *Homo sapiens* UniProt Swiss—Prot protein database, with the incorporation of an equal amount of decoy sequences; using the MSFragger search engine[226,227] (version 3.7). MS/MS spectra were searched using the following criteria: precursor-ion mass tolerance of 20 ppm, fragment mass tolerance of 20 ppm (isotope errors 0/1/2); as fixed modifications, cysteine carbamylation (+57.0215); and as variable modifications, methionine oxidation (+15.9949), and N-terminal protein acetylation (+42.0106). As digestion enzyme, trypsin was chosen, allowing up to two missed cleavage sites. The search results were processed with the Philosopher toolkit[228] (version 4.8.0), which comprised PSM validation with Percolator[229], MS1 quantification and match-between-runs with IonQuant[230] (version 1.8.10), and the use of PeptideProphet and ProteinProphet for protein inference[231]. Protein groups were filtered to 1% false discovery rate (FDR) using the target-decoy strategy.

Lastly, isobaric TMT 16-plex data from the platelet lysates of patients and controls was also processed with FragPipe, with the same settings as for LFQ, with the following exceptions: fragment mass tolerance of 0.6 Da (isotope errors 0/1/2/3); as fixed modifications, cysteine carbamylation (+57.0215) and lysine TMT labeling (+304.2072); and as variable modifications, methionine oxidation (+15.9949), N-terminal protein

acetylation (+42.0106), and TMT labeling of peptide N-terminus. In this case, TMTIntegrator was not used for the normalization of the data.

LFQ data analysis of the platelet lysate proteome and secretome

For the MaxQuant and FragPipe comparison, the 'proteinGroups.txt' and 'combined_protein.tsv' output tables were used. Additionally, in the case of FragPipe, the protein coverage information was retrieved from the 'protein.tsv' files. In both instances (and in all proteomics analysis), the data were analyzed within the R environment[169] (version 4.0.3). Firstly, the data was cleaned of contaminants, log2-transformed, and filtered so that proteins with more than 50% of missing values, across all samples, were dropped. Additionally, for the characterization of the control platelet lysate, coefficients of variation were calculated per protein, using all available sample intensities. Gene ontology enrichment was performed using the 'enrighGO' function from the clusterProfiler[219] R package, using the whole human proteome as background.

For the secretome analysis, the 'combined_protein.tsv' output table from Fragpipe was used. Proteins were filtered for potential contaminants, only identified by site and reverse hits, intensities were log2-transformed, and 0 were changed to NA. The filtering strategy comprised, firstly, the removal of proteins that were only identified (*i.e.*, presented with missing values across all samples and groups), and then of those that are not present in at least two of the three replicates, of at least one group. The remaining dataset was normalized to the median, across all samples, and sequentially imputed using the 'impSeq' function from the rrcovNA[232] R package. A linear model combined with empirical Bayesian statistics implemented by the limma[171] R package was used to determine the differential expression analysis of proteins among all pairwise comparisons against the control. Differential expression of proteins hits with adjusted *p*-values (Benjamini−Hochberg method) lower than 0.05 were considered significant.

Phosphoproteomics data analysis

Data transformation and inference

The data from 'Phospho (STY)Sites.txt' output table from MaxQuant were transformed and analyzed as in the secretomes analysis, with the exception of an extra step that allowed only for high quality phosphosites (localization probability > 0.75).

Phosphoproteomics database search

The phosphorylation site and kinase substrate datasets from PhosphoSitePlus (PPS) were downloaded on January 2023 (https://www.phosphosite.org/), while the Phospho.ELM database was downloaded on August, 2022 (http://phospho.elm.eu.org/). All were filtered for human phosphopeptides, and the "ON_FUNCTION" and "ON_PROCESS" were used for the enrichment of regulatory roles. Additionally, post translational modification information from UniProt was accessed using the rbioapi R package.

Data clustering and enrichment

Hierarchical soft clustering was performed using the fuzzy c-means algorithm of the mfuzz R package[233], which is based on the minimization of a weighted square error function (ref). A number of clusters, ranging from 1 to 7, were tested, and the minimum distance (Dmin) between cluster centroids was utilized to select the optimal number of clusters.

Gene ontology enrichment was performed using the 'enrichGO' function from the clusterProfiler R package[219], interrogating the three orthogonal ontologies (*i.e.*, biological process [BP], molecular function [MF], and cellular component [CC]). Reactome pathway over-representation analysis was conducted using the 'enrichPathway' function from the ReactomePA R package[234], which implements a hypergeometric model. Lastly, phosphosite-level ontology enrichment was performed employing the PPS kinase substrate dataset previously mentioned, by means of the hypeR R package[235], which also performs a hypergeometric test to determine if a group of proteins is over-

represented. As background, all confidently identified phosphosites across all samples were used, and each term was required to have at least 5 overlapping proteins.

KinSwing analysis

To predict kinase activity from phosphoproteomics data, the KinSwingR R package was used, which is based on the algorithm described by Engholm-Keller *et al*. (2019)[236]. It integrates kinase-substrate predictions, with the fold change and its significance, of phosphopeptide sequences obtained from the study. Since KinSwing does not need data to be pre-filtered or clustered beforehand, the total of phosphopeptides used for inference was fed to the algorithm, along with their fold changes in respect to the control condition, and the associated *p* values. Additionally, the curated substrate sequences for all human protein kinases, along with their respective substrates, were taken from the aforementioned PPS dataset. This database was used to build position weight matrices (PWMs), with the 'buildPWM' function, for all human curated kinases. Subsequently, the 'scoreSequences' function scored the resulting PWMs against the input data, and thus building the kinase-substrate network. Lastly, the 'swing' function integrated all the available information (*i.e.*, directionality and significance of the fold change), to assess the local connectivity of the networks. It outputs a normalized (z-score) 'swing' score that has been weighted for the number of substrates used in the PWM model, and the number of phosphopeptides in the local network; as well as accompanying *p* values, which are determined through 1000 random permutations of the network. Volcano plots of the 'swing' scores for each agonist, which represent the predicted kinase activity, were constructed.

TMT data analysis

Data transformation

For this analysis, the starting data were the raw intensities, without any normalization to the reference channel. Thus, the 'protein.tsv' output tables from

Philosopher, one per experiment / run (three in total), were merged to have a single dataset. Intensities were log2-transformed, 0 were converted to NAs, and common platelet contaminants (namely immunoglobulins, transthyretin, hemoglobins, band 3 protein, spectrins, and carbonic anhydrases), were removed. A subsequent filtering step was conducted, where both only-identified proteins, and proteins with only 20% of observed values, across all experiments, were dropped. The resulting data matrix was quantile normalized, and imputed. To avoid introducing artifacts that may alter downstream analysis, non-ignorable missing data (*i.e.*, proteins that are absent in all samples of the same experiment, but observed in the other batches) were not imputed in that specific batch, while ignorable missing data were imputed, by means of multivariate imputation by chained equations algorithm, using the 'mice' R package[222], with the following input parameters: m = 5 (number of imputed data sets), method = 'pmm' (predictive mean matching), maxit = 0 (number of iterations), and a group argument stating the grouping variable (imputation by condition).

Univariate mixed-effects selection model

To analyze labeled proteomics data presenting with non-ignorable missing values, severe batch effects caused by the batch processing of samples, and presence of a reference sample, a univariate mixed-effects selection model was implemented. Listwise deletion of missing values would dramatically reduce the number of proteins, especially in platelet proteomics where the number is already low. Therefore, an alternative approach is necessary, which still takes into consideration the batch-processing design and uses the reference channel. This model was developed by Chen *et al*. (2017b)[237] and Wang *et al*. (2018)[238], and was implemented in the mvMISE R package. For it to work, proteins have to be observed in more than one batch/experiment, and even if that protein is partially observed within the run, the reference channel has to be present (which is taken care of by the imputation step). Thus, the model is computed for each individual protein using the 'mvMISE_b' function, in a recursive manner, and

where the first sample of each experiment corresponds to the reference sample. The covariate matrix is composed of an intercept, followed by indicators for both the reference sample, and the groups that are going to be compared against the control, in that order. Additionally, batch identifications for each sample have to be provided, and the 'sigma_diff' argument has to be TRUE, to indicate that the error variance of the first sample (reference sample) in each batch is different from the rest. The resulting *p* values have to undergo an extra correction step, to account for the multiple testing, using the Benjamini & Hochberg adjustment method.

Batch-correcting normalization between runs

For fold change calculation and plotting purposes, since the model does not output this information, the raw intensity values of the proteins fed to the model were normalized to correct the batch effect of the different runs, ignoring the missing values. For this, an initial sample loading (SL) normalization followed by an internal reference scaling (IRS) were performed[239]. SL normalization consists of calculating how much the sum of each channel deviates from the total average, and using the resulting factor (ratio) to scale each column accordingly. Likewise, the IRS normalization calculates the geometric average intensity for each protein, across all reference channels, and then computes how much each protein deviates from it, to yield a factor per reference channel and experiment, which will be used to scale each channel of the respective experiment. This strategy did not fully correct the batch effect between runs, so the IRS was substituted by submitting the SL-normalized, log2-transformed intensities to the removeBatchEffect function from the 'limma' package[171]. PCAs to check the clustering of samples after each normalization were performed with the PCA function from the FactoMineR R package[240]. Lastly, the fold change was calculated by averaging the protein log2-intensities per group, and then subtracting them from the control averages.

Enrichment analysis

The GO enrichment analysis was performed as stipulated in the previous phosphoproteomics section, using the ‘enrighGO’ function from the clusterProfiler R package[219], and interrogating the three orthogonal ontologies. For enrichment of all up-regulated proteins, the proteins fed to the model were set as background; while for the rest, the default was used.

Results

Chapter I – Platelet proteomics to understand the pathophysiology of immune thrombocytopenia: Studies in mouse models

Primary immune thrombocytopenia (ITP) is an acquired autoimmune condition characterized by low platelet counts (<100 x 10^9/L). The causes behind its onset and progression are not yet fully understood, although it is acknowledged that a dysregulated immune response is a critical aspect of ITP pathophysiology[241]. The generation of autoantibodies targeting platelet receptors and the presence of cytotoxic T cells translates into platelet destruction and impaired platelet production[242]. The management of ITP patients comprises a number of treatment lines (immunosuppressants, Thrombopoietin receptor agonists [TPO-RA's] and splenectomy), which are indicated in a trial-error manner, alone or combined[243]. A deeper insight into the disease at the molecular level may aid in developing better, personalized treatment regimes[244,245].

Here, we characterize the platelet proteome in two different ITP (passive and active) mouse models at the thrombocytopenic stage and upon platelet count recovery (reached naturally or upon IVIg-treatment, depending on the model). These two models could phenocopy, as we propose, the acute/newly-diagnosed and persistent/chronic stages of ITP in human, respectively[246]. Our results support the notion that the platelet proteome may be used to clearly distinguish ITP models and thrombocytopenic stages, and suggest that the alterations observed in the ITP platelet proteome might reflect potential fine-tuning of megakaryopoiesis and/or platelet priming in the circulation. Furthermore, the potential associated cellular processes affected in each ITP model are discussed.

Proteomics exploration of the two murine proteomes

We obtained the platelet proteome from two ITP mouse models at the thrombocytopenic and recovered platelet count states to identify distinct protein signatures and dynamics in each model (Figure 1A). We excluded samples with > 35% missing values, as quality control[247]. Interestingly, ITP samples had more missing values, which could be considered as an ITP-specific trait (Figure S1A and Table S1). Principal Component Analysis (PCA) of the proteomes after data adjustment (Figure S1B), separated samples according to disease status (thrombocytopenia or recovery; PC1), and showed that day 3 and 7 controls (C D3 and C D7) clustered together, along with D7 passive ITP (P-ITP D7, recovered) samples (Figure 1B). Therefore, we joined C D3 and C D7 samples as healthy platelet control proteome for further analyses. Thrombocytopenic ITP samples (P-ITP D3 and A-ITP) separated from the rest (PC1), while the A-ITP IVIg samples positioned closer, but not overlapping, to controls or P-ITP D7 samples, suggesting that a normal platelet count may not necessarily reflect a complete proteome restoration after ITP induction (at the time points of study and in the active model). PC2 distinguished both ITP models at the thrombocytopenic state, showing that there are model-specific differences.

Weighted gene correlation analysis to study protein dynamics

From the identified 1866 proteins, 544 were differentially expressed (DEPs) across all comparisons (Table S2). Weighted gene correlation analysis (WGCNA) of DE proteins after dynamic tree cutting identified 10 co-expression clusters, which were reduced to 7 modules after cluster merging (Figure S1C). Cluster profiling of each module showed different dynamics across groups (Figure 1C). The grey module (not depicted) comprises proteins that do not cluster to any other module. Sample clustering in the heatmap of the module eigenproteins (Figure 1D) followed the PCA clustering (Figure 1B), where ITP samples at the thrombocytopenic state separate from controls

and platelet-count recovered respective samples, with the particularities mentioned above.

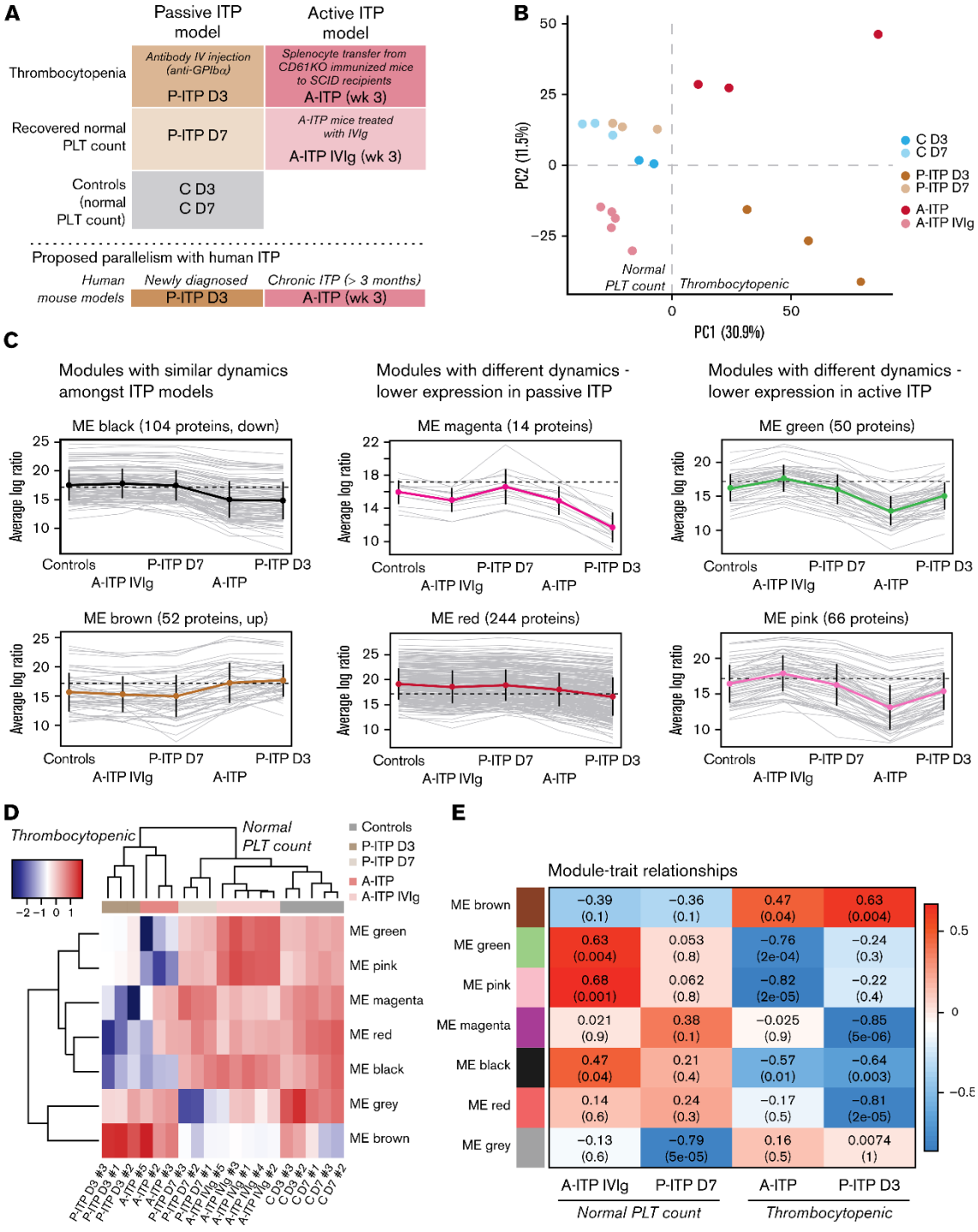

Figure 1. Experimental sample groups and proteome clustering. (A) Schematic representations of the preclinical mouse models of ITP and their respective study groups, and the proposed parallelism with human ITP. **(B)** PCA of the platelet proteomes (post-adjustment data) from both ITP models, at the thrombocytopenic and recovered normal platelet-count stage, and controls. **(C)** Cluster profile for each expression module, grouped by their common dynamics. Each gray line represents 1 protein, and the thick colored line represents the average for all. **(D)** Eigen protein heat map and dendrograms. Eigen proteins for each module

are calculated by singular value decomposition and can be seen as linear combinations of the actual module proteins. **(E)** Heat map showing the correlation between modules and each of the groups (except the control), where red and blue represent high and low correlations, respectively. Each cell is composed of the correlation coefficient and, in brackets, the corresponding P value. A-ITP samples shared the same most significant modules, green and pink, but in opposite directions, pointing to a recovery of the phenotype via IVIg treatment. In addition, both ITP groups correlated with the black module, indicating a potential global ITP signature. Distinctively, the P-ITP D3 group correlated with the magenta and red modules, and to a lesser extent, with the brown module. Last, the P-ITP D7 group was associated only with the gray module, which comprises the set of proteins that have not been clustered in any module. SCID, severe combined immunodeficiency.

The A-ITP IVIg samples, albeit closer to the control samples, have their own unique profile, pointing towards a partial recovery (or a persistent phenotype) of the platelet proteome after IVIg treatment. Furthermore, it showed that the ITP models possess common dynamics between them (black and brown modules), aside from their inherent, model-specific ones (green, pink, magenta and red) (Table S3). These results were substantiated with module-trait correlation analyses performed against the control group (Figure 1E).

Functional and pathway enrichment analyses were performed module- and model-wise (shown in Figures S2-3, and Table S4). Common to both models of ITP, the black module represented downregulated proteins, involved in receptor signaling (Itgb1, Itgb3, Gp1ba, Gp1bb, Gp9, Clec1b, Lyn, Src, Rac1, Rap1a/b)[54], metabolism (Ndufs, Acads, Aldh2, Ak3)[51,248], and exo/endocytosis (Vamp3, Vps37b, Stx11/12, Snap23)[249]. Upregulated proteins (brown module) were structural proteins, proteases (Serpins)[250] or immunomodulators (Orm1, C1ra)[251,252]. It appears as if ITP platelets in general lose protein content through basal degranulation or vesiculation, and upregulated proteins are those of the structural components. Of note, upregulated proteins included Histones, which could derive (potentially) from neutrophil extracellular traps (NETs), or from megakaryocytes[253,254].

Proteins linked to a more severe downregulation in P-ITP D3 samples (red and magenta modules) indicate significant dysfunction in the cytoskeleton compartment

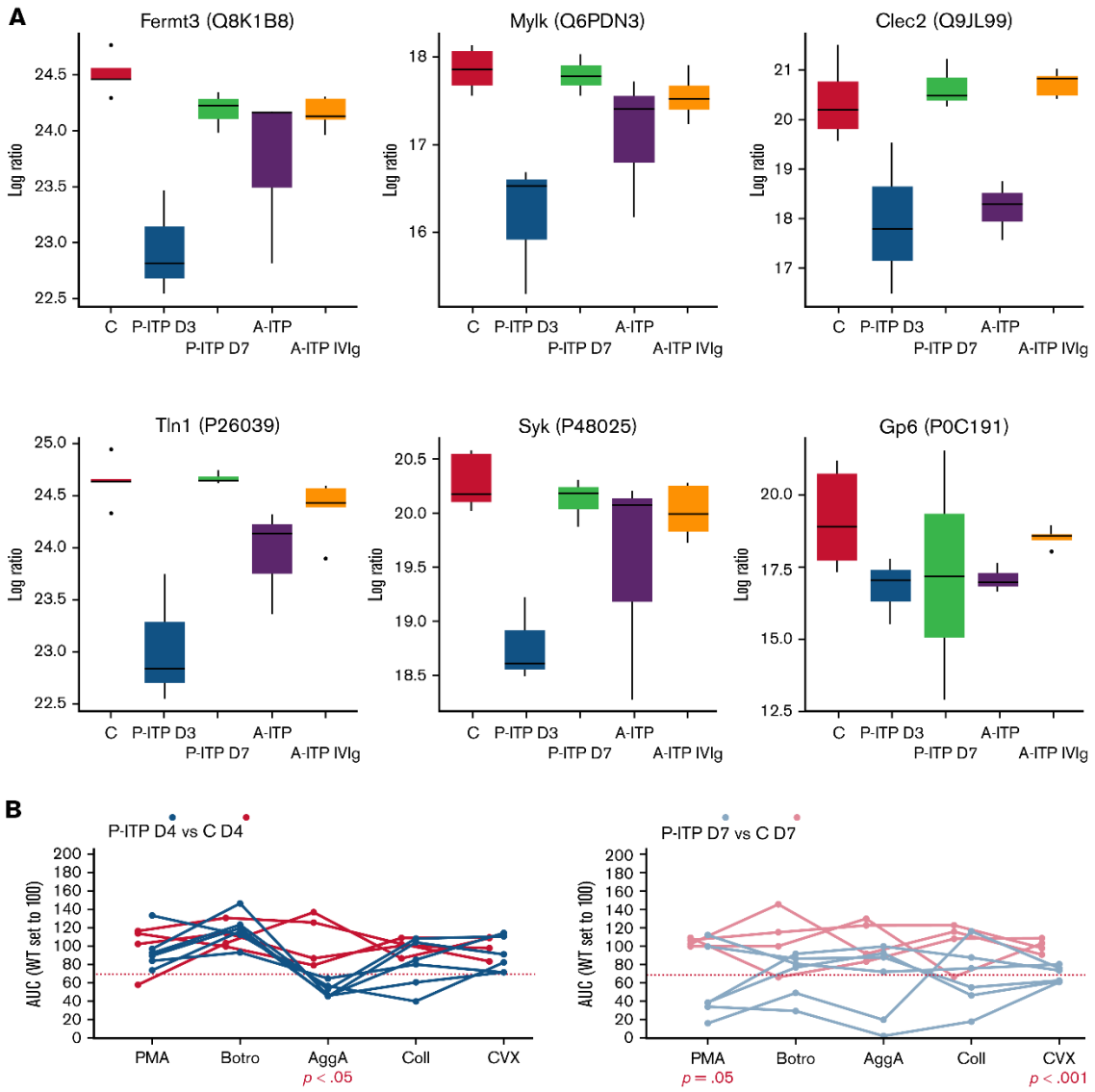

Figure 2. ITP affects specific platelet signaling pathways: proteomics and functional evidence. (A) Protein expression across ITP preclinical models of selected proteins and key players in hem-ITAM receptor (Gp6 and Clec2) signaling are represented. **(B)** Flow cytometry–based platelet aggregation assays were performed with platelets of the P-ITP model and respective controls at days 4 and 7 after platelet depletion. Studied single receptors by using the following agonists: PMA, botrocetin (Botro); aggretin A (AggA); collagen (Coll); convulxin (CVX). The area under the curve of each aggregation reaction was calculated and plotted after the average in control mice was set to 100, for each condition. The values obtained from platelets from the same mouse are joined by lines. At D4, P-ITP platelets had a homogeneous platelet aggregation profile, characterized by impairment toward AggA stimulation. At day 7, platelets from most of the mice showed a normal platelet aggregation profile, although not all mice had fully recovered platelets at that time point.

(Actb, Myh9, Capza's, Tubb's)[255], general metabolism (Pdi's, Alox12)[256,257], degranulation (PF4, Mmrn1, Emilin1, Nbeal2, vWF)[258], and integrin signaling (Itga2b, Fermt3, Tln1, Mylk; see also Figure 2A)[64]. While these proteins are also downregulated

in the A-ITP samples, they are markedly affected in the P-ITP D3 samples, suggesting that in chronic ITP there may be an accommodation or adaptation of the platelet phenotype as disease progresses. These results suggest that the level of hyporesponsiveness due to platelet pre-activation might be superior in P-ITP D3 platelets than on those form A-ITP mice.

Proteins linked to a more severe downregulation in A-ITP samples (green and pink modules) showed a strong association with mitochondrial metabolism, impaired in the case of the A-ITP group, but recovered (partially) upon IVIg-treatment. The reduced levels of mitochondrial electron transport chain enzymes may induce overproduction of reactive oxygen species (although there are no evident signs of platelet damage or apoptosis) compromising platelet ATP synthesis[51], resulting in dysfunctional platelet activation. On the other hand, we cannot discard platelet mitochondria release, which has been reported as a bactericidal tool[248]. Furthermore, strong downregulation of key proteins in the lineage, such as Pear1, Pecam1 or Stim1,[54,259,260] appear unique to the "chronic" ITP state.

Furthermore, we performed platelet functional studies in P-ITP mice, which allow a better monitorization of the timing of platelet count recovery and measured the platelet aggregation capacity towards 5 different agonists at D4 and D7 after platelet depletion. Interestingly, results revealed a marked defect in the aggregation response upon Aggretin A stimulation (Clec2-mediated) in P-ITP D4 samples (Figure 2B) which was largely recovered in P-ITP D7 samples. These results are supported by the proteomics dynamics observed, as key players in the Clec2-mediated platelet aggregation, including Clec2 itself, are downregulated at D3 and recovered in P-ITP D7 platelets (Figure 2A). Of note, not all P-ITP D7 mice displayed a balanced platelet aggregation profile at that time point, suggesting that a longer period might be required for full recovery of platelet function (Figure 2B), and that can be seen by the variation in the expression levels of other proteins such as the other immunoreceptor tyrosine-based activation motif (ITAM)

receptor, Gp6, which may affect responses towards other agonists such as collagen or convulxin.

In summary, in this Chapter, our results showed that the platelet proteome was able to differentiate between health and ITP states, and even between ITP subtypes (active and passive), and after phenotype rescuing by IVIg treatment. Furthermore, it displayed a common ITP signature that pointed to the existence of an hyperresponsive state in these platelets, as well as a mitochondrial dysfunction exclusive to the active model. Additionally, functional aggregation assays in the passive model showed a defect on the signaling pathway triggered by the Clec2 receptor. In light of these results, next we wondered if the platelet proteomics results obtained in murine models could be extrapolated to humans.

Chapter II – Proteomics-wise, how similar are mouse and human platelets?

The use of mice as pre-clinical models

In spite of the fact that there are obvious differences between mice and humans, the use of the former as preclinical models is sufficiently justified by the conservation of physiological, anatomic, and genetic features[261]. Needless to say, preclinical models have provided essential knowledge and facilitated various clinical applications that range from surgery and vaccine development, to diagnosis and treatment of disease, amongst others. However, there are social, scientific and ethical concerns regarding their usage[262]. The detailed knowledge acquired so far from interspecies studies, makes it clear that conclusions drawn from animal studies cannot be carelessly transferred to human. Still, some studies require a living organism, which allows observation and experimental manipulation, in order to answer biological questions where multiple tissues or systems contribute in health and disease. In parallel, *in vitro* tools with increasing levels of complexity *(i.e.*, human organoids) are being developed, which can potentially substitute many in vivo studies[263]. All in all, many variables have to be pondered before engaging in animal studies, and always bearing in mind that, ultimately, the experimental option has to translate into a benefit for human clinical research.

While differences in the platelet formation process between mouse and human have been identified, their genetic similarity to humans and our ability to genetically/physiologically modify them, have positioned mice as a suitable model for studying human megakaryopoiesis, thrombopoiesis, and platelet function[261,264]. For example, murine preclinical models have been essential to demonstrate the function of various proteins *(i.e.*, transcription factors, receptors, signaling molecules, or hormones, among others) in megakaryopoiesis and hemostasis, and have aided to better understand the process of megakaryocyte differentiation[265,266]. However, whenever a murine preclinical model is used with the intention to extrapolate results into human,

either when studying normal physiological processes or when phenocopying a human disease or pathology, it is important to be aware of the differences and similitudes.

Key features of megakaryopoiesis and platelets in mice and humans

In the last stages of megakaryopoiesis, bone marrow-resident megakaryocytes release platelets into the blood circulation through a process of cell-remodeling[267], which appears to be conserved between mice and humans, with some species-specific particularities. While human megakaryocytes are chiefly located within the bone marrow, murine megakaryocytes are also present in clusters in the red pulp of the spleen, at least in the normal adult state[264]. Furthermore, murine and human megakaryocytes have also been observed within the lungs and pulmonary circulation, where they may contribute to platelet production[34,264]. In addition, murine and human megakaryocytes display similar ploidy distribution (modal ploidy of 16N), their density within the bone marrow is greater in mice than in humans, while the size of mature megakaryocytes appears to be significantly smaller in mice[268]. Proplatelets are formed in megakaryocytes from both species, however, human megakaryocyte proplatelets have been described as “long strands with regular constrictions (collar of pearls)”, while murine megakaryocyte proplatelets are shorter and interconnected with other proplatelets[264].

Mice have approximately five times more platelets in the circulation compared to humans, although murine platelets are overall smaller. Their lifespan is also shorter, around 4 days, while human platelets remain in the circulation for 8- to 12-days; the faster turnover is probably counterbalanced in mice by a constant splenic platelet production[264,266]. Schmitt *et al*. (2007) reported that murine platelets have an increased granule heterogeneity, although reduced in number per platelet section, and it seems this heterogeneity affects specially the α-granules, as dense granules are quite similar morphologically between the two species[264].

Evolutionary aspects and platelet function

Aside from the classical role that platelets play in maintaining hemostasis, the ancestral immune function of thrombocytes has not been lost through evolution, as they participate in immunomodulation and inflammation, in the separation of blood and lymphatic vessels during ontogeny, and are also active players on pathogenic processes such as thrombo-inflammation or cancer metastasis (see Introduction).

Polyploid megakaryocytes and enucleated platelets are only found in mammals (placentals, marsupials and monotremes)[269]. It seems that these acquired characteristics have resulted from the necessity to enhance the hemostatic function of platelets in detriment of their prominent immune ancestral role in other vertebrates. The fact that in mice platelets are more numerous, smaller and with a shorter lifespan, might be to cover a greater demand to protect against injury, which implies faster and more efficient clotting reactions, while facilitating, at the same time, the clearance of potential circulating pathogens.

Many other differences have already been put forward between mouse and human platelets, such as the absence of FCγRIIA[270] and PAR1[271] in mouse. Additionally, several studies with Eltrombopag, a non-competitive agonist of TPO, found that the juxtamembrane domain of MPL (at residue H499) is not conserved in mice, which means that it is specific to humans and nonhuman primates[272]. In this context, studies with Eltrombopag may seem intuitively useless in mice, however, this particular feature is the basis for the rationale to use mouse models to study MPL-independent mechanisms, which seem to play a role in the recovery of immune thrombocytopenia patients treated with this drug. Another example of interspecies differences is the case of the protein kinase C (PKC) isoforms, PKCδ and PKCε, whose expression levels display an opposite balance between mouse and human platelets, with PKCδ being highly expressed in human platelets, while in murine platelets it is PKCε the one expressed at higher levels[273]. However, the kinase universe of platelets is so promiscuous (or pleiotropic) that

these differences do not seem to make a difference in the functional capacities between murine and human platelets.

An interspecies proteomics overview of platelets

Given the plethora of functions in which platelets are involved, in addition to the fact that they are produced differently or altered somehow by the health status[108,274], that they even uptake molecules from neighboring cells, and release microvesicles in the circulation, they constitute biosensors worth exploring and delineating[275,276]. Proteomics stands as a one of the most interesting tools to study platelets, due to their inherent characteristics (*i.e.*, absence of a nucleus). This tool might be used to understand disease, and to identify biomarkers for prognosis and diagnosis of pathologies of different etiology[277,278]. In this regard, if we employ mice as preclinical models, how similar are they, proteomic-wise? Do we have a basis to claim that they represent a good model?

The platelet and megakaryocyte proteome

The comparison of the mouse and human genomes at the sequence level has revealed that, albeit harboring striking differences, especially in non-coding regions, the protein-coding regions are evolutionary conserved, with approximately an 85% overlap in identity, on average[279], driven by physiological function requirements. In order to obtain a comprehensive comparison of the platelet proteome between species, we have selected different publicly available proteomics datasets, as described in the Experimental and Bioinformatics Procedures, and Tables S1-2.

The core platelet proteome in each species –that is, the subset of platelet proteins detected in at least half of the datasets included in this review (see Tables S1-2 and Figure S1A)– represents about 10% of the respective species reference proteome (Figure 1A). Additionally, the comparison after bidirectional orthologue translation of the core platelet proteome protein lists, confirms an overlap of approximately 85% of the identified proteins (Figure 1B). This is a very important aspect to consider, since the bidirectional orthologue translation of the reference proteome between species is 70-

80% (Figure 1B), suggesting a strong function-driven evolutionary conservation in the protein content of platelets of both species.

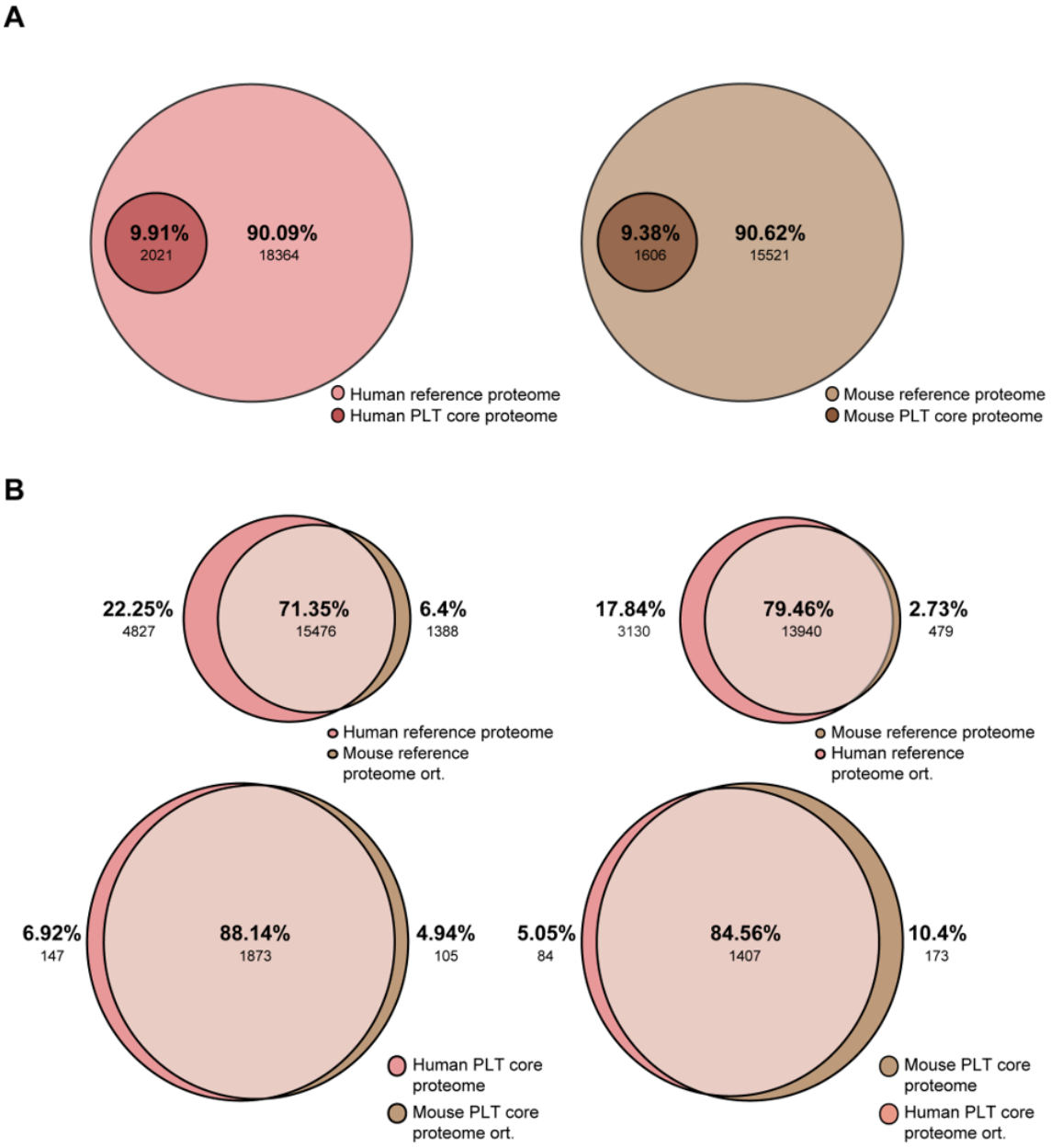

Figure 1. Interspecies comparison of the human and mouse reference and platelet core proteomes. **(A)** Venn diagrams showing the overlap between the human (left) and mouse (right) reference proteomes, and the respective platelet core proteome. **(B)** Venn diagrams showing the overlap between the reference proteomes or the platelet core proteomes, of mouse and human (top left and right, and bottom left and right, respectively), and their respective mouse and human orthologs. PLT: platelet.

We next compared the relative quantification distribution of the identified proteins in platelets from the respective mouse and human chosen datasets, as indicated in the Experimental and Bioinformatics Procedures. We could observe a high overlap of the

highly and intermediately expressed proteins between species, while low abundant proteins differed more, suggesting that they either do not have an essential role in platelet function (*i.e.*, residual proteins, plasma/erythrocyte contamination), that they are different components of unitary functional protein-complexes (*i.e.*, redundancy), and/or that the heterogeneity is subject to technical limitations in the detection, due to their low abundance expression or other protein-specific constraints[277] (Figures S2-S3). Enrichment analysis of the protein lists based on abundance (*i.e.*, per expression slot), further supported these results, confirming conservation of function between species (Figures S2-S3). According to this, we can suggest that human and mouse platelets share a highly conserved proteome, considering identified proteins, and most importantly, their relative abundance.

These conclusions are parallel to those extrapolated from the isolated comparison of the mouse and human platelet transcriptomes[212]. Therefore, we next set out to determine the mirroring level of the platelet transcriptome and proteome, species-wise. Both species showed a similar overlap, around 18% (suggesting that the majority of platelet RNA is either inherited residual RNA or exogenous), which constitutes 85% and 75% of the human and mouse core proteome, respectively (Figure 2A). However, they both showed a weak correlation (R ~ 0.4) in terms of relative abundance (Figure 2B), in accordance with what has been published[280], and supporting the idea of a desynchronized protein and RNA homeostasis in platelets. Still, a multi-Omics approach (proteomics, transcriptomics) in the study of platelets and their megakaryocytic progenitors may be determinant, especially considering that platelets contain exogenous proteins, as mentioned above. Studies that intended to identify the transcription origin of identified platelet proteins, have included megakaryocyte transcriptomics in their

experimental design, proving the reliability of the multi-Omics approach in this regard[164,281].

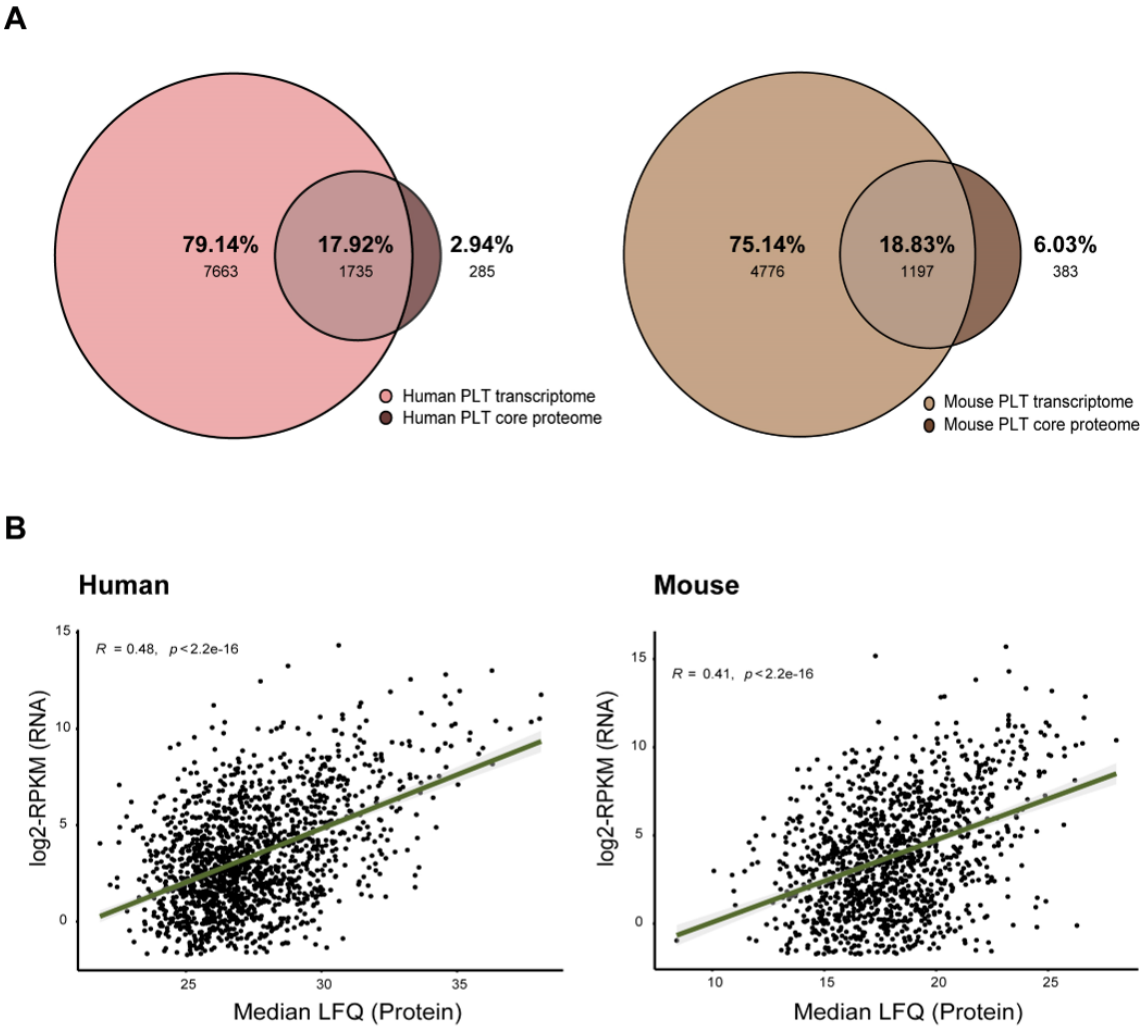

Figure 2. Interspecies comparison of the human and mouse platelet core proteomes and transcriptomes. (A) Venn diagrams showing the overlap between the human (left) and mouse (right) transcriptome and platelet core proteome. **(B)** Scatterplot showing the Pearson correlation between the relative transcriptomics (log2-RPKM) and proteomics (log2-LFQ) abundances both in human (left) and in mouse (right). The proteomics data belong to the x11 and x39 datasets (as in Tables S1-2), respectively. PLT: platelet, RPKM: reads per kilobase million.

Literature search regarding the megakaryocyte proteome showed that it is scarcely studied from an unbiased perspective, and a characterization of both mouse and human primary megakaryocytes is lacking. A study focusing on mouse megakaryocytes, aimed at comparing the total proteome of embryonic stem cell-derived and fetal liver megakaryocytes[282]. As for the human studies, one of them aimed at identifying the proteome of megakaryocytes differentiated from induced pluripotent stem

cells (iPSCs)[283], while the other was performed on megakaryocytes differentiated from the DAMI cell line[230]. Additionally, no raw data was available from any of the mentioned studies. This points towards the difficulty of working with primary megakaryocytes, due to its low abundance in peripheral blood and *in vitro*, its asynchrony when differentiated from progenitor cells, and the issues regarding their isolation (*i.e.*, flow cytometry cell-sorting), evidencing that the application of proteomics to the megakaryocyte compartment has a promising but long journey ahead[221,284,285].

The platelet secretome

Since platelets secrete their granule cargo upon activation, a process highly relevant in their hemostatic and non-hemostatic functions, we set out to compare the proteomic profile of platelet secretomes of mouse and human from publicly available datasets (see Tables S1-2 and Figure S1B). Of these, all save one were using thrombin as the stimulating agonist. The secretome constitutes around 20% of the core platelet proteome both in mouse and human (Figure 3A). Of note, the platelet secretome proteins that do not overlap with the respective core platelet proteomes (Figure 3A) are detected as part of the platelet proteome, when all the proteins of all datasets are taken into consideration (data not shown). The overlap of the identified secretome proteins, in bidirectional orthologue translations, is around 75% (Figure 3B).

Following the same analysis performed with the platelet core proteome, we next compared the identified proteins in the platelet secretomes from mouse and human depending on their relative abundance, in the different datasets. We observed a great overlap of the highly and intermediately expressed proteins between species, while low abundant proteins showed more variation, similarly as with the platelet core proteome (Figure S4). However, the separation of the proteins that are present in the high and intermediate abundances slots did not appear as relevant, functionally, as with the platelet core proteome. Enrichment analysis of the protein lists further supported these results, confirming the conservation of function between species, and supporting the

notion that the high and intermediate abundance slots constitute a functional joint fraction (Figure S4).

Figure 3. Interspecies comparison of the human and mouse platelet core proteomes and secretomes. **(A)** Venn diagrams showing the overlap between the human (left) and mouse (right) platelet core proteomes, and their respective platelet secretomes. **(B)** Venn diagrams showing the overlap between the platelet human (left) and mouse (right) secretomes, and their respective mouse and human orthologs. PLT: platelet.

In summary, in this Chapter, and using publicly available platelet proteomics datasets, our results showed a high agreement between the murine and human whole platelet proteomes and secretomes, which was especially evident when it came to the most abundant proteins. Notably, this occurred in spite of the different sample preparation and bioinformatics workflows employed. Given the utility of proteomics to study the platelet proteome and sub-proteomes, and the fact that can be extrapolated

across species, we then set out to compare two of the most used, publicly available software tools to analyze these type of data (namely, MaxQuant and FragPipe). Additionally, and using both proteomics and cell biology tools, we performed a thorough characterization of platelets in health.

Chapter III – Multilayered proteomics picture of quiescent and activated platelets in health

Comparison of freely available proteomics analysis tools

Proteomics is becoming a widely used tool to interrogate the platelet proteome and sub-proteomes, both in health and disease. However, there is still little consensus regarding the many aspects of the sample collection and preparation, and subsequent bioinformatics analysis. Concerning the latter, within the available open-source software for the identification and quantification of the proteins of a sample, from the raw spectra yielded by a mass spectrometer, MaxQuant (and thus its search engine, Andromeda) is one of the most stablished ones[166,168]. FragPipe's MSFragger[226], on the other hand, is relatively new in comparison, but it is increasingly being used. Using our own data, we set out to benchmarking each of them, in terms of their protein identification performance, and coverage.

Additionally, in this Chapter, we characterized platelets from healthy donors in depth, making special emphasis on the utility of proteomics to map the whole platelet proteome, as well as the complex signaling dynamics that occurs during platelet activation and posterior protein release. Hence, by using a wide range of techniques, we pursued the profiling of the different layers that compose the platelet phenotype, regarding both the composition and stability of their proteome, and their functionality. We were particularly interested in studying the response of platelets after single stimulation of a selection of their receptors, under equal experimental conditions, since most studies so far have primarily focused on the characterization of the signaling after activation of the ITAM receptors. Here, we targeted hemostatic and non-hemostatic receptors, including non-ITAM receptors, with different agonists (see Figure 6 of the Introduction), namely: GPVI, with convulxin (CVX); CLEC2, with aggretin A (AggA); vWF receptor GPIb-V-IX, with ristocetin; PAR1, with thrombin receptor-activating peptide-6 (TRAP6); integrin $\alpha_{II}\beta_1$, with low-dose collagen; and integrin $\alpha_{IIb}\beta_3$, with phorbol 12-myristate 13-

acetate (PMA), although PMA is also able to elicit platelet activation without stimulating the integrin, but rather diffusing through the membrane and interacting with the PKC kinase directly.

Thus, on top of studying the overall aggregation and degranulation responses elicited after the triggering of each receptor, we delved in the different layers that compose two of the most important platelet sub-proteomes: the phosphoproteome, and the releasate or secretome. With this, we not only aimed at setting the basis on what to study later study the changes exerted by disease, but also further advancing and adding to the knowledge in relation to the different aspects of platelets. A more precise and deep understanding of the complex platelet activation signaling pathways, and the synergy between them, will helps us understand their significance in disease, and also develop new generations of drugs to treat them. After all, our understanding of the mechanisms of health and disease determines how precise medicine can be.

Comparison between FragPipe and MaxQuant for basic LFQ analysis

We carried out a comparison between the Andromeda (MaxQuant) and MSFragger (FragPipe) search engines, to elucidate which one was able to map and quantify a greater number of proteins with reliability. Therefore, both search engines were run with the same data and FASTA file, and keeping the engine parameters and computational requirements as similar to each other as possible (see Experimental and Bioinformatics Procedures).

Firstly, the same search took around 15 min to complete in FragPipe, while MaxQuant finished after 5 hours (run in the same computational environment, in terms of RAM memory and cores available). When comparing the actual data, it could be seen that FragPipe identified a higher number of proteins per sample, although at the same time, it presented with a higher number of missing values (Figure S1A). After a filtering step (as a rule of thumb, it was required that the protein was observed in at least half of

the samples), that difference in number was preserved. Furthermore, interrogation of the distribution of those missing values showed that it was similar between the two engines, and that FragPipe displayed a higher number of complete cases (*i.e.*, proteins observed across all samples) (Figure S1B-C). Regarding the percentage of coverage (percentage representing the number of amino acids of a protein that were identified), the median was higher for MaxQuant (16.4 vs 9.6 %) (Figure S1D). Additionally, the overlap between the two search engines in terms of protein identified and quantified was high (77 and 83%, for MaxQuant and FragPipe, respectively), with 1362 common proteins, which displayed a high intensity correlation (R = 0.87), except for three proteins, which belonged to the cytoskeleton (Figure S1E-F). Lastly, the proteins that were detected only with FragPipe showed a lower median log2-intensity (22.6) than that of the common proteins (26.6), which did not occur in the case of MaxQuant, pointing to the former being able to recover more proteins from the left tail of the intensity distribution. Thus, given all of the above, FragPipe was selected as the search engine of choice, when possible. The exception lied with the phosphoproteomics data, due to the fact that, to date, there is a higher availability of tools for MaxQuant data.

Describing the steady-state platelet proteome

MS analysis of FragPipe output data resulted, then, in the identification of 2478 proteins, with a median of 32% of missing values across samples. After removing contaminants and dropping those proteins identified in less than 50% of the samples, the resulting 1758 proteins were explored to decipher the qualitative and quantitative characteristics of the platelet proteome of this cohort of healthy donors. Correlation analysis of the ten samples indicated a very high agreement between them (median R ~ 0.935) (Figure S2A). In addition, plotting of the mean intensities against the ranked abundance displayed a span of intensities that ranged across several orders of magnitude. Highly abundant proteins comprised members of the cytoskeleton (ACTB, TLN1), along with other proteins that present with a high copy number on platelets

(THBS1, PPBP, FERMT3, ITGB3, PF4); while in the mid-range, there were kinases essential for platelet signaling (SYK, MYLK, PRKG1) and several surface receptors (GPVI, CLEC2). In the lower range of detection, there were proteins similar in function (AKT1-2, FYN, PRKCA), among others with high variability (Figure S2B). Furthermore, interrogation of the variability of protein quantifications by means of the coefficient of variation (CV) showed that, although it inversely correlated with the protein intensity (*i.e.*, higher CV in low-abundance proteins), the highest CV did not reach 20%, and almost all of them could be found under 10% (median CV ~3%) (Figure S2C). In line with this, the most variable proteins, were also those who were partially detected (*i.e.*, proteins that were not quantified in one or more samples), and presented with a median log2-intensity significantly lower than those proteins that were reliably quantified in all samples (Figure S2D). Further GO enrichment confirmed the nature of the protein profile, with two distinct clusters related to platelet and mitochondrial functions, especially in the biological process ontology, as well as terms related the cytoskeleton, in the cellular compartment ontology (Figure S2E).

The functional capabilities of healthy platelets

To study platelet aggregation, one of the endpoints of platelet activation, we performed a functional assay (an aggregation assay), by means of the platelet count drop method. In this assay, which was conducted in whole blood and thus recreating physiological conditions, the device measures the number of remaining platelets, at several time points, after agonist stimulation. This count negatively correlates with the magnitude of the response, where an aggregation rate of a 100% means that all platelets in the sample have aggregated. In addition, it makes it possible to calculate the area under the curve (AUC), a measurement that allows the study of the dynamics of the aggregation response. That is, with this assay not only can the maximum aggregation rate (MAR) be calculated, to study how much platelets aggregate; but also, with the AUC,

the relative speed at which those platelets reached that MAR (*i.e.*, if a delayed response took place, or the opposite) can also be studied.

Thus, study of the platelet aggregation in a group of healthy donors revealed a high inter-individual variability in the dynamics of the responses triggered by the agonists ristocetin, collagen and AggA, although it was rather consistent in terms of the MAR, where the responses were almost comparable to those of the other agonists (Figure 1A). That is, even if these three agonists elicited responses at different speeds, most of said responses reached roughly the same percentage aggregation. On the other hand, CVX, PMA and TRAP6 presented with very fast, reproducible responses at all time points, both in terms of the AUC and MAR (Figure 1B). Lastly, within the unstimulated condition that served as internal control, it could be noticed that although all of them displayed low rates, as time passed, there was a tendency towards an increased aggregation. This was most likely due to the fact that, with less volume remaining, contacts among platelets increased, and thus some residual aggregation occurred.

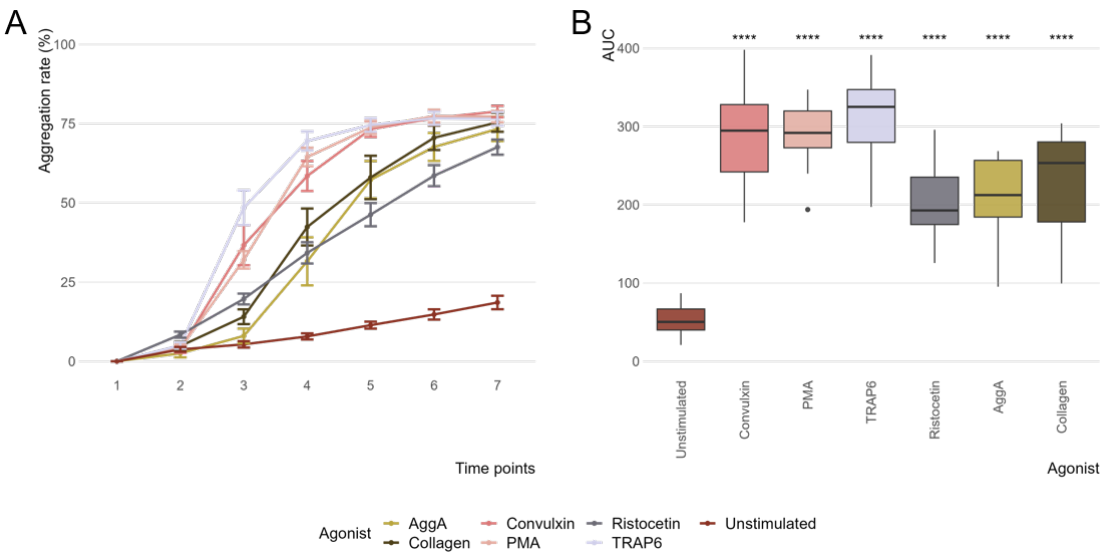

Figure 1. Aggregation assay in platelets of healthy donors. (A) Mean aggregation curves for each agonist. Error bars represent the standard error of the mean. **(B)** Boxplots representing the area under the curve (AUC) of each aggregation assay. Asterisks represent the *p* value (**** < 0.0001) after ANOVA, comparing against the unstimulated condition.

On the other hand, to characterize the extent of the degranulation response after stimulation with the same battery of agonists, a set of proteins that reflect that activation

were interrogated by flow cytometry: P-selectin (CD62p) and CD63, which are found in the membrane of alpha and dense granules; fibrinogen, which binds to the high affinity conformation of integrin $\alpha_{IIb}\beta_3$ in activated platelets; and annexin V, which attaches to phosphatidylserine (PS) after its translocation from the inner to the outer side of the plasma membrane, as a response to the activation (or the apoptosis) of platelets. The gating strategy consisted of selecting the $CD9^+$ population, and then extracting the mean fluorescence intensities (MFIs) of the other markers (Figure 2A). In line with what was seen in the aggregation assay, CVX, PMA and TRAP6 elicited the most acute responses, in terms of both alpha and dense granule secretion, and fibrinogen binding. They were

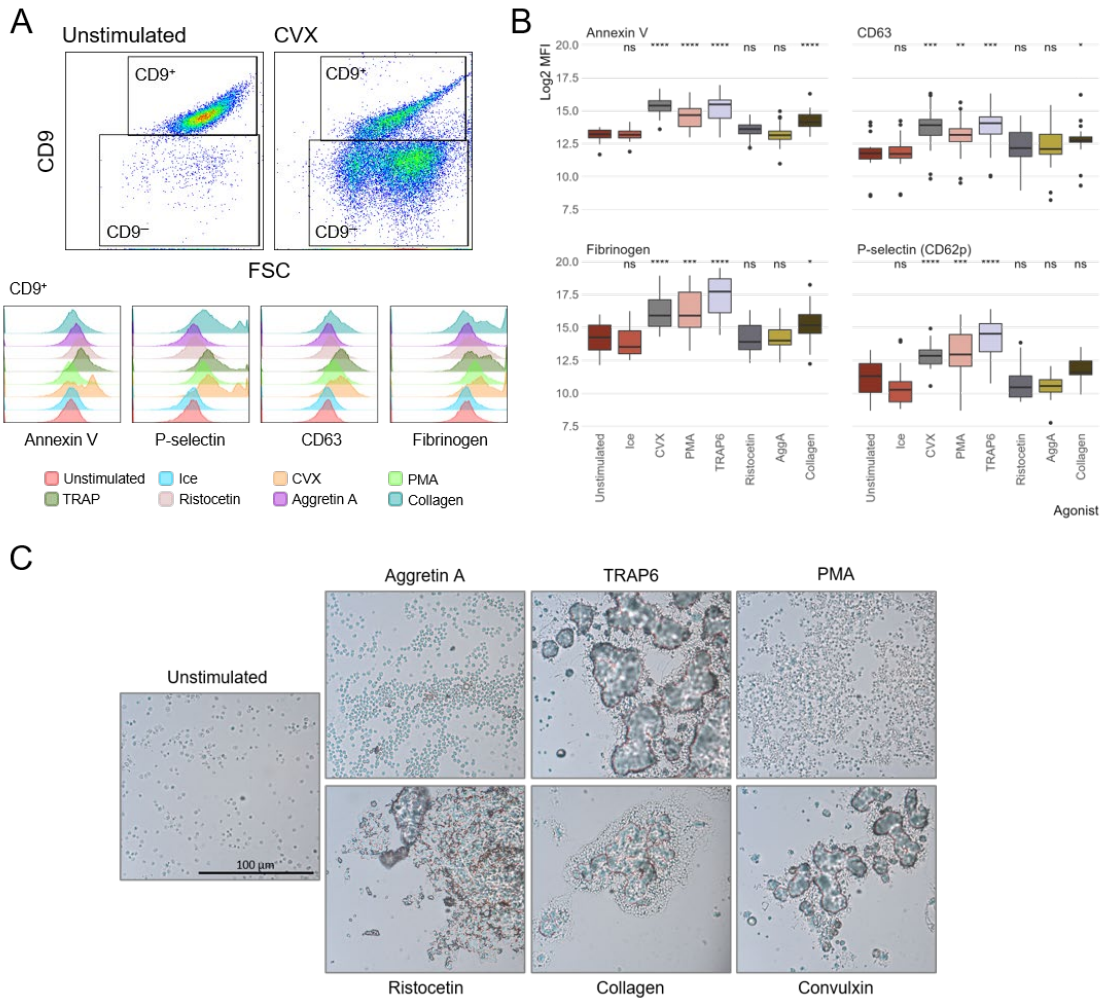

Figure 2. Degranulation assay in platelets of healthy donors. (A) Top: Gating strategy to evaluate the degranulation response. As examples, the unstimulated and convulxin (CVX) conditions of one of the donors are shown. Bottom: modal histograms of the $CD9^+$ populations for each marker and agonist. **(B)** Boxplots representing the log2-transformed mean fluorescence intensities (MFI) for each marker (parent gate $CD9^+$) and agonist. Asterisks represent the *p* value (**** < 0.0001) after ANOVA, comparing against the unstimulated condition. **(C)** Microscopy images taken from cytospin preparations of platelets after the degranulation assay, for each agonist. Scale bar: 100 µm.

followed by collagen, although in all cases the degranulation was milder, as if the stimulation was not firing the same number of receptors. Interestingly, AggA and ristocetin bore a closer resemblance to the unstimulated condition, although both seemed to display a preference towards dense granule and lysosome exocytosis (Figure 2B). Light microscopy images of cytospin preparations of the activated platelets revealed that there was indeed aggregation in all cases, although in varying degrees, mirroring the count drop assay (Figure 2C). Furthermore, and consistent with what has already been described, ristocetin triggers platelet agglutination rather than aggregation.

All in all, CVX, PMA and TRAP6 elicited very rapid, drastic aggregation and degranulation responses in our conditions, most likely due to the synergy and positive feedback triggered by the release of second mediators, which further amplified the platelet activation response. On the other hand, AggA, ristocetin and low-dose collagen triggered more variable, muffled responses, especially when degranulating; although they still managed to reach an optimal aggregation rate, comparable to the other three agonists.

Phosphoproteomics analysis of single stimulation of platelet receptors

Based on the degranulation responses analyzed in the previous section, we selected three donors with optimal platelet activation to further study the platelet phosphoproteome. Study of the post-translational modifications, more specifically phosphorylations, sheds light on the complex dynamics of protein kinases and phosphorylases, and therefore on the signaling pathways triggered after the stimulation of receptors. Thus, in this particular case, changes in the phosphorylation levels of differently-activated platelets relative to the unstimulated control were determined using a global quantitative phosphoproteomics workflow.

The phosphoproteomics data were processed and further interrogated using a robust bioinformatics approach, based on the existing literature. Thus, only high-

confidence phosphopeptides (class 1 sites, with probability ≥ 0.75) were used for downstream analyses. A total of 1657 unique phosphopeptides were quantified across all conditions from 706 proteins (no isoforms). Detection and quantification, both at the peptide and protein levels, was roughly the same across the three donors, and it was higher for PMA stimulation, followed closely by TRAP6; and lower for ristocetin and the unstimulated control (Figure S3A). Additionally, a strict filtering step was performed, in order to remove phosphopeptides that were identified but not quantified, and to keep those that were present in at least two of the three replicates of at least one of the groups. This resulted in 203 phosphopeptides and 71 corresponding proteins being dropped. Our statistical workflow involved further normalization and missing value imputation of the data. The percentage of missing values per sample ranged between 37% and 61%, so the fact that these high percentages had to be imputed was taken into account for the downstream analysis and interpretation of the data (Figure S3B). Unsupervised principal component analysis (PCA) of all phosphopeptides separated the different agonists in three clusters along the first three principal components, with ristocetin, ice and unstimulated samples clustering together, as CVX, AggA and TRAP6; and PMA distancing itself from the rest (Figure 3A). This further confirms what was seen with the functional assays, and thus the phosphorylation of peptides was largely occurring in an activation-grade-dependent manner.

Comparison of the phosphoproteome of all conditions against the unstimulated control, yielded a total of 899 significantly up- and down-regulated phosphopeptides, corresponding to 431 proteins. Significance was determined using a moderated t-statistic adjusted for multiple hypothesis testing, and thus an adjusted-*p* value < 0.05 was required as inclusion criteria. There were no differences between the ice and unstimulated conditions, while the PMA stimulation elicited the most dramatic activation of all agonists. The rest of the conditions displayed a gradual perturbation, resembling the cluster disposition showed with the PCA. Additionally, as it could be expected, the

number of up-regulated phosphopeptides is higher in all conditions, except for the ristocetin agonist (Figure 3B). Ristocetin displayed the highest number of missing values, and thus was the most thoroughly imputed.

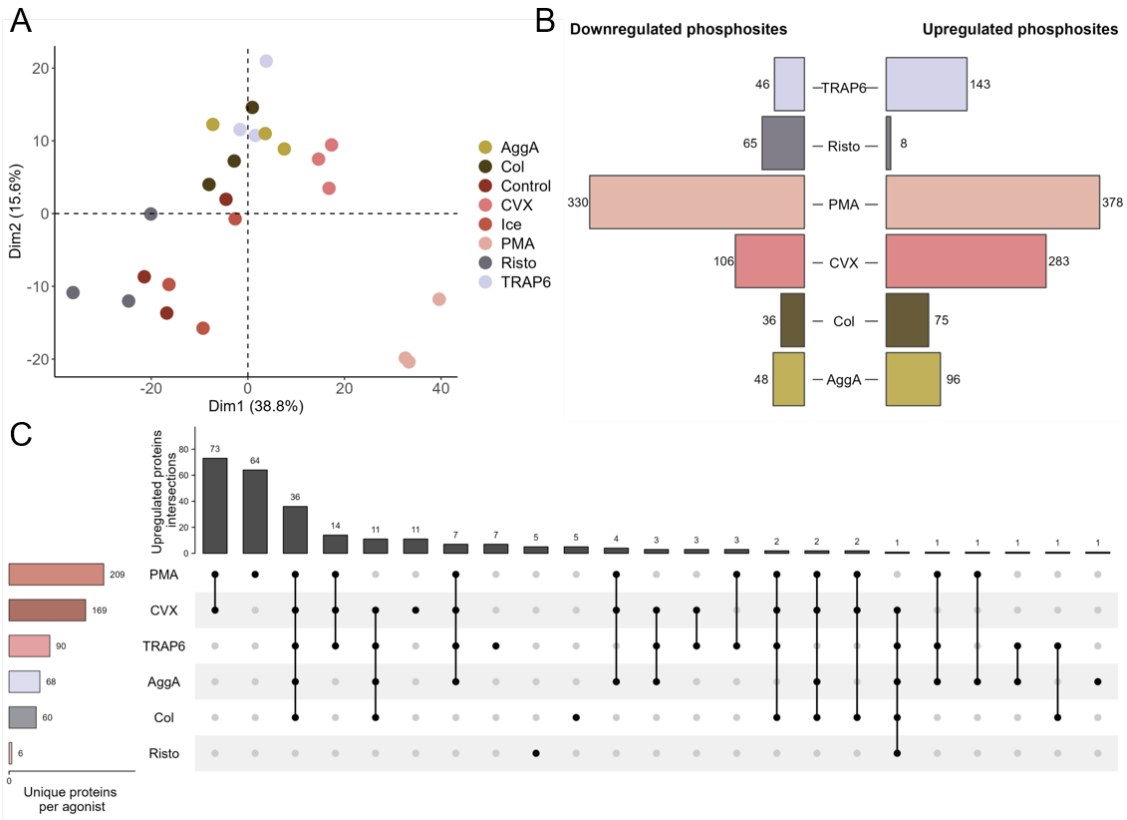

Figure 3. The different platelet agonists display a gradual activation size effect. (A) Principal component analysis (PCA) of the phosphorylation profiles of the different agonists. **(B)** Barplots showing the number of upregulated (right) and downregulated (left) phosphosites per agonist. **(C)** Upset plot of the overlapping upregulated phosphosites across agonists.

Interrogation of the protein overlap of the respective up-regulated phosphopeptides revealed a high agreement between the PMA and CVX conditions, followed by a cluster of proteins encompassing all agonists except for ristocetin (73 and 36 unique proteins, respectively, see Figure 3C). Pathway enrichment analysis of these proteins, followed by term clustering, showed PMA and CVX dominating most of the terms related to platelet activation (*i.e.*, RHO GTPase cycle, platelet degranulation, MAPK activation, integrin and other signaling pathways), there were a handful of them were TRAP6, collagen and AggA were more present, such as in ROCK and PAK kinase activation (Figure S4C).

All 899 phosphopeptides were search against three different post-translation modifications databases (namely PhosphoSitePlus[286], ELM[287] and UniProt[288]), and it was found that 87.7% - 83% - 37% of them, in respect to each database, had already been identified. Interestingly, only 9-13% of these sites have a known function or regulatory role. This indicates, firstly, a very low agreement between different databases as far as platelet proteins is concerned, and a very large gap in the knowledge of the signaling mechanisms involved in the different pathways of platelet activation.

Data clustering and enrichment analysis

To determine which groups of proteins and/or biological processes had similar phospho-signaling dynamic, the 899 significantly regulated phosphopeptides across all conditions were clustered using the fuzzy c-means algorithm[289]. Three clusters were determined as optimal for enrichment analysis (Dmin). Clusters were summarized as (1) opposite dynamics for ristocetin-PMA, (2) down-regulation of PMA-CVX, and (3) up-regulation of all agonists (except for ristocetin). Figure 4A show the standardized log2 intensities for each cluster, grouped by agonist, and it is provided to allow comparison of each cluster trend using a mean line profile graph. Thus, cluster 1 revealed an opposed phosphorylation dynamic, with high up-regulation under PMA stimulation, followed by CVX activation, albeit less pronounced; while ristocetin stimulation displayed the opposite tendency, due to imputation. On the other hand, cluster 2 also exhibited an overall bidirectionality, although one that only affected PMA and CVX, this time by means of down-regulation. Lastly, cluster 3 revealed common activation pathways for all agonists, except for ristocetin, which presented with a similar phosphorylation status as the control and ice conditions. Thus, clustering enabled the identification of three specific patterns of phosphopeptide regulation, implying the existence of non-specific, ubiquitous kinases, which are going to be involved in platelet activation regardless of the triggered

receptor; and also, the presence of other kinases specific to the ITAM signaling, shared by both PMA and CVX.

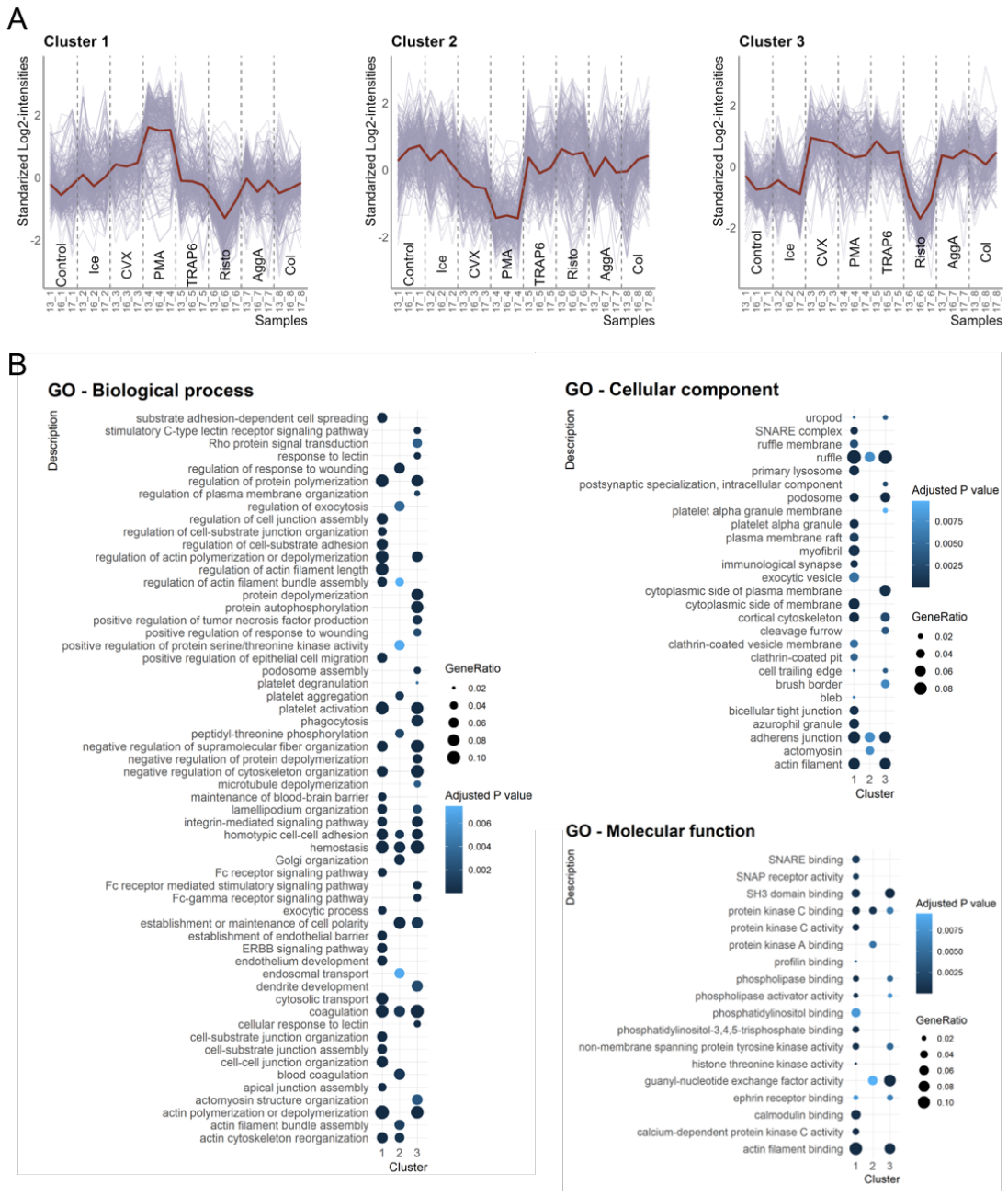

Figure 4. Differentially expressed proteins across all conditions / agonists group in three distinct clusters. (A) Profile plot of each cluster, organized so that the three replicates of each agonist are positioned together. **(B)** Dotplots of the three gene ontologies (GO), after enrichment analysis, for each cluster.

Each cluster was subsequently investigated for gene ontology (GO, see Figure 4B) and Reactome enrichment analyses. The cellular component (CC) terms related to cytoskeleton and cytoskeleton remodeling (*i.e.*, “ruffle”, “actin filament”, “adherent

junctions") are present in all three cluster, but especially clusters 1 and 2, and a high number of these terms can also be seen, in the same way, both in the biological process (BP, *i.e.*, terms related to "actin polymerization") and molecular function (MF, *i.e.*, "actin filament") enrichment. There was also an enrichment of secretion of alpha granule terms, skewed towards cluster 1 ("SNARE complex" in CC and MF, "platelet alpha granule" and "platelet activation" in MF and BP); although the three clusters presented with BP terms related to hemostasis and coagulation. As for the MF enrichment, it was composed of mostly kinase-related terms, and chiefly in cluster 1. Lastly, the Reactome enrichment map, which organizes enriched terms so that mutually overlapping gene sets cluster together, identified 5 functional modules (Figure S4A). Two of them (1 and 2), related to MAPK and calcium-dependent signaling, showed major contributions of clusters 1 and 2; while another two (3 and 4), referring to RHO GTPase activity and platelet activation-related terms, were shared by the three clusters. The biggest cluster could be considered as made of two, one being similar to the 3 and 4 clusters in terms of cluster contribution and related terms; while the remaining, which pointed to the CLEC2 and GPVI signaling, had some input of cluster 1, but mainly from cluster 3.

In light of these results, it can be seen that both the enriched gene ontology and Reactome terms lacked cluster specificity. It seems as if the enrichment analyses, which is of protein-centric nature, had been undermined by proteins whose phosphorylation sites are present across more than one cluster. Inquiry of this overlap revealed that 19 proteins were common to the three clusters, namely: several proteins related to the cytoskeleton and adherent junctions (MYH9, FLNA, WASF2, MY18A, INF2, ZYX, TJP2, ABI1), kinases/phosphatases and binding partners (FYB1, SRC, STK10, TNIK, KPCD, PTN12), granule release (SYTL4, CAVN2, BIN2, STIM1), and aggregation (SREC). Additionally, phosphosites of 9 of them were among the 20 most abundant for each comparison. However, the number of differentially expressed phosphosites was neither correlated to the length of its parent protein, nor to the total number of phosphosites

described for its parent protein by PSP. The number of total phosphosites did however correlate with the protein length (Figure S4B). This kind of ubiquitous representation across clusters suggests participation in multiple phospho-signaling pathways, pointing to a similar activation outcome (*i.e.*, cytoskeletal reorganization, degranulation, calcium dynamics, among others); and potentially to a more widespread response, where several receptors are involved due to positive feedback loops, even when just one receptor was originally triggered.

As platelet activation triggers a number of pathways, where many kinases are being phosphorylated and de-phosphorylated, we set out to investigate what non-kinase substrates were involved in these clusters, and in what processes they were involved. To do this, we repeated the GO and Reactome enrichment analyses after removing the kinases from every cluster (Figure S5A-B). As a whole, in the GO enrichment, there was a reduction in the number of significant terms, which affected particularly to cluster 2. Specifically, BP terms that remained were those related to conformational changes of the platelets, both of the cytoskeleton and the membrane; hemostasis, and signal transduction. For CC, the main themes were conserved, and only some of the redundancy was lost; while for MF the changes were more drastic, albeit expected, with the disappearance of cluster 2 altogether. Almost all terms related to kinase activity were lost, and those related the act of binding remained. Overall, the removal of the phosphorylated kinases did not affect the previous results, except for cluster 2. Lastly, Reactome enrichment after kinase removal also suffered a trimming of significant terms, but conserving the overall structure. That is, RHO GTPase cycles presented evenly in the three clusters, as well as platelet activation and degranulation; while terms referring to integrin and MAPK signaling were prominent for cluster 1, and as in the GO enrichment, cluster 2 accounted for the highest loss.

Due to the lack of cluster specificity of the previous enrichment analyses, we investigated phosphosite-level ontology using a publicly available curated dataset from

PhosphoSitePlus, which contained information on the regulatory role of specific phosphosites. We conducted this enrichment for each cluster, which showed that terms such as “cytoskeletal reorganization” and “signaling pathway regulation” were enriched for the three clusters, but skewed towards 1 and 3; while “regulation of molecular association” and “intracellular localization” were evenly distributed (Figure S5C). This all pointed to cluster 2 being conformed with phosphorylated substrates that either do not directly participate in the signaling pathways, or which phosphorylation had an inhibitory nature (“protein degradation”). Of note, the low number of phosphosites that could be found associated with phospho-regulation terms (< 12%) limited the power of the analysis.

Exploration of the signaling pathways triggered by each agonist

The clustering and enrichment analyses point to common and synergic dynamics among receptors, as it was made evident by the presence of RHO GTPases, which are heavily involved in the regulation of the cytoskeleton, and calcium-related and degranulation terms. In the end, the outcome of platelet activation, regardless of the firing receptor, involves precisely those three things. However, there are differences among the pathways. Close examination of the up- and down-regulated phosphosites and corresponding proteins showed that, of the three agonists targeting the ITAM receptors, CVX showed the highest number of differences in respect to the control than AggA and collagen (Figure S6). Thus, activation of GPVI resulted in phosphorylation of G6b-B, and the kinases SYK, MYLK, and FYN/LYN (SFKs), as well as of GADS, PLC, and kinases PKC and MAPK. This signaling pathway resulted in degranulation, as well as inside-out integrin signaling, as evidenced by the phosphorylation of VAMP-3 and SNAP23, and cytoskeleton proteins talin-1 and filamin-A (FLNA), respectively. Of note, and as it was shown with the proteins common to all clusters, proteins BIN2 and STIM-1 displayed a highly phosphorylated signature, along with DOCK10, which underscored the importance of calcium dynamics during platelet activation. On the other hand,

significantly dephosphorylated proteins included PKA, as well as pleckstrin and the serum deprivation response protein (SDPR), and the kinase suppressor of Ras 1 (KSR1).

Interestingly, this is all shared by stimulation with PMA, albeit with higher number of phosphosites and fold changes. Additionally, although PMA stimulates the integrin αIIbβIII, which shares a similar pathway with CVX, it is also able to interact with PKC directly, and this is reflected in the data. Additionally, and as a response to its enhanced response, members of that pathway that could not be seen with the other agonists are detected, such as LAT. On the other hand, PAK2 phosphosites were detected in all agonists, but not with PMA, and collagen presented with phosphorylation in DAPP1.

Unbiased assessment of protein kinase contribution using KinSwing

Next, we set out to identify and determine the contribution of the major protein kinases involved in the platelet activation by each agonist, in addition to the ones already detected by proteomics for being themselves also kinase substrates. To do this, we used KinSwing, which is a statistical approach that predicts the positive or negative inferred activity for specific protein kinases (*i.e.*, their contribution to the signaling) by integrating kinase-substrate predictions, curated protein kinase substrate motifs, and the fold change and significance of phospho-regulation from the data available.

Depiction of the predicted kinase activity for each agonist showed a great similarity between the PMA and CVX agonists, mostly due to the presence of several members of the PKC family, with PKCA being the most prominent member (Figure 5). Additionally, CVX showed a positive activity for the ILK kinase, which was not present in PMA. This high overlap can be explained by the common pathways that are shared by the integrin $\alpha_{IIb}\beta_3$ outside-in signaling and the GPVI receptor. Although both CVX and AggA stimulation showed regulation by the GRK1 kinase, it was more pronounced under TRAP6 activation; while PAK2 was predicted in both AggA and TRAP6 conditions, but

seemed to played a more central role in the former. On the other hand, collagen showed a positive kinase activity profile similar to that of AggA. Lastly, and in contrast, CSNK2A1 kinase showed an acute negative activity in almost all conditions (Figure 5).

Interestingly, a number of well-known kinases involved in platelet activation, namely SYK, LYN and BTK, displayed a negative predicted activity (Figure 5). This points to the fact that protein kinase activity should be regarded as opposed to protein phosphatase activity, that is to say, phosphorylation is a highly dynamic process, and intermediate kinases are de- and phosphorylated in a tightly regulated manner. This would coincide with the experimental data, which points to some of the phosphosites of these Src kinases being upregulated. Thus, it is possible that, given the duration of the experiment, these key proteins exerted their function at the very first stages of the platelet activation, and were afterwards de-phosphorylated by phosphatases. However, since substrate motifs for phosphatases are not as specific, studies tend to focus on kinase-centric approaches.

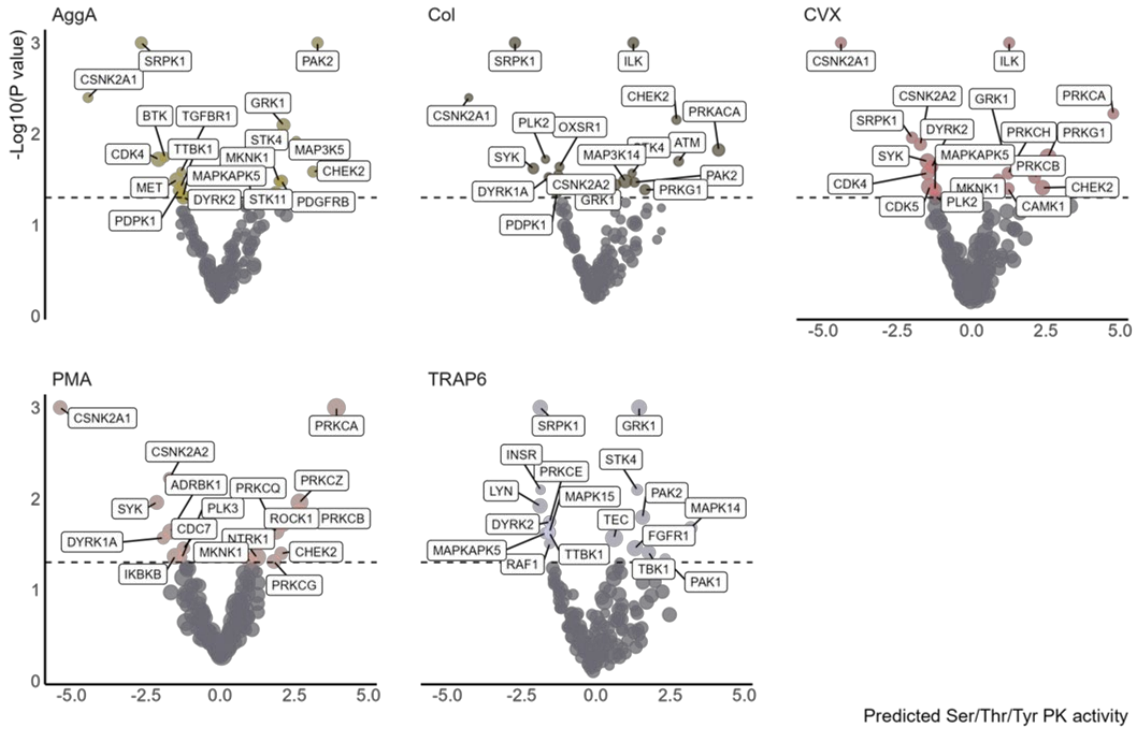

Figure 5. Volcano plots representing the positive and negative predicted kinase activities of each agonist, except for ristocetin. Colored and labeled kinases were found to be significant. PK: protein kinase, Ser: serine, Thr: threonine, Tyr: tyrosine.

Proteomics analysis of the secretome resulting from single stimulation of platelet receptors

The last characterization step regarding the activation of platelets consisted of interrogating the platelet secretome after agonist stimulation, to complement the information given by the phosphoproteome. For this, the supernatant generated after the degranulation assay was isolated and subject to proteomics analysis, where the same amount of protein from each reaction was fed to the mass spectrometer. The raw spectra data was processed using the same MSFragger protocol used with the whole platelet proteome, and the subsequent global quantitative workflow resembled the one used with the phosphoproteomics data, in terms of filtering, normalization, imputation and inference.

At the very start of the analysis, common contaminants in platelet proteomics (namely, immunoglobulins, albumin, and erythrocyte-specific proteins) were removed, as it is understood that, although these contaminants can be trapped in the open canalicular system of platelets, they are not found within the alpha and dense granules, and in consequence were dropped. This resulted in the detection of 339 proteins across all conditions, with ristocetin having the least number of identifications, followed by the control and ice conditions, while CVX and AggA seemed to induce the release of the highest number of proteins (Figure 6A). PCA showed a clear clustering of ristocetin and unstimulated conditions versus the rest of conditions, along the first component, hinting to the degranulation capacity of each agonist (Figure 6B). Further differential expression analysis revealed, as expected, that quantitative differences compared to the unstimulated condition leaned towards the over-secretion, in all cases (Figure 6C). The one exception was found after ristocetin stimulation. As per the previous results, it seems as if platelets activated with this agonist did aggregate, or rather, agglutinate, but this did not translate to another of the usual outcomes, which is granule secretion. This fact resulted in a lot of missing values that had to be imputed, and thus the inference results took this fact into account.

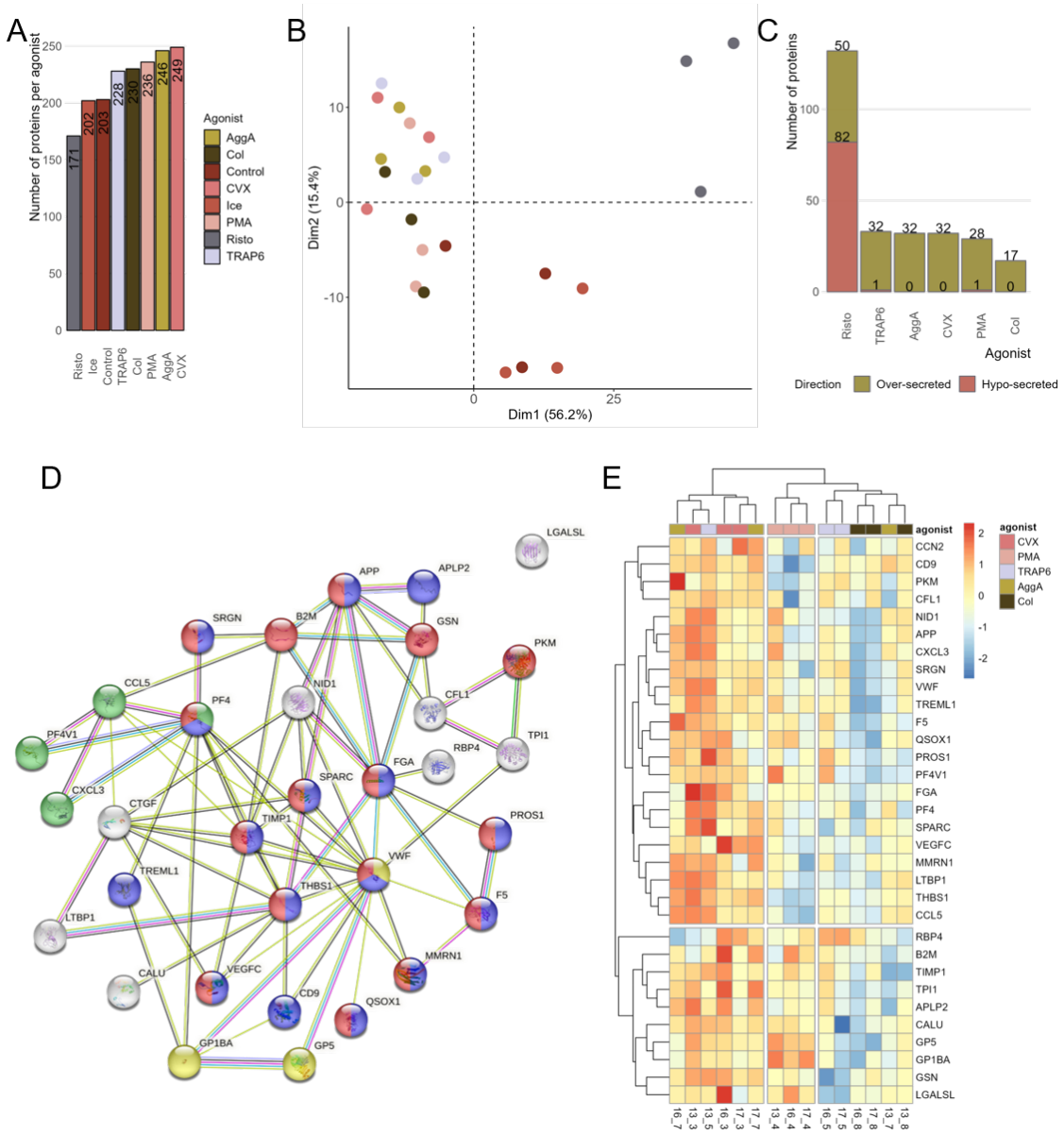

Figure 6. Proteomics investigation of the secretion profile of platelets after single receptor stimulation. (A) Barplot showing the number of proteins detected in each condition. **(B)** Principal component analysis (PCA) of the secretion / degranulation profiles of the different agonists. **(C)** Barplot representing the number of over- or hypo-secreted proteins, per agonists. **(D)** STRING network of the unique over-expressed proteins present across all conditions, save for ristocetin. Yellow represents proteins of the GO:0007597 term (blood coagulation, intrinsic pathway); green, the GO:0008009 term (chemokine activity); blue, the GO:0031091 (platelet alpha granule); and red, GO:0034774 (secretory granule lumen). **(E)** Heatmap showing the fold changes of the same proteins represented in the network.

STRING analysis was employed to explore potential interactions between the unique 32 differentially expressed proteins across all comparisons (save for the ristocetin comparison, Figure 6D). The protein-protein interaction enrichment *p*-value was near 0, indicating that they were biologically connected. Furthermore, all proteins (except for LGALSL) formed an interactive cluster, with vWF, thrombospondin-1 (THBS1), amyloid-

beta precursor protein (APP), platelet factor 4 (PF4), and fibrinogen (FGA) as main nodes, which are not only well-known platelet alpha granule proteins, but also are among the most abundant molecules in platelets. Other similar proteins are SPARC, multimerin-1 (MMRN1), calumenin (CALU), coagulation factor V (F5), or the vascular endothelial growth factor (VEGFC). In addition, there were proteins with chemokine activity (CCL5, CXCL3) and shed receptors (GP5, GP1BA). Study of the overlap between conditions revealed a high agreement among them, with 12 proteins shared by all agonists, and 10 by at least four of the five conditions (Figure S7A). Heatmap of those common proteins showed that CVX and AggA elicited their secretion in higher quantities, that is, the activation in terms of the degranulation response was more drastic than with the other agonists (Figure 6E). It was closely followed by PMA activation, and then collagen and TRAP6.

Lastly, ristocetin presented with 32 over-secreted proteins that did not coincide with those of the other agonists, and 44 proteins under-secreted (Figure S7A). Gene ontology enrichment of the former revealed terms related to lipoprotein particles, since there were various members of the apolipoprotein family, as well as cytoskeleton-related (myosin, actin, tropomyosins) and alpha granule (insulin growth factor, kininogen-1) terms. Interestingly, there were also specific terms related to the dense granules, due to the presence of tetranectin (CLEC3B) and selenoprotein P (Figure S7B). The latter displayed the highest fold-change of them all, potentially pointing to ristocetin mobilizing this type of granules more than the other agonists.

Overall, these data highlight the common profiles of all agonists in terms of the identity of the proteins secreted. The synergy of the activation pathways that are triggered not only are noticeable in their phosphorylation dynamics, but also in regard to their secretion profile, which converged chiefly in the exocytosis of the alpha granule cargo. The one exception throughout this characterization is the response elicited after

ristocetin addition, which results in a secretory profile distinct from the other agonists, and which seems to favor the release by dense granules, although not exclusively.

In summary, in this Chapter, we provided an extensive data resource of platelets in health, both in resting and activated states. In the case of the latter, we performed a complete mapping of the signaling pathways and degranulation after activation of five of the most important hemostatic and non-hemostatic receptors. Thus, we set the basis for the study of platelets in disease.

Chapter IV – Megakaryopoiesis and platelets under chronic low-grade inflammation – a proteomics and cell biology approach

It has been extensively studied that situations of acute stress or inflammation, such as those that occur in sepsis or cytopenias, have a great impact not only on hematopoiesis as a whole, but also on the megakaryocyte-platelet axis. As explained before, studies have shown that there is a subpopulation of HSCs with restricted megakaryocyte potential that are able to differentiate directly to megakaryocyte progenitors, bypassing intermediate multi- and bipotent stages[9]. Furthermore, the presence of certain cytokines might be modulating how platelets are produced, and making megakaryocytes choose an alternative pathway to the formation of proplatelets[39]. However, these changes were observed under emergency conditions, where dramatic events are more likely to occur, and therefore be seen. Chronic low-grade inflammation, on the other hand, has not been as thoroughly investigated, especially in the context of megakaryopoiesis, thrombopoiesis and platelet characterization[290].

Chronic low-grade, systemic inflammation is a subclinical feature not yet completely defined, but consensus establishes the presence of elevated levels of cytokines (*i.e.*, IL-6, IL-8 or TNF-α, among others), and other biomarkers (*i.e.*, C-reactive protein, fibrinogen, or VCAM-1, among others)[291]. It is present in a number of diseases, such as cancer, and neurodegenerative diseases, as well as others of metabolic or autoimmune origin, such as diabetes or rheumatoid arthritis. In addition, it is a definitory characteristic of aging —a phenomenon carrying its own term: inflammaging[292] —, and thus a risk factor for the development of the aforementioned diseases.

One of the features that lies at the core of it, and shared by all of these diseases of different etiologies, is thromboinflammation, which is driven by a state of platelet hyperreactivity that preludes the onset of associated cardiovascular diseases, one of the main causes of morbidity and mortality in these patients[198,293]. The mechanism by which

this enhanced activation occurs is not yet defined, although it is most likely multifactorial and disease-specific. For instance, in diabetes, one study found that hyperglycemia seems to be increasing platelet glucose uptake by the GLUT1 and GLUT3 receptors, as well as its subsequent metabolism, and in turn promoting platelet activation in circulation[294]. Other studies also point to hyperglycemia being able to tune megakaryopoiesis, by means of eliciting the release of S100 calcium-binding protein A8/A9 by neutrophils, which in turn bind to Kupffer cells of the liver and promote their increased TPO production[295]. In this setting, megakaryocytes not only display an augmented ploidy, but also produce reticulated, immature platelets with upregulated expression of $\alpha_{IIb}\beta_3$, CD61, CD63, thromboxane and thrombospondin, which translates in an enhanced aggregation response[296]. However, in a more general capacity, platelets are also activated in the presence of IL-6, via its receptor GP130 using the GPVI receptor signaling pathway[297]; and of TNF-α, which directly affects megakaryopoiesis by means of reprogramming inflammatory, metabolic, and mitochondrial pathways, which in turn promotes the generation of platelets with a high number and enhanced activity of mitochondria, leading to a hyperactive platelet profile[40]. Additionally, there is also evidence of a crosstalk between inflammation and platelets in the form of a positive feedback loop with leukocytes, which result in a mutual activation by both the secretion of cytokines, and the formation of aggregates[298]. This behavior constitutes one of the hallmarks of psoriasis and, to a lesser extent, of atopic dermatitis: the infiltration of low-density granulocytes (LDGs) into the skin lesions[299]. Platelets seem to interact and aggregate with these LDGs, increasing their vascular rolling, and also infiltrating the skin.

However, although the relationship between subclinical inflammation and platelet reactivity has been established, the characterization of this phenomenon has been done mainly in murine models, and in little depth. So much so, that it is not entirely clear what platelet molecules or surface receptors are changing, how they are changing, and the impact that low-grade inflammation has in megakaryopoiesis. In this study, we

investigate the multifaceted effect of low-grade inflammation on megakaryopoiesis and, more specifically, in the platelet phenotype and function. For this, five cohorts presenting with this kind of inflammation, albeit with different etiologies, were selected: type 1 diabetes mellitus, psoriasis, atopic dermatitis, and major depressive disorder concurrent with (MDD) or without suicide attempt (MDD SA); as well as a sex- and age-matched healthy group. Individuals in each group were selected using stringent inclusion and exclusion criteria, so that certain confounders were removed. We employed an assortment of cellular and molecular techniques to interrogate the function, immunophenotype and protein profile of platelets, as well as the phenotype of the differentiating megakaryocytes at different time points. Therefore, by unraveling how the different aspects of subclinical inflammation impacts the megakaryocyte/platelet axis, our study advances not only the understanding of the biology of each specific disease, but also provides potential diagnostic and prognostic markers, as well as testable therapeutic approaches.

Chronic low-grade inflammation had no impact on the blood count

To study the effect of inflammation on platelets, we recruited patients from five different cohorts, all presenting with chronic, subclinical inflammation, as well as a group of healthy volunteers (N = 20, N = 10 for proteomics). The patient cohorts included: (1) type 1 diabetes (N = 10), (2) moderate dermatitis (N = 4), (3) mild-to-moderate psoriasis (N = 4), (4) major depression (N = 10), and (5) major depression with recent suicidal attempt (N = 6). No significant differences among groups were identified with regard to sociodemographic characteristics (sex and age), after post-hoc pairwise analysis (Tukey).

Additionally, study of the complete blood count (CBC) of each cohort showed that all of the analyzed blood parameters were within the normal range, for both patients and controls. This included white blood cell and differential count (neutrophils, lymphocytes, monocytes, eosinophils, and basophils), nucleated and enucleated red blood cell count,

mean corpuscular volume, hematocrit, and hemoglobin-related variables (hemoglobin, mean corpuscular hemoglobin, mean corpuscular hemoglobin concentration), and platelet-related indices (count, plateletcrit, mean platelet volume, distribution width, and larger cell ratio). Descriptive information can be found in Table S1. From these data, the neutrophil-to-lymphocyte, monocyte-to-lymphocyte, and platelet-to-lymphocyte ratios, as well as the systemic immune-inflammation index, were calculated. Analysis of covariance (ANCOVA) of each variable, controlling for both sex and age, revealed that only the mean corpuscular hemoglobin concentration significantly varied between the diabetes and psoriasis groups, while the rest yielded no differences against the control, or among groups. Hence, low-grade inflammation had no impact in either the platelet count or associated indexes, in these cohorts.

Functional assays of inflammation-primed platelets

Two different functional assays were performed on samples of all cohorts to determine if chronic low-grade inflammation caused a dysfunction in the aggregation and degranulation capabilities of platelets. In both cases, platelets were stimulated with a battery of agonists targeting single receptors (see Chapter III), and each individual response was recorded. Additionally, AggA aggregation responses in half of the control group had to be filtered out due to suboptimal agonist concentration.

In the aggregation assay, two different parameters were assessed: the maximum aggregation rate (MAR), which is defined as the highest (maximum) recorded aggregation percentage at any given time point; and the area under the curve (AUC), which is used to measure the dynamics of the aggregation. Although in all groups and under all agonists the responses had a high dispersion, pointing to an equally high inter-donor variability, an analysis of variance (ANOVA) followed by Tukey *post-hoc* pairwise analysis among the different patient groups and the control, for both the unstimulated condition and all agonists, showed no anomalous responses (Figure S1). However, it did reveal a significantly diminished MAR in response to AggA in the dermatitis cohort, with

a correspondent, similar reduction in the AUC, which was observed also after CVX, and even collagen (p = 0.08), stimulation (Figure 1A).

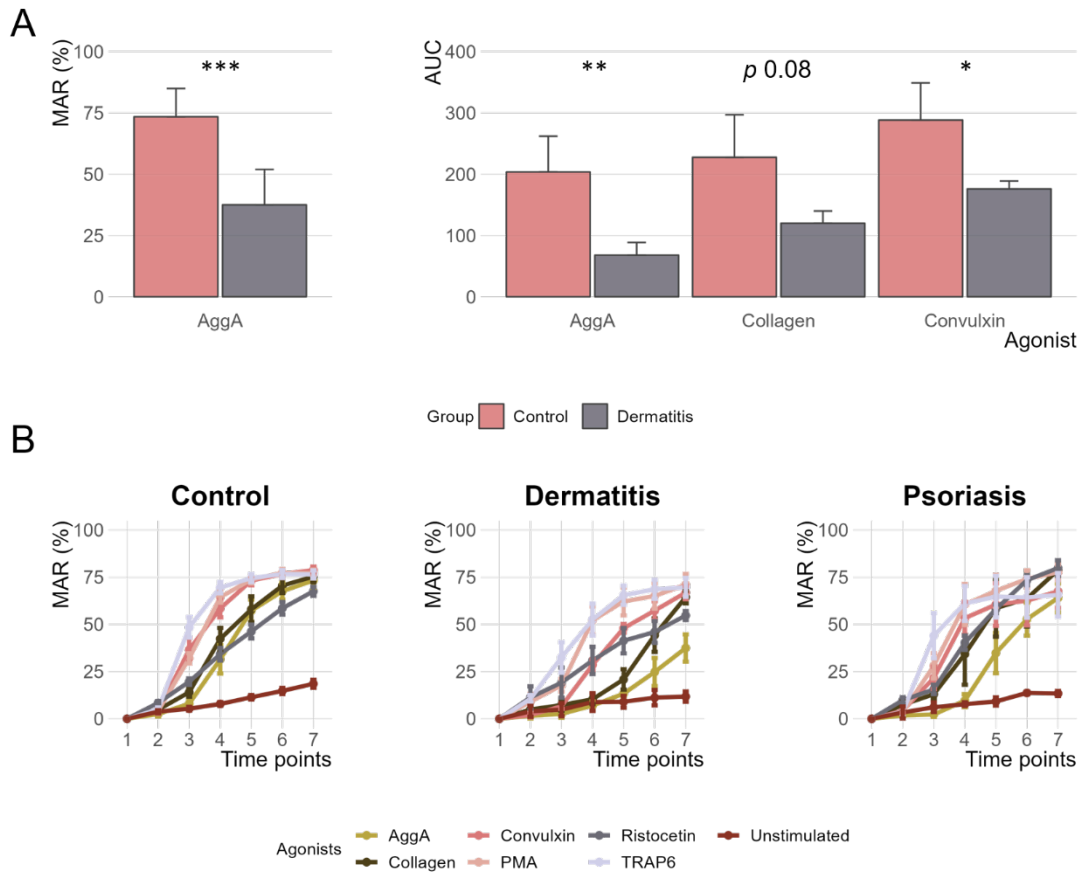

Figure 1. Dermatitis and psoriasis platelets displayed an aggregation defect. (A) Boxplots of the maximum aggregation rate (MAR) and area under the curve (AUC) in dermatitis, after aggretin A (AggA), collagen and convulxin stimulation. **(B)** Aggregation curves of all agonists of the healthy, dermatitis and psoriasis platelets. Error bars represent the standard error of the mean. *: p <= 0.05, **: p <= 0.01, ***: p <= 0.001.

This means that with AggA, dermatitis platelets failed to aggregate to the same extent as healthy ones; while those same platelets, after AggA, CVX and collagen addition, had a different aggregation dynamic, starting off with difficulty, and taking longer to reach the same aggregation rates as the controls, at the same time points. Of note, AggA and CVX trigger the CLEC2 and GPVI receptors, respectively, which are known to participate in the non-hemostatic functions of platelets; while collagen is able to activate both GPVI and integrin $\alpha_{II}\beta_1$. Additionally, although not significant, psoriasis platelets displayed a similar tendency in the AUC, for the same agonists, pointing towards the overlapping etiology of both diseases (Figure 1B and S1).

In the case of the degranulation assay, flow cytometry analysis of unstimulated platelets (basal condition) revealed a diminished phosphatidylserine (PS) exposure in the diabetes, dermatitis and MDD SA groups; as well as a reduced fibrinogen binding capability, and an increase in P-selectin expression only in diabetic patients, with respect to the control group. Thus, platelets from the diabetes patients are already activated in resting conditions, although they are not procoagulant.

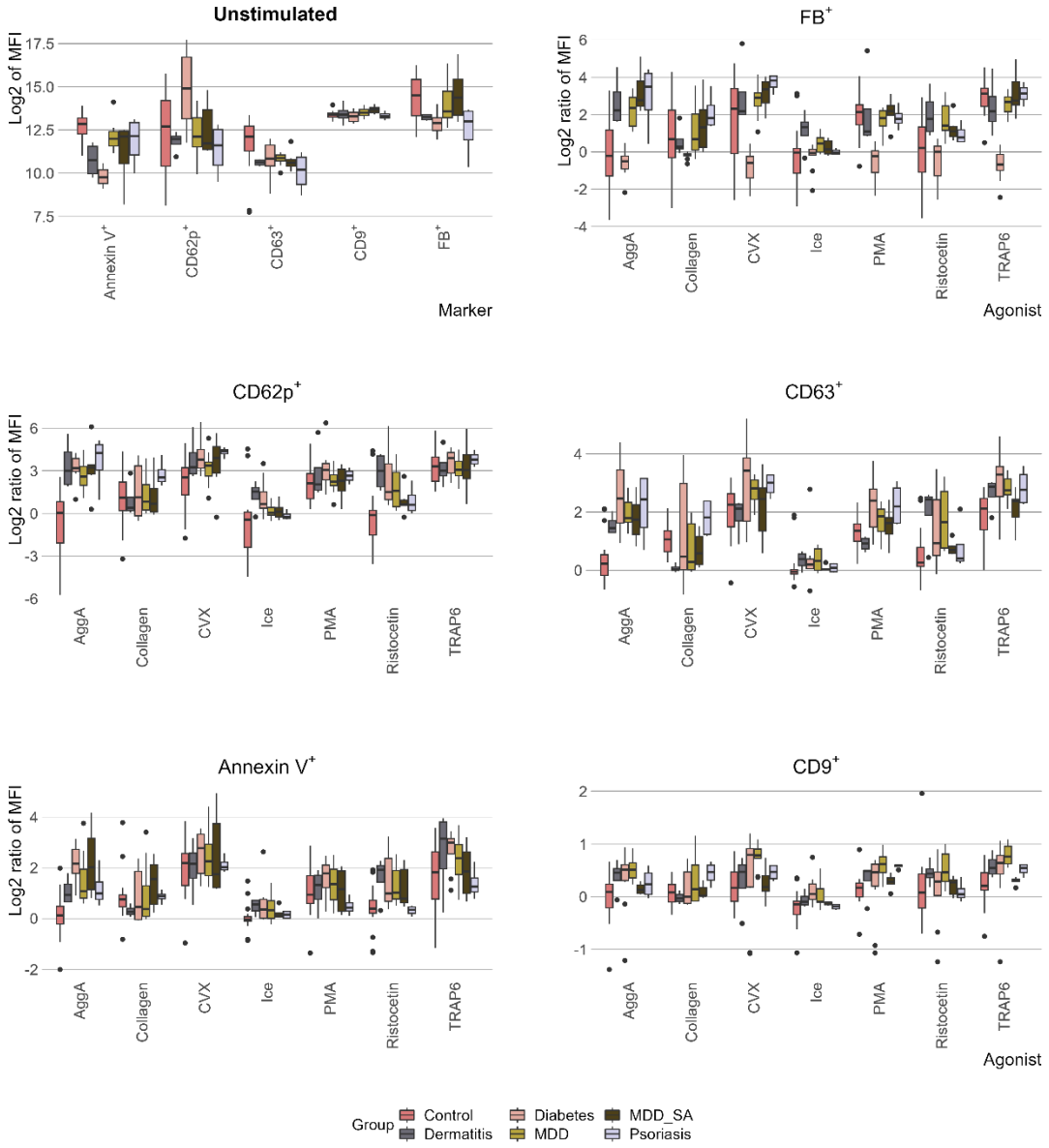

Figure 2. The degranulation response for each agonist. Boxplots depicting either the log2-transform mean fluorescence intensity (MFI) of the unstimulated platelets, for all markers (top left); or the log2 ratio (to the unstimulated condition) MFI for each agonist and marker. MDD: major depressive disorder, SA: suicidal attempt.

Further analysis of the activation and reactivity of platelets following agonist addition was performed, after normalization against the unstimulated condition. It showed that, although they are already pre-activated, diabetic platelets still reached a greater activation (augmented P-selectin) than controls after AggA, CVX and ristocetin stimulation. Similarly, AggA, CVX, TRAP6, and PMA induced a higher dense granule and lysosome secretion (CD63) in these platelets; while collagen, CVX, PMA and TRAP6 addition resulted in a reduced fibrinogen binding ability. AggA, in turn, induced a higher overall fibrinogen binding and granule secretion in all groups, except for CD63 in the dermatitis cohort; while a higher PS exposure was measured for both MDD and MDD SA, besides diabetes. Lastly, ristocetin elicited a similar, overall heightened response in the MDD cohort; while only an enhanced alpha granule secretion in dermatitis platelets. Interestingly, MDD platelets showed increased CD9 expression after AggA, CVX, PMA and TRAP6 stimulation, although only with AggA this was accompanied by an increased granule secretion.

All in all, the platelets of the diabetes cohort sustained the most dramatic degranulation changes, with an enhanced alpha and dense granule secretion response, especially after the stimulation of the CLEC2 and GPVI receptors, which was already present in steady-state conditions; but a reduced fibrinogen binding, even after the addition of AggA and CVX. These agonists induce the inside-out activation of the integrin GPIIbIIa (the main hemostatic receptor), making it switch from a low- to high-affinity state for fibrinogen (among other ligands). Lastly, AggA promoted a hyper-secreting response in all cohorts.

Immunophenotype of inflammation-primed platelets

To assess whether the changes seen in the functional assays were due to either an up- or down-regulation of the respective receptors, the immunophenotype of the resting platelets was studied by flow cytometry (Figure 3). In regard to the two non-hemostatic receptors, GPVI and CLEC2, a tendency towards a lower expression on the

former could be observed in both dermatitis and psoriasis patients (p ~ 0.1), while no differences were reported in the case of the latter. Similarly, a tendency towards the overexpression of the integrin $\alpha_{II}\beta_1$ (CD49b) was found for MDD platelets (p = 0.05). Furthermore, the diabetes cohort displayed a selective down-regulation of GPIbα (CD42b), but not of GPIX (CD42a), both subunits of the von Willebrand factor receptor; as well as a reduction of PS and the integrin subunit GPIIb (CD41). MDD SA, and dermatitis and psoriasis platelets also showed a reduction of these two molecules, respectively.

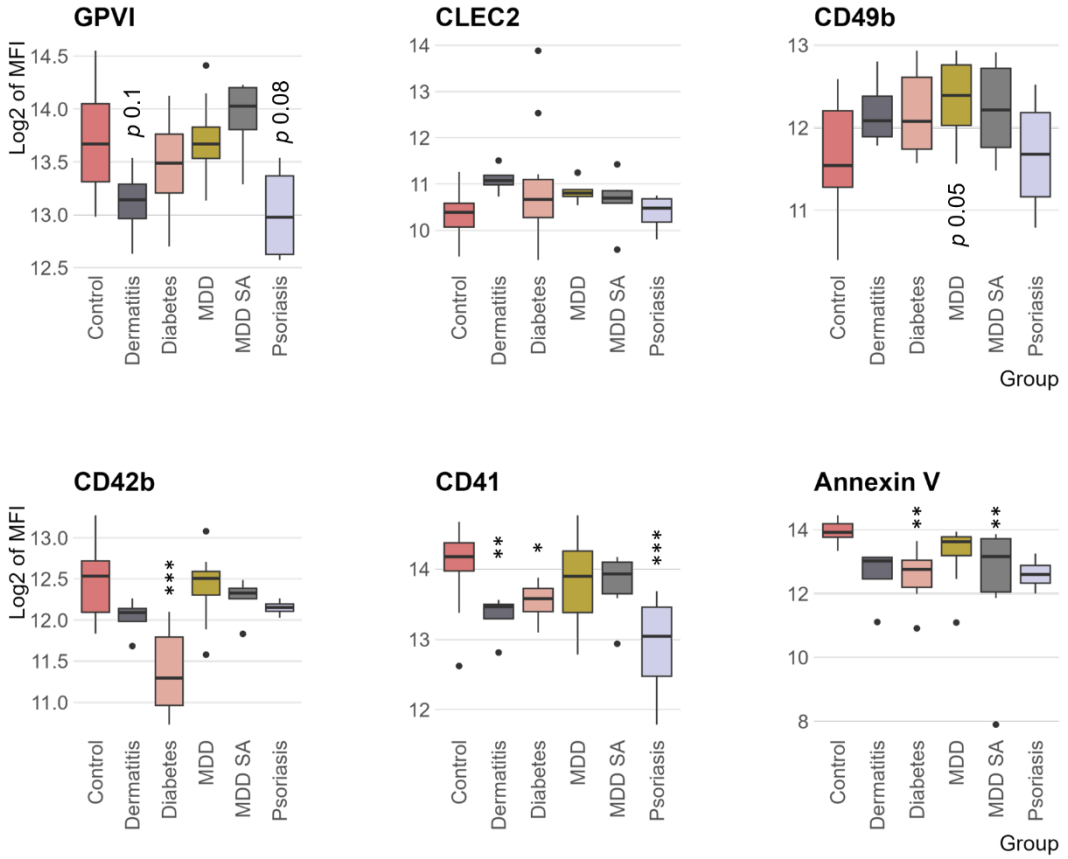

Figure 3. Immunophenotype of the platelets of the different diseases. Boxplots represent the log2-transformed mean fluorescence intensities (MFI) of the representative markers. Alternative names: integrin $\alpha_{II}\beta_1$ (CD49b), GPIbα (CD42b, subunit of the vWF receptor), GPIIb (CD41, subunit of the integrin $\alpha_{IIb}\beta_3$). MDD: major depressive disorder, SA: suicidal attempt. *: p <= 0.05, **: p <= 0.01, ***: p <= 0.001.

In summary, although low-grade inflammation seemed to have a different effect depending on the disease, in all cases it points to a fine-tuning affecting the responses elicited by triggering of the CLEC2 and GPVI receptors. Hence, despite the fact that

diabetic platelets displayed a hyperreactive profile, with an over-representation of P-selectin on the surface membrane, they had normal aggregation responses. It did affect, however, to their degranulation response, which showed an increase secretion of biomolecules regardless of the agonists used. The overall low fibrinogen binding could be explained by the reduced levels of the integrin subunit GPIIb; and it also showed a significant and specific reduction of one of the subunits of the von Willebrand factor receptor, although it did not seem to affect the response. For their part, dermatitis and psoriasis were affected in a lesser extent by this inflammation, which seemed to favor their degranulation response, at the expense of the aggregation, especially when the CLEC2 receptor was involved. Lastly, MDD and MDD SA platelets were the ones least affected by this inflammatory milieu, and demonstrated their hyperactivated secretory activity only when stimulated by AggA.

Low-grade inflammation is able to shape megakaryopoiesis

To further study the impact of inflammation on the megakaryocyte-platelet axis, primary peripheral blood mononuclear cells (PBMCs) were isolated from the patients and healthy controls, and cultured under specific conditions to promote their differentiation towards and the growth of megakaryocytes, without having to initially isolate $CD34^+$ precursors. To study the evolution of this differentiation, cells were taken for immunophenotyping at days 0 (start of the culture), 7 and 11 (end of the culture). The gating strategy was based on the CD31 (platelet endothelial cell adhesion molecule-1, PECAM-1), CD71 (transferrin receptor), Lin 2, CD41 (GPIIb) and CD42a (GPIbα) antibodies (Figure S2). CD31, a glycoprotein found on endothelial cells and immature and mature circulating hematopoietic cells, including megakaryocytes, was used both to select nucleated cells and to further divide that population based on its level of expression ($CD31^{high}$, $CD31^{mid}$ and $CD31^-$). In addition, both the $CD31^{high}$ and $CD31^{mid}$ subpopulations were used to extract the megakaryocyte fraction, by means of combining either the Lin 2 cocktail or CD71, respectively, with CD41 or CD42b, two markers specific

to megakaryocytes. The analysis of days 7 and 11 had an additional step to check for pro-erythroblasts and related progenitors ($CD31^{-}$ $cKIT^{+}$). Positioning of the three CD31 compartment against the side and forward scatters indicated that the $CD31^{mid}$ and $CD31^{-}$ populations seemed to be composed of lymphocytes, while the $CD31^{high}$ population contained a higher proportion of leukocytes and cells with higher internal complexity.

Notably, along the differentiation process, there was an imbalance within the CD31 compartment of nucleated cells (Figure 4A). Thus, it can be seen that at day 0, there is a dramatic shift towards the $CD31^{-}$ compartment, at the expense of the other two ($CD31^{high}$ and $CD31^{mid}$), in the psoriasis and dermatitis cohorts, albeit less pronounced in the latter; and which returned to levels comparable to the control group for the remaining of the maturation process. Since at day 0 the culture resembled what was happening systemically in the blood, there seemed to be an overall loss of CD31, that recovered when the culture started differentiating and producing new cells, and the ones not targeted by the medium died. Furthermore, by the end of the culture, the MDD SA cohort suffered a similar disparity. Meanwhile, the diabetes cohort underwent a mid-differentiation decompensation that favored the $CD31^{mid}$ compartment, from which it also recovered.

Additionally, megakaryocytes were selected in each of the two CD31 positive compartments ($CD31^{high}$ and $CD31^{mid}$), using the CD41 and CD42a markers. Thus, in line with what was reported above, the psoriasis and dermatitis cohorts displayed a reduced percentage of $CD31^{high}CD41^{+}$ and $CD31^{high}CD42a^{+}$ megakaryocytes, which is sustained throughout the differentiation (Figure 4B). In the $CD31^{mid}$ compartment, where in general there were less megakaryocytes, at day 0, the percentages resembled more closely those of the control, although at days 7 and 11 only the $CD31^{mid}CD41^{+}$ presented these differences; and at day 11, just the psoriasis cohort (Figure 4C). These results showed a gradual recovery as the culture advanced, which may reflect a higher impact of the environment in the circulation than in megakaryopoiesis, although the psoriasis

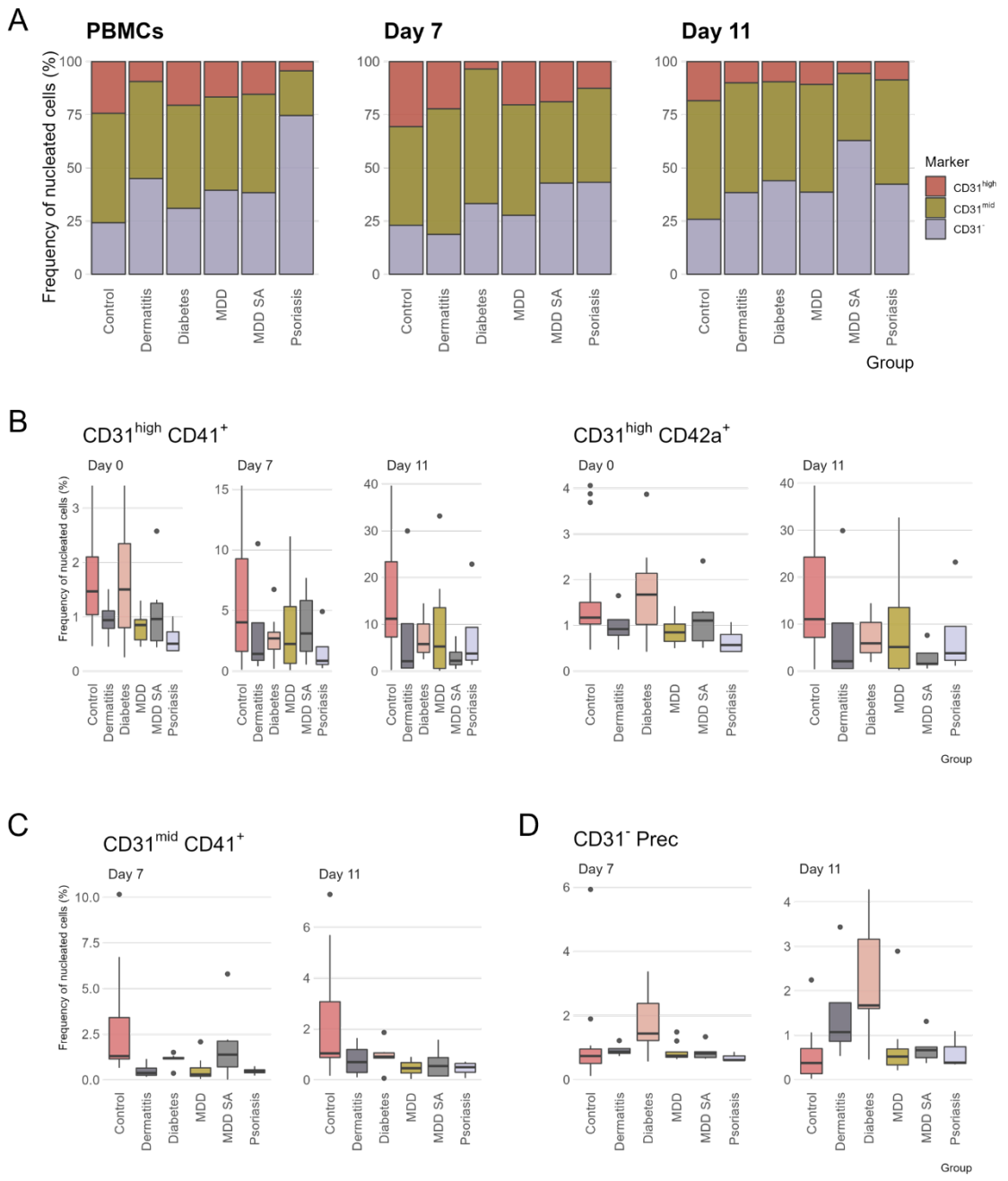

Figure 4. Immunophenotype of peripheral blood mononucleate cells (PBMCs) and cells from the differentiation of the megakaryocyte lineage, at different time points. (A) Percentage distribution of the CD31 (PECAM-1) populations within the nucleated cell compartment. **(B)** Boxplots representing the percentage of CD31^{high} maturing megakaryocytes within the nucleated compartment, at different time points. **(C)** Boxplots representing the percentage of CD31^{mid} maturing megakaryocytes within the nucleated compartment, at different time points. **(D)** Boxplots representing the percentage of pro-erythroblasts and other early progenitors (CD31^{high} cKIT^{+}) within the nucleated compartment, at different time points. Alternative names: GPIX (CD42a, subunit of the vWF receptor), GPIIb (CD41, subunit of the integrin $\alpha_{IIb}\beta_3$). MDD: major depressive disorder, Prec: erythrocyte precursor, SA: suicidal attempt.

group was the most affected. Interestingly, the MDD and MDD SA groups displayed a similar behavior at days 0 and 7 as the dermatitis cohort; and at day 7, the MDD SA behaved as the psoriasis group. Lastly, the diabetes group was the less affected, with a

decrease in the percentage of megakaryocytes which started at day 7, hand in hand with the loss of cells in the CD31 positive compartment, and extended into the day 11.

Further use of the cKIT marker revealed an enrichment of this compartment ($CD31^{-}$ $CD71^{-}$ KIT^{+}), which comprised pro-erythroblasts and early erythroid progenitors, within the diabetes cohort, both at days 7 and 11 (Figure 4D). It could also be seen in the case of the dermatitis group, at day 11.

Overall, these results indicate that the inflammatory environment is indeed having an impact on the hematopoietic cells, as made evident with the results regarding the CD31 compartments at day 0. Nonetheless, it is also shaping megakaryopoiesis, affecting the balance of megakaryocyte production. This is noted especially in the diabetes group, where even in a pro-megakaryocytic environment, there is a shift towards another lineage, since these precursors are almost non-existent in the healthy donors.

Platelet proteomics of patients displays an inflammatory signature

To elucidate the impact of low-grade inflammation on the proteomic profile of platelets, and understand the differences in protein expression of each specific cohort, we took advantage of the increased throughput of multiplexed TMT proteomics. In this case, we included 10 controls, which did not introduce any differences in terms of sex and age, and all patients from the different cohorts. Thus, we generated a quantitative platelet proteome profile of a total of 42 samples, using a robust data analysis pipeline.

The samples were arranged into three experimental groups, according to the labelling capacity of a 16-plex TMT isobaric kit (n = 15 samples; 14 platelet lysate samples, 1 reference sample consisting of a pool of all 42 samples, and an empty channel). Each proteomic TMT experiment identified 5546, 5568, and 5882 peptides, respectively, which translated in 1370 unique proteins across all samples (1% protein and 1% PSM false discovery rate). For all steps of the identification and quantification of

peptides, and protein inference from the raw spectral data, the MSFragger and Philosopher tools were used.

After removal of common contaminants in platelet proteomics (namely remnants of plasma and erythrocytes) and proteins that were only identified, but not quantified (*i.e.*, presented with missing values across all samples), an initial quality assessment was performed. PCA of samples indicated the presence of a severe batch effect, resulting from the processing of the TMT experiments, which also caused the appearance of batch-dependent, non-ignorable missing values (*i.e.*, a protein abundance is either all observed or all missing in the samples corresponding to the same TMT experiment). Due to the fact that roughly half of the proteins detected presented this pattern, listwise deletion of missing values would not only lead to biased estimation and inference, but also to a drastic and unwanted reduction of statistical power and sample size. Thus, to avoid this, a univariate mixed-effects selection model was performed, after transformation, quantile normalization, and imputation of ignorable missing data, using the multivariate imputation by chained equations from the 'mice' package (see Experimental and Bioinformatics Procedures).

Furthermore, since the model did not return fold changes, and to be able to study the direction and effect of the change, an alternative route to acquire batch-corrected intensities was conducted. Sample loading normalization of the raw data, followed by normalization to the reference channel did not fully address the batch effect (Figure 5A – top), most likely due to the high inter-variability of human samples. Instead, the removeBatchEffect function from the 'limma' R package was performed in its stead, resulting in a clear distinction between normal and pathological proteomes, albeit demonstrating a modest distinction among the latter (Figure 5A – bottom). Although some of the information was lost in the process, the resulting expression matrix retained the general trends observed with the model.

Thus, differential expression analysis followed by multiple comparison correction yielded 416 unique proteins significantly up- or down-regulated across all groups. Diabetes disease induced major proteomic changes, with > 200 differentially abundant proteins, while dermatitis presented with the least (~ 80 proteins) (Figure 5B). Additionally, gene ontology (GO) enrichment of all up-regulated proteins (n = 311), regardless of disease, revealed an overrepresentation of terms related to inflammation and the immune response, pointing towards a distinct protein profile in this group of inflammation-mediated pathologies (Figure 5C).

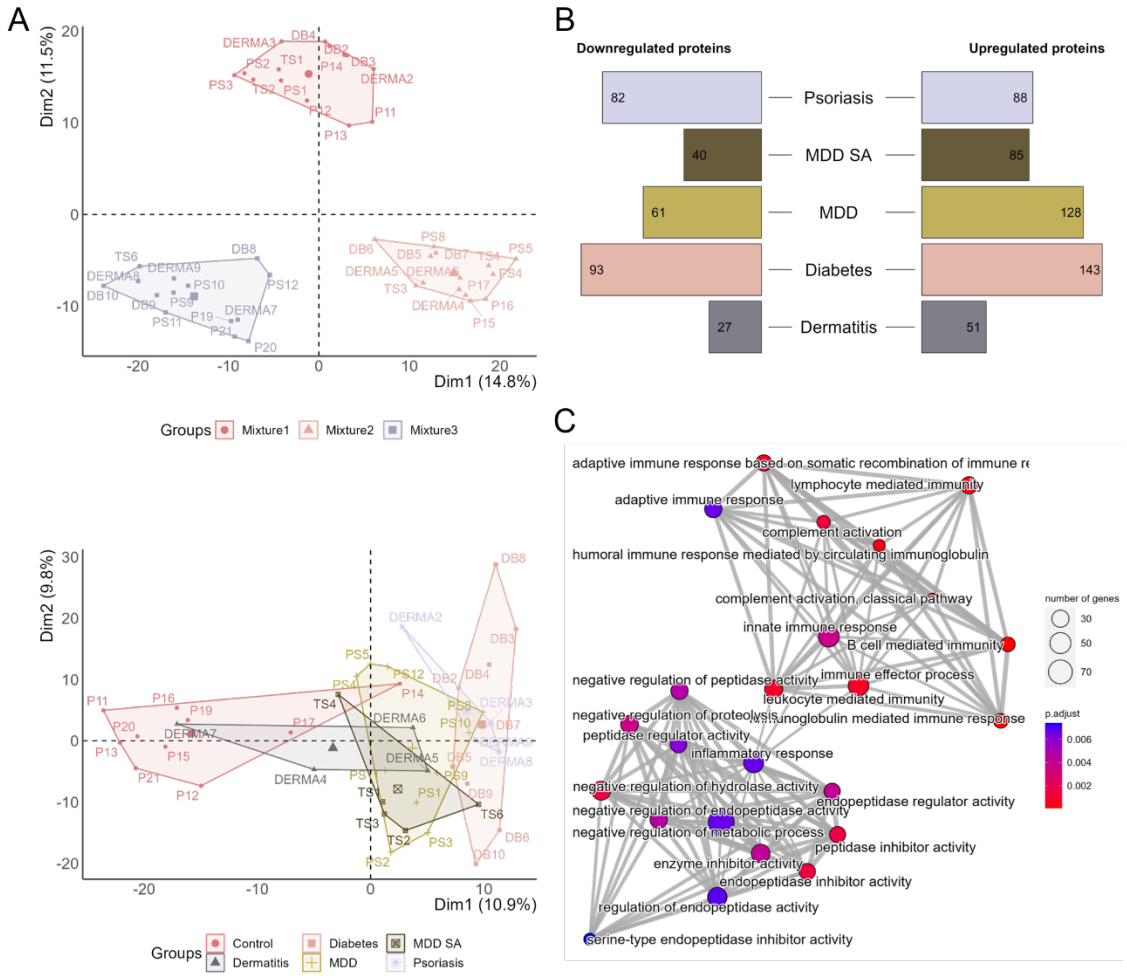

Figure 5. The proteomics profile of platelets in chronic low-grade inflammation. (A) Principal component analysis (PCA) before (top) and after (bottom) the removal of the batch effect caused by the nature of the proteomics experimental design (three different runs / mixtures). **(B)** Barplot showing the number of down- and up-regulated proteins for each condition, against the control. **(C)** Enrichment map showing the significantly over-represented terms (comprising the three orthogonal ontologies) of the up-regulated proteins across all conditions. MDD: major depressive disorder, SA: suicidal attempt.

Not all of the studied receptors were able to be detected by mass spectrometry, such as GPVI, GPIIb, and the GPV subunit of the vWF receptor, and those that did, displayed certain dynamics. For instance, the CLEC2 receptor, although not significant, displayed a marked downregulation in the dermatitis cohort (Figure 6A). Of note, this could explain the impaired aggregation response seen after AggA stimulation, although it did not show in the immunophenotype. Additionally, the other two subunits of the vWF receptor, GPIX and GPIbα, were downregulated in diabetes and psoriasis (trending in dermatitis), and in diabetes, MDD and MDD SA, respectively; although the immunophenotype only pointed to the latter as being shed. As for the integrins, the GPIIIa subunit was downregulated in the psoriasis and diabetes cohorts, complementing the same dynamic of the complementary GPIIb signaling; and the GPIIα integrin is specifically downregulated in MDD (Figure 6A). These results showed that, under inflammation, platelets tend to reduce their hemostatic responses. Interestingly, all groups displayed a significantly upregulation of the linker for activation of T cells protein (LAT), an adaptor protein required for the signaling pathway downstream of GPVI and CLEC2. The dermatitis cohort further showed an increase in the accompanying proteins of LAT: GADS and SLP-76.

To gain a better understanding of the functional differences and similarities within the different cohorts, an analogous GO enrichment was performed for each of them, taking into account the direction of the change. Concordant with what was previously seen, the up-regulated terms showed a preference for immune- and inflammation-related labels. On the other hand, down-regulated proteins seemed to be enriched with cytoskeleton-related terms. Group-specific terms referred to granule and organelle trafficking in MDD SA and psoriasis, and histones in MDD (Figure S3). Diabetes displayed platelet- and hemostasis-related terms both in the up- and down-regulated protein groups (Figure S3). Interestingly, in both dermatitis and psoriasis, there were terms referring to cysteines and S-S bonds, as well as “Protein disulfide isomerase (PDI)

activity" (Figure S4). PDI has been shown to promote the interaction of the platelet GPIbα with neutrophils, in conditions of thromboinflammation. Furthermore, it is precisely this partnership which results in the skin lesions characteristic of both atopic dermatitis and psoriasis. Although the 3 PDIs relevant to that term (PDIA1, PDIA4 and TMX3) are only significantly upregulated in dermatitis, there is a tendency also in psoriasis patients (Figure 6B).

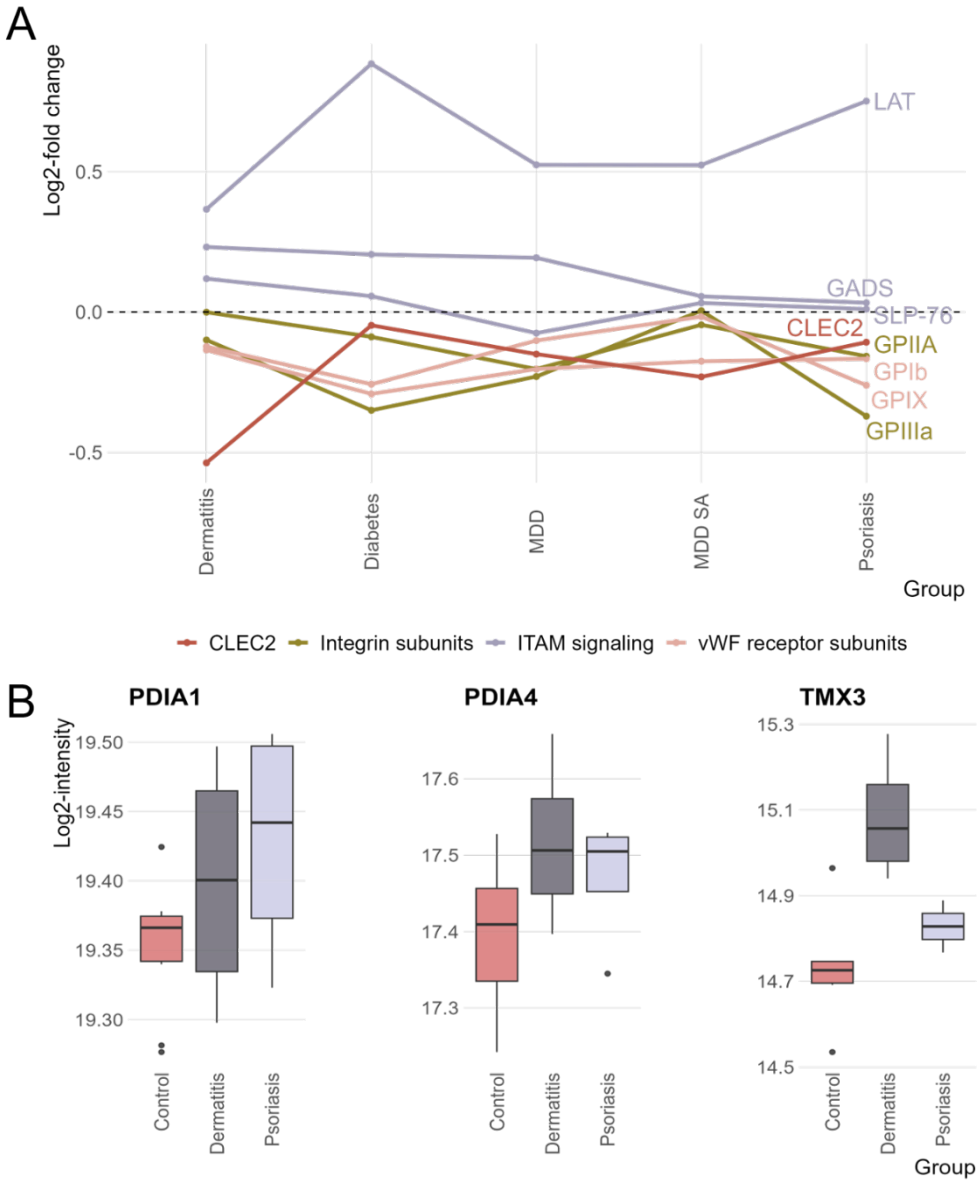

Figure 6. Specific protein dynamics across groups. (A) Profile plot of the studied receptors and proteins related to the immunoreceptor tyrosine-based activation motif (ITAM) signaling. **(B)** Boxplots of the expression of disulfide isomerases (PDI) in the dermatitis and psoriasis groups, against the healthy controls. vWF: von Willebrand factor.

Discussion

Platelet proteomics to differentiate between and study two murine models of ITP

Primary immune thrombocytopenia (ITP) is an autoimmune disease that is currently poorly understood, in terms of both the factors that trigger its onset and its management. In the first Chapter of this Thesis, we set out to characterize the platelet proteome of two murine ITP models, with the two-fold objective of further advancing our understanding of this disease, at the molecular level; and determining if the platelet proteome was able to distinguish between health and disease.

Firstly, our results show that the platelet proteomes between the healthy platelets and those from the two ITP murine models are indeed different, and not only that, but that the proteomics analysis was also able to differentiate between the two murine models, and even the treatment condition. Furthermore, they suggest that platelets may be generally dysfunctional, or hyporesponsive, probably due to the effects of basal activation and degranulation in the circulation. This hyporesponsiveness particularly affected platelets from the P-ITP model, while those from the A-ITP model showed a marked tendency towards mitochondrial dysfunction.

However, another level to consider is the “age” of the platelets analyzed in each model at the thrombocytopenic or recovered (PLT count) states. The pathological dynamics of platelet clearance and platelet production in ITP may affect their quality and function, as well as their turn-over. Interestingly, the mitochondrial defects we observed in active ITP are comparable to aging platelets[181]. Noteworthy, a slower turn-over of platelets has been reported in ITP patients[300], which might be the reason behind the proteome differences identified in our active ITP model, characterized, hypothetically, by circulating older and hyporeactive platelets.

A previous proteomics analysis of bone marrow megakaryocytes showed the down-regulation of five apoptosis-related proteins (HSPA6, HSPA8, ITGB3, YWHAH, and PRDX6) in newly diagnosed ITP patients without treatment[301]. Four of those proteins

(HSPA6 is not found in mice) are also differentially down-regulated in P-ITP D3, which we proposed as equivalent to newly diagnosed ITP. These data support the notion that, in addition to proteomics alterations caused in the circulation, some of the protein dynamics observed may occur at the megakaryocyte level. Another proteomics study achieved similar results as us, but associated the resulting proteins to autophagy[302].

Interestingly, treatment of ITP patients with Fostamatinib, a Syk inhibitor, is more effective in PLT count recovery and results in less bleeding events when implemented as second-line compared to third-or-later-line of treatment[303] (*i.e.*, chronic ITP). We observed downregulation of Syk in P-ITP D3 platelets (*i.e.*, acute), and partial restoration in A-ITP (*i.e.*, chronic). Extrapolated to human, our results may explain why Fostamatinib is safer in terms of bleeding as second-line treatment: it does not affect platelet functionality through Syk inhibition, because it is already downregulated in newly diagnosed ITP. However, variation in Syk levels in chronic ITP may result in an increased risk of bleeding events, and reduced clinical responses. Our results highlight the potential of applying platelet proteomics to profile human ITP, aiming at the adjusted personalized patient management.

Investigation of the similarities between the platelet (and megakaryocytic) proteomes of mouse and human

Clinical applications of platelet and megakaryocyte proteomics studies

We devoted Chapter II to study the similarity between mouse and human in terms of the platelet proteome, and thus respond to the question of whether results on this front could be extrapolated between species. The analysis of the platelet proteome and sub-proteomes (releasates / secretomes, phospho-proteome, platelet-derived extracellular vesicles, etc.) poses as a promising means not only to better understand platelet function and production, but also to identify novel biomarkers for disease diagnosis and prognosis. Furthermore, the increasing demand to develop novel and more-specific anti-platelet / anti-aggregant drugs for the management of thrombosis will benefit from the

rigorous dissection of platelet signaling cascades, where phospho-proteomics may play a relevant role.

Platelets represent a critical factor in the onset and progression of cardiovascular diseases, which globally account for one of the top-ten leading causes of death worldwide[304]. A study by Maguire *et al*. (2020)[305] identified distinct proteomic signatures in platelet releasates from patients at different stages of progression of symptomatic cardiovascular disease, and another study by García *et al*. (2016)[306] even observed differences in the proteomes of intracoronary and peripheral platelets in patients of acute myocardial infarction. Regarding genetic platelet disorders, a comprehensive quantitative proteomics analysis revealed that platelets of patients carrying individual mutations in the transcription factors GATA1, GFI1B or RUNX1 had a distinct proteome profile, while displaying similar platelet morphological and functional abnormalities[205].

In the field of transfusion medicine, there is a concern on how to maintain the integrity and functionality of platelets in the platelet concentrates to be transfused. The so-called platelet storage lesion (PSL), appears with more evidence in longer-stored platelet concentrates, and manifests conditioned by all the steps involved in platelet concentrate production and storage[307]. The application of proteomics identified a number of hallmarks that could be associated with PSL, starting from proteomic differences related to platelet apoptosis[308], to a differential expression of proteins related to platelet degranulation or structural ones[192]. Another aspect of concern is the impact of pathogen reduction treatments on platelet concentrates, a safety measure to reduce the inherent risk for bacterial contamination of platelet concentrates[309]. Proteomics studies on platelet concentrates treated or not with Mirasol Pathogen Reduction Technology, also revealed specific alterations, although marginal, which were not exclusively due to an accelerated PSL, contrary to what was earlier thought[165].

The similarity of the mouse and human platelet proteome provides a solid foundation to the studies performed on mouse models, such as the one depicted in the

previous Chapter, where we characterized and compared the platelet proteome of two mouse models of ITP, at the thrombocytopenic stage and after platelet count recovery[204]. Interestingly, the application of proteomics in the field has allowed the exploration of the platelet proteomes and secretomes in other species, such as squirrels, dogs and, more recently, bears[310-312]. The particular physiological or pathological condition on each model provides with new knowledge with potential direct applications in evolutionary science, veterinary medicine, and importantly, with potential translation into humans. An example is the case of the study of the platelet proteomes of hibernating squirrels, that reach body temperatures of 4–8°C. Physiological differences have been observed in the platelet proteome of squirrels (hibernating vs active) which might translate into developments to improve the cold storage of human platelets used for transfusion, in an effort to minimize platelet activation at the same time as relenting the storage lesion[310]. Also in hibernating animals, in this case bears, and in comparison with humans subject to chronic immobilization, another study found a conserved thromboprotective platelet proteomics signature (chiefly led by the heat-shock protein HSP47), which could aid in the development of new therapeutic targets for the treatment of thrombotic events in immobilized patients[312].

In summary, given the function of platelets to facilitate thrombosis and hemostasis, quantitative (phospho)proteomics analyses of platelet proteomes/sub-proteomes, and of megakaryocytes, will provide molecular biomarkers for diagnosis and prognosis of platelet related pathologies or dysfunction, and even provide targets for anti-platelet drug development. On the other hand, considering the various and diverse roles of platelets during ontogeny, or in inflammation, platelet proteomics might pose a significant biomarker discovery tool in other pathologies, beyond those primarily related to platelets[274,277,278,313].

However, as it has been acknowledged by experts in the field, there are certain issues of concern regarding the application of high-throughput proteomics to the study

of platelet biology, ranging from the field-specific ones (such as blood sampling collection variables and sample processing), to the aspects related to mass spectrometry technological characteristics and data analysis themselves (detection low abundance peptides, modifications altering digestion, etc.). When applying proteomics to megakaryocytes, certain variables will also require to be acknowledged, such as the source (primary, or cultured *in vitro*), the homogeneity of the sample (differentiation status, contamination with other cell types), to name a few. Such variables account for inter-laboratory procedural differences that might limit cross-comparison of data and extrapolation of results to the clinical setting. As of today, mass-spectrometry proteomic analyses are still costly, many studies comprise a low number of samples, and data should be validated in larger cohorts; however, few institutions can afford to perform studies with an optimal number of samples that allows rigorous data analysis. As a consequence, regarding the applicability of platelet proteomics to the clinical field, there is a concern that the equipment may not be affordable by clinical institutions, and that proteomics analysis is complex and requires trained staff, precluding a globalized usage of the technique at the diagnostic clinical laboratory[314-316].

Considering all this, and despite having observed experimental differences in the datasets used in this study, we have also noticed consistency and reproducibility if we consider the relative abundance of detected proteins, and the identified GO terms from the enrichment analysis. Supporting our findings, Bayés *et al*. (2012)[317] studied human and mouse postsynaptic membranes at the protein level, and found a ~70% overlap after orthologue translation, similarly to what we have observed with the interspecies platelet proteomes and combining data from datasets from independent experiments. These suggests that it is possible to identify differences in the platelet proteome (or sub-proteome) associated with pathology, also inter-species wise.

In general, we propose that, for the field to move forward, common guidelines and points of concern should be established that help to improve the multi-laboratory

reproducibility of platelet preparation, sample processing and data analysis. Most importantly, all these variables should be carefully described in scientific communications, and access to raw data and/or data analysis through public repositories should be mandatory. Objectively, technological developments of mass spectrometers, with deeper detection capacities and more compact, will allow the reduction of costs for the analysis of large sample groups. The implementation of comprehensive pipelines of analysis, which are globally evolving in parallel, will also provide with more robust information at the clinical level. The quality of the generated data is improving over the years, and when technical limitations and heterogeneity are overcome, cross-study comparisons will be possible, aiding in the advance of the field. While crude mass spectrometry might be as of today unthinkable in the clinical diagnostic lab, it will surely aid biomarker discovery with potential application in the clinic, as customized protein multiplex detection assays can be designed with the information obtained from unbiased proteomic studies and implemented in the diagnostic lab. Lastly, we conclude from our *in silico* analysis that platelets from mice and humans share a proteome with high identity, which portrays mouse as an optimal pre-clinical model. The same conclusion was reached by Balkenhol *et al*. (2020)[318] on their systems biology study aimed at the *in silico* analysis of the central platelet signaling cascade and inter-species comparison. Furthermore, obtaining blood samples requires non-invasive methods, and if platelets (and their proteome) should reflect the health status of a patient, the application of platelet proteomics for diagnostic/prognostic purposes could potentially invade other clinical fields beyond haematopoiesis and transfusion medicine.

Multilayered proteomics picture of quiescent and activated platelets in health

In this third Chapter, we presented a complete characterization of the function, protein composition, signaling pathways and secretion of platelets under steady-state, healthy conditions, in the quiescent state or upon stimulation with a battery of agonists.

Furthermore, we put the focus on proteomics as an invaluable tool to study the different aspects of platelets, and delved into the challenges that stem from its use. Overall, we aimed at painting a picture that would not only advance and integrate our knowledge of how platelets function in health, but also set the basis for the study of platelets and platelet function under pathological states.

Firstly, and given the importance that proteomics had in the study, we set out to compare, in the case of platelet proteomics, two of the most widely used, open source softwares to analyze proteomics data at the spectra level: MaxQuant and FragPipe. We were interested in seeing which one, in our particular case *(i.e.*, lower number of proteins in the sample, and thus less peptide-spectrum matches [PSM], with no previous fractionation that could enhance the sensitivity), yielded a higher number of reliable identifications, and thus tackled the missing value problem better. In the end, and in line with what have been already been reported[319], FragPipe displayed a superior performance, identifying more PSMs per protein and thus providing more reliable quantification, and doing so almost 20 times faster. The one drawback of using FragPipe is that there are far less bioinformatic tools adapted to its output format and provided information, due to its more recent release.

Having settled in the tool of choice, we next characterized the proteome of the platelet lysate, that is, the whole platelet proteome. Although the field is still halfway in the detection of the predicted platelet proteome[156], studies using fractionation have been reporting the identification of around 4-5k proteins[320], and pointing to its high stability across healthy donors[158]. Since our data lacked that detection depth, we were interested in elucidating whether both the stability and the identification were also reliable and stable when the identification depth was much lower (*i.e.*, no fractionation), as it was the case of this study. The results confirmed the low variability of a core of proteins, across donors, which mostly correspond to the proteins with the highest abundance, which are reliably detected in all studies (see Chapter II). These observations confirm that, even at

lower detection rates, the platelet proteome remains stable, with the highest swing in both identification and quantification owing to the low-abundance proteins. However, although this provides with confidence when it comes to the study of the platelet proteome in disease, the low identification and quantification rates in relation to the least abundant proteins hampers the detection of the more subtle changes, and thus the studies might be biased towards the changes that affect highly abundant proteins.

Following the depiction of the protein cargo, we engaged on the study of the functionality of platelets. In spite of their small size, platelets display a myriad of surface receptors that interact with their environment and orchestrate how they behave[54]. For this set of studies, we chose five of the most important hemostatic and non-hemostatic receptors in platelets, namely: vWF receptor or GPIb-V-IX, PAR1, integrins $\alpha_{II}\beta_1$ and $\alpha_{IIb}\beta_3$, CLEC2 and GPVI, and stimulated them with dedicated agonists. We performed two functional assays to study the aggregation and degranulation responses of platelets, under each stimulus, which revealed that in both cases, the stimulation of GPVI, integrin $\alpha_{IIb}\beta_3$ and PAR1 elicited the most dramatic responses. Activation of GPIb-V-IX by ristocetin seemed to trigger a very different response, promoting the agglutination of platelets, without little impact on the degranulation response.

To further investigate the underlying signaling pathways, we used a proteomics approach to quantify the different dynamics of the platelet phosphoproteome. Across all conditions, we detected 1454 phosphorylation sites, and up to 899 (62%) were differently regulated in a collective manner, similar to or even above the numbers reported in other studies[321]. We found the biggest changes after PMA and CVX stimulation, followed by TRAP6, and revealed that they were also very similar amongst them. This points to the fact that, under physiological conditions (or close to them), platelets undergo two waves of activation: the first one owing to the triggering of the individual receptor, followed by a feedback potentiation by ADP release, TXA_2 generation, and integrin inside-out $\alpha_{IIb}\beta_3$ activation[322]. Our analysis measured many well-known modifications that are primarily

associated with the different steps of GPVI activation[323], such as members of the SFK family, GADS, or PKC; as well as cytoskeleton proteins and members of the degranulation machinery[324]. In parallel, dephosphorylation events were detected in inhibitory proteins, such as PKA and phosphatases, but also in the pleckstrin-SDPR complex, which are both phosphorylated by PCK[325]. Interestingly, these dynamics were also observed after PMA stimulation, an agonist that is capable of not only interacting with the outside-in signaling of the $\alpha_{IIb}\beta_3$ integrin, but also eliciting activation by directly interacting with PKC. This last fact is reflected in the data by the high levels of phosphorylation presented by FLNA, which has been shown to mediate PKC activation and promote β1 integrin activation[326]. For its part, collagen was the only agonist that showed hyperphosphorylation of DAPP1, which could potentially explain the lesser response, since it has been shown it is a negative regulator of collagen-mediated activation[327]. At the same time, it is known that activation of both GPVI and integrin $\alpha_{II}\beta_1$ by collagen is dependent on the release of the secondary mediators, which explains the delayed aggregation curve, and thus the strength of the response is not as robust as with CVX[328,329]. As for AggA, it displayed a profile resembling that of GPVI, but with less identifications, corroborating what was seen in the degranulation assay. Lastly, ristocetin exhibited an interesting profile, which greatly differed from the other conditions. Not only did it hardly activate, as its high number of missing values portrayed (*i.e.*, no phosphorylation is occurring), but also presented with an opposite dynamic as far as the phosphorylation of KSR1 was concerned. KSR1 is an intriguing protein, barely characterized in platelets, and only recently seen involved in their signaling[323,330]. It is known to be a scaffold for the Raf/MEK/ERK kinase cascade[331], and a binding partner of the 14-3-3 family of proteins in platelets, which mediate the signal transduction of the ristocetin receptor, GPIb-V-IX[332].

The proteomics analysis of the proteins released after activation (*i.e.*, secretome) further confirmed that ristocetin triggered a distinct platelet response, hinting to an equal

preference in the degranulation of both alpha and dense granules, which was not seen with the other agonists, whose profiles were mostly of the former. However, these results have to be interpreted carefully. The fact that almost all identified proteins were also present in the control condition, and thus the reported differences came only from the quantitative side, pointed to a basal, albeit light, unavoidable activation of platelets resulting from their handling. In addition, this could also originate from the fact that the same amount of protein was fed to the spectrometer in all cases, which hinders the normalization of the data and thus does not fully reflect the nature of the experiment (*i.e.*, the control condition does not secrete to the extent of the agonist conditions). This problem, added to the inherent limitations of the data-dependent acquisition (DDA) proteomics (*i.e.*, selection of the most abundant peptides/proteins)[143], hampers the sensitivity of the experiment. However, there was a clear quantitative profile that was dependent on the agonist, were both CVX and AggA elicited the most robust degranulation responses. On the other hand, in terms of identification, all the aforementioned proteins were also detected in similar studies[206,209,210,333] —although most of them used thrombin or PAR agonists—, with the sole exception of ristocetin, whose secretory profile was mostly unique.

Overall, after integration of the different layers of platelet activation, it is apparent that stimulation of GPVI with CVX triggered the most robust, fast response in terms of aggregation with other platelets, firing of signaling pathways and release of granule content[329]. Activation of CLEC2 by AggA, although sharing most of its signaling machinery with GPVI, presented with more modest responses, as it was made evident in the functional assays. For their part, activation of PKC and outside-in integrin signaling by PMA, and stimulation of PAR1, both translated also in drastic responses; while the interaction between ristocetin and the GPIb-V-IX complex induced an agglutination response, with little and distinct degranulation. This gradient in the effect of the activation loosely correlates with the expression of these receptors on the platelet surface (*i.e.*,

copy number)[158], pointing to additional factors controlling the process. These factors include successive activation loops or amplification signals, as a result of the synergy among pathways and receptors, so that an optimal response can be reached[334,335]. This fact makes it difficult to discern the individual contributions of each of the receptors, which would entail the use of dedicated cocktail of inhibitors to prevent the release of secondary mediators (ADP, TXA_2) and thus the propagation of the response[336].

In summary, we provide extensive data resources of the activation of each of the receptors, along with a robust analysis, that aims at profiling how platelets behave in steady-state conditions, at the cellular and molecular level. Although we report overall signaling changes, our findings also discern steps of the specific pathways. This is particularly important, because most studies so far had focus on the characterization of the activation of ITAM receptors. Hence, this opens the door not only to the study of how therapeutical agents may affect platelet signaling, but also to the characterization of the platelet phenotypes in disease. Additionally, we underscore the utility of quantitative proteomics, let it be labelled or label-free, in the profiling of platelet activation mechanisms, and the connection of the platelet phenotypes with health and disease.

Multilayer proteomics picture of quiescent and activated platelets in health

Lastly, in Chapter IV, we presented a multilayered cellular and molecular description, by means of functional assays, flow cytometry, *in vitro* culture, and proteomics, of how chronic low-grade inflammation impacts megakaryocytes and platelets, and we further demonstrate that there are differences between pathologies, but with a consistency within those with a similar etiology (*i.e.*, psoriasis and atopic dermatitis).

Although the relationship between this type of inflammation and an affected megakaryocyte-platelet axis has already been stablished, there is little knowledge regarding the details of how it affects said axis, and without the presence of certain

cofounders. In this study, we selected patients so that any influence caused by medication, comorbidities, or hyperglycemia (in the case of the diabetes group) was removed, and thus to be able to investigate the single impact of low-grade inflammation, as isolated as possible. Our results showed that, although inflammation is affecting all cohorts at all phenotypic levels, while CBC parameters remained the same, it is doing so in varying intensity, correlating in a way with its systemic contribution to each disease.

In diabetes, the general consensus points to a pro-thrombotic state, characterized by altered platelet indices, enhanced surface adhesion, increased membrane surface expression of activation markers such as P-selectin, and hyperactivity both in their aggregation and degranulation responses, which increase after agonist stimulation[337-339]. All of this, however, does not entirely match what was seen in this study, despite the fact that the platelets from this cohort displayed an hyperactivated state, too, with augmented P-selectin and increased degranulation responses, although it did not extend to the adhesion or aggregation responses. Interestingly, two surface receptors were underrepresented: the GPIbα subunit of the vWF receptor (GPIb-V-IX), and the GPIIbα subunit of the integrin $\alpha_{IIb}\beta_3$, which are the two receptors chiefly involved in the hemostatic function of platelets, and thus potentially pointing to the environment favoring an inflammation profile in platelets. In the case of GPIbα, it is well-documented that they are subject to metalloproteinase-induced shedding in circulation[340,341]; however, GPIIbα does not, so it could be plausible that its downregulation is inherited from the megakaryocytic progenitors.

Thus, in the absence of hyperglycemia, this shift that seems to favor the inflammatory function of platelets rather than the thrombotic role, points to a potential fine-tuning driven by the inflammatory milieu. The impact of the insulin treatment cannot be ruled out as a potential cause, although one study found increased levels of P-selectin in platelets from first degree relatives of diabetic patients[342]. As for the impact in megakaryopoiesis, the higher abundance of MEP and related progenitors, which

correlated with a small decrease in the percentage of megakaryocytes, did not seem to affect the final platelet count or related indices, meaning that other paths are taken to assure the balance (*i.e.*, extramedullary megakaryopoiesis, in the spleen or lung). All in all, the prothrombotic platelet phenotype seems to follow the appearance of hyperglycemia, but already-present low-grade inflammation at the onset of the disease preludes some of the changes that are seen later on.

For their part, it is well-known that atopic dermatitis and psoriasis patients present with a pathogenesis mainly driven by regulatory T cells (Tregs), which contribute to the prevention of autoimmune disease by suppressing immune responses[343,344]. However, in these skin-related diseases, Tregs display an impairment in this suppression leading to an altered T-helper (Th)/Treg balance[345]. Interestingly, immunophenotyping of the nucleated, CD31 compartment of PBMCs, showed a marked disbalance that favored the $CD31^{-}$ subpopulation in these two pathologies. CD31 or PECAM-1, traditionally an endothelial marker, is also expressed by platelets and megakaryocytes, but also by all leukocytes[346]. Several studies have highlighted its key role in the regulation of T-cell (and also B-cell) homeostasis and function, helping to maintain peripheral tolerance by means of raising the activation threshold of their antigen-receptor signaling[347]. Therefore, impairment of CD31 function is associated with excessive immunoreactivity, as the one that occurs in atopic dermatitis and psoriasis, where we have observed a loss in this marker. However, although we cannot confidently determine what lineage (or lineages) of cells are the ones losing this marker, the shift specially affected the $CD31^{mid}$ subpopulation, where lymphocytes are most present.

Furthermore, the reduced aggregation capacity of platelets when the two main non-hemostatic receptors, CLEC2 and GPVI, when stimulated (due to a downregulation of both of them), or the reduced expression of PF4 (with contributes to the recruitment of inflammatory cells)[348], may point to a response of the megakaryocyte-platelet axis to prevent an exacerbation of the immune response. However, the respective enhanced

secretory response and the upregulation of proteins belonging to their signaling pathway, might be favoring the secretory function of platelets, under this setting. On the other hand, upregulation of the PDIs might be enhancing platelets interactions with neutrophils[349], and thus directly contributing to their extravasation to the skin, further sustaining the injuries[350].

Lastly, the case of the MDD relationship with inflammation is an intriguing one, since it seems to go both ways[351,352], that is, MDD patients display an inflammatory signature per se, which may lead to CVD complications[353]; but also patients with inflammatory-based diseases, such as the ones mentioned in this study, have a higher risk of developing MDD in the long run[354]. Nevertheless, many studies have reported MDD displaying hyperactivated platelets, both in steady-state and after agonist stimulation; and having an impact on thrombopoiesis, since the most reported alterations are related to platelet count and indices[355,356]. In this study, the MDD cohorts showed mild inflammation-driven changes compared to the other cohorts, and while there was indeed a hypersecretion after CLEC2 stimulation, we did not find any differences regarding the immunophenotype of platelets, other than a slight upregulation of the $\alpha_{II}\beta_1$ receptor and a downregulation of the GPIbα subunit. Similarly, no changes were observed on the CBC, although they displayed reduced megakaryocyte percentages throughout the differentiation process *in vitro*. Of note, we did observe a consistent overexpression of CD9 after stimulation with all agonists. CD9 is a member of the tetraspanin superfamily, present both in the surface and alpha granule membranes of platelets[357]. Since no overexpression was found in the immunophenotype, we can conclude that this increased expression occurs within the alpha granules. Interestingly, CD9 has been reported to have a physical link with the $\alpha_{IIb}\beta_3$ integrin, and could act as a repressor of said integrin inside-out signaling[358], meaning that the activation elicited by CLEC2 and GPVI could have potential anti-hemostatic functions in this particular setting. Lastly, this milder response to low-grade inflammation in comparison to the other cohorts

could be in response to lower cytokine levels in circulation, due to either the disorder per se, or the antidepressant regiment of the patients, which has been seen to modulate – to some extent – said levels[359,360].

However, some limitations in this study should be taken into consideration, such as the small number of patients per group, and the fact that it was focused chiefly on platelets, and to a lesser extent on megakaryocytes, and thus other hematopoietic lineages were not studied to see how low-grade inflammation globally impacts hematopoiesis. Additionally, we could not rule out the modulating impact that indispensable medication (*i.e.*, drugs needed to control the studied diseases, such as insulin or antidepressants) could have had; and that the proteomics experiment was conducted without any previous fractionation, and thus there was a bias towards highly abundant proteins.

In summary, the study of the different patient cohorts identified common, low-grade inflammation signatures in respect to the megakaryocyte-platelet axis, at the same time that underscored the existence of specific profiles underlying each of them, grouped by etiology. It also pointed to a capital role of the two non-hemostatic receptors, CLEC2 and GPVI, in regulating both the immune role of platelets, and the hemostatic one, and whose signaling pathways and interactions could be potential therapeutic agents to ameliorate or alleviate the progression of these diseases. At the same time, it showed that the platelet surface and cargo displayed an accentuated inflammatory and immune profile, further supporting the fine-tuning caused by the environment. All of this highlights the importance and concrete roles of platelets in low-grade inflammatory diseases, and how the specifics of each setting are able to further tune all aspects of their phenotype and function, advancing our knowledge of these diseases and uncovering potential therapeutic targets.

General overview

Throughout this Thesis, we set out to study platelets and megakaryocytes in health and disease, in different species, and to highlight the use of proteomics as an essential tool for the study of the many aspects of the platelet biology. Firstly, we used this very same technique to interrogate the platelet proteome of two different murine models of immune thrombocytopenia, to see whether it was able to discern between the healthy and pathological states. We found notable differences not only between these two, but also between the two murine models, and even the treated (recovery) condition, further proving the sensibility and utility of this tool. Furthermore, we performed a systematic review and a complementary data analysis on the differences and similarities of the murine and human platelet proteomes, pondering on whether the potential results found in the former could be extrapolated to the latter.

Given the positive results found in the first two Chapters, we then set out to perform a thorough characterization of the platelet functionality and proteomics in health, to set the basis for its study in disease. For this, we first compared which of the two most common, freely available software for the processing of proteomics data was best suited to the interrogation of our data. Having settled on that, we checked the stability and variability of the platelet proteome, and studied the process involved in all of the functions of platelets: their activation. Continuing with our goal of mapping, as meticulously as possible, the many aspects of platelet activation, we conducted functional assays, and subsequent phosphoproteomics and secretome analysis, after stimulation with a battery of agonists, something that had never been done before. This exhaustive profiling, aiming at mapping the signaling pathways of the key hemostatic and non-hemostatic platelet receptors, revealed the extent and specificity of the responses, but also the underlying synergy that characterizes platelet activation. Interestingly, it unveiled the particular response elicited after ristocetin activation, which displayed a unique profile

aimed at promoting an agglutination response, rather than a full secretion and aggregation response.

Lastly, we wondered whether chronic low-grade inflammation had an impact on megakaryopoiesis, thrombopoiesis and platelets themselves, hypothesizing that this particular environment could be tailoring the megakaryocytic lineage to suit its needs. However, we were also interested in elucidating if those changes were happening only at the progenitor level, or whether inflammation also affected platelets in circulation. Or whether it was a combination of the two. We investigated the influence of this kind of inflammation in non-hemostatic diseases (namely diabetes type 1, psoriasis, atopic dermatitis, and major depressive disorder, concurrent or not with suicidal attempt), and similarly to what it was done in health, we performed functional, immunophenotyping and proteomics assays, as well as *in vitro* cultures to map megakaryopoiesis. The results showed that chronic low-grade inflammation was indeed affecting all aspects of platelets (and to a lesser extent, of megakaryocytes), and that it was doing so in a specific manner, where each disease had a particular functional and phenotypic platelet profile, suggesting that inflammation has a distinct impact depending on the origin and extent of the pathology. It also showed a common proteomics inflammatory signature, further underscoring the potential of proteomics to unravel the consequences of this fine-tuning on platelets, and how we could harness it in the search for biomarkers and new therapeutical targets, as well as advancing our knowledge of the underlying disease.

It is worth mentioning that, since this Thesis started, a handful of studies were published that corroborated our results. For instance, several groups investigated the differences in the platelet proteome of a number of inherited platelet disorders[205,320], or in the phosphoproteome of an obese cohort[361], and the platelet releasate of pregnant women[210]. All of them found that the platelet proteome and sub-proteomees differed in this pathological / non-physiological conditions, and that did so specifically, similarly to what we found. In addition, another group pointed to the extravascular vesicles (EVs)

produced by platelet themselves under inflammation, as the means by which megakaryopoiesis was been altered[122]. This all adds to growing body of evidence that confirms that the health status has an impact on the platelet cargo and functionality, as well as megakaryopoiesis.

However, although there has been plenty of studies highlighting the role of acute inflammation in affecting the phenotype and activation of platelets, not many had directed their efforts towards their study under chronic low-grade inflammation. Although many interesting observations were shown during this Thesis, specific to each of the studied diseases, there was an emerging common thread regarding the CLEC2 and, to a lesser extent, GPVI receptors, both of which are considered the platelet immune receptors[61]. The ligands of both receptors, collagen and podoplanin, respectively, can be found at sites of vascular injury, although their participation in the hemostatic response[362,363]. Thus, both in the murine models of ITP as well as in the chronic low-grade diseases studied in human, a delay in the aggregation response after CLEC2 stimulation was seen. This phenomenon could be a response of the organism to prevent further exacerbation of the inflammatory response. However, the underlying mechanism that potentially explains why this is happening seems to differ between diseases. In ITP, the proteomics data points to a down-regulation of this receptor, although in the human diseases, nor these type of data or the immunophenotype alludes to a defect in its expression, and thus it could be plausible that this could be caused by a dysfunction in its signaling pathway. Future studies could delve in this particular question.

Limitations and future perspectives

In spite of the fact that the experimental design was conceived to take into account possible cofounding factors and the effect size, we are aware that a larger cohort, for each disease, will be necessary to confirm these results. This extends to the results in preclinical models, which should be further confirmed in human cohorts. It would also be interesting to replicate the phosphoproteomics analysis perform on the

healthy donors, in the disease groups. It is likely that many of the defects seen at the functional and phenotype level further propagate, or have their roots, in signaling abnormalities. Furthermore, the main way by which platelets exert their different functions is by secreting a myriad of bioactive molecules, either directly or by the exocytosis of EVs. Hence the study of the different releasates or EV cargo in disease will also hint at this directed modulation. Of note, all the samples required to address the aforementioned future perspectives are already collected (namely, ITP human patients, and phosphoproteome and secretome of chronic low-grade inflammation cohorts).

This leads us to another limitation of the study, which is related to the cost of the proteomics experiments. Even though this particular omic has greatly advanced in recent years, it is still falling behind the other omics (namely genomics and transcriptomics), and this is chiefly highlighted in its cost. This fact precluded not only the performance of certain experiments (*i.e.*, phosphoproteomics and secretome), but also the depth at which we could interrogate the different platelet proteomes. And although we made sure that this did not reflect on the reproducibility and stability of our results, it is nonetheless true that, if no previous fractionation is performed, the identification depth shrinks considerably.

Lastly, it would also be interesting to expand the results seen in *in vitro*, widening the characterization to other lineages, as well as corroborating the results regarding the biomarkers, so that we can start investigating their true potential in designing new therapeutical targets, as well as tools for the diagnosis and prognosis of these diseases.

Conclusions

1. The platelet proteome allows the discrimination of healthy and pathological states, since platelet specific protein profiles associate with different subtypes within a disease or recovery status, as it was seen with the two murine preclinical models of immune thrombocytopenia.

2. Platelet proteomics coupled with functional assays revealed a downregulation and defect in the Clec2 pathway in the passive (acute) model of immune thrombocytopenia, which recovered only partially after treatment with IVIg.

3. The murine and human platelet proteomes and sub-proteomes are comparable, and thus allowing for the extrapolation of results between species.

4. Technological advances in the proteomics field allow the comparison of datasets from different labs, whenever certain quality thresholds are abode, disrupting the paradigm.

5. Differential activation of platelet receptors highlights the existing synergy between them at the phosphoproteome and secretome levels, save the stimulation of the vWF receptor by ristocetin, that elicits an agglutination response with minimal pathway activation.

6. Chronic low-grade inflammation impacts hematopoiesis, megakaryopoiesis and platelets, and it does so differently, depending on the disease, albeit maintaining common features when there is a common etiology (*i.e.*, psoriasis and atopic dermatitis).

7. Chronic low-grade inflammation affects hematopoiesis by provoking a loss of CD31/PECAM-1 in the PBMC compartment in psoriasis and atopic dermatitis; and megakaryopoiesis, by reducing the percentages of the different stages of megakaryocytic maturation in all diseases. It also induces a blockade at the MEP stage in diabetes or unrestricted erythroid development at the expense of megakaryocytes, despite megakaryocytic promoting conditions in culture.

8. Chronic low-grade inflammation shapes platelets via the tailoring of the CLEC2 and GPVI receptors, and corresponding pathways. This promotes an hyperresponsive degranulation profile after dedicated agonist stimulation, with a limited or no effect on the aggregation response, suggesting a targeted tuning of the two non-hemostatic receptors to deal with the inflammatory environment.

9. The proteomic profile of platelets under chronic low-grade inflammation displays an inflammatory signature.

10. The proteomic profile of platelets can be used as a source of biomarkers in diseases beyond those that inherently affect platelets. Platelets are mirrors of the health status.

Conclusiones

1. El proteoma de las plaquetas permite discriminar entre estados de salud y patológicos, puesto que cada perfil proteico se asocia con diferentes subtipos bien de enfermedad o de recuperación, como se ha podido ver con los dos modelos murinos preclínicos de trombocitopenia inmune.

2. El uso conjunto de la proteómica de plaquetas y de ensayos funcionales ha mostrado una disminución o defecto en la ruta del receptor Clec2 en el modelo pasivo (agudo) de trombocitopenia inmune, cuya recuperación tras administración de IVIg fue solo parcial.

3. Los proteomas y sub-proteomas de plaquetas de ratón y humano son comparables, y por tanto permiten la extrapolación de resultados entre las dos especies.

4. Los avances tecnológicos en el campo de la proteómica permiten la comparación de bases de datos entre diferentes laboratorios, siempre y cuando se alcancen ciertos umbrales de calidad.

5. La activación diferencial de los receptores plaquetarios subraya la sinergia existente entre los mismos, a nivel tanto del fosfoproteoma como del secretoma. La excepción se encuentra en la estimulación con el agonista ristocetina del receptor de von Willebrand, que induce una aglutinación con una mínima activación de su ruta.

6. La inflamación crónica de bajo grado tiene un impacto sobre la hematopoyesis, megacariopoyesis y las plaquetas, y además, este es distinto dependiendo de la enfermedad, aunque con rasgos comunes cuando la etiología es común (*i.e.*, psoriasis y dermatitis atópica).

7. La inflamación crónica de bajo grado afecta a la hematopoyesis provocando la pérdida del marcador CD31/PECAM-1 en el compartimento de células mononucleadas de sangre periférica, en psoriasis y dermatitis atópica. Afecta también a la megacariopoyesis, reduciendo los porcentajes de los megacariocitos en diferentes estadios de diferenciación, en todas las enfermedades estudiadas. Por

último, induce un bloqueo madurativo en diabetes, a nivel del progenitor megacariocítico-eritrocítico bipotente, promoviendo la diferenciación del linaje eritrocítico a expensas del megacariocítico, a pesar de que las condiciones de cultivo favorecen la maduración de este último.

8. La inflamación crónica de bajo grado afecta a las plaquetas por medio de la modulación de los receptores CLEC2 y GPVI, y sus rutas de activación correspondientes. Esto promueve un perfil de degranulación hiperreactivo tras estimulación con agonistas, y un efecto limitado o inexistente sobre la respuesta de agregación. Este hecho sugiere una afectación dirigida de los dos receptores no hemostáticos, con el objetivo de adaptarse al ambiente inflamatorio.

9. El perfil proteómico de las plaquetas bajo una inflamación crónica de bajo grado muestra una firma inflamatoria.

10. El perfil proteómico de las plaquetas puede ser utilizado como una fuente de biomarcadores en enfermedades que van más allá de las que afectan de forma inherente a las plaquetas. Las plaquetas son espejos del estado de salud.

Bibliography

1. Olson OC, Kang Y-A, Passegué E. Normal hematopoiesis is a balancing act of self-renewal and regeneration. *Cold Spring Harbor perspectives in medicine*. 2020;10(12):a035519.

2. Zhu J, Emerson SG. Hematopoietic cytokines, transcription factors and lineage commitment. *Oncogene*. 2002;21(21):3295-3313.

3. Seita J, Weissman IL. Hematopoietic stem cell: self-renewal versus differentiation. *WIREs Systems Biology and Medicine*. 2010;2(6):640-653.

4. Cheng H, Zheng Z, Cheng T. New paradigms on hematopoietic stem cell differentiation. *Protein & Cell*. 2019;11(1):34-44.

5. Velten L, Haas SF, Raffel S, et al. Human haematopoietic stem cell lineage commitment is a continuous process. *Nature Cell Biology*. 2017;19(4):271-281.

6. Karamitros D, Stoilova B, Aboukhalil Z, et al. Single-cell analysis reveals the continuum of human lympho-myeloid progenitor cells. *Nature Immunology*. 2018;19(1):85-97.

7. Sanjuan-Pla A, Macaulay IC, Jensen CT, et al. Platelet-biased stem cells reside at the apex of the haematopoietic stem-cell hierarchy. *Nature*. 2013;502(7470):232-236.

8. Shin JY, Hu W, Naramura M, Park CY. High c-Kit expression identifies hematopoietic stem cells with impaired self-renewal and megakaryocytic bias. *Journal of Experimental Medicine*. 2014;211(2):217-231.

9. Haas S, Hansson J, Klimmeck D, et al. Inflammation-Induced Emergency Megakaryopoiesis Driven by Hematopoietic Stem Cell-like Megakaryocyte Progenitors. *Cell Stem Cell*. 2015;17(4):422-434.

10. Huang H, Cantor AB. Common features of megakaryocytes and hematopoietic stem cells: What's the connection? *Journal of Cellular Biochemistry*. 2009;107(5):857-864.

11. Yoshihara H, Arai F, Hosokawa K, et al. Thrombopoietin/MPL Signaling Regulates Hematopoietic Stem Cell Quiescence and Interaction with the Osteoblastic Niche. *Cell Stem Cell*. 2007;1(6):685-697.

12. Rodriguez-Fraticelli AE, Wolock SL, Weinreb CS, et al. Clonal analysis of lineage fate in native haematopoiesis. *Nature*. 2018;553(7687):212-216.

13. Machlus KR, Italiano JE, Jr. The incredible journey: From megakaryocyte development to platelet formation. *Journal of Cell Biology*. 2013;201(6):785-796.

14. Mazzi S, Lordier L, Debili N, Raslova H, Vainchenker W. Megakaryocyte and polyploidization. *Experimental Hematology*. 2018;57:1-13.

15. Eckly A, Heijnen H, Pertuy F, et al. Biogenesis of the demarcation membrane system (DMS) in megakaryocytes. *Blood*. 2014;123(6):921-930.

16. Richardson JL, Shivdasani RA, Boers C, Hartwig JH, Italiano JE, Jr. Mechanisms of organelle transport and capture along proplatelets during platelet production. *Blood*. 2005;106(13):4066-4075.

17. Avecilla ST, Hattori K, Heissig B, et al. Chemokine-mediated interaction of hematopoietic progenitors with the bone marrow vascular niche is required for thrombopoiesis. *Nature Medicine*. 2004;10(1):64-71.

18. Mbiandjeu S, Balduini A, Malara A. Megakaryocyte Cytoskeletal Proteins in Platelet Biogenesis and Diseases. *Thrombosis and Haemostasis*. 2021;122(05):666-678.

19. Lagrue-Lak-Hal A-H, Debili N, Kingbury G, et al. Expression and Function of the Collagen Receptor GPVI during Megakaryocyte Maturation. *Journal of Biological Chemistry*. 2001;276(18):15316-15325.

20. Malara A, Currao M, Gruppi C, et al. Megakaryocytes Contribute to the Bone Marrow-Matrix Environment by Expressing Fibronectin, Type IV Collagen, and Laminin. *Stem Cells*. 2014;32(4):926-937.

21. Kelemen E, Lehoczky D, Cserhati I, Krizsa F, Rak K. Demonstrability of a serum factor inducing thrombocytosis prior to acute rises of platelets in mice and men. *Acta Haematologica*. 1963;29:16-26.

22. Bartley TD, Bogenberger J, Hunt P, et al. Identification and cloning of a megakaryocyte growth and development factor that is a ligand for the cytokine receptor Mpl. *Cell*. 1994;77(7):1117-1124.

23. Doré LC, Crispino JD. Transcription factor networks in erythroid cell and megakaryocyte development. *Blood*. 2011;118(2):231-239.

24. Xavier-Ferrucio J, Krause DS. Concise Review: Bipotent Megakaryocytic-Erythroid Progenitors: Concepts and Controversies. *Stem Cells*. 2018;36(8):1138-1145.

25. Kanaji T, Vo M-N, Kanaji S, et al. Tyrosyl-tRNA synthetase stimulates thrombopoietin-independent hematopoiesis accelerating recovery from thrombocytopenia. *Proceedings of the National Academy of Sciences*. 2018;115(35):E8228-E8235.

26. Nakamura-Ishizu A, Matsumura T, Stumpf PS, et al. Thrombopoietin Metabolically Primes Hematopoietic Stem Cells to Megakaryocyte-Lineage Differentiation. *Cell Reports*. 2018;25(7):1772-1785.e1776.

27. Junt T, Schulze H, Chen Z, et al. Dynamic Visualization of Thrombopoiesis Within Bone Marrow. *Science*. 2007;317(5845):1767-1770.

28. Thon JN, Montalvo A, Patel-Hett S, et al. Cytoskeletal mechanics of proplatelet maturation and platelet release. *Journal of Cell Biology*. 2010;191(4):861-874.

29. Schachtner H, Calaminus SDJ, Sinclair A, et al. Megakaryocytes assemble podosomes that degrade matrix and protrude through basement membrane. *Blood*. 2013;121(13):2542-2552.

30. Abbonante V, Di Buduo CA, Malara A, Laurent P-A, Balduini A. Mechanisms of platelet release: in vivo studies and in vitro modeling. *Platelets*. 2020;31(6):717-723.

31. Bluteau O, Langlois T, Rivera-Munoz P, et al. Developmental changes in human megakaryopoiesis. *Journal of Thrombosis and Haemostasis*. 2013;11(9):1730-1741.

32. Orkin SH, Zon LI. Hematopoiesis: An Evolving Paradigm for Stem Cell Biology. *Cell*. 2008;132(4):631-644.

33. Crane GM, Jeffery E, Morrison SJ. Adult haematopoietic stem cell niches. *Nature Reviews Immunology*. 2017;17(9):573-590.

34. Lefrançais E, Ortiz-Muñoz G, Caudrillier A, et al. The lung is a site of platelet biogenesis and a reservoir for haematopoietic progenitors. *Nature*. 2017;544(7648):105-109.

35. Yeung AK, Villacorta-Martin C, Hon S, Rock JR, Murphy GJ. Lung megakaryocytes display distinct transcriptional and phenotypic properties. *Blood Advances*. 2020;4(24):6204-6217.

36. Erlacher M, Strahm B. Missing Cells: Pathophysiology, Diagnosis, and Management of (Pan)Cytopenia in Childhood. *Frontiers in Pediatrics*. 2015;3.

37. Fujisaki J, Wu J, Carlson AL, et al. In vivo imaging of Treg cells providing immune privilege to the haematopoietic stem-cell niche. *Nature*. 2011;474(7350):216-219.

38. Bogeska R, Mikecin A-M, Kaschutnig P, et al. Inflammatory exposure drives long-lived impairment of hematopoietic stem cell self-renewal activity and accelerated aging. *Cell Stem Cell*. 2022;29(8):1273-1284.e1278.

39. Nishimura S, Nagasaki M, Kunishima S, et al. IL-1α induces thrombopoiesis through megakaryocyte rupture in response to acute platelet needs. *Journal of Cell Biology*. 2015;209(3):453-466.

40. Davizon-Castillo P, McMahon B, Aguila S, et al. TNF-α–driven inflammation and mitochondrial dysfunction define the platelet hyperreactivity of aging. *Blood*. 2019;134(9):727-740.

41. Middleton EA, Rowley JW, Campbell RA, et al. Sepsis alters the transcriptional and translational landscape of human and murine platelets. *Blood*. 2019;134(12):911-923.

42. Roweth HG, Malloy MW, Goreczny GJ, et al. Pro-inflammatory megakaryocyte gene expression in murine models of breast cancer. *Science Advances*. 2022;8(41):eabo5224.

43. Tomaiuolo M, Brass LF, Stalker TJ. Regulation of Platelet Activation and Coagulation and Its Role in Vascular Injury and Arterial Thrombosis. *Interventional Cardiology Clinics*. 2017;6(1):1-12.

44. Sharda A, Flaumenhaft R. The life cycle of platelet granules [version 1; peer review: 2 approved]. *F1000Research*. 2018;7(236).

45. Holinstat M. Normal platelet function. *Cancer and Metastasis Reviews*. 2017;36(2):195-198.

46. Durán-Saenz NZ, Serrano-Puente A, Gallegos-Flores PI, et al. Platelet Membrane: An Outstanding Factor in Cancer Metastasis. *Membranes*. 2022;12(2):182.

47. Weyrich AS, Dixon DA, Pabla R, et al. Signal-dependent translation of a regulatory protein, Bcl-3, in activated human platelets. *Proceedings of the National Academy of Sciences*. 1998;95(10):5556-5561.

48. Quach ME, Chen W, Li R. Mechanisms of platelet clearance and translation to improve platelet storage. *Blood*. 2018;131(14):1512-1521.

49. Mason KD, Carpinelli MR, Fletcher JI, et al. Programmed Anuclear Cell Death Delimits Platelet Life Span. *Cell*. 2007;128(6):1173-1186.

50. Li J, van der Wal DE, Zhu G, et al. Desialylation is a mechanism of Fc-independent platelet clearance and a therapeutic target in immune thrombocytopenia. *Nature Communications*. 2015;6(1):7737.

51. Melchinger H, Jain K, Tyagi T, Hwa J. Role of Platelet Mitochondria: Life in a Nucleus-Free Zone. *Frontiers in Cardiovascular Medicine*. 2019;6.

52. Jin RC, Voetsch B, Loscalzo J. Endogenous Mechanisms of Inhibition of Platelet Function. *Microcirculation*. 2005;12(3):247-258.

53. Bye AP, Unsworth AJ, Gibbins JM. Platelet signaling: a complex interplay between inhibitory and activatory networks. *Journal of Thrombosis and Haemostasis*. 2016;14(5):918-930.

54. Rivera J, Lozano ML, Navarro-Núñez L, Vicente V. Platelet receptors and signaling in the dynamics of thrombus formation. *Haematologica*. 2009;94(5):700-711.

55. Offermanns S. Activation of Platelet Function Through G Protein–Coupled Receptors. *Circulation Research*. 2006;99(12):1293-1304.

56. Koupenova M, Ravid K. Biology of Platelet Purinergic Receptors and Implications for Platelet Heterogeneity. *Frontiers in Pharmacology*. 2018;9.

57. Koessler J, Hermann S, Weber K, et al. Role of Purinergic Receptor Expression and Function for Reduced Responsiveness to Adenosine Diphosphate in Washed Human Platelets. *PLOS ONE*. 2016;11(1):e0147370.

58. Cattaneo M. Platelet P2 receptors: old and new targets for antithrombotic drugs. *Expert Review of Cardiovascular Therapy*. 2007;5(1):45-55.

59. Nonne C, Lenain N, Hechler B, et al. Importance of Platelet Phospholipase Cγ2 Signaling in Arterial Thrombosis as a Function of Lesion Severity. *Arteriosclerosis, Thrombosis, and Vascular Biology*. 2005;25(6):1293-1298.

60. Watson SP, Herbert JMJ, Pollitt AY. GPVI and CLEC-2 in hemostasis and vascular integrity. *Journal of Thrombosis and Haemostasis*. 2010;8(7):1456-1467.

61. Rayes J, Watson SP, Nieswandt B. Functional significance of the platelet immune receptors GPVI and CLEC-2. *The Journal of Clinical Investigation*. 2019;129(1):12-23.

62. Zhi H, Rauova L, Hayes V, et al. Cooperative integrin/ITAM signaling in platelets enhances thrombus formation in vitro and in vivo. *Blood*. 2013;121(10):1858-1867.

63. Durrant TN, van den Bosch MT, Hers I. Integrin αIIbβ3 outside-in signaling. *Blood*. 2017;130(14):1607-1619.

64. Huang J, Li X, Shi X, et al. Platelet integrin αIIbβ3: signal transduction, regulation, and its therapeutic targeting. *Journal of Hematology & Oncology*. 2019;12(1):26.

65. Andonegui G, Kerfoot SM, McNagny K, Ebbert KVJ, Patel KD, Kubes P. Platelets express functional Toll-like receptor-4. *Blood*. 2005;106(7):2417-2423.

66. Hally K, Fauteux-Daniel S, Hamzeh-Cognasse H, Larsen P, Cognasse F. Revisiting Platelets and Toll-Like Receptors (TLRs): At the Interface of Vascular Immunity and Thrombosis. *International Journal of Molecular Sciences*. 2020;21(17):6150.

67. Heijnen H, van der Sluijs P. Platelet secretory behaviour: as diverse as the granules... or not? *Journal of Thrombosis and Haemostasis*. 2015;13(12):2141-2151.

68. Smith CW. Release of α-granule contents during platelet activation. *Platelets*. 2022;33(4):491-502.

69. Herter JM, Rossaint J, Zarbock A. Platelets in inflammation and immunity. *Journal of Thrombosis and Haemostasis*. 2014;12(11):1764-1775.

70. Nishikawa M, Tanaka T, Hidaka H. Ca2+-calmodulin-dependent phosphorylation and platelet secretion. *Nature*. 1980;287(5785):863-865.

71. Polgár Jn, Chung S-H, Reed GL. Vesicle-associated membrane protein 3 (VAMP-3) and VAMP-8 are present in human platelets and are required for granule secretion. *Blood*. 2002;100(3):1081-1083.

72. Ren Q, Wimmer C, Chicka MC, et al. Munc13-4 is a limiting factor in the pathway required for platelet granule release and hemostasis. *Blood*. 2010;116(6):869-877.

73. Italiano JE, Jr, Richardson JL, Patel-Hett S, et al. Angiogenesis is regulated by a novel mechanism: pro- and antiangiogenic proteins are organized into separate platelet α granules and differentially released. *Blood*. 2008;111(3):1227-1233.

74. Kamykowski J, Carlton P, Sehgal S, Storrie B. Quantitative immunofluorescence mapping reveals little functional coclustering of proteins within platelet α-granules. *Blood*. 2011;118(5):1370-1373.

75. Swinkels M, Hordijk S, Bürgisser PE, et al. Quantitative super-resolution imaging of platelet degranulation reveals differential release of von Willebrand factor and von Willebrand factor propeptide from alpha-granules. *Journal of Thrombosis and Haemostasis*. 2023.

76. Bizzozero G. Su di un nuovo elemento morfologico del sangue dei mammiferi e della sua importanza nella trombosi e nella coagulazione. *L'Osservatore*. 1881;17(3).

77. Scridon A. Platelets and Their Role in Hemostasis and Thrombosis—From Physiology to Pathophysiology and Therapeutic Implications. *International Journal of Molecular Sciences*. 2022;23(21):12772.

78. Martin JF, Paolo D'Avino P. A theory of rapid evolutionary change explaining the de novo appearance of megakaryocytes and platelets in mammals. *Journal of Cell Science*. 2022;135(24).

79. Anitua E, Prado R, Padilla S. Evolutionary Insight into Immunothrombosis as a Healing Mechanism. *International Journal of Molecular Sciences*. 2022;23(15):8346.

80. Martin JF, Wagner GP. The origin of platelets enabled the evolution of eutherian placentation. *Biology Letters*. 2019;15(7):20190374.

81. Claver JA, Quaglia AIE. Comparative Morphology, Development, and Function of Blood Cells in Nonmammalian Vertebrates. *Journal of Exotic Pet Medicine*. 2009;18(2):87-97.

82. Suzuki-Inoue K, Inoue O, Ding G, et al. Essential in Vivo Roles of the C-type Lectin Receptor CLEC-2: Embryonic/neonatal lethality of CLEC-2 deficient mice by blood/lymphatic misconnections and impaired thrombus formation of CLEC-2 deficient platelets. *Journal of Biological Chemistry*. 2010;285(32):24494-24507.

83. Carramolino L, Fuentes J, García-Andrés C, Azcoitia V, Riethmacher D, Torres M. Platelets Play an Essential Role in Separating the Blood and Lymphatic Vasculatures During Embryonic Angiogenesis. *Circulation Research*. 2010;106(7):1197-1201.

84. Echtler K, Stark K, Lorenz M, et al. Platelets contribute to postnatal occlusion of the ductus arteriosus. *Nature Medicine*. 2010;16(1):75-82.

85. Bénézech C, Nayar S, Finney BA, et al. CLEC-2 is required for development and maintenance of lymph nodes. *Blood*. 2014;123(20):3200-3207.

86. Gawaz M, Vogel S. Platelets in tissue repair: control of apoptosis and interactions with regenerative cells. *Blood*. 2013;122(15):2550-2554.

87. Levoux J, Prola A, Lafuste P, et al. Platelets Facilitate the Wound-Healing Capability of Mesenchymal Stem Cells by Mitochondrial Transfer and Metabolic Reprogramming. *Cell Metabolism*. 2021;33(2):283-299.e289.

88. Maouia A, Rebetz J, Kapur R, Semple JW. The Immune Nature of Platelets Revisited. *Transfusion Medicine Reviews*. 2020;34(4):209-220.

89. Aslam R, Speck ER, Kim M, et al. Platelet Toll-like receptor expression modulates lipopolysaccharide-induced thrombocytopenia and tumor necrosis factor-α production in vivo. *Blood*. 2006;107(2):637-641.

90. Carestia A, Kaufman T, Rivadeneyra L, et al. Mediators and molecular pathways involved in the regulation of neutrophil extracellular trap formation mediated by activated platelets. *Journal of Leukocyte Biology*. 2015;99(1):153-162.

91. Aloui C, Prigent A, Sut C, et al. The Signaling Role of CD40 Ligand in Platelet Biology and in Platelet Component Transfusion. *International Journal of Molecular Sciences*. 2014;15(12):22342-22364.

92. Engelmann B, Massberg S. Thrombosis as an intravascular effector of innate immunity. *Nature Reviews Immunology*. 2013;13(1):34-45.

93. Boilard E, Blanco P, Nigrovic PA. Platelets: active players in the pathogenesis of arthritis and SLE. *Nature Reviews Rheumatology*. 2012;8(9):534-542.

94. Scherlinger M, Richez C, Tsokos GC, Boilard E, Blanco P. The role of platelets in immune-mediated inflammatory diseases. *Nature Reviews Immunology*. 2023.

95. Caudrillier A, Kessenbrock K, Gilliss BM, et al. Platelets induce neutrophil extracellular traps in transfusion-related acute lung injury. *The Journal of Clinical Investigation*. 2012;122(7):2661-2671.

96. Palacios-Acedo AL, Mège D, Crescence L, Dignat-George F, Dubois C, Panicot-Dubois L. Platelets, Thrombo-Inflammation, and Cancer: Collaborating With the Enemy. *Frontiers in Immunology*. 2019;10.

97. Suzuki-Inoue K. Platelets and cancer-associated thrombosis: focusing on the platelet activation receptor CLEC-2 and podoplanin. *Hematology*. 2019;2019(1):175-181.

98. Amo L, Tamayo-Orbegozo E, Maruri N, et al. Involvement of Platelet–Tumor Cell Interaction in Immune Evasion. Potential Role of Podocalyxin-Like Protein 1. *Frontiers in Oncology*. 2014;4.

99. Leiter O, Walker TL. Platelets in Neurodegenerative Conditions—Friend or Foe? *Frontiers in Immunology*. 2020;11.

100. Leiter O, Seidemann S, Overall RW, et al. Exercise-Induced Activated Platelets Increase Adult Hippocampal Precursor Proliferation and Promote Neuronal Differentiation. *Stem Cell Reports*. 2019;12(4):667-679.

101. Hayon Y, Dashevsky O, Shai E, Varon D, Leker RR. Platelet Microparticles Promote Neural Stem Cell Proliferation, Survival and Differentiation. *Journal of Molecular Neuroscience*. 2012;47(3):659-665.

102. Ferrer-Raventós P, Beyer K. Alternative platelet activation pathways and their role in neurodegenerative diseases. *Neurobiology of Disease*. 2021;159:105512.

103. Pariser DN, Hilt ZT, Ture SK, et al. Lung megakaryocytes are immune modulatory cells. *The Journal of Clinical Investigation*. 2021;131(1).

104. Zufferey A, Speck ER, Machlus KR, et al. Mature murine megakaryocytes present antigen-MHC class I molecules to T cells and transfer them to platelets. *Blood Advances*. 2017;1(20):1773-1785.

105. Campbell RA, Schwertz H, Hottz ED, et al. Human megakaryocytes possess intrinsic antiviral immunity through regulated induction of IFITM3. *Blood*. 2019;133(19):2013-2026.

106. Claushuis TAM, van Vught LA, Scicluna BP, et al. Thrombocytopenia is associated with a dysregulated host response in critically ill sepsis patients. *Blood*. 2016;127(24):3062-3072.

107. Valle-Jiménez Xareni R, Sánchez-García Juan C, Revilla-Rodríguez E, et al. Modification of immunological features in human platelets during sepsis. *Immunological Investigations*. 2018;47(2):196-211.

108. Villa-Fajardo M, Palma MCY, Acebes-Huerta A, et al. Platelet number and function alterations in preclinical models of sterile inflammation and sepsis patients: implications in the pathophysiology and treatment of inflammation. *Transfusion and Apheresis Science*. 2022;61(2).

109. Montague SJ, Delierneux C, Lecut C, et al. Soluble GPVI is elevated in injured patients: shedding is mediated by fibrin activation of GPVI. *Blood Advances*. 2018;2(3):240-251.

110. Freishtat RJ, Natale J, Benton AS, et al. Sepsis Alters the Megakaryocyte–Platelet Transcriptional Axis Resulting in Granzyme B–mediated Lymphotoxicity. *American Journal of Respiratory and Critical Care Medicine*. 2009;179(6):467-473.

111. Goebel S, Li Z, Vogelmann J, et al. The GPVI-Fc Fusion Protein Revacept Improves Cerebral Infarct Volume and Functional Outcome in Stroke. *PLOS ONE*. 2013;8(7):e66960.

112. Pachel C, Mathes D, Arias-Loza A-P, et al. Inhibition of Platelet GPVI Protects Against Myocardial Ischemia–Reperfusion Injury. *Arteriosclerosis, Thrombosis, and Vascular Biology*. 2016;36(4):629-635.

113. Kleinschnitz C, Pozgajova M, Pham M, Bendszus M, Nieswandt B, Stoll G. Targeting Platelets in Acute Experimental Stroke. *Circulation*. 2007;115(17):2323-2330.

114. Lakka Klement G, Yip T-T, Cassiola F, et al. Platelets actively sequester angiogenesis regulators. *Blood*. 2009;113(12):2835-2842.

115. Reilmann R, Rolf LH, Lange HW. Huntington's disease: The neuroexcitotoxin aspartate is increased in platelets and decreased in plasma. *Journal of the Neurological Sciences*. 1994;127(1):48-53.

116. Denis HL, Lamontagne-Proulx J, St-Amour I, et al. Platelet abnormalities in Huntington’s disease. *Journal of Neurology, Neurosurgery & Psychiatry*. 2019;90(3):272.

117. Ferrarese C, Zoia C, Pecora N, et al. Reduced platelet glutamate uptake in Parkinson's disease. *Journal of Neural Transmission*. 1999;106(7):685-692.

118. Hishizawa M, Yamashita H, Akizuki M, Urushitani M, Takahashi R. TDP-43 levels are higher in platelets from patients with sporadic amyotrophic lateral sclerosis than in healthy controls. *Neurochemistry International*. 2019;124:41-45.

119. Dupuis L, Spreux-Varoquaux O, Bensimon G, et al. Platelet Serotonin Level Predicts Survival in Amyotrophic Lateral Sclerosis. *PLOS ONE*. 2010;5(10):e13346.

120. Leimkühler NB, Schneider RK. Inflammatory bone marrow microenvironment. *Hematology*. 2019;2019(1):294-302.

121. Caiado F, Pietras EM, Manz MG. Inflammation as a regulator of hematopoietic stem cell function in disease, aging, and clonal selection. *Journal of Experimental Medicine*. 2021;218(7).

122. French SL, Butov KR, Allaeys I, et al. Platelet-derived extracellular vesicles infiltrate and modify the bone marrow during inflammation. *Blood Advances*. 2020;4(13):3011-3023.

123. Boilard E, Nigrovic PA, Larabee K, et al. Platelets Amplify Inflammation in Arthritis via Collagen-Dependent Microparticle Production. *Science*. 2010;327(5965):580-583.

124. Balko J, Havlin J, Casas-Mendez F, et al. Mapping of the lung megakaryocytes: A role in pathogenesis of idiopathic pulmonary arterial hypertension? *Pathology - Research and Practice*. 2022;237:154060.

125. Mandal RV, Mark EJ, Kradin RL. Megakaryocytes and platelet homeostasis in diffuse alveolar damage. *Experimental and Molecular Pathology*. 2007;83(3):327-331.

126. Roncati L, Ligabue G, Nasillo V, et al. A proof of evidence supporting abnormal immunothrombosis in severe COVID-19: naked megakaryocyte nuclei increase in the bone marrow and lungs of critically ill patients. *Platelets*. 2020;31(8):1085-1089.

127. Wang J, Xie J, Wang D, et al. CXCR4high megakaryocytes regulate host-defense immunity against bacterial pathogens. *eLife*. 2022;11:e78662.

128. Sulkowski S, Terlikowski S, Sulkowska M. Occlusion of Pulmonary Vessels by Megakaryocytes after Treatment with Tumour Necrosis Factor-alpha (TNF-α). *Journal of Comparative Pathology*. 1999;120(3):235-245.

129. Aronson JK, Ferner RE. Biomarkers—A General Review. *Current Protocols in Pharmacology*. 2017;76(1):9.23.21-29.23.17.

130. Zhu X, Cao Y, Lu P, et al. Evaluation of platelet indices as diagnostic biomarkers for colorectal cancer. *Scientific Reports*. 2018;8(1):11814.

131. Alessandro G, Benedetta I, Augusto Di C, et al. Revisiting the link between platelets and depression through genetic epidemiology: new insights from platelet distribution width. *Haematologica*. 2020;105(5):e246-e248.

132. Welder D, Jeon-Slaughter H, Ashraf B, et al. Immature platelets as a biomarker for disease severity and mortality in COVID-19 patients. *British Journal of Haematology*. 2021;194(3):530-536.

133. Post E, Sol N, Best MG, Wurdinger T. Blood platelets as an RNA biomarker platform for neuro-oncological diseases. *Neuro-Oncology Advances*. 2022;4(Supplement_2):ii61-ii65.

134. Wegrzyn G, Walborn A, Rondina M, Fareed J, Hoppensteadt D. Biomarkers of Platelet Activation and Their Prognostic Value in Patients With Sepsis-Associated Disseminated Intravascular Coagulopathy. *Clinical and Applied Thrombosis/Hemostasis*. 2021;27:1076029620943300.

135. Pandey A, Mann M. Proteomics to study genes and genomes. *Nature*. 2000;405(6788):837-846.

136. Yates I, JR. Recent technical advances in proteomics [version 1; peer review: 2 approved]. *F1000Research*. 2019;8(351).

137. Macklin A, Khan S, Kislinger T. Recent advances in mass spectrometry based clinical proteomics: applications to cancer research. *Clinical Proteomics*. 2020;17(1):17.

138. Adhikari S, Nice EC, Deutsch EW, et al. A high-stringency blueprint of the human proteome. *Nature Communications*. 2020;11(1):5301.

139. Jiang L, Wang M, Lin S, et al. A Quantitative Proteome Map of the Human Body. *Cell*. 2020;183(1):269-283.e219.

140. Sinitcyn P, Richards AL, Weatheritt RJ, et al. Global detection of human variants and isoforms by deep proteome sequencing. *Nature Biotechnology*. 2023.

141. Gatto L, Aebersold R, Cox J, et al. Initial recommendations for performing, benchmarking and reporting single-cell proteomics experiments. *Nature Methods*. 2023;20(3):375-386.

142. Gevaert K, Eggermont L, Demol H, Vandekerckhove J. A fast and convenient MALDI-MS based proteomic approach: identification of components scaffolded by the actin cytoskeleton of activated human thrombocytes. *Journal of Biotechnology*. 2000;78(3):259-269.

143. Dupree EJ, Jayathirtha M, Yorkey H, Mihasan M, Petre BA, Darie CC. A Critical Review of Bottom-Up Proteomics: The Good, the Bad, and the Future of This Field. *Proteomes*. 2020;8(3):14.

144. García Á. Clinical proteomics in platelet research: challenges ahead. *Journal of Thrombosis and Haemostasis*. 2010;8(8):1784-1785.

145. Tassi Yunga S, Gower AJ, Melrose AR, et al. Effects of ex vivo blood anticoagulation and preanalytical processing time on the proteome content of platelets. *Journal of Thrombosis and Haemostasis*. 2022;20(6):1437-1450.

146. van der Meer PF, Korte Dd. Platelet preservation: Agitation and containers. *Transfusion and Apheresis Science*. 2011;44(3):297-304.

147. Ferroni P, Riondino S, Vazzana N, Santoro N, Guadagni F, Davì G. Biomarkers of platelet activation in acute coronary syndromes. *Thrombosis and Haemostasis*. 2012;108(12):1109-1123.

148. Lazar C, Gatto L, Ferro M, Bruley C, Burger T. Accounting for the Multiple Natures of Missing Values in Label-Free Quantitative Proteomics Data Sets to Compare Imputation Strategies. *Journal of Proteome Research*. 2016;15(4):1116-1125.

149. Karpievitch YV, Dabney AR, Smith RD. Normalization and missing value imputation for label-free LC-MS analysis. *BMC Bioinformatics*. 2012;13(16):S5.

150. Zufferey A, Schvartz D, Nolli S, Reny J-L, Sanchez J-C, Fontana P. Characterization of the platelet granule proteome: Evidence of the presence of MHC1 in alpha-granules. *Journal of Proteomics*. 2014;101:130-140.

151. Maynard DM, Heijnen HFG, Horne MK, White JG, Gahl WA. Proteomic analysis of platelet α-granules using mass spectrometry. *Journal of Thrombosis and Haemostasis*. 2007;5(9):1945-1955.

152. Lewandrowski U, Wortelkamp S, Lohrig K, et al. Platelet membrane proteomics: a novel repository for functional research. *Blood*. 2009;114(1):e10-e19.

153. Zahedi RP, Lewandrowski U, Wiesner J, et al. Phosphoproteome of Resting Human Platelets. *Journal of Proteome Research*. 2008;7(2):526-534.

154. Coppinger AJ, Maguire BP. Insights into the Platelet Releasate. *Current Pharmaceutical Design*. 2007;13(26):2640-2646.

155. Burkhart JM, Gambaryan S, Watson SP, et al. What Can Proteomics Tell Us About Platelets? *Circulation Research*. 2014;114(7):1204-1219.

156. Huang J, Swieringa F, Solari FA, et al. Assessment of a complete and classified platelet proteome from genome-wide transcripts of human platelets and megakaryocytes covering platelet functions. *Scientific Reports*. 2021;11(1):12358.

157. Lee H, Chae S, Park J, et al. Comprehensive Proteome Profiling of Platelet Identified a Protein Profile Predictive of Responses to An Antiplatelet Agent Sarpogrelate. *Molecular & Cellular Proteomics*. 2016;15(11):3461-3472.

158. Burkhart JM, Vaudel M, Gambaryan S, et al. The first comprehensive and quantitative analysis of human platelet protein composition allows the comparative analysis of structural and functional pathways. *Blood*. 2012;120(15):e73-e82.

159. Sabrkhany S, Kuijpers MJE, Knol JC, et al. Exploration of the platelet proteome in patients with early-stage cancer. *Journal of Proteomics*. 2018;177:65-74.

160. Cervi D, Yip T-T, Bhattacharya N, et al. Platelet-associated PF-4 as a biomarker of early tumor growth. *Blood*. 2008;111(3):1201-1207.

161. Chow L, Aslam R, Speck ER, et al. A murine model of severe immune thrombocytopenia is induced by antibody- and CD8+ T cell–mediated responses that are differentially sensitive to therapy. *Blood*. 2010;115(6):1247-1253.

162. De Cuyper IM, Meinders M, van de Vijver E, et al. A novel flow cytometry–based platelet aggregation assay. *Blood*. 2013;121(10):e70-e80.

163. Meinders M, Hoogenboezem M, Scheenstra MR, et al. Repercussion of Megakaryocyte-Specific Gata1 Loss on Megakaryopoiesis and the Hematopoietic Precursor Compartment. *PLOS ONE*. 2016;11(5):e0154342.

164. Meinders M, Kulu DI, van de Werken HJG, et al. Sp1/Sp3 transcription factors regulate hallmarks of megakaryocyte maturation and platelet formation and function. *Blood*. 2015;125(12):1957-1967.

165. Salunkhe V, De Cuyper IM, Papadopoulos P, et al. A comprehensive proteomics study on platelet concentrates: Platelet proteome, storage time and Mirasol pathogen reduction technology. *Platelets*. 2019;30(3):368-379.

166. Cox J, Mann M. MaxQuant enables high peptide identification rates, individualized p.p.b.-range mass accuracies and proteome-wide protein quantification. *Nature Biotechnology*. 2008;26(12):1367-1372.

167. Sinitcyn P, Tiwary S, Rudolph J, et al. MaxQuant goes Linux. *Nature Methods*. 2018;15(6):401-401.

168. Cox J, Neuhauser N, Michalski A, Scheltema RA, Olsen JV, Mann M. Andromeda: A Peptide Search Engine Integrated into the MaxQuant Environment. *Journal of Proteome Research*. 2011;10(4):1794-1805.

169. R Core Team. R: A language and environment for statistical computing. Vienna, Austria: R Foundation for Statistical Computing; 2022.

170. Lazar C. imputeLCMD: a collection of methods for left-censored missing data imputation. *R package, version*. 2015;2.

171. Ritchie ME, Phipson B, Wu D, et al. limma powers differential expression analyses for RNA-sequencing and microarray studies. *Nucleic Acids Research*. 2015;43(7):e47-e47.

172. Langfelder P, Horvath S. WGCNA: an R package for weighted correlation network analysis. *BMC Bioinformatics*. 2008;9(1):559.

173. Wu JX, Pascovici D, Wu Y, Walker AK, Mirzaei M. Workflow for Rapidly Extracting Biological Insights from Complex, Multicondition Proteomics Experiments with WGCNA and PloGO2. *Journal of Proteome Research*. 2020;19(7):2898-2906.

174. Pagès H, Carlson M, Falcon S, Li N. AnnotationDbi: Manipulation of SQLite-based annotations in Bioconductor; 2022.

175. Carlson M. org.Mm.eg.db: Genome wide annotation for Mouse; 2022.

176. Young MD, Wakefield MJ, Smyth GK, Oshlack A. Gene ontology analysis for RNA-seq: accounting for selection bias. *Genome Biology*. 2010;11(2):R14.

177. Dolgalev I. msigdbr: MSigDB Gene Sets for Multiple Organisms in a Tidy Data Format; 2022.

178. Wickham H. ggplot2: Elegant Graphics for Data Analysis. *Wiley interdisciplinary reviews: computational statistics*. 2011;3(2):180-185.

179. Shannon P, Markiel A, Ozier O, et al. Cytoscape: A Software Environment for Integrated Models of Biomolecular Interaction Networks. *Genome Research*. 2003;13(11):2498-2504.

180. Deutsch EW, Bandeira N, Sharma V, et al. The ProteomeXchange consortium in 2020: enabling 'big data' approaches in proteomics. *Nucleic Acids Research*. 2019;48(D1):D1145-D1152.

181. Allan HE, Hayman MA, Marcone S, et al. Proteome and functional decline as platelets age in the circulation. *Journal of Thrombosis and Haemostasis*. 2021;19(12):3095-3112.

182. Bergemalm D, Ramstrom S, Kardeby C, et al. Platelet proteome and function in X-linked thrombocytopenia with thalassemia and in silico comparisons with gray platelet syndrome. *Haematologica*. 2021;106(11):2947-2959.

183. Bhat A, Das S, Yadav G, et al. Hyperoxidized Albumin Modulates Platelets and Promotes Inflammation Through CD36 Receptor in Severe Alcoholic Hepatitis. *Hepatology Communications*. 2020;4(1):50-65.

184. Bianchetti A, Chinello C, Guindani M, et al. A Blood Bank Standardized Production of Human Platelet Lysate for Mesenchymal Stromal Cell Expansion: Proteomic

Characterization and Biological Effects. *Frontiers in Cell and Developmental Biology*. 2021;9:650490.

185. Cimmino G, Tarallo R, Nassa G, et al. Activating stimuli induce platelet microRNA modulation and proteome reorganisation. *Thrombosis and Haemostasis*. 2015;114(1):96-108.

186. de Almeida LGN, Young D, Chow L, et al. Proteomics and Metabolomics Profiling of Platelets and Plasma Mediators of Thrombo-Inflammation in Gestational Hypertension and Preeclampsia. *Cells*. 2022;11(8).

187. Linge CP, Jern A, Tyden H, et al. Enrichment of Complement, Immunoglobulins, and Autoantibody Targets in the Proteome of Platelets from Patients with Systemic Lupus Erythematosus. *Thrombosis and Haemostasis*. 2022;122(9):1486-1501.

188. Loroch S, Trabold K, Gambaryan S, et al. Alterations of the platelet proteome in type I Glanzmann thrombasthenia caused by different homozygous delG frameshift mutations in ITGA2B. *Thrombosis and Haemostasis*. 2017;117(3):556-569.

189. Mirlashari MR, Vetlesen A, Nissen-Meyer LSH, et al. Proteomic study of apheresis platelets made HLA class I deficient for transfusion of refractory patients. *PROTEOMICS – Clinical Applications*. 2021;15(6):e2100022.

190. Nassa G, Giurato G, Cimmino G, et al. Splicing of platelet resident pre-mRNAs upon activation by physiological stimuli results in functionally relevant proteome modifications. *Scientific Reports*. 2018;8(1):498.

191. Nebie O, Carvalho K, Barro L, et al. Human platelet lysate biotherapy for traumatic brain injury: preclinical assessment. *Brain*. 2021;144(10):3142-3158.

192. Rijkers M, van den Eshof BL, van der Meer PF, et al. Monitoring storage induced changes in the platelet proteome employing label free quantitative mass spectrometry. *Scientific Reports*. 2017;7(1):11045.

193. Rodrigues RM, Valim VS, Berger M, et al. The proteomic and particle composition of human platelet lysate for cell therapy products. *Journal of Cellular Biochemistry*. 2022;123(9):1495-1505.

194. Sereni L, Castiello MC, Marangoni F, et al. Autonomous role of Wiskott-Aldrich syndrome platelet deficiency in inducing autoimmunity and inflammation. *Journal of Allergy and Clinical Immunology*. 2018;142(4):1272-1284.

195. Shah P, Yang W, Sun S, Pasay J, Faraday N, Zhang H. Platelet glycoproteins associated with aspirin-treatment upon platelet activation. *Proteomics*. 2017;17(6).

196. Solari FA, Mattheij NJ, Burkhart JM, et al. Combined Quantification of the Global Proteome, Phosphoproteome, and Proteolytic Cleavage to Characterize Altered Platelet Functions in the Human Scott Syndrome. *Molecular & Cellular Proteomics*. 2016;15(10):3154-3169.

197. Stokhuijzen E, Koornneef JM, Nota B, et al. Differences between Platelets Derived from Neonatal Cord Blood and Adult Peripheral Blood Assessed by Mass Spectrometry. *Journal of Proteome Research*. 2017;16(10):3567-3575.

198. Yeh T-L, Hsu M-S, Hsu H-Y, et al. Risk of cardiovascular diseases in cancer patients: A nationwide representative cohort study in Taiwan. *BMC Cancer*. 2022;22(1):1198.

199. Thiele T, Braune J, Dhople V, et al. Proteomic profile of platelets during reconstitution of platelet counts after apheresis. *PROTEOMICS – Clinical Applications*. 2016;10(8):831-838.

200. Trugilho MRO, Azevedo-Quintanilha IG, Gesto JSM, et al. Platelet proteome reveals features of cell death, antiviral response and viral replication in covid-19. *Cell Death Discovery*. 2022;8(1):324.

201. Trugilho MRO, Hottz ED, Brunoro GVF, et al. Platelet proteome reveals novel pathways of platelet activation and platelet-mediated immunoregulation in dengue. *PLOS Pathogens*. 2017;13(5):e1006385.

202. Wright B, Stanley RG, Kaiser WJ, Mills DJ, Gibbins JM. Analysis of protein networks in resting and collagen receptor (GPVI)-stimulated platelet sub-proteomes. *Proteomics*. 2011;11(23):4588-4592.

203. Zeiler M, Moser M, Mann M. Copy number analysis of the murine platelet proteome spanning the complete abundance range. *Molecular & Cellular Proteomics*. 2014;13(12):3435-3445.

204. Martínez-Botía P, Meinders M, De Cuyper IM, Eble JA, Semple JW, Gutiérrez L. Dissecting platelet proteomics to understand the pathophysiology of immune thrombocytopenia: studies in mouse models. *Blood Advances*. 2022;6(11):3529-3534.

205. Van Bergen MGJM, Marneth AE, Hoogendijk AJ, et al. Specific proteome changes in platelets from individuals with GATA1-, GFI1B-, and RUNX1-linked bleeding disorders. *Blood*. 2021;138(1):86-90.

206. van Holten TC, Bleijerveld OB, Wijten P, et al. Quantitative proteomics analysis reveals similar release profiles following specific PAR-1 or PAR-4 stimulation of platelets. *Cardiovascular Research*. 2014;103(1):140-146.

207. Au AE, Sashindranath M, Borg RJ, et al. Activated platelets rescue apoptotic cells via paracrine activation of EGFR and DNA-dependent protein kinase. *Cell Death and Disease*. 2014;5(9):e1410.

208. Servais L, Wera O, Dibato Epoh J, et al. Platelets contribute to the initiation of colitis-associated cancer by promoting immunosuppression. *Journal of Thrombosis and Haemostasis*. 2018;16(4):762-777.

209. Parsons MEM, Szklanna PB, Guerrero JA, et al. Platelet Releasate Proteome Profiling Reveals a Core Set of Proteins with Low Variance between Healthy Adults. *Proteomics*. 2018;18(15):e1800219.

210. Szklanna PB, Parsons ME, Wynne K, et al. The Platelet Releasate is Altered in Human Pregnancy. *PROTEOMICS – Clinical Applications*. 2019;13(3):1800162.

211. Posit team. RStudio: Integrated Development Environment for R. Boston, MA: Posit Software, PBC; 2022.

212. Rowley JW, Oler AJ, Tolley ND, et al. Genome-wide RNA-seq analysis of human and mouse platelet transcriptomes. *Blood*. 2011;118(14):e101-111.

213. Wickham H, François R, Henry L, Müller K, Vaughan D. dplyr: A Grammar of Data Manipulation; 2023.

214. Wickham H. stringr: Simple, Consistent Wrappers for Common String Operations; 2022.

215. Kassambara A. ggpubr: 'ggplot2' Based Publication Ready Plots; 2023.

216. Larsson J. eulerr: Area-Proportional Euler and Venn Diagrams with Ellipses; 2022.

217. Carlson M. org.Hs.eg.db: Genome wide annotation for Human; 2022.

218. Kolberg L, Raudvere U, Kuzmin I, Vilo J, Peterson H. gprofiler2 -- an R package for gene list functional enrichment analysis and namespace conversion toolset g:Profiler [version 2; peer review: 2 approved]. *F1000Research*. 2020;9(709).

219. Yu G, Wang L-G, Han Y, He Q-Y. clusterProfiler: an R Package for Comparing Biological Themes Among Gene Clusters. *OMICS: A Journal of Integrative Biology*. 2012;16(5):284-287.

220. Salunkhe V, Papadopoulos P, Gutiérrez L. Culture of Megakaryocytes from Human Peripheral Blood Mononuclear Cells. *Bio-protocol*. 2015;5(21):e1639.

221. Acebes-Huerta A, Martínez-Botía P, Martín Martín C, et al. Immunophenotyping and Cell Sorting of Human MKs from Human Primary Sources or Differentiated In Vitro from Hematopoietic Progenitors. *Journal of Visualized Experiments*. 2021(174):e62569.

222. van Buuren S, Groothuis-Oudshoorn K. mice: Multivariate Imputation by Chained Equations in R. *Journal of Statistical Software*. 2011;45(3):1 - 67.

223. Fox J, Weisberg S. An R companion to applied regression: Sage publications; 2018.

224. Hothorn T, Bretz F, Westfall P. Simultaneous Inference in General Parametric Models. *Biometrical Journal*. 2008;50(3):346-363.

225. Adusumilli R, Mallick P. Data Conversion with ProteoWizard msConvert. In: Comai L, Katz JE, Mallick P, eds. Proteomics: Methods and Protocols. New York, NY: Springer New York; 2017:339-368.

226. Kong AT, Leprevost FV, Avtonomov DM, Mellacheruvu D, Nesvizhskii AI. MSFragger: ultrafast and comprehensive peptide identification in mass spectrometry–based proteomics. *Nature Methods*. 2017;14(5):513-520.

227. Teo GC, Polasky DA, Yu F, Nesvizhskii AI. Fast Deisotoping Algorithm and Its Implementation in the MSFragger Search Engine. *Journal of Proteome Research*. 2021;20(1):498-505.

228. da Veiga Leprevost F, Haynes SE, Avtonomov DM, et al. Philosopher: a versatile toolkit for shotgun proteomics data analysis. *Nature Methods*. 2020;17(9):869-870.

229. Käll L, Canterbury JD, Weston J, Noble WS, MacCoss MJ. Semi-supervised learning for peptide identification from shotgun proteomics datasets. *Nature Methods*. 2007;4(11):923-925.

230. Jin X, Yu H, Wang B, et al. Airborne particulate matters induce thrombopoiesis from megakaryocytes through regulating mitochondrial oxidative phosphorylation. *Particle and Fibre Toxicology*. 2021;18(1):19.

231. Nesvizhskii AI, Keller A, Kolker E, Aebersold R. A Statistical Model for Identifying Proteins by Tandem Mass Spectrometry. *Analytical Chemistry*. 2003;75(17):4646-4658.

232. Todorov V. rrcovNA: Scalable Robust Estimators with High Breakdown Point for Incomplete Data; 2020.

233. Kumar L, Futschik ME. Mfuzz: a software package for soft clustering of microarray data. *Bioinformation*. 2007;2(1):5.

234. Yu G, He Q-Y. ReactomePA: an R/Bioconductor package for reactome pathway analysis and visualization. *Molecular BioSystems*. 2016;12(2):477-479.

235. Federico A, Monti S. hypeR: an R package for geneset enrichment workflows. *Bioinformatics*. 2019;36(4):1307-1308.

236. Engholm-Keller K, Waardenberg AJ, Müller JA, et al. The temporal profile of activity-dependent presynaptic phospho-signalling reveals long-lasting patterns of poststimulus regulation. *PLOS Biology*. 2019;17(3):e3000170.

237. Chen LS, Wang J, Wang X, Wang P. A mixed-effects model for incomplete data from labeling-based quantitative proteomics experiments. *The Annals of Applied Statistics*. 2017;11(1):114-138, 125.

238. Wang J, Wang P, Hedeker D, Chen LS. Using multivariate mixed-effects selection models for analyzing batch-processed proteomics data with non-ignorable missingness. *Biostatistics*. 2018;20(4):648-665.

239. Plubell DL, Wilmarth PA, Zhao Y, et al. Extended Multiplexing of Tandem Mass Tags (TMT) Labeling Reveals Age and High Fat Diet Specific Proteome Changes in Mouse Epididymal Adipose Tissue. *Molecular & Cellular Proteomics*. 2017;16(5):873-890.

240. Lê S, Josse J, Husson F. FactoMineR: An R Package for Multivariate Analysis. *Journal of Statistical Software*. 2008;25(1):1 - 18.

241. McKenzie CGJ, Guo L, Freedman J, Semple JW. Cellular immune dysfunction in immune thrombocytopenia (ITP). *British Journal of Haematology*. 2013;163(1):10-23.

242. Swinkels M, Rijkers M, Voorberg J, Vidarsson G, Leebeek FWG, Jansen AJG. Emerging Concepts in Immune Thrombocytopenia. *Frontiers in Immunology*. 2018;9(880).

243. Kochhar M, Neunert C. Immune thrombocytopenia: A review of upfront treatment strategies. *Blood Reviews*. 2021:100822.

244. García Á. Platelet clinical proteomics: Facts, challenges, and future perspectives. *PROTEOMICS – Clinical Applications*. 2016;10(8):767-773.

245. Hell L, Lurger K, Mauracher L-M, et al. Altered platelet proteome in lupus anticoagulant (LA)-positive patients—protein disulfide isomerase and NETosis as new players in LA-related thrombosis. *Experimental & Molecular Medicine*. 2020;52(1):66-78.

246. Neunert C, Terrell DR, Arnold DM, et al. American Society of Hematology 2019 guidelines for immune thrombocytopenia. *Blood Advances*. 2019;3(23):3829-3866.

247. Liu M, Dongre A. Proper imputation of missing values in proteomics datasets for differential expression analysis. *Briefings in Bioinformatics*. 2020;22(3).

248. Boudreau LH, Duchez A-C, Cloutier N, et al. Platelets release mitochondria serving as substrate for bactericidal group IIA-secreted phospholipase A2 to promote inflammation. *Blood*. 2014;124(14):2173-2183.

249. Tang BL. A unique SNARE machinery for exocytosis of cytotoxic granules and platelets granules. *Molecular Membrane Biology*. 2015;32(4):120-126.

250. Rau JC, Beaulieu LM, Huntington JA, Church FC. Serpins in thrombosis, hemostasis and fibrinolysis. *Journal of Thrombosis and Haemostasis*. 2007;5:102-115.

251. Luo Z, Lei H, Sun Y, Liu X, Su D-F. Orosomucoid, an acute response protein with multiple modulating activities. *Journal of Physiology and Biochemistry*. 2015;71(2):329-340.

252. Eriksson O, Mohlin C, Nilsson B, Ekdahl KN. The Human Platelet as an Innate Immune Cell: Interactions Between Activated Platelets and the Complement System. *Frontiers in Immunology*. 2019;10.

253. Fuchs TA, Bhandari AA, Wagner DD. Histones induce rapid and profound thrombocytopenia in mice. *Blood*. 2011;118(13):3708-3714.

254. Frydman GH, Tessier SN, Wong KHK, et al. Megakaryocytes contain extranuclear histones and may be a source of platelet-associated histones during sepsis. *Scientific Reports*. 2020;10(1):4621.

255. Flaumenhaft R, Dilks JR, Rozenvayn N, Monahan-Earley RA, Feng D, Dvorak AM. The actin cytoskeleton differentially regulates platelet α-granule and dense-granule secretion. *Blood*. 2005;105(10):3879-3887.

256. Kim K, Hahm E, Li J, et al. Platelet protein disulfide isomerase is required for thrombus formation but not for hemostasis in mice. *Blood*. 2013;122(6):1052-1061.

257. Mitsui T, Makino S, Tamiya G, et al. ALOX12 mutation in a family with dominantly inherited bleeding diathesis. *Journal of Human Genetics*. 2021;66(8):753-759.

258. Wijten P, Holten Tv, Woo LL, et al. High Precision Platelet Releasate Definition by Quantitative Reversed Protein Profiling—Brief Report. *Arteriosclerosis, Thrombosis, and Vascular Biology*. 2013;33(7):1635-1638.

259. Kardeby C, Fälker K, Haining EJ, et al. Synthetic glycopolymers and natural fucoidans cause human platelet aggregation via PEAR1 and GPIbα. *Blood Advances*. 2019;3(3):275-287.

260. Lopez JJ, Salido GM, Rosado JA. Cardiovascular and Hemostatic Disorders: SOCE and Ca2+ Handling in Platelet Dysfunction. In: Groschner K, Graier WF, Romanin C, eds. Store-Operated Ca^{2+} Entry (SOCE) Pathways: Emerging Signaling Concepts in Human (Patho)physiology. Cham: Springer International Publishing; 2017:453-472.

261. Monaco G, van Dam S, Casal Novo Ribeiro JL, Larbi A, de Magalhães JP. A comparison of human and mouse gene co-expression networks reveals conservation and divergence at the tissue, pathway and disease levels. *BMC Evolutionary Biology*. 2015;15(1):259.

262. eBioMedicine. The 3Rs of Animal Research. *eBioMedicine*. 2022;76.

263. Kim J, Koo B-K, Knoblich JA. Human organoids: model systems for human biology and medicine. *Nature Reviews Molecular Cell Biology*. 2020;21(10):571-584.

264. Schmitt A, Guichard J, Massé J-M, Debili N, Cramer EM. Of mice and men: Comparison of the ultrastructure of megakaryocytes and platelets. *Experimental Hematology*. 2001;29(11):1295-1302.

265. Thijs T, Deckmyn H, Broos K. Model systems of genetically modified platelets. *Blood*. 2012;119(7):1634-1642.

266. Jirouskova M, Shet AS, Johnson GJ. A guide to murine platelet structure, function, assays, and genetic alterations. *Journal of Thrombosis and Haemostasis*. 2007;5(4):661-669.

267. Tilburg J, Becker IC, Italiano JE. Don't you forget about me(gakaryocytes). *Blood*. 2022;139(22):3245-3254.

268. Corash L, Levin J, Mok Y, Baker G, McDowell J. Measurement of megakaryocyte frequency and ploidy distribution in unfractionated murine bone marrow. *Experimental Hematology*. 1989;17(3):278-286.

269. Levin J. The Evolution of Mammalian Platelets. In: Kuter DJ, Hunt P, Sheridan W, Zucker-Franklin D, eds. Thrombopoiesis and Thrombopoietins: Molecular, Cellular, Preclinical, and Clinical Biology. Totowa, NJ: Humana Press; 1997:63-78.

270. McKenzie SE, Taylor SM, Malladi P, et al. The role of the human Fc receptor Fc gamma RIIA in the immune clearance of platelets: a transgenic mouse model. *Journal of Immunology*. 1999;162(7):4311-4318.

271. Ware J. Dysfunctional platelet membrane receptors: from humans to mice. *Thrombosis and Haemostasis*. 2004;92(09):478-485.

272. Kuter DJ. The biology of thrombopoietin and thrombopoietin receptor agonists. *International Journal of Hematology*. 2013;98(1):10-23.

273. Pears CJ, Thornber K, Auger JM, et al. Differential Roles of the PKC Novel Isoforms, PKCδ and PKCε, in Mouse and Human Platelets. *PLOS ONE*. 2008;3(11):e3793.

274. Gianazza E, Brioschi M, Baetta R, Mallia A, Banfi C, Tremoli E. Platelets in Healthy and Disease States: From Biomarkers Discovery to Drug Targets Identification by Proteomics. *International Journal of Molecular Sciences*. 2020;21(12):4541.

275. Antunes-Ferreira M, Koppers-Lalic D, Würdinger T. Circulating platelets as liquid biopsy sources for cancer detection. *Molecular Oncology*. 2021;15(6):1727-1743.

276. Grande R, Dovizio M, Marcone S, et al. Platelet-Derived Microparticles From Obese Individuals: Characterization of Number, Size, Proteomics, and Crosstalk With Cancer and Endothelial Cells. *Frontiers in Pharmacology*. 2019;10.

277. Huang J, Zhang P, Solari FA, et al. Molecular Proteomics and Signalling of Human Platelets in Health and Disease. *International Journal of Molecular Sciences*. 2021;22(18):9860.

278. Shevchuk O, Begonja AJ, Gambaryan S, et al. Proteomics: A Tool to Study Platelet Function. *International Journal of Molecular Sciences*. 2021;22(9):4776.

279. Yue F, Cheng Y, Breschi A, et al. A comparative encyclopedia of DNA elements in the mouse genome. *Nature*. 2014;515(7527):355-364.

280. Londin ER, Hatzimichael E, Loher P, et al. The human platelet: strong transcriptome correlations among individuals associate weakly with the platelet proteome. *Biology Direct*. 2014;9(1):3.

281. Senis YA, Tomlinson MG, García Á, et al. A Comprehensive Proteomics and Genomics Analysis Reveals Novel Transmembrane Proteins in Human Platelets and Mouse Megakaryocytes Including G6b-B, a Novel Immunoreceptor Tyrosine-based Inhibitory Motif Protein. *Molecular & Cellular Proteomics*. 2007;6(3):548-564.

282. Merico V, Zuccotti M, Carpi D, et al. The genomic and proteomic blueprint of mouse megakaryocytes derived from embryonic stem cells. *Journal of Thrombosis and Haemostasis*. 2012;10(5):907-915.

283. Kammers K, Taub MA, Mathias RA, et al. Gene and protein expression in human megakaryocytes derived from induced pluripotent stem cells. *Journal of Thrombosis and Haemostasis*. 2021;19(7):1783-1799.

284. Martínez-Botía P, Acebes-Huerta A, Seghatchian J, Gutiérrez L. On the Quest for In Vitro Platelet Production by Re-Tailoring the Concepts of Megakaryocyte Differentiation. *Medicina*. 2020;56(12):671.

285. Martínez-Botía P, Acebes-Huerta A, Seghatchian J, Gutiérrez L. In vitro platelet production for transfusion purposes: Where are we now? *Transfusion and Apheresis Science*. 2020;59(4).

286. Hornbeck PV, Kornhauser JM, Tkachev S, et al. PhosphoSitePlus: a comprehensive resource for investigating the structure and function of experimentally determined post-translational modifications in man and mouse. *Nucleic Acids Research*. 2011;40(D1):D261-D270.

287. Kumar M, Gouw M, Michael S, et al. ELM—the eukaryotic linear motif resource in 2020. *Nucleic Acids Research*. 2019;48(D1):D296-D306.

288. The UniProt Consortium. UniProt: the Universal Protein Knowledgebase in 2023. *Nucleic Acids Research*. 2022;51(D1):D523-D531.

289. Suganya R, Shanthi R. Fuzzy c-means algorithm-a review. *International Journal of Scientific and Research Publications*. 2012;2(11):1.

290. Marialaura B, Augusto Di C, George P, et al. A score of low-grade inflammation and risk of mortality: prospective findings from the Moli-sani study. *Haematologica*. 2016;101(11):1434-1441.

291. Barbaresko J, Koch M, Schulze MB, Nöthlings U. Dietary pattern analysis and biomarkers of low-grade inflammation: a systematic literature review. *Nutrition Reviews*. 2013;71(8):511-527.

292. Franceschi C, Garagnani P, Parini P, Giuliani C, Santoro A. Inflammaging: a new immune–metabolic viewpoint for age-related diseases. *Nature Reviews Endocrinology*. 2018;14(10):576-590.

293. Wang CCL, Hess CN, Hiatt WR, Goldfine AB. Clinical Update: Cardiovascular Disease in Diabetes Mellitus. *Circulation*. 2016;133(24):2459-2502.

294. Fidler TP, Marti A, Gerth K, et al. Glucose Metabolism Is Required for Platelet Hyperactivation in a Murine Model of Type 1 Diabetes. *Diabetes*. 2019;68(5):932-938.

295. Kraakman MJ, Lee MKS, Al-Sharea A, et al. Neutrophil-derived S100 calcium-binding proteins A8/A9 promote reticulated thrombocytosis and atherogenesis in diabetes. *The Journal of Clinical Investigation*. 2017;127(6):2133-2147.

296. Brown AS, Hong Y, Belder Ad, et al. Megakaryocyte Ploidy and Platelet Changes in Human Diabetes and Atherosclerosis. *Arteriosclerosis, Thrombosis, and Vascular Biology*. 1997;17(4):802-807.

297. Houck KL, Yuan H, Tian Y, et al. Physical proximity and functional cooperation of glycoprotein 130 and glycoprotein VI in platelet membrane lipid rafts. *Journal of Thrombosis and Haemostasis*. 2019;17(9):1500-1510.

298. Stephen J, Emerson B, Fox KAA, Dransfield I. The Uncoupling of Monocyte–Platelet Interactions from the Induction of Proinflammatory Signaling in Monocytes. *The Journal of Immunology*. 2013;191(11):5677-5683.

299. Teague HL, Varghese NJ, Tsoi LC, et al. Neutrophil Subsets, Platelets, and Vascular Disease in Psoriasis. *JACC: Basic to Translational Science*. 2019;4(1):1-14.

300. P. Heyns Ad, Badenhorst PN, Lotter MG, Pieters H, Wessels P, F. Kotze H. Platelet Turnover and Kinetics in Immune Thrombocytopenic Purpura: Results With Autologous 111In-Labeled Platelets and Homologous 51Cr-Labeled Platelets Differ. *Blood*. 1986;67(1):86-92.

301. Liu S-y, Yuan D, Sun R-J, Zhu J-j, Shan N-n. Significant reductions in apoptosis-related proteins (HSPA6, HSPA8, ITGB3, YWHAH, and PRDX6) are involved in immune thrombocytopenia. *Journal of Thrombosis and Thrombolysis*. 2021;51(4):905-914.

302. Sun R-J, Yin D-m, Yuan D, Liu S-y, Zhu J-j, Shan N-n. Quantitative LC–MS/MS uncovers the regulatory role of autophagy in immune thrombocytopenia. *Cancer Cell International*. 2021;21(1):548.

303. Boccia R, Cooper N, Ghanima W, et al. Fostamatinib is an effective second-line therapy in patients with immune thrombocytopenia. *British Journal of Haematology*. 2020;190(6):933-938.

304. Papapanagiotou A, Daskalakis G, Siasos G, Gargalionis A, Papavassiliou GA. The Role of Platelets in Cardiovascular Disease: Molecular Mechanisms. *Current Pharmaceutical Design*. 2016;22(29):4493-4505.

305. Maguire PB, Parsons ME, Szklanna PB, et al. Comparative Platelet Releasate Proteomic Profiling of Acute Coronary Syndrome versus Stable Coronary Artery Disease. *Frontiers in Cardiovascular Medicine*. 2020;7.

306. Vélez P, Ocaranza-Sánchez R, López-Otero D, et al. 2D-DIGE-based proteomic analysis of intracoronary versus peripheral arterial blood platelets from acute myocardial infarction patients: Upregulation of platelet activation biomarkers at the culprit site. *PROTEOMICS – Clinical Applications*. 2016;10(8):851-858.

307. Shrivastava M. The platelet storage lesion. *Transfusion and Apheresis Science*. 2009;41(2):105-113.

308. Thiele T, Steil L, Gebhard S, et al. Profiling of alterations in platelet proteins during storage of platelet concentrates. *Transfusion*. 2007;47(7):1221-1233.

309. Salunkhe V, van der Meer PF, de Korte D, Seghatchian J, Gutiérrez L. Development of blood transfusion product pathogen reduction treatments: A review of methods, current applications and demands. *Transfusion and Apheresis Science*. 2015;52(1):19-34.

310. Cooper S, Wilmarth PA, Cunliffe JM, et al. Platelet proteome dynamics in hibernating 13-lined ground squirrels. *Physiological Genomics*. 2021;53(11):473-485.

311. Cremer SE, Catalfamo JL, Goggs R, Seemann SE, Kristensen AT, Brooks MB. Proteomic profiling of the thrombin-activated canine platelet secretome (CAPS). *PLOS ONE*. 2019;14(11):e0224891.

312. Thienel M, Müller-Reif JB, Zhang Z, et al. Immobility-associated thromboprotection is conserved across mammalian species from bear to human. *Science*. 2023;380(6641):178-187.

313. Hermida-Nogueira L, García Á. Extracellular vesicles in the transfusion medicine field: The potential of proteomics. *Proteomics*. 2021;21(13-14):2000089.

314. Looße C, Swieringa F, Heemskerk JWM, Sickmann A, Lorenz C. Platelet proteomics: from discovery to diagnosis. *Expert Review of Proteomics*. 2018;15(6):467-476.

315. Mischak H, Apweiler R, Banks RE, et al. Clinical proteomics: A need to define the field and to begin to set adequate standards. *PROTEOMICS – Clinical Applications*. 2007;1(2):148-156.

316. Tabb DL, Vega-Montoto L, Rudnick PA, et al. Repeatability and Reproducibility in Proteomic Identifications by Liquid Chromatography−Tandem Mass Spectrometry. *Journal of Proteome Research*. 2010;9(2):761-776.

317. Bayés À, Collins MO, Croning MDR, van de Lagemaat LN, Choudhary JS, Grant SGN. Comparative Study of Human and Mouse Postsynaptic Proteomes Finds High Compositional Conservation and Abundance Differences for Key Synaptic Proteins. *PLOS ONE*. 2012;7(10):e46683.

318. Balkenhol J, Kaltdorf KV, Mammadova-Bach E, et al. Comparison of the central human and mouse platelet signaling cascade by systems biological analysis. *BMC Genomics*. 2020;21(1):897.

319. Yu F, Haynes SE, Nesvizhskii AI. IonQuant Enables Accurate and Sensitive Label-Free Quantification With FDR-Controlled Match-Between-Runs. *Molecular & Cellular Proteomics*. 2021;20.

320. Kreft IC, Huisman EJ, Cnossen MH, et al. Proteomic landscapes of inherited platelet disorders with different etiologies. *Journal of Thrombosis and Haemostasis*. 2023;21(2):359-372.e353.

321. Zimman A, Titz B, Komisopoulou E, Biswas S, Graeber TG, Podrez EA. Phosphoproteomic Analysis of Platelets Activated by Pro-Thrombotic Oxidized Phospholipids and Thrombin. *PLOS ONE*. 2014;9(1):e84488.

322. Cho MJ, Liu J, Pestina TI, et al. The roles of αIIbβ3-mediated outside-in signal transduction, thromboxane A2, and adenosine diphosphate in collagen-induced platelet aggregation. *Blood*. 2003;101(7):2646-2651.

323. Babur Ö, Melrose AR, Cunliffe JM, et al. Phosphoproteomic quantitation and causal analysis reveal pathways in GPVI/ITAM-mediated platelet activation programs. *Blood*. 2020;136(20):2346-2358.

324. Lai KC, Flaumenhaft R. SNARE protein degradation upon platelet activation: Calpain cleaves SNAP-23. *Journal of Cellular Physiology*. 2003;194(2):206-214.

325. Baig A, Bao X, Wolf M, Haslam RJ. The platelet protein kinase C substrate pleckstrin binds directly to SDPR protein. *Platelets*. 2009;20(7):446-457.

326. Kim H, McCulloch CA. Filamin A mediates interactions between cytoskeletal proteins that control cell adhesion. *FEBS Letters*. 2011;585(1):18-22.

327. Durrant TN, Hutchinson JL, Heesom KJ, et al. In-depth PtdIns(3,4,5)P3 signalosome analysis identifies DAPP1 as a negative regulator of GPVI-driven platelet function. *Blood Advances*. 2017;1(14):918-932.

328. Nieswandt B, Watson SP. Platelet-collagen interaction: is GPVI the central receptor? *Blood*. 2003;102(2):449-461.

329. Asazuma N, Wilde JI, Berlanga O, et al. Interaction of Linker for Activation of T Cells with Multiple Adapter Proteins in Platelets Activated by the Glycoprotein VI-selective Ligand, Convulxin. *Journal of Biological Chemistry*. 2000;275(43):33427-33434.

330. Beck F, Geiger J, Gambaryan S, et al. Temporal quantitative phosphoproteomics of ADP stimulation reveals novel central nodes in platelet activation and inhibition. *Blood*. 2017;129(2):e1-e12.

331. Kortum RL, Lewis RE. The Molecular Scaffold KSR1 Regulates the Proliferative and Oncogenic Potential of Cells. *Molecular and Cellular Biology*. 2004;24(10):4407-4416.

332. Chen Y, Ruggeri ZM, Du X. 14-3-3 proteins in platelet biology and glycoprotein Ib-IX signaling. *Blood*. 2018;131(22):2436-2448.

333. Coppinger JA, Cagney G, Toomey S, et al. Characterization of the proteins released from activated platelets leads to localization of novel platelet proteins in human atherosclerotic lesions. *Blood*. 2004;103(6):2096-2104.

334. Shen J, Sampietro S, Wu J, et al. Coordination of platelet agonist signaling during the hemostatic response in vivo. *Blood Advances*. 2017;1(27):2767-2775.

335. Huang EM, Detwiler TC. Characteristics of the Synergistic Actions of Platelet Agonists. *Blood*. 1981;57(4):685-691.

336. Dawood BB, Wilde J, Watson SP. Reference curves for aggregation and ATP secretion to aid diagnose of platelet-based bleeding disorders: Effect of inhibition of ADP and thromboxane A2 pathways. *Platelets*. 2007;18(5):329-345.

337. Puig Domingo M. Platelet Function and Hyperglycemia in Acute Coronary Syndrome. *Revista Española de Cardiología (English Edition)*. 2014;67(1):3-5.

338. Kassassir H, Siewiera K, Talar M, Przygodzki T, Watala C. Flow cytometry analysis reveals different activation profiles of thrombin- or TRAP-stimulated platelets in db/db mice. The regulatory role of PAR-3. *Blood Cells, Molecules, and Diseases*. 2017;65:16-22.

339. Kakouros N, Rade JJ, Kourliouros A, Resar JR. Platelet Function in Patients with Diabetes Mellitus: From a Theoretical to a Practical Perspective. *International Journal of Endocrinology*. 2011;2011:742719.

340. Montague SJ, Andrews RK, Gardiner EE. Mechanisms of receptor shedding in platelets. *Blood*. 2018;132(24):2535-2545.

341. Bergmeier W, Burger PC, Piffath CL, et al. Metalloproteinase inhibitors improve the recovery and hemostatic function of in vitro–aged or –injured mouse platelets. *Blood*. 2003;102(12):4229-4235.

342. Tschoepe D, Driesch E, Schwippert B, Lampeter EF, Group Denis S. Activated platelets in subjects at increased risk of IDDM. *Diabetologia*. 1997;40(5):573-577.

343. Cai Y, Fleming C, Yan J. New insights of T cells in the pathogenesis of psoriasis. *Cellular & Molecular Immunology*. 2012;9(4):302-309.

344. Nussbaum L, Chen YL, Ogg GS. Role of regulatory T cells in psoriasis pathogenesis and treatment. *British Journal of Dermatology*. 2021;184(1):14-24.

345. Hu P, Wang M, Gao H, et al. The Role of Helper T Cells in Psoriasis. *Frontiers in Immunology*. 2021;12.

346. Woodfin A, Voisin M-B, Nourshargh S. PECAM-1: A Multi-Functional Molecule in Inflammation and Vascular Biology. *Arteriosclerosis, Thrombosis, and Vascular Biology*. 2007;27(12):2514-2523.

347. Liu L, Shi G-P. CD31: beyond a marker for endothelial cells. *Cardiovascular Research*. 2012;94(1):3-5.

348. Dib PRB, Quirino-Teixeira AC, Merij LB, et al. Innate immune receptors in platelets and platelet-leukocyte interactions. *Journal of Leukocyte Biology*. 2020;108(4):1157-1182.

349. Li J, Kim K, Jeong S-Y, et al. Platelet Protein Disulfide Isomerase Promotes Glycoprotein Ibα–Mediated Platelet-Neutrophil Interactions Under Thromboinflammatory Conditions. *Circulation*. 2019;139(10):1300-1319.

350. Herster F, Bittner Z, Codrea MC, et al. Platelets Aggregate With Neutrophils and Promote Skin Pathology in Psoriasis. *Frontiers in Immunology*. 2019;10.

351. Gold SM, Köhler-Forsberg O, Moss-Morris R, et al. Comorbid depression in medical diseases. *Nature Reviews Disease Primers*. 2020;6(1):69.

352. Beurel E, Toups M, Nemeroff CB. The Bidirectional Relationship of Depression and Inflammation: Double Trouble. *Neuron*. 2020;107(2):234-256.

353. Osimo EF, Pillinger T, Rodriguez IM, Khandaker GM, Pariante CM, Howes OD. Inflammatory markers in depression: A meta-analysis of mean differences and variability in 5,166 patients and 5,083 controls. *Brain, Behavior, and Immunity*. 2020;87:901-909.

354. Benros ME, Waltoft BL, Nordentoft M, et al. Autoimmune Diseases and Severe Infections as Risk Factors for Mood Disorders: A Nationwide Study. *JAMA Psychiatry*. 2013;70(8):812-820.

355. Izzi B, Tirozzi A, Cerletti C, et al. Beyond Haemostasis and Thrombosis: Platelets in Depression and Its Co-Morbidities. *International Journal of Molecular Sciences*. 2020;21(22):8817.

356. Morel-Kopp MC, McLean L, Chen Q, et al. The association of depression with platelet activation: evidence for a treatment effect. *Journal of Thrombosis and Haemostasis*. 2009;7(4):573-581.

357. Higashihara M, Takahata K, Yatomi Y, Nakahara K, Kurokawa K. Purification and partial characterization of CD9 antigen of human platelets. *FEBS Letters*. 1990;264(2):270-274.

358. Mangin PH, Kleitz L, Boucheix C, Gachet C, Lanza F. CD9 negatively regulates integrin αIIbβ3 activation and could thus prevent excessive platelet recruitment at sites of vascular injury. *Journal of Thrombosis and Haemostasis*. 2009;7(5):900-902.

359. Hannestad J, DellaGioia N, Bloch M. The Effect of Antidepressant Medication Treatment on Serum Levels of Inflammatory Cytokines: A Meta-Analysis. *Neuropsychopharmacology*. 2011;36(12):2452-2459.

360. Arteaga-Henríquez G, Simon MS, Burger B, et al. Low-Grade Inflammation as a Predictor of Antidepressant and Anti-Inflammatory Therapy Response in MDD Patients: A Systematic Review of the Literature in Combination With an Analysis of Experimental Data Collected in the EU-MOODINFLAME Consortium. *Frontiers in Psychiatry*. 2019;10.

361. Barrachina MN, Hermida-Nogueira L, Moran LA, et al. Phosphoproteomic Analysis of Platelets in Severe Obesity Uncovers Platelet Reactivity and Signaling Pathways Alterations. *Arteriosclerosis, Thrombosis, and Vascular Biology*. 2021;41(1):478-490.

362. Hatakeyama K, Kaneko MK, Kato Y, et al. Podoplanin expression in advanced atherosclerotic lesions of human aortas. *Thrombosis Research*. 2012;129(4):e70-e76.

363. Kee MF, Myers DR, Sakurai Y, Lam WA, Qiu Y. Platelet Mechanosensing of Collagen Matrices. *PLOS ONE*. 2015;10(4):e0126624.

Supplementary materials

Chapter I

Figure S1. Proteomic analysis of platelets from ITP mouse models. (A) On the left, bar-plot graph depicting the percentage of missing values in each sample; the dotted line represents the arbitrary threshold (35%) for filtering out poor quality samples. On the right, box-plot graph representing the number of missing values within each group, after removal of samples with >35% of missing values. **(B)** Box-plot graph of the log2 transformed and filtered label-free iBAQ intensities for each sample before (left) and after (right) quantile normalization, imputation, and batch effect removal. **(C)** Clustering dendrogram of the differentially expressed proteins (DEPs) related to both ITP mouse models, before (up) and after (down) cluster merging. Colors represent the modules assigned to the protein clusters.

Figure S2. Protein–protein interaction graphics of ITP affected proteins module- and model-wise using STRING database. (A) Proteins affected on both ITP models. Modules black (downregulated) and brown (upregulated) are represented. **(B)** Proteins affected more severely on one ITP model (*i.e.*, lower expression in P-ITP D3). A selection of proteins from the red module are represented. **(C)** Proteins affected more severely on one ITP model (*i.e.*, lower expression in A-ITP). Proteins from the green and pink modules are represented.

Figure S3. GO Term analysis after cooperative analysis of protein dynamics in platelets from ITP mouse models. Bar-graphs representing the significant Gene Ontology (GO), Kyoto Encyclopedia of Genes and Genomes (KEGG), and Reactome enrichments on gene lists from the **(A)** black module (with the same protein dynamics on platelets from both ITP mouse models); **(B)** red module (with different protein dynamics – lower expression in the passive ITP model) and **(C)** green and pink modules (with different protein dynamics -lower expression in the active ITP model). BP, biological process; CF, cellular function; CC, cellular compartment.

Figure S1

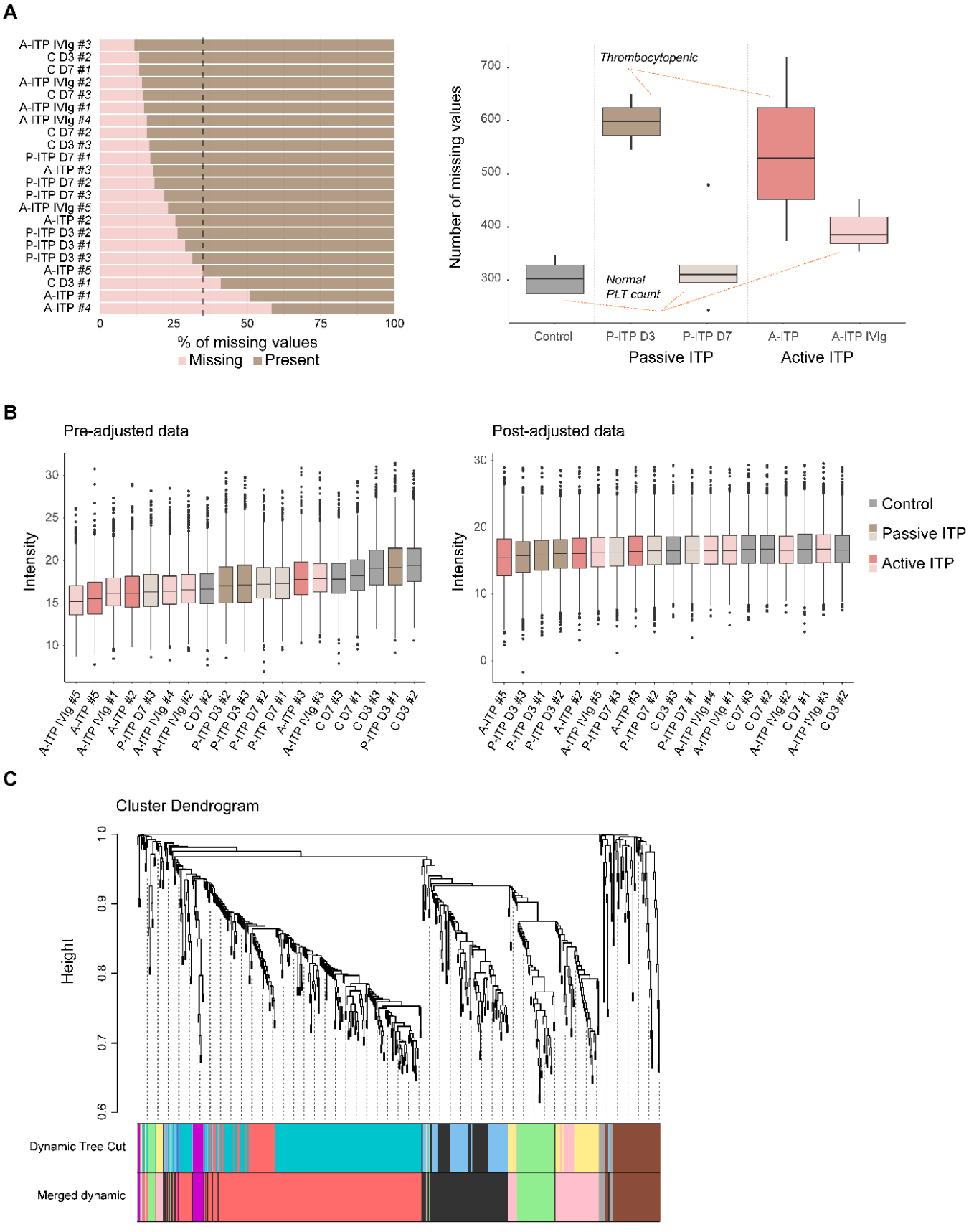
A
A-ITP IVIg #3
C D3 #2
C D7 #1
A-ITP IVIg #2
C D7 #3
A-ITP IVIg #1
A-ITP IVIg #4
C D7 #2
C D3 #3
P-ITP D7 #1
A-ITP #3
P-ITP D7 #2
P-ITP D7 #3
A-ITP IVIg #5
A-ITP #2
P-ITP D3 #2
P-ITP D3 #1
P-ITP D3 #3
A-ITP #5
C D3 #1
A-ITP #1
A-ITP #4
0
25
50
75
100
% of missing values
Missing
Present
Number of missing values
700
600
500
400
300
Thrombocytopenic
Normal
PLT count
Control
P-ITP D3
P-ITP D7
A-ITP
A-ITP IVIg
Passive ITP
Active ITP
B
Pre-adjusted data
Post-adjusted data
Intensity
30
25
20
15
10
0
A-ITP IVIg #5
A-ITP #5
A-ITP IVIg #1
A-ITP #2
P-ITP D7 #3
A-ITP IVIg #4
A-ITP IVIg #2
C D7 #2
P-ITP D3 #2
P-ITP D3 #3
P-ITP D7 #2
P-ITP D7 #1
A-ITP #3
A-ITP IVIg #3
C D7 #3
C D7 #1
C D3 #3
P-ITP D3 #1
C D3 #2
A-ITP #5
P-ITP D3 #3
P-ITP D3 #1
P-ITP D3 #2
A-ITP #2
A-ITP IVIg #5
P-ITP D7 #3
A-ITP #3
P-ITP D7 #2
C D3 #3
P-ITP D7 #1
A-ITP IVIg #4
A-ITP IVIg #1
C D7 #3
C D7 #2
A-ITP IVIg #2
C D7 #1
A-ITP IVIg #3
C D3 #2
Control
Passive ITP
Active ITP
C
Cluster Dendrogram
Height
1.0
0.9
0.8
0.7
0.6
Dynamic Tree Cut
Merged dynamic

Figure S2

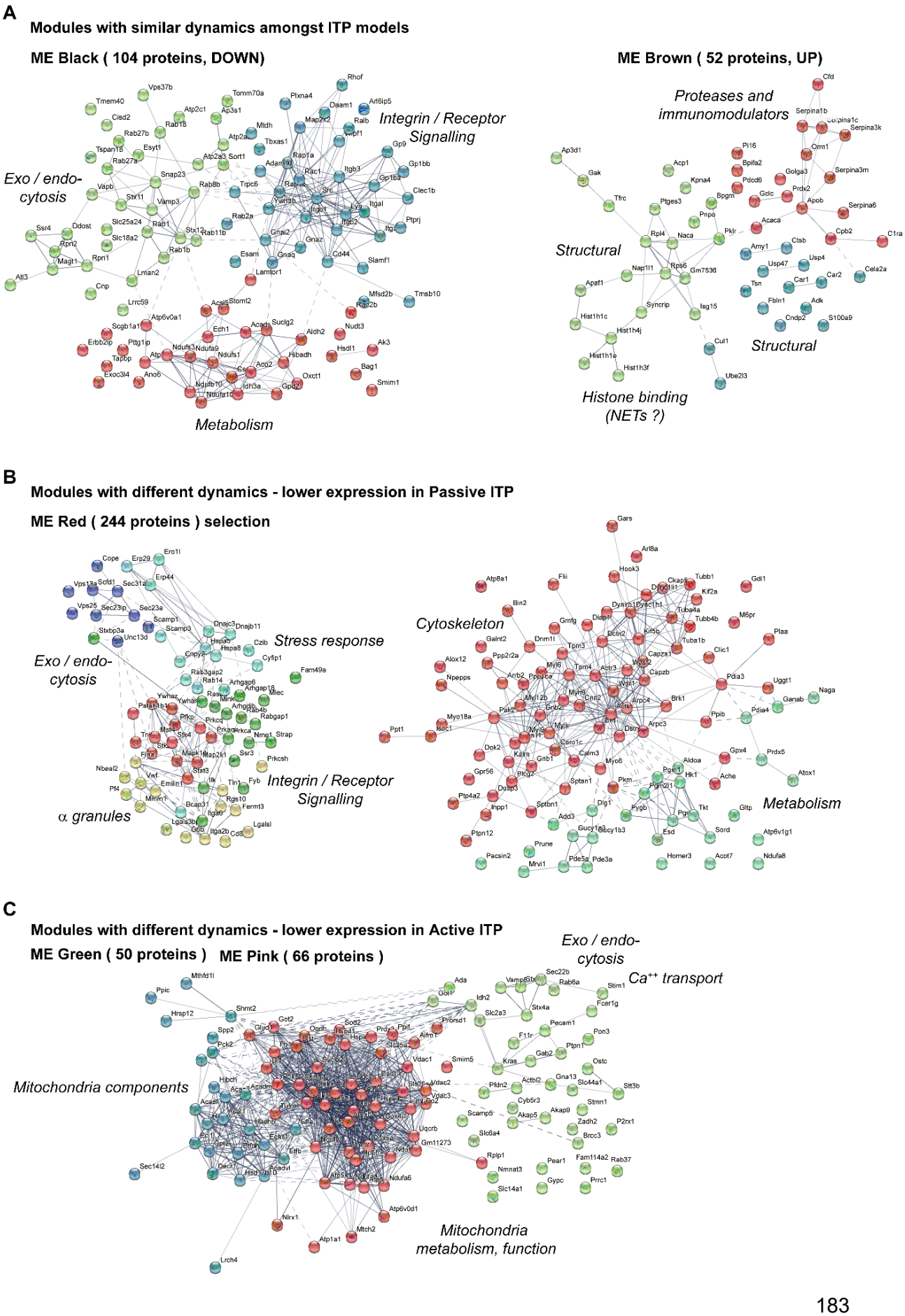
A
Modules with similar dynamics amongst ITP models
ME Black (104 proteins, DOWN)
Integrin / Receptor Signalling
Exo / endo-cytosis
Metabolism
ME Brown (52 proteins, UP)
Proteases and immunomodulators
Structural
Structural
Histone binding (NETs ?)
B
Modules with different dynamics - lower expression in Passive ITP
ME Red (244 proteins) selection
Stress response
Exo / endo-cytosis
Integrin / Receptor Signalling
α granules
Cytoskeleton
Metabolism
C
Modules with different dynamics - lower expression in Active ITP
ME Green (50 proteins)
ME Pink (66 proteins)
Exo / endo-cytosis
Ca++ transport
Mitochondria components
Mitochondria metabolism, function

Figure S3

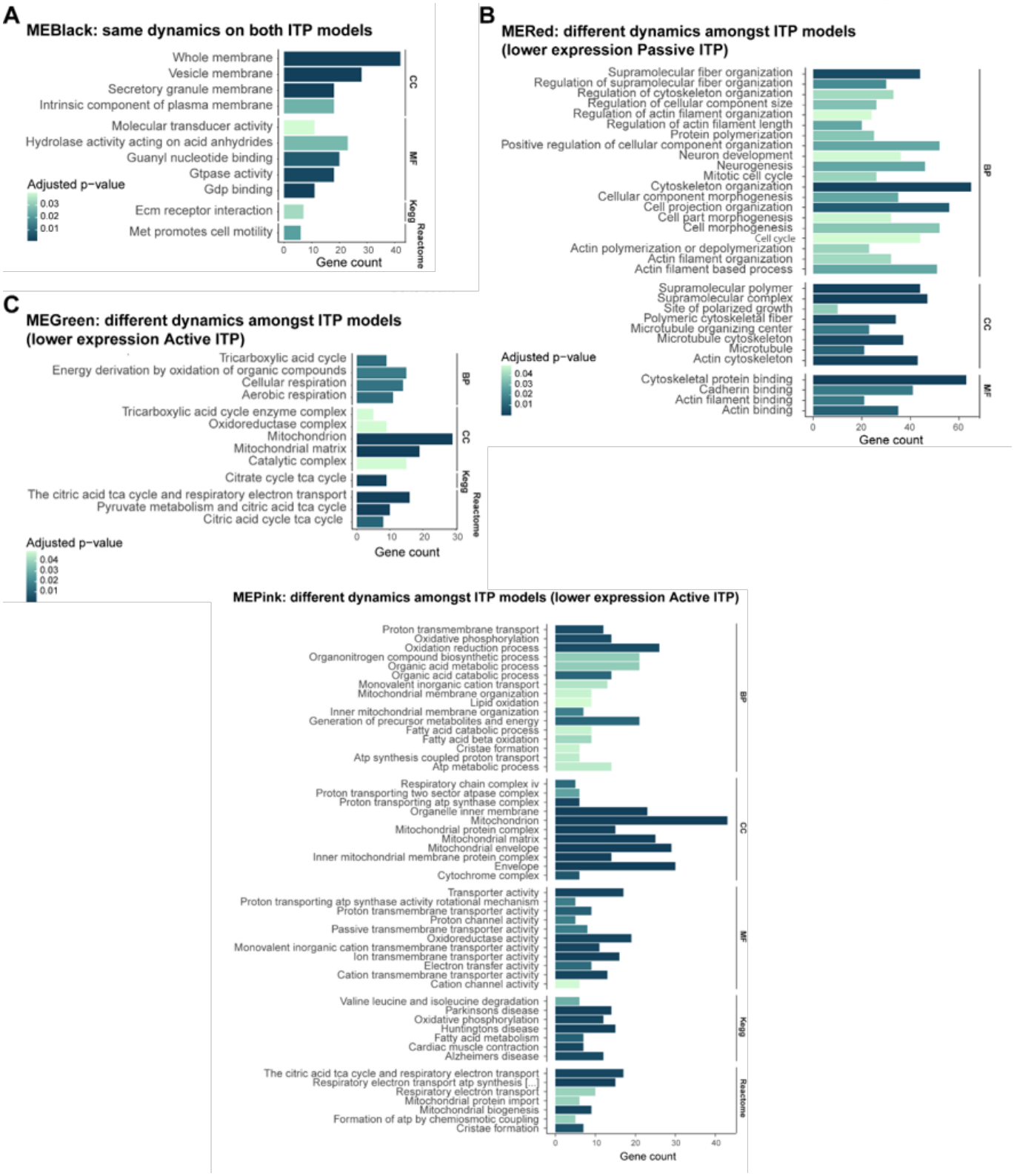
A
MEBlack: same dynamics on both ITP models
Whole membrane
Vesicle membrane
Secretory granule membrane
Intrinsic component of plasma membrane
Molecular transducer activity
Hydrolase activity acting on acid anhydrides
Guanyl nucleotide binding
Gtpase activity
Gdp binding
Ecm receptor interaction
Met promotes cell motility
CC
MF
Kegg
Reactome
Adjusted p-value
0.03
0.02
0.01
0 10 20 30 40
Gene count
B
MERed: different dynamics amongst ITP models
(lower expression Passive ITP)
Supramolecular fiber organization
Regulation of supramolecular fiber organization
Regulation of cytoskeleton organization
Regulation of cellular component size
Regulation of actin filament organization
Regulation of actin filament length
Protein polymerization
Positive regulation of cellular component organization
Neuron development
Neurogenesis
Mitotic cell cycle
Cytoskeleton organization
Cellular component morphogenesis
Cell projection organization
Cell part morphogenesis
Cell morphogenesis
Cell cycle
Actin polymerization or depolymerization
Actin filament organization
Actin filament based process
Supramolecular polymer
Supramolecular complex
Site of polarized growth
Polymeric cytoskeletal fiber
Microtubule organizing center
Microtubule cytoskeleton
Microtubule
Actin cytoskeleton
Cytoskeletal protein binding
Cadherin binding
Actin filament binding
Actin binding
BP
CC
MF
Adjusted p-value
0.04
0.03
0.02
0.01
0 20 40 60
Gene count
C
MEGreen: different dynamics amongst ITP models
(lower expression Active ITP)
Tricarboxylic acid cycle
Energy derivation by oxidation of organic compounds
Cellular respiration
Aerobic respiration
Tricarboxylic acid cycle enzyme complex
Oxidoreductase complex
Mitochondrion
Mitochondrial matrix
Catalytic complex
Citrate cycle tca cycle
The citric acid tca cycle and respiratory electron transport
Pyruvate metabolism and citric acid tca cycle
Citric acid cycle tca cycle
BP
CC
Kegg
Reactome
Adjusted p-value
0.04
0.03
0.02
0.01
0 10 20 30
Gene count
MEPink: different dynamics amongst ITP models (lower expression Active ITP)
Proton transmembrane transport
Oxidative phosphorylation
Oxidation reduction process
Organonitrogen compound biosynthetic process
Organic acid metabolic process
Organic acid catabolic process
Monovalent inorganic cation transport
Mitochondrial membrane organization
Lipid oxidation
Inner mitochondrial membrane organization
Generation of precursor metabolites and energy
Fatty acid catabolic process
Fatty acid beta oxidation
Cristae formation
Atp synthesis coupled proton transport
Atp metabolic process
Respiratory chain complex iv
Proton transporting two sector atpase complex
Proton transporting atp synthase complex
Organelle inner membrane
Mitochondrion
Mitochondrial protein complex
Mitochondrial matrix
Mitochondrial envelope
Inner mitochondrial membrane protein complex
Envelope
Cytochrome complex
Transporter activity
Proton transporting atp synthase activity rotational mechanism
Proton transmembrane transporter activity
Proton channel activity
Passive transmembrane transporter activity
Oxidoreductase activity
Monovalent inorganic cation transmembrane transporter activity
Ion transmembrane transporter activity
Electron transfer activity
Cation transmembrane transporter activity
Cation channel activity
Valine leucine and isoleucine degradation
Parkinsons disease
Oxidative phosphorylation
Huntingtons disease
Fatty acid metabolism
Cardiac muscle contraction
Alzheimers disease
The citric acid tca cycle and respiratory electron transport
Respiratory electron transport atp synthesis [...]
Respiratory electron transport
Mitochondrial protein import
Mitochondrial biogenesis
Formation of atp by chemiosmotic coupling
Cristae formation
BP
CC
MF
Kegg
Reactome
0 10 20 30 40
Gene count

Chapter II

Figure S1. Descriptive parameters of human and mouse proteomics datasets used for the analysis. (A) Barplots showing the number of proteins (Y-axis) that are detected across datasets (X-axis), (*i.e.*, 8 proteins were consistently detected in the 27 datasets), both in human (top) and mouse (bottom) platelet lysates; and **(B)** human platelet secretomes independently of the agonist used (left) and those obtained upon stimulation with thrombin (right). The core proteomes (lysate and secretome) were built with the proteins contained in the bars shaded in a darker color, representing dataset intersections.

Figure S2. Ranked distributions of human platelet proteome selected datasets. (A) Ranked distributions based on the relative abundance of the platelet proteins of datasets x11 (see Tables S1-2), and dotplots showing the main GO terms after enrichment analysis of the three different subsets based on the distribution quartiles of said distribution (high, intermediate, and low abundance). Vertical grey lines show the quartile breaks. **(B)** Ranked distributions based on the relative abundance of the platelet proteins of three other selected datasets in human (x25, x28 and x42).

Figure S3. Ranked distributions of mouse platelet proteome selected datasets. (A) Ranked distributions based on the relative abundance of the platelet proteins of datasets x39 (see Tables S1-2), and dotplots showing the main GO terms after enrichment analysis of the three different subsets based on the distribution quartiles of said distribution (high, intermediate, and low abundance). Vertical grey lines show the quartile breaks. **(B)** Ranked distributions based on the relative abundance of the platelet proteins of another dataset in mouse (x35).

Figure S4. Ranked distributions of human and mouse platelet secretome selected datasets. Ranked distributions based on the relative abundance of the platelet secretome proteins of two selected datasets (s5 and s4 as in Tables S1-2, top and

bottom, for human and mouse, respectively), and dotplots showing the main GO terms after enrichment analysis of the three different subsets based on the distribution quartiles of said distribution (high, intermediate, and low abundance). Vertical grey lines show the quartile breaks.

Tables S1 and S2. Summary of the datasets used in this study, and the corresponding processing and bioinformatics information, and data availability.

Figure S1

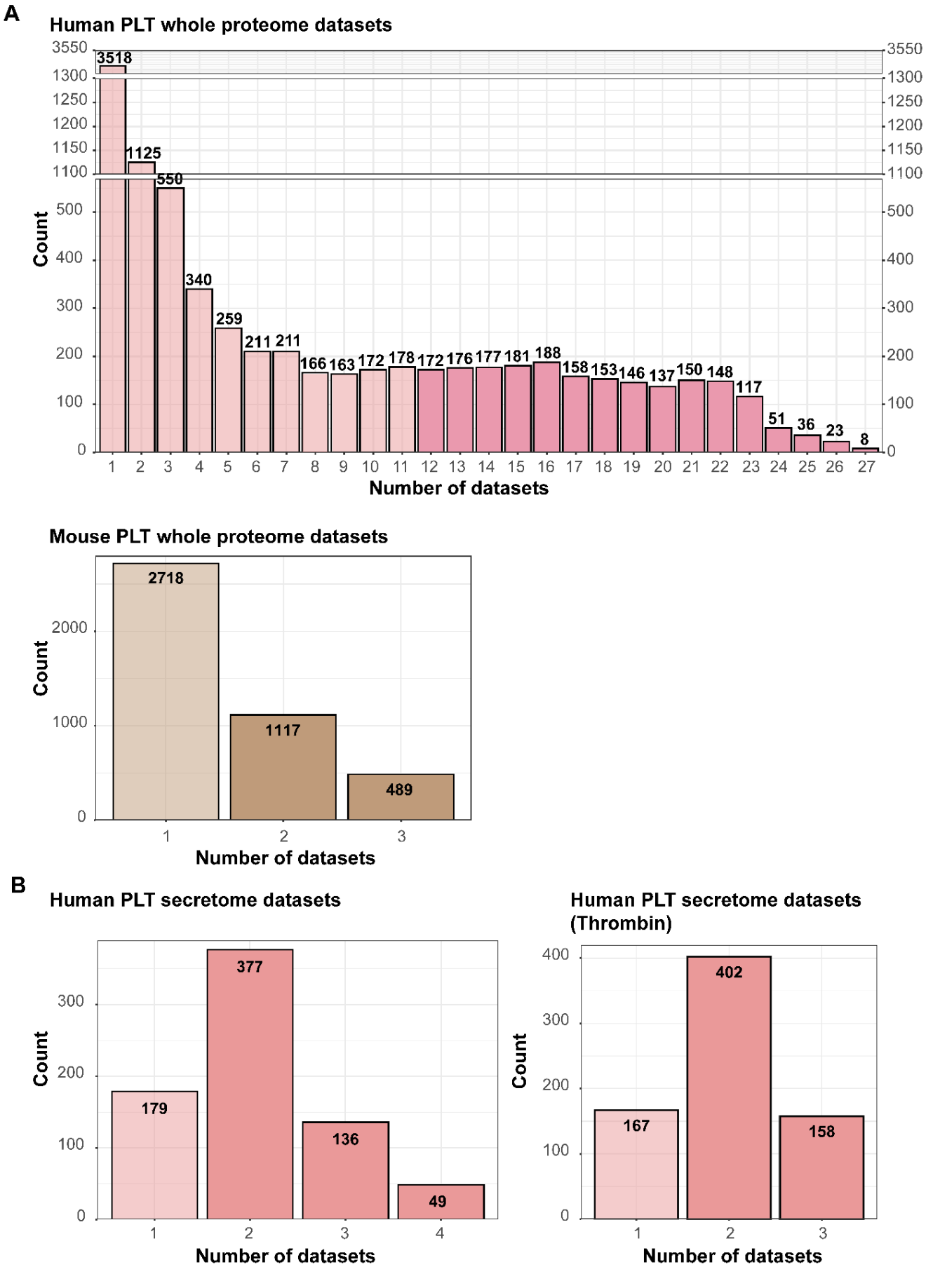
A
Human PLT whole proteome datasets
Count
Number of datasets
3518
1125
550
340
259
211 211
166 163 172 178 172 176 177 181 188
158 153 146 137 150 148
117
51
36
23
8
Mouse PLT whole proteome datasets
2718
1117
489
B
Human PLT secretome datasets
179
377
136
49
Human PLT secretome datasets (Thrombin)
167
402
158

Figure S2

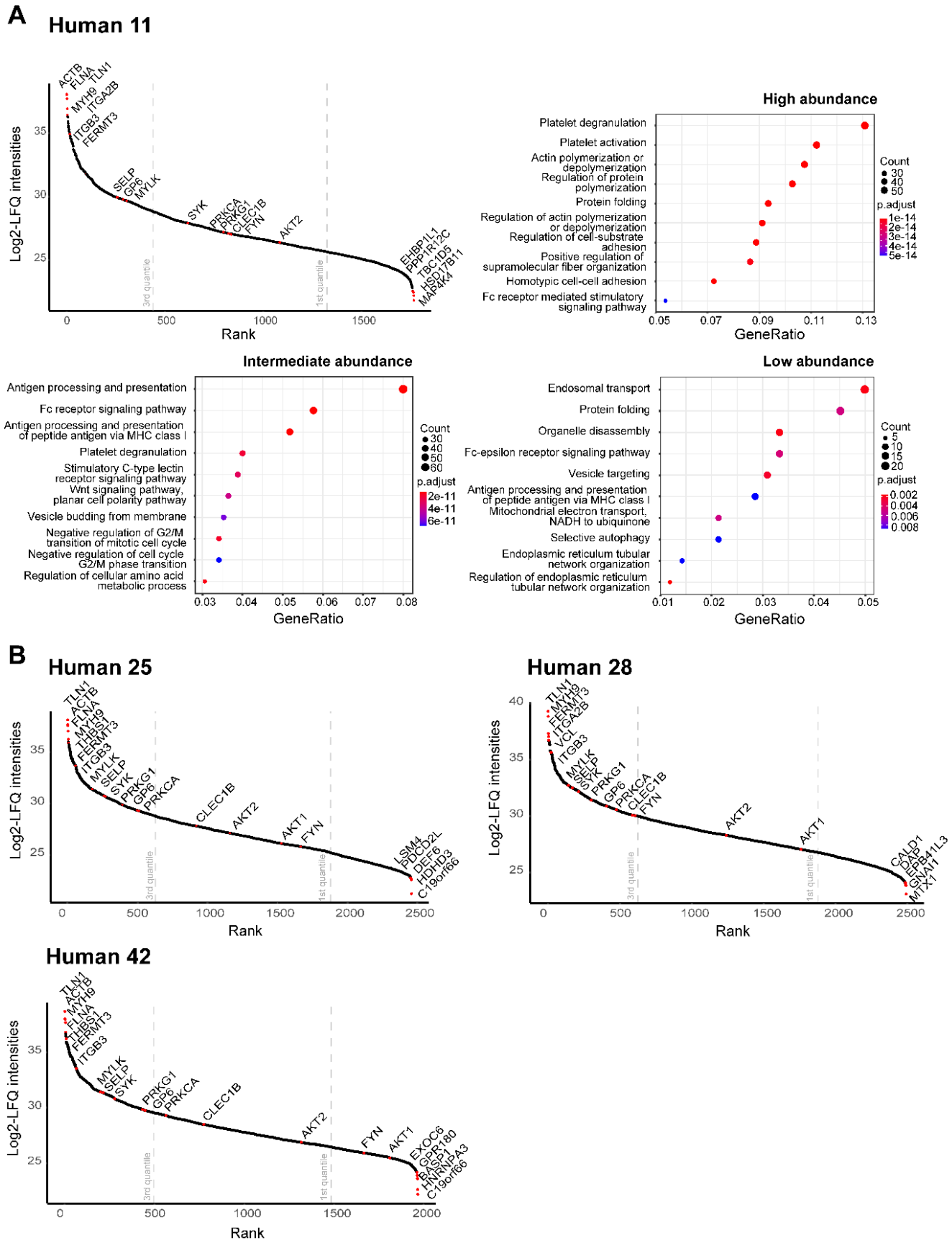
A
Human 11
Log2-LFQ intensities
Rank
3rd quantile
1st quantile
ACTB
FLNA
TLN1
MYH9
ITGA2B
ITGB3
FERMT3
SELP
GP6
MYLK
SYK
PRKCA
PRKG1
CLEC1B
FYN
AKT2
EHBP1L1
PPP1R12C
TBC1D5
HSD17B11
MAP4K4
High abundance
Platelet degranulation
Platelet activation
Actin polymerization or depolymerization
Regulation of protein polymerization
Protein folding
Regulation of actin polymerization or depolymerization
Regulation of cell-substrate adhesion
Positive regulation of supramolecular fiber organization
Homotypic cell-cell adhesion
Fc receptor mediated stimulatory signaling pathway
GeneRatio
Count
p.adjust
Intermediate abundance
Antigen processing and presentation
Fc receptor signaling pathway
Antigen processing and presentation of peptide antigen via MHC class I
Platelet degranulation
Stimulatory C-type lectin receptor signaling pathway
Wnt signaling pathway, planar cell polarity pathway
Vesicle budding from membrane
Negative regulation of G2/M transition of mitotic cell cycle
Negative regulation of cell cycle G2/M phase transition
Regulation of cellular amino acid metabolic process
Low abundance
Endosomal transport
Protein folding
Organelle disassembly
Fc-epsilon receptor signaling pathway
Vesicle targeting
Antigen processing and presentation of peptide antigen via MHC class I
Mitochondrial electron transport, NADH to ubiquinone
Selective autophagy
Endoplasmic reticulum tubular network organization
Regulation of endoplasmic reticulum tubular network organization
B
Human 25
LSM4
PRCD2L
DEF6
HDHD3
C19orf66
Human 28
VCL
CALD1
DAB2
EPB41L3
GNAI1
MTX1
Human 42
EXOC6
GPR180
RASD1
HNRNPA3
C19orf66

Figure S3

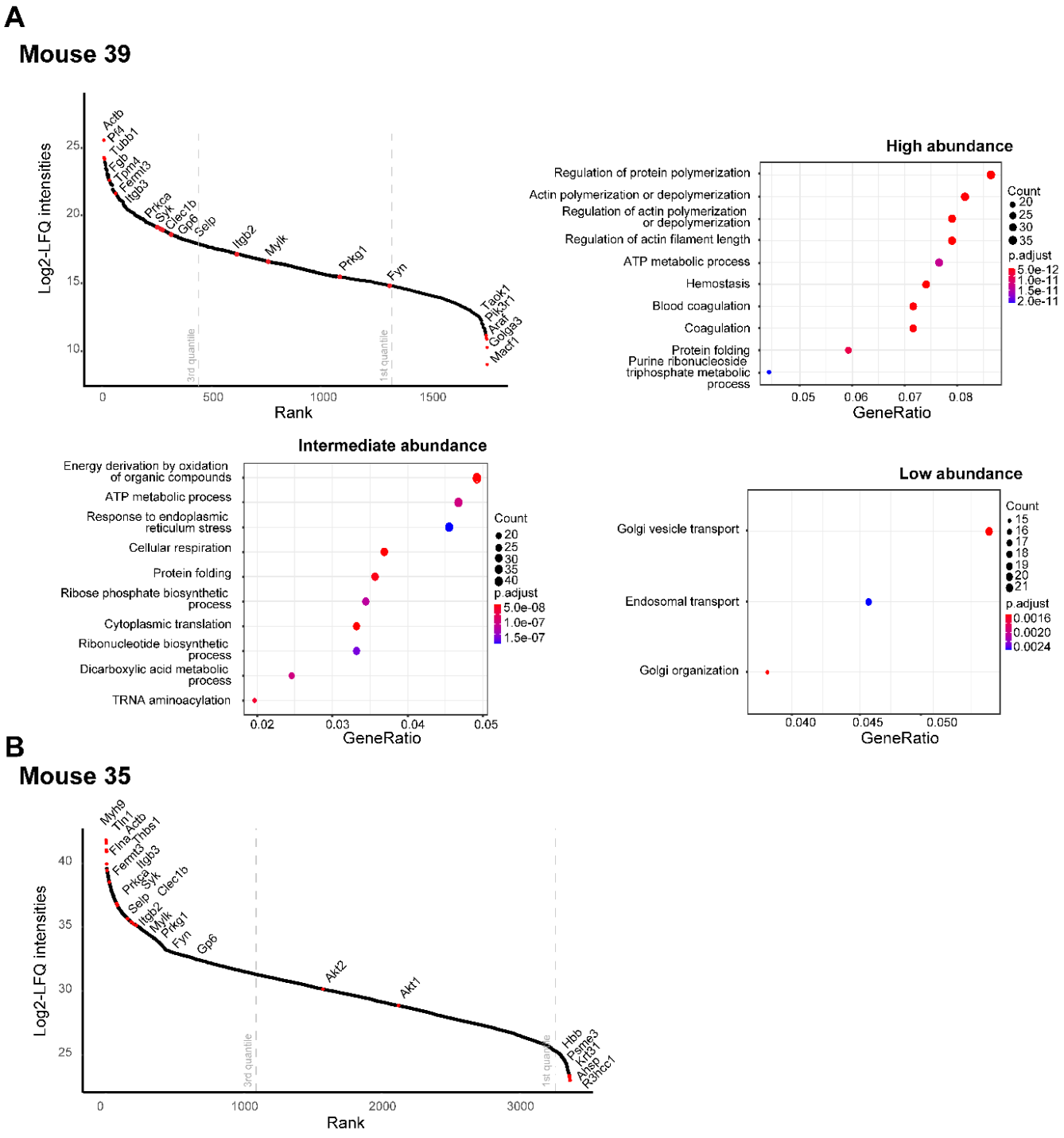
A
Mouse 39
Log2-LFQ intensities
Rank
3rd quantile
1st quantile
Actb
Pf4
Tubb1
Fgb
Tpm4
Fermt3
Itgb3
Prkca
Syk
Clec1b
Gp6
Selp
Itgb2
Mylk
Prkg1
Fyn
Tagk1
Pik3r1
Araf
Golga3
Macf1
High abundance
Regulation of protein polymerization
Actin polymerization or depolymerization
Regulation of actin polymerization or depolymerization
Regulation of actin filament length
ATP metabolic process
Hemostasis
Blood coagulation
Coagulation
Protein folding
Purine ribonucleoside triphosphate metabolic process
GeneRatio
Count
p.adjust
Intermediate abundance
Energy derivation by oxidation of organic compounds
ATP metabolic process
Response to endoplasmic reticulum stress
Cellular respiration
Protein folding
Ribose phosphate biosynthetic process
Cytoplasmic translation
Ribonucleotide biosynthetic process
Dicarboxylic acid metabolic process
TRNA aminoacylation
Low abundance
Golgi vesicle transport
Endosomal transport
Golgi organization
B
Mouse 35
Log2-LFQ intensities
Rank
Myh9
Tln1
Flna
Actb
Thbs1
Fermt3
Itgb3
Prkca
Syk
Clec1b
Selp
Itgb2
Mylk
Prkg1
Fyn
Gp6
Akt2
Akt1
Hbb
Psme3
Kif3a
Arsp
R3hcc1

Figure S4

Human

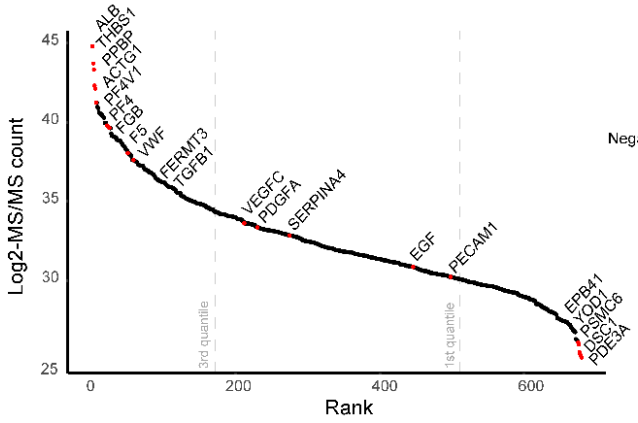

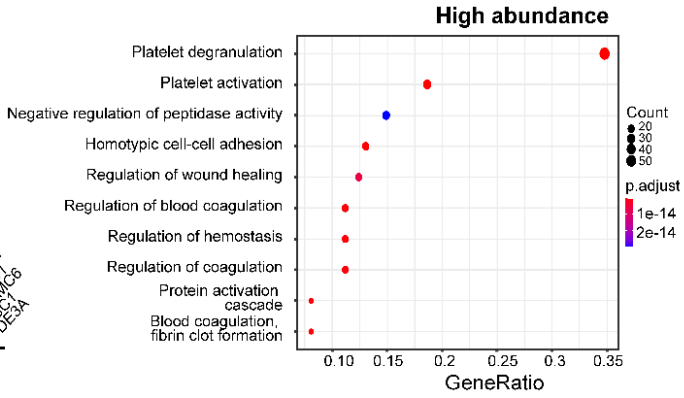

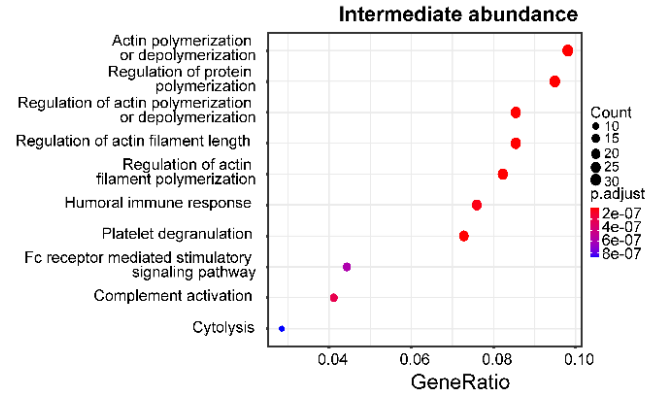

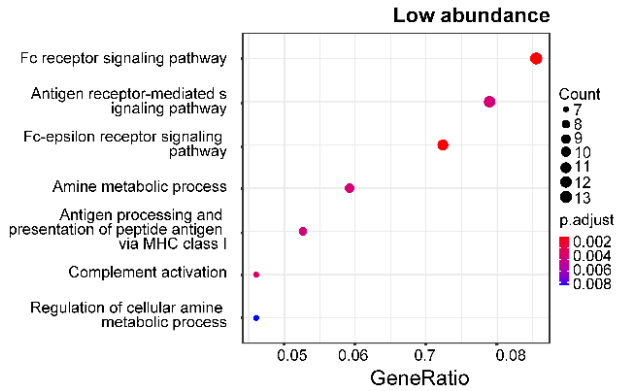

Mouse

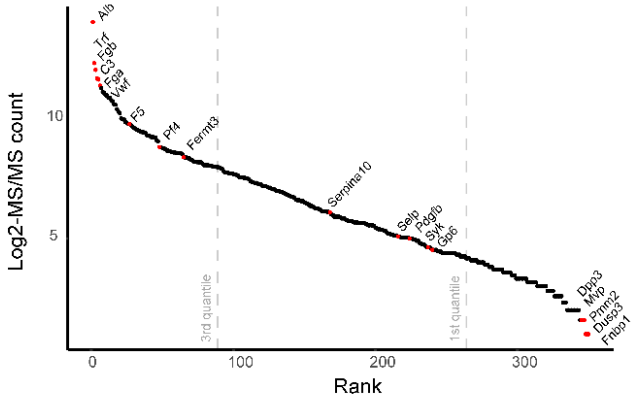

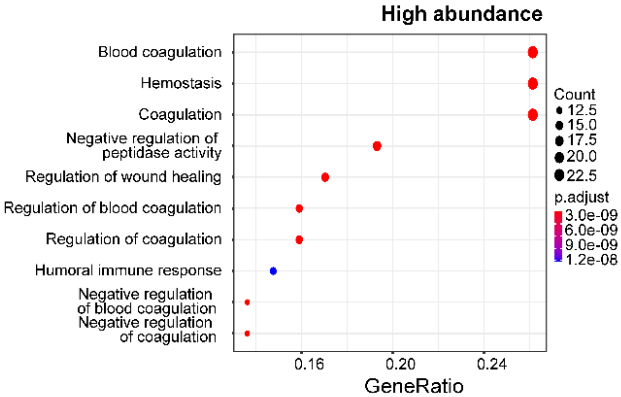

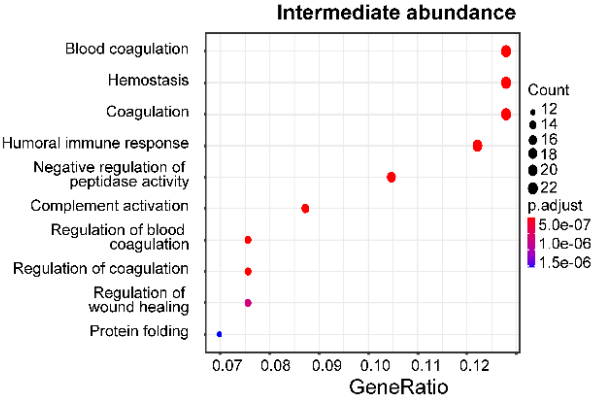

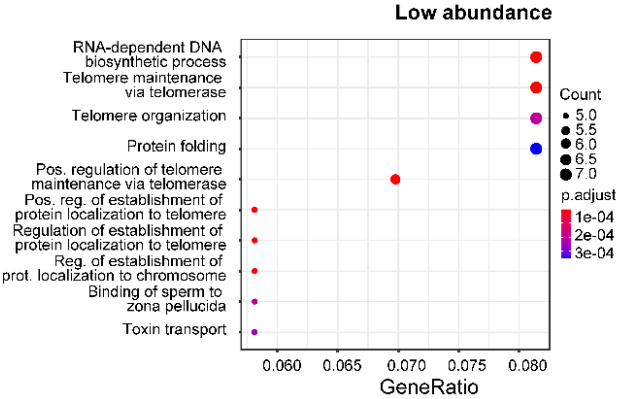

db_id	PMID	pride_id	species	type	complete_data	clear_samples	n_control	sample_pool	n_proteins	prot_type	enzyme	mass_spec	search_engine
x1	35892149		human	PLT lysate	yes	yes	6	yes	252	label_free	trypsin	LTQ Orbitrap XL	IP2
x2	35419777	PXD031202	human	PLT lysate	yes	no	10	no	2572	label_free	trypsin	tribid	PD
x4	35842415	PXD031251	human	PLT lysate	yes	yes	6	no	3778	label_free	trypsin	Q-Exactive	PatternLab/Coment
x6	35253976	PXD030225	human	PLT lysate	yes	yes	18	no	3358	TMT11plex	trypsin	Orbitrap Fusion	COMET/PAW
x7	35455936	PXD031278	human	PLT lysate	yes	yes	3	no	552	TMT6plex	trypsin	tribid	MaxQuant
x8	35967457	OMIX001255	human	PLT lysate	yes	yes	3	no	3542	DIA	trypsin	Q-Exactive	MaxQuant, Spectronaut
x9	34390534	PXD014490	human	PLT lysate	yes	yes	8	no	583	label_free	trypsin	Q-Exactive	MaxQuant
x10	34086871		human	PLT lysate	yes	no		yes	1210	label_free	trypsin	tribid	PD
x11	34510746	PXD027893	human	PLT lysate	yes	yes	7	no	1717	label_free	trypsin	Q-Exactive	MaxQuant
x12	33054111		human	PLT lysate	yes	yes	5	no	2275	TMT10plex	trypsin	Q-Exactive / tribid	PD
x15	33690840	PXD020343	human	PLT lysate	yes	yes	28	no	2871	label_free	trypsin	tribid	MaxQuant
x17	34055779	PXD023745	human	PLT lysate	yes	yes	3	yes	383	label_free	trypsin	QqToF	PEAKS Studio X+
x21	31909355		human	PLT lysate	yes	yes	10	no	1235	itraq	trypsin	TripleTOF	Protein Pilot
x24	29421274		mouse	PLT lysate	yes	yes	6	no	1477	label_free	trypsin	Q-Exactive	PD
x25	29553857	PXD008119	human	PLT lysate	yes	yes	3	yes	2505	label_free	trypsin	tribid	MaxQuant
x26	29323256	PXD006559	human	PLT lysate	yes	yes	3	yes	5816	TMT10plex	trypsin	Q-Exactive	PD
x28	28887518	PXD005610	human	PLT lysate	yes	yes	21	yes	2501	label_free	trypsin	Orbitrap Fusion	MaxQuant
x29	28542641		human	PLT lysate	yes	yes	5	no	2896	label_free	trypsin	LTQ Orbitrap XL	
x30	27601597	PXD003613	human	PLT lysate	yes	yes	14	no	5423	label_free	trypsin	LTQ-FT	MS-GF+
x31	27040998		human	PLT lysate	yes	no	1	no	1017	label_free	trypsin	Orbitrap Velos	PD
x33	25903651	PXD000621	human	PLT lysate	yes	no	2	no	919	itraq3plex	trypsin	QStar Elite	Protein Pilot
x35	25205226	PXD000747	mouse	PLT lysate	yes	yes	3	no	4376	label_free	trypsin	Q-Exactive	MaxQuant
x36	22869793	22201-22203, 22206	human	PLT lysate	yes	yes	4	no	4191	itraq4plex	trypsin	Orbitrap XL, Qstar Elite	Mascot, OMSSA and X!Tandem - PeptideShaker
x37	22114104	18827–18850	human	PLT lysate, others	yes	yes	3	no	663	label_free	trypsin	Esquire-HCT	GeneBio PhenyxOnLine
x39	35298626	PXD028814	mouse	PLT lysate	yes	yes	6	no	2035	label_free	trypsin	tribid	MaxQuant
x40	27535140	PXD002883	human	PLT lysate	yes	yes	1	no	2278	itraq8plex	trypsin	Q-Exactive	PD
x41	28078347	PXD003912	human	PLT lysate	yes	yes	2	no	2335	label_free	trypsin	Orbitrap Velos	Progenesis, PeptideShaker
x42	28823163	PXD004578	human	PLT lysate	yes	yes	5	no	1999	label_free	trypsin	tribid	MaxQuant
x43	27452734		human	PLT lysate	yes	yes	10	no	1532	itraq4plex	trypsin	Q-Exactive	PD
x44	24776597	PXD000228	human	PLT lysate	yes	yes	3	no	3142	Stable isotope dimethyl labelling	Lys-C, trypsin	Orbitrap Velos	PD
s2	25210793		human	releasate	yes	no		yes	266	label_free	trypsin	Q-Exactive	X! tandem
s3	24776597	PXD000228	human	releasate	yes	yes	3	no	93	iTRAQ	Lys-C,trypsin	Orbitrap Velos	PD
s4	29369476	PXD006478	mouse	releasate	yes	no	5	no	395				
s5	29932309	PXD009310	human	releasate	yes	yes	32	no	894	label_free	Lys-C, trypsin	Q-Exactive	MaxQuant
s6	30318839		human	releasate	yes	yes	13	no	723	label_free	Lys-C, trypsin	Q-Exactive	MaxQuant

Supplementary Table 1:

Datasets used for the analysis, and obtained information related to the samples, proteomics procedures and mass spectrometry analysis.

db_id	Dataset identification for data analysis
PMID	PubMed Identifier
pride_id	PRIDE identification (if any)
species	Species (human or mouse)
type	Platelet fraction analyzed
complete_data	Are all the detected proteins reported?
clear_samples	Are the groups/bioreplicates clearly identified?
n_control	Number of controls used
sample_pool	Do the analyzed samples result from a previous pooling?
n_proteins	Number of proteins detected (per the Results section)
prot_type	Type of proteomics performed
enzyme	Enzyme used for the protein digestion
mass_spec	Mass spectrometer used
search_engine	Software used for the spectra analysis

Table S2

db_id	PMID	pride_id	species	type	plt_source	anticoagulant	day_after_collection	anti_activation_PLT	n centrifugations	check purity	check activation	agonist	Observations / Notes
x1	35892149		human	PLT lysate	bag	sodium citrate	7	no	0	yes	no		Each batch consisted of platelet concentrate bags of a median of six donors (5–8 range)
x2	35419777	PXD031202	human	PLT lysate	donor	ACD	0	prostaglandin	2	yes	yes		
x4	35842415	PXD031251	human	PLT lysate	donor	ACD	0	prostaglandin	2	yes	no		
x6	35253976	PXD030225	human	PLT lysate	donor	ACD, EDTA, heparin	0, 1	prostacyclin	3	yes	yes		
x7	35455936	PXD031278	human	PLT lysate	donor	ACD	0	no	2	no	no		
x8	35967457	OMIX001255	human	PLT lysate	donor	trisodium citrate	0	prostaglandin	2	yes	no		
x9	34390534	PXD014490	human	PLT lysate	donor	trisodium citrate	0	prostaglandin	2	yes	yes		Sorted PLTs
x10	34086871		human	PLT lysate	bag		5	no	1	yes	no		
x11	34510746	PXD027893	human	PLT lysate	bag	ACD	1	no	2	yes	yes		List of proteins includes contaminants
x12	33054111		human	PLT lysate	donor	EDTA	0	no	4	no	no		
x15	33690840	PXD020343	human	PLT lysate	donor		0	prostaglandin	4	no	no		
x17	34055779	PXD023745	human	PLT lysate	bag		1	no	1	yes	no		3 pools made of 18 donors each
x21	31909355		human	PLT lysate	donor	sodium citrate	0	prostaglandin	3	yes	no		List of proteins includes contaminants
x24	29421274		mouse	PLT lysate	donor	ACD	0	no	2	no	yes		
x25	29553857	PXD008119	human	PLT lysate	donor, bag	sodium citrate	0, 1, 2, 6, 8	no	2	yes	no		3 pools made of 6 donors each and splitted
x26	29323256	PXD006559	human	PLT lysate	donor	sodium citrate	0	no	2	yes	no		3 pools made of 5 donors each
x28	28887518	PXD005610	human	PLT lysate	bag	ACD	1, 2, 5, 7, 9, 13, 16	no	4	yes	no		21 pools made of 22 donors each, 7 groups
x29	28542641		human	PLT lysate	donor	ACD	0	prostaglandin	4	yes	no		
x30	27601597	PXD003613	human	PLT lysate	donor	ACD	0	no	2	yes	no		
x31	27040998		human	PLT lysate	donor	ACD	0	no	5	no	no		Day 1 referes to the day before the treatment
x33	25903651	PXD000621	human	PLT lysate	donor	sodium citrate	0	no	1	yes	no		
x35	25205226	PXD000747	mouse	PLT lysate	donor	heparin	0	no	4	yes	no		The ultra-purified fraction was used
x36	22869793	22201-22203, 22206	human	PLT lysate	donor	ACD	0	no	4	yes	no		Proteins with detected with high confidence were used
x37	22114104	18827–18850	human	PLT lysate, others	donor		0	prostacyclin	3	yes	no		not sure
x39	35298626	PXD028814	mouse	PLT lysate	donor	EDTA, CPDA	0	no	2	yes	no		
x40	27535140	PXD002883	human	PLT lysate	donor	ACD	0	no	3	yes	no		
x41	28078347	PXD003912	human	PLT lysate	donor	ACD	0	no	4	yes	no		
x42	28823163	PXD004578	human	PLT lysate	donor	sodium citrate	0	prostaglandin	4	yes	no		
x43	27452734		human	PLT lysate	donor	sodium citrate	0	prostaglandin	2	no	no		
x44	24776597	PXD000228	human	PLT lysate	donor	trisodium citrate, ACD	0	prostacyclin	2	no	yes		Unstimulated platelets are the controls
s2	25210793		human	releasate	donor, bag	ACD	0, 5	theophylline	3	no	yes	bovine thrombin	Supernatants were pooled across 4–15 donors
s3	24776597	PXD000228	human	releasate	donor	trisodium citrate	0	prostacyclin, acetylsalicylic acid, AR-C69931MX	3	no	yes	SFLLRN, AYPGKF	3 donors per experiment - filtering needed to differentiate receptors
s4	29369476	PXD006478	mouse	releasate	donor	ACD	0	Clopidogrel			yes	thrombin	Lacks methodology information
s5	29932309	PXD009310	human	releasate	donor	ACD	0	no	4	no	no	thrombin	A core set of 277 proteins were reproducibly found in every donor
s6	30318839		human	releasate	donor	ACD	0	no	4	no	no	thrombin	

Supplementary Table 2:

Datasets used for the analysis, and obtained information related to the sample processing prior proteomics analysis.

db_id	Dataset identification for data analysis
PMID	PubMed Identifier
pride_id	PRIDE identification (if any)
species	Species (human or mouse)
type	Platelet fraction analyzed
plt_source	Platelet source (collection bag or tube from donor)
anticoagulant	Anticoagulant used in the collection tube
day_after_collection	Days passed after blood collection (0 = processed on the same day)
anti_activation_PLT	Anti-platelet activation molecule (if any)
n centrifugations	Number of centrifugations
check purity	Do the authors check the purity of the samples?
check activation	Do the authors check whether the platelets have been activated in the process?
agonist	Only in the case of type = "releasate", agonist used to stimulate the PLTs
Observations/Notes	Observations

Chapter III

Figure S1. Comparison between FragPipe and MaxQuant using the whole platelet proteome of healthy donors. (A) Barplots representing the percentage of missing values per sample, and between softwares. **(B)** Barplots of the number of detected proteins in each sample, and between softwares. **(C)** Number of missing values per protein, across samples (*i.e.*, there are 999 proteins that have no missing values, with MaxQuant). The X-axis goes from 0 (no missing values per protein) to 5 (5 missing values per protein), because an arbitrary threshold for dropping proteins with more than 5 missing values was previously set. **(D)** Violin plots of the coverage percentage for each software. **(E)** Venn diagram representing the overlap between the two softwares. **(F)** Scatter plot showing the correlation between the intensities quantified in each software, of the common proteins displayed in the Venn diagram.

Figure S2. Profiling of the healthy platelet proteome and its variability. (A) Plot showing the Pearson correlation between each sample. **(B)** Ranked distribution based on the relative log10-iBAQ intensities of the platelet proteome (*i.e.*, proteins present in all samples, 1758). **(C)** Scatter plot displaying the coefficient of variation percentages for each protein, against their mean log-2 intensities. Additionally, on the right, a boxplot showing the distribution of the coefficients. **(D)** Density plot showing the distribution of the intensities for proteins present in all samples (red) or proteins present in some, but not all, of the samples (grey). **(E)** Enrichment map showing the significantly over-represented biological process (left), molecular function (center), and cellular component (right) terms of the 1758 proteins present in all samples.

Figure S3. Overview of the phosphoproteomics data of healthy platelets. (A) Barplot showing the number of detected phosphosites per agonist. **(B)** Barplot of the percentage of missing values across samples. **(C)** Network of the Reactome terms resulting from a biological theme comparison of the significantly upregulated proteins

across all comparisons (ristocetin did not have any significant terms). The proportion of clusters in the pie chart is determined by the number of proteins.

Figure S4. Interrogation of the different clusters, at the protein level. (A) Network of the Reactome terms resulting from a biological theme comparison of the differentially expressed proteins of each cluster. The proportion of clusters in the pie chart is determined by the number of proteins. **(B)** Scatter plots representing the number of differentially expressed (DE) phosphosites per protein against the respective protein length (left), and number of total phosphosites reported for the corresponding protein (center), and the protein length against the number of total phosphosites (right). The 19 proteins displayed are the ones present across the three clusters, and in red, those who are also found within the top 20 most abundant proteins.

Figure S5. Interrogation of the different clusters, at the protein level, after removal of kinases. (A) Dotplots of the three gene ontologies (GO), after enrichment analysis, for each cluster. **(B)** Network of the Reactome terms resulting from a biological theme comparison of the differentially expressed proteins of each cluster. The proportion of clusters in the pie chart is determined by the number of proteins. **(C)** Dotplots of the phosphosite-level ontology, after enrichment analysis of phospho-regulation terms, for each cluster (kinases were included in this instance).

Figure S6. Heatmap representing the fold-changes of the differentially expressed phosphosites of selected proteins. Extreme fold-changes were truncated to either 2 or -2, so that the color code was easier to understand.

Figure S7. (A) Upset plot of the overlapping over-secreted proteins across agonists (ristocetin not displayed). **(B)** Enrichment map showing the significantly over-represented biological process terms for the over-expressed proteins of the ristocetin condition.

Figure S1

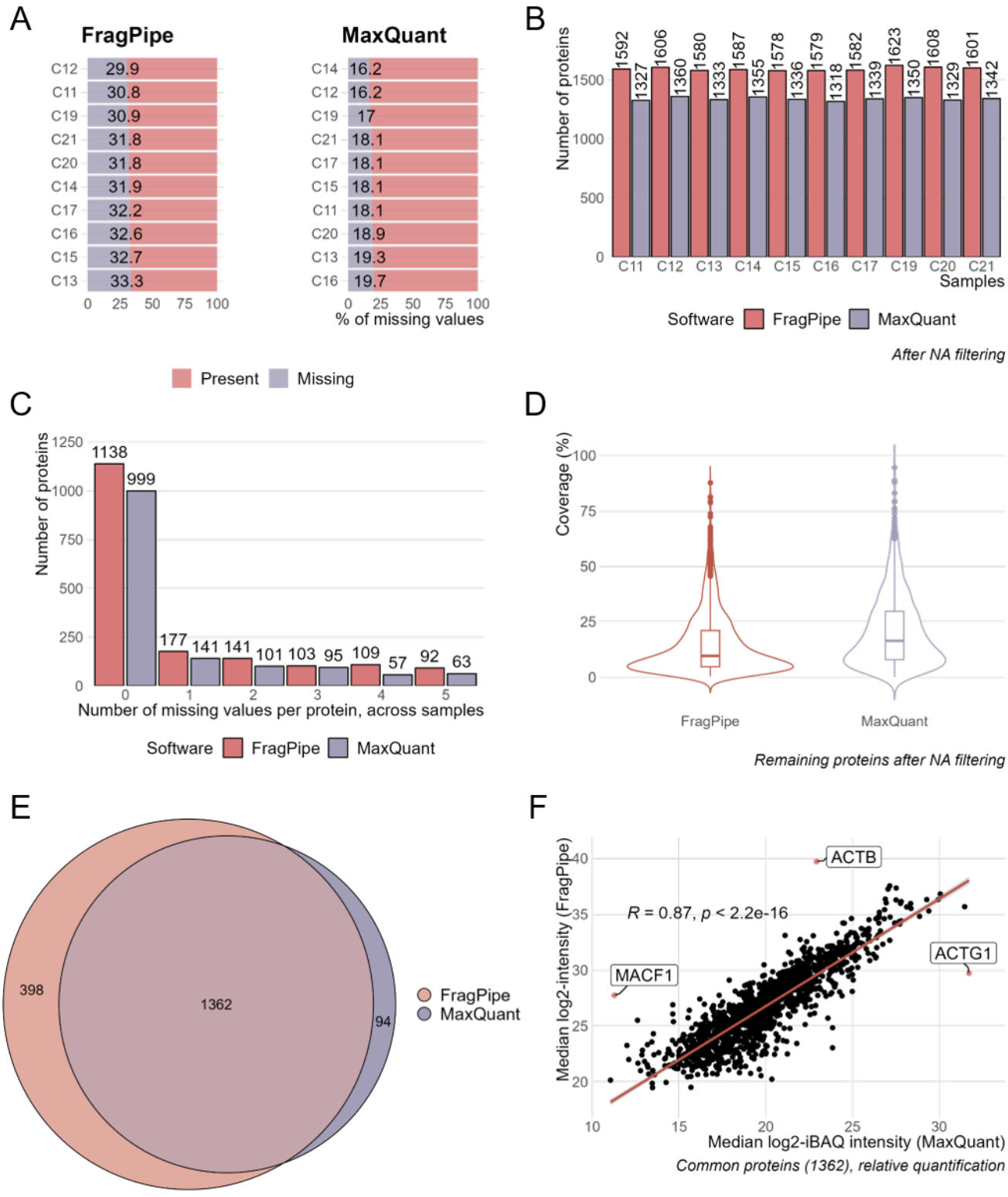
A
FragPipe
C12 29.9
C11 30.8
C19 30.9
C21 31.8
C20 31.8
C14 31.9
C17 32.2
C16 32.6
C15 32.7
C13 33.3
0 25 50 75 100
MaxQuant
C14 16.2
C12 16.2
C19 17
C21 18.1
C17 18.1
C15 18.1
C11 18.1
C20 18.9
C13 19.3
C16 19.7
0 25 50 75 100
% of missing values
Present Missing
B
Number of proteins
1592 1606 1580 1587 1578 1579 1582 1623 1608 1601
1327 1360 1333 1355 1336 1318 1339 1350 1329 1342
0 500 1000 1500
C11 C12 C13 C14 C15 C16 C17 C19 C20 C21
Samples
Software FragPipe MaxQuant
After NA filtering
C
Number of proteins
1138 999 177 141 141 101 103 95 109 57 92 63
0 250 500 750 1000 1250
0 1 2 3 4 5
Number of missing values per protein, across samples
Software FragPipe MaxQuant
D
Coverage (%)
0 25 50 75 100
FragPipe
MaxQuant
Remaining proteins after NA filtering
E
398
1362
94
FragPipe
MaxQuant
F
Median log2-intensity (FragPipe)
10 15 20 25 30 35 40
ACTB
R = 0.87, p < 2.2e-16
ACTG1
MACF1
Median log2-iBAQ intensity (MaxQuant)
Common proteins (1362), relative quantification

Figure S2

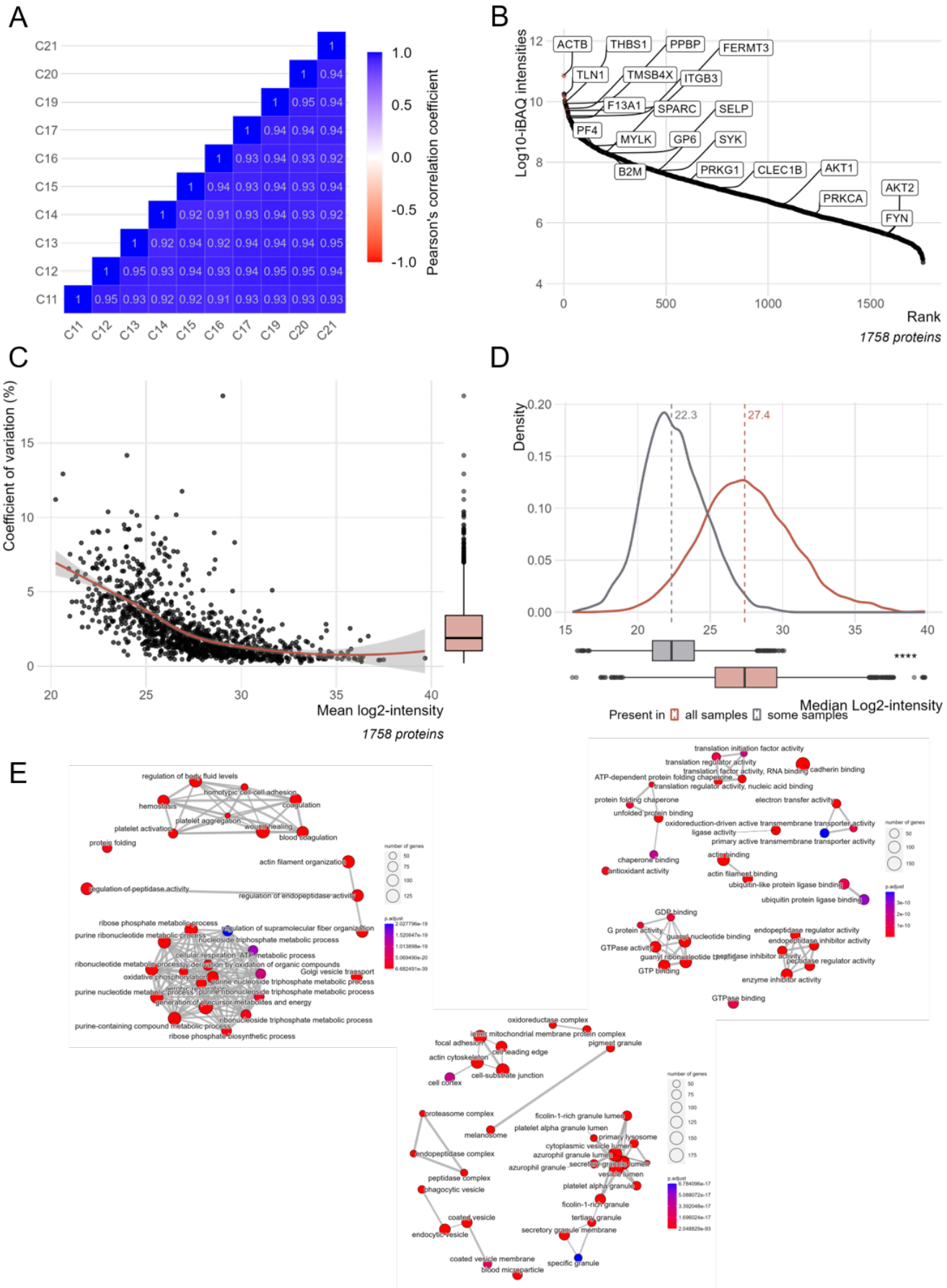
A
C21
C20
C19
C17
C16
C15
C14
C13
C12
C11
Pearson's correlation coefficient
1.0
0.5
0.0
-0.5
-1.0
B
Log10-iBAQ intensities
ACTB
THBS1
PPBP
FERMT3
TLN1
TMSB4X
ITGB3
F13A1
SPARC
SELP
PF4
MYLK
GP6
SYK
B2M
PRKG1
CLEC1B
AKT1
AKT2
PRKCA
FYN
Rank
1758 proteins
C
Coefficient of variation (%)
Mean log2-intensity
1758 proteins
D
Density
22.3
27.4
****
Median Log2-intensity
Present in all samples some samples
E
regulation of body fluid levels
homotypic cell-cell adhesion
hemostasis
coagulation
platelet aggregation
platelet activation
wound healing
blood coagulation
protein folding
actin filament organization
regulation of endopeptidase activity
ribose phosphate metabolic process
regulation of supramolecular fiber organization
purine ribonucleotide metabolic process
nucleoside triphosphate metabolic process
cellular respiration
ATP metabolic process
Golgi vesicle transport
oxidative phosphorylation
purine nucleoside triphosphate metabolic process
purine nucleoside triphosphate biosynthetic process
generation of precursor metabolites and energy
ribonucleoside triphosphate metabolic process
purine-containing compound metabolic process
ribose phosphate biosynthetic process
translation initiation factor activity
translation regulator activity
translation factor activity, RNA binding
cadherin binding
ATP-dependent protein folding chaperone
translation regulator activity, nucleic acid binding
protein folding chaperone
electron transfer activity
unfolded protein binding
oxidoreduction-driven active transmembrane transporter activity
ligase activity
primary active transmembrane transporter activity
actin binding
chaperone binding
antioxidant activity
actin filament binding
ubiquitin-like protein ligase binding
ubiquitin protein ligase binding
GDP binding
G protein activity
guanyl-nucleotide binding
endopeptidase regulator activity
endopeptidase inhibitor activity
GTPase activity
guanyl ribonucleotide binding
peptidase inhibitor activity
peptidase regulator activity
GTP binding
enzyme inhibitor activity
GTPase binding
oxidoreductase complex
inner mitochondrial membrane protein complex
focal adhesion
pigment granule
cell leading edge
actin cytoskeleton
cell-substrate junction
cell cortex
proteasome complex
ficolin-1-rich granule lumen
platelet alpha granule lumen
melanosome
primary lysosome
cytoplasmic vesicle lumen
endopeptidase complex
azurophil granule lumen
azurophil granule
secretory granule lumen
vesicle lumen
peptidase complex
phagocytic vesicle
platelet alpha granule
ficolin-1-rich granule
coated vesicle
tertiary granule
endocytic vesicle
secretory granule membrane
coated vesicle membrane
specific granule
blood microparticle
number of genes
p.adjust

Figure S3

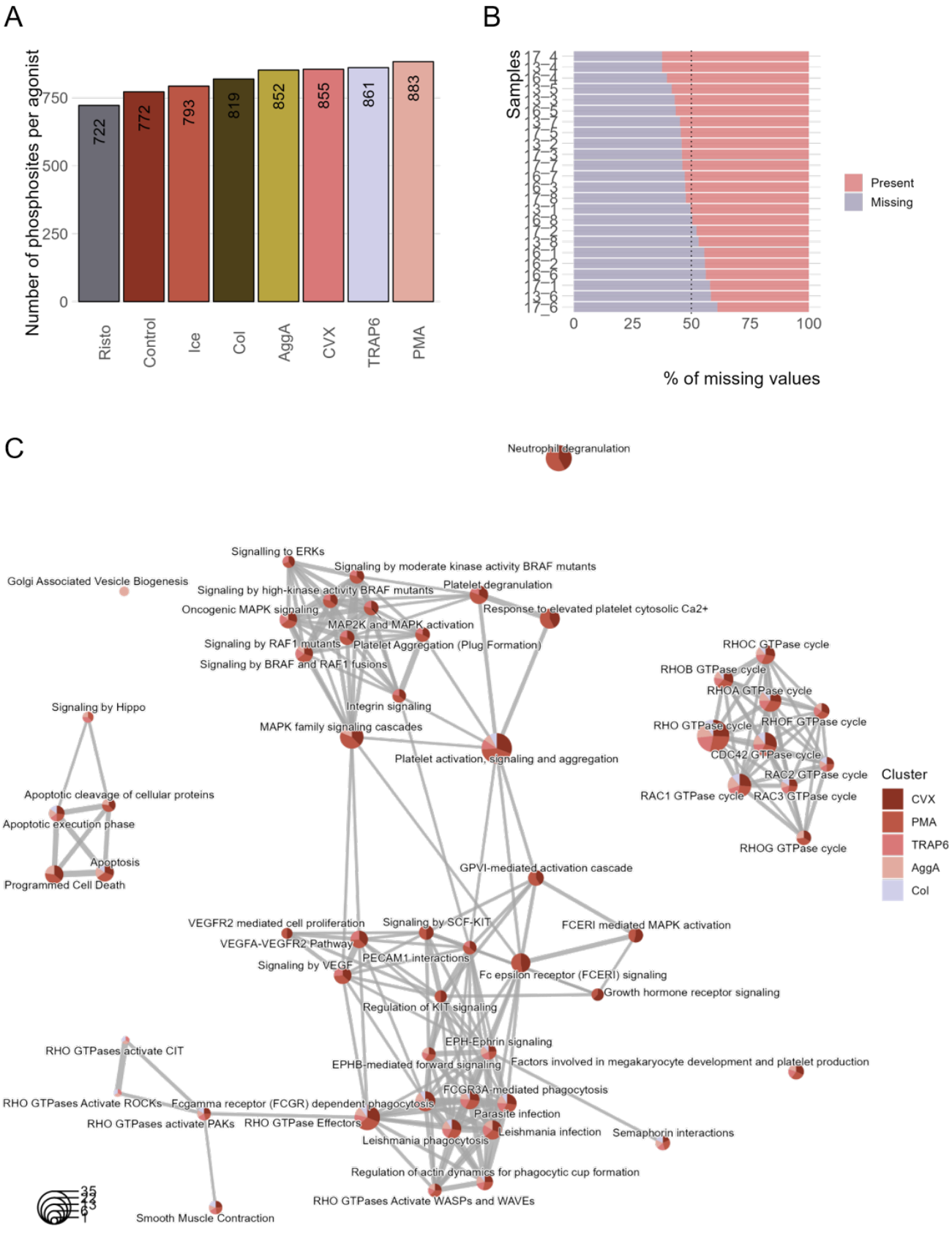
A
Number of phosphosites per agonist
0
250
500
750
722
772
793
819
852
855
861
883
Risto
Control
Ice
Col
AggA
CVX
TRAP6
PMA
B
Samples
0
25
50
75
100
% of missing values
Present
Missing
C
Neutrophil degranulation
Signalling to ERKs
Signaling by moderate kinase activity BRAF mutants
Golgi Associated Vesicle Biogenesis
Signaling by high-kinase activity BRAF mutants
Platelet degranulation
Oncogenic MAPK signaling
Response to elevated platelet cytosolic Ca2+
MAP2K and MAPK activation
Signaling by RAF1 mutants
Platelet Aggregation (Plug Formation)
Signaling by BRAF and RAF1 fusions
Integrin signaling
Signaling by Hippo
MAPK family signaling cascades
Platelet activation, signaling and aggregation
RHOC GTPase cycle
RHOB GTPase cycle
RHOA GTPase cycle
RHO GTPase cycle
RHOF GTPase cycle
CDC42 GTPase cycle
RAC2 GTPase cycle
RAC1 GTPase cycle
RAC3 GTPase cycle
RHOG GTPase cycle
Cluster
CVX
PMA
TRAP6
AggA
Col
Apoptotic cleavage of cellular proteins
Apoptotic execution phase
Apoptosis
Programmed Cell Death
GPVI-mediated activation cascade
VEGFR2 mediated cell proliferation
Signaling by SCF-KIT
FCERI mediated MAPK activation
VEGFA-VEGFR2 Pathway
PECAM1 interactions
Signaling by VEGF
Fc epsilon receptor (FCERI) signaling
Growth hormone receptor signaling
Regulation of KIT signaling
EPH-Ephrin signaling
RHO GTPases activate CIT
EPHB-mediated forward signaling
Factors involved in megakaryocyte development and platelet production
FCGR3A-mediated phagocytosis
RHO GTPases Activate ROCKs
Fcgamma receptor (FCGR) dependent phagocytosis
Parasite infection
RHO GTPases activate PAKs
RHO GTPase Effectors
Leishmania infection
Semaphorin interactions
Leishmania phagocytosis
Regulation of actin dynamics for phagocytic cup formation
RHO GTPases Activate WASPs and WAVEs
Smooth Muscle Contraction

Figure S4

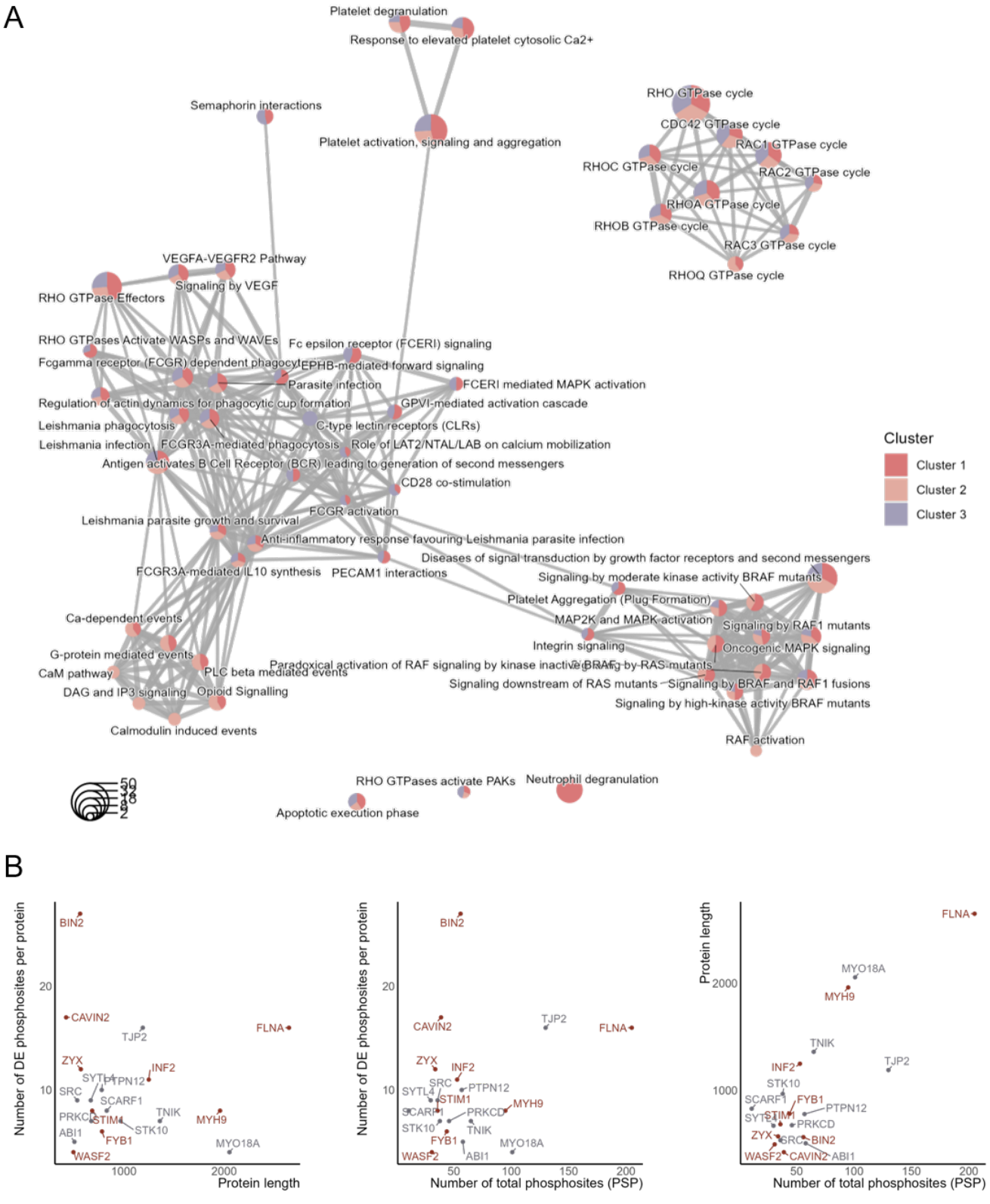
A
Platelet degranulation
Response to elevated platelet cytosolic Ca2+
Semaphorin interactions
Platelet activation, signaling and aggregation
RHO GTPase cycle
CDC42 GTPase cycle
RAC1 GTPase cycle
RHOC GTPase cycle
RAC2 GTPase cycle
RHOA GTPase cycle
RHOB GTPase cycle
RAC3 GTPase cycle
RHOQ GTPase cycle
VEGFA-VEGFR2 Pathway
Signaling by VEGF
RHO GTPase Effectors
RHO GTPases Activate WASPs and WAVEs
Fc epsilon receptor (FCERI) signaling
Fcgamma receptor (FCGR) dependent phagocytosis
EPHB-mediated forward signaling
Parasite infection
FCERI mediated MAPK activation
Regulation of actin dynamics for phagocytic cup formation
GPVI-mediated activation cascade
Leishmania phagocytosis
C-type lectin receptors (CLRs)
Leishmania infection
FCGR3A-mediated phagocytosis
Role of LAT2/NTAL/LAB on calcium mobilization
Antigen activates B Cell Receptor (BCR) leading to generation of second messengers
CD28 co-stimulation
FCGR activation
Leishmania parasite growth and survival
Anti-inflammatory response favouring Leishmania parasite infection
Diseases of signal transduction by growth factor receptors and second messengers
FCGR3A-mediated IL10 synthesis
PECAM1 interactions
Signaling by moderate kinase activity BRAF mutants
Platelet Aggregation (Plug Formation)
Ca-dependent events
MAP2K and MAPK activation
Signaling by RAF1 mutants
Integrin signaling
Oncogenic MAPK signaling
G-protein mediated events
Paradoxical activation of RAF signaling by kinase inactive BRAF by RAS mutants
CaM pathway
PLC beta mediated events
Signaling downstream of RAS mutants
Signaling by BRAF and RAF1 fusions
DAG and IP3 signaling
Opioid Signalling
Signaling by high-kinase activity BRAF mutants
Calmodulin induced events
RAF activation
Cluster
Cluster 1
Cluster 2
Cluster 3
50
100
150
200
250
RHO GTPases activate PAKs
Neutrophil degranulation
Apoptotic execution phase
B
Number of DE phosphosites per protein
Protein length
Number of total phosphosites (PSP)
BIN2
CAVIN2
TJP2
FLNA
ZYX
INF2
SYTL4
PTPN12
SRC
SCARF1
PRKCD
STIM1
TNIK
MYH9
STK10
ABI1
FYB1
MYO18A
WASF2

Figure S5

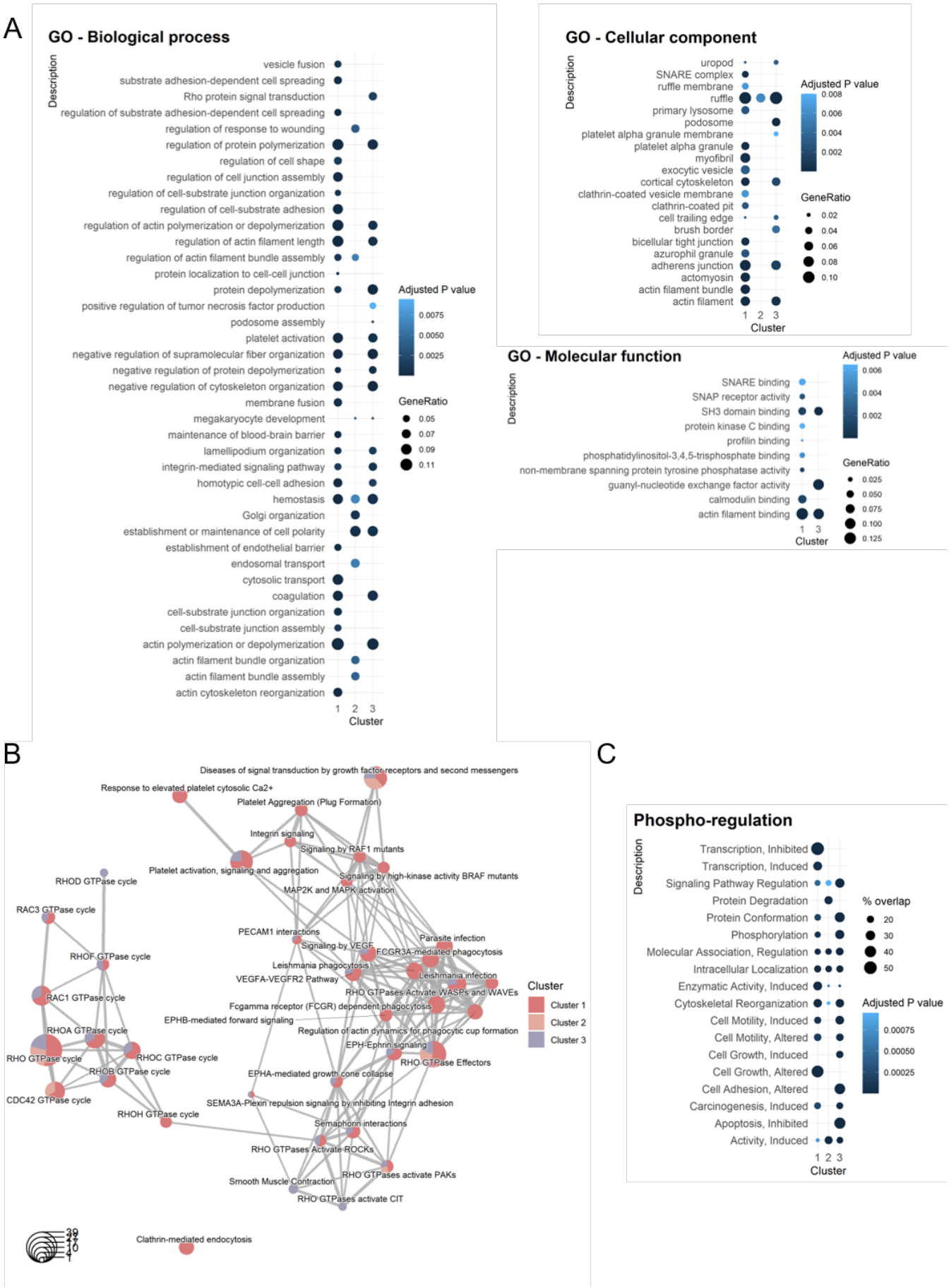
A
GO - Biological process
Description
vesicle fusion
substrate adhesion-dependent cell spreading
Rho protein signal transduction
regulation of substrate adhesion-dependent cell spreading
regulation of response to wounding
regulation of protein polymerization
regulation of cell shape
regulation of cell junction assembly
regulation of cell-substrate junction organization
regulation of cell-substrate adhesion
regulation of actin polymerization or depolymerization
regulation of actin filament length
regulation of actin filament bundle assembly
protein localization to cell-cell junction
protein depolymerization
positive regulation of tumor necrosis factor production
podosome assembly
platelet activation
negative regulation of supramolecular fiber organization
negative regulation of protein depolymerization
negative regulation of cytoskeleton organization
membrane fusion
megakaryocyte development
maintenance of blood-brain barrier
lamellipodium organization
integrin-mediated signaling pathway
homotypic cell-cell adhesion
hemostasis
Golgi organization
establishment or maintenance of cell polarity
establishment of endothelial barrier
endosomal transport
cytosolic transport
coagulation
cell-substrate junction organization
cell-substrate junction assembly
actin polymerization or depolymerization
actin filament bundle organization
actin filament bundle assembly
actin cytoskeleton reorganization
1 2 3
Cluster
Adjusted P value
0.0075
0.0050
0.0025
GeneRatio
0.05
0.07
0.09
0.11
GO - Cellular component
Description
uropod
SNARE complex
ruffle membrane
ruffle
primary lysosome
podosome
platelet alpha granule membrane
platelet alpha granule
myofibril
exocytic vesicle
cortical cytoskeleton
clathrin-coated vesicle membrane
clathrin-coated pit
cell trailing edge
brush border
bicellular tight junction
azurophil granule
adherens junction
actomyosin
actin filament bundle
actin filament
1 2 3
Cluster
Adjusted P value
0.008
0.006
0.004
0.002
GeneRatio
0.02
0.04
0.06
0.08
0.10
GO - Molecular function
Description
SNARE binding
SNAP receptor activity
SH3 domain binding
protein kinase C binding
profilin binding
phosphatidylinositol-3,4,5-trisphosphate binding
non-membrane spanning protein tyrosine phosphatase activity
guanyl-nucleotide exchange factor activity
calmodulin binding
actin filament binding
1 3
Cluster
Adjusted P value
0.006
0.004
0.002
GeneRatio
0.025
0.050
0.075
0.100
0.125
B
Diseases of signal transduction by growth factor receptors and second messengers
Response to elevated platelet cytosolic Ca2+
Platelet Aggregation (Plug Formation)
Integrin signaling
Signaling by RAF1 mutants
Platelet activation, signaling and aggregation
Signaling by high-kinase activity BRAF mutants
MAP2K and MAPK activation
RHOD GTPase cycle
RAC3 GTPase cycle
PECAM1 interactions
Signaling by VEGF
Parasite infection
FCGR3A-mediated phagocytosis
RHOF GTPase cycle
Leishmania phagocytosis
VEGFA-VEGFR2 Pathway
Leishmania infection
RAC1 GTPase cycle
RHO GTPases Activate WASPs and WAVEs
Fcgamma receptor (FCGR) dependent phagocytosis
EPHB-mediated forward signaling
RHOA GTPase cycle
Regulation of actin dynamics for phagocytic cup formation
EPH-Ephrin signaling
RHO GTPase cycle
RHOC GTPase cycle
RHO GTPase Effectors
RHOB GTPase cycle
EPHA-mediated growth cone collapse
CDC42 GTPase cycle
SEMA3A-Plexin repulsion signaling by inhibiting Integrin adhesion
RHOH GTPase cycle
Semaphorin interactions
RHO GTPases Activate ROCKs
RHO GTPases activate PAKs
Smooth Muscle Contraction
RHO GTPases activate CIT
Clathrin-mediated endocytosis
Cluster
Cluster 1
Cluster 2
Cluster 3
39
27
17
10
4
1
C
Phospho-regulation
Description
Transcription, Inhibited
Transcription, Induced
Signaling Pathway Regulation
Protein Degradation
Protein Conformation
Phosphorylation
Molecular Association, Regulation
Intracellular Localization
Enzymatic Activity, Induced
Cytoskeletal Reorganization
Cell Motility, Induced
Cell Motility, Altered
Cell Growth, Induced
Cell Growth, Altered
Cell Adhesion, Altered
Carcinogenesis, Induced
Apoptosis, Inhibited
Activity, Induced
1 2 3
Cluster
% overlap
20
30
40
50
Adjusted P value
0.00075
0.00050
0.00025

Figure S6

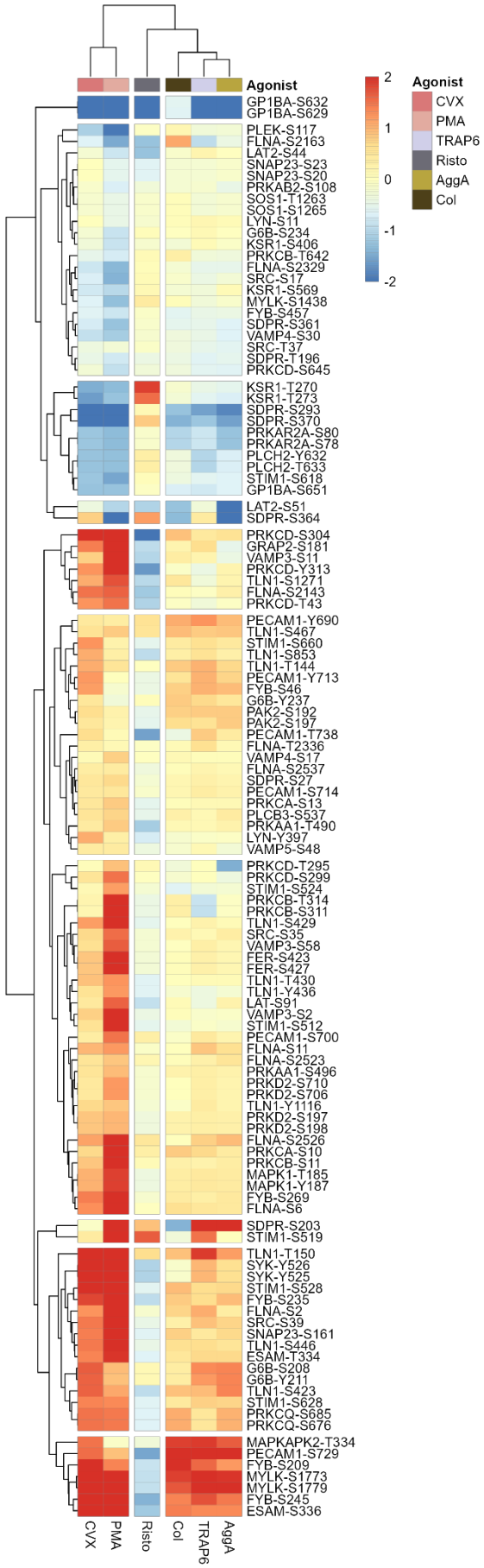
Agonist
GP1BA-S632
GP1BA-S629
PLEK-S117
FLNA-S2163
LAT2-S44
SNAP23-S23
SNAP23-S20
PRKAB2-S108
SOS1-T1263
SOS1-S1265
LYN-S11
G6B-S234
KSR1-S406
PRKCB-T642
FLNA-S2329
SRC-S17
KSR1-S569
MYLK-S1438
FYB-S457
SDPR-S361
VAMP4-S30
SRC-T37
SDPR-T196
PRKCD-S645
KSR1-T270
KSR1-T273
SDPR-S293
SDPR-S370
PRKAR2A-S80
PRKAR2A-S78
PLCH2-Y632
PLCH2-T633
STIM1-S618
GP1BA-S651
LAT2-S51
SDPR-S364
PRKCD-S304
GRAP2-S181
VAMP3-S11
PRKCD-Y313
TLN1-S1271
FLNA-S2143
PRKCD-T43
PECAM1-Y690
TLN1-S467
STIM1-S660
TLN1-S853
TLN1-T144
PECAM1-Y713
FYB-S46
G6B-Y237
PAK2-S192
PAK2-S197
PECAM1-T738
FLNA-T2336
VAMP4-S17
FLNA-S2537
SDPR-S27
PECAM1-S714
PRKCA-S13
PLCB3-S537
PRKAA1-T490
LYN-Y397
VAMP5-S48
PRKCD-T295
PRKCD-S299
STIM1-S524
PRKCB-T314
PRKCB-S311
TLN1-S429
SRC-S35
VAMP3-S58
FER-S423
FER-S427
TLN1-T430
TLN1-Y436
LAT-S91
VAMP3-S2
STIM1-S512
PECAM1-S700
FLNA-S11
FLNA-S2523
PRKAA1-S496
PRKD2-S710
PRKD2-S706
TLN1-Y1116
PRKD2-S197
PRKD2-S198
FLNA-S2526
PRKCA-S10
PRKCB-S11
MAPK1-T185
MAPK1-Y187
FYB-S269
FLNA-S6
SDPR-S203
STIM1-S519
TLN1-T150
SYK-Y526
SYK-Y525
STIM1-S528
FYB-S235
FLNA-S2
SRC-S39
SNAP23-S161
TLN1-S446
ESAM-T334
G6B-S208
G6B-Y211
TLN1-S423
STIM1-S628
PRKCQ-S685
PRKCQ-S676
MAPKAPK2-T334
PECAM1-S729
FYB-S209
MYLK-S1773
MYLK-S1779
FYB-S245
ESAM-S336
CVX
PMA
Risto
Col
TRAP6
AggA
2
1
0
-1
-2
Agonist
CVX
PMA
TRAP6
Risto
AggA
Col

Figure S7

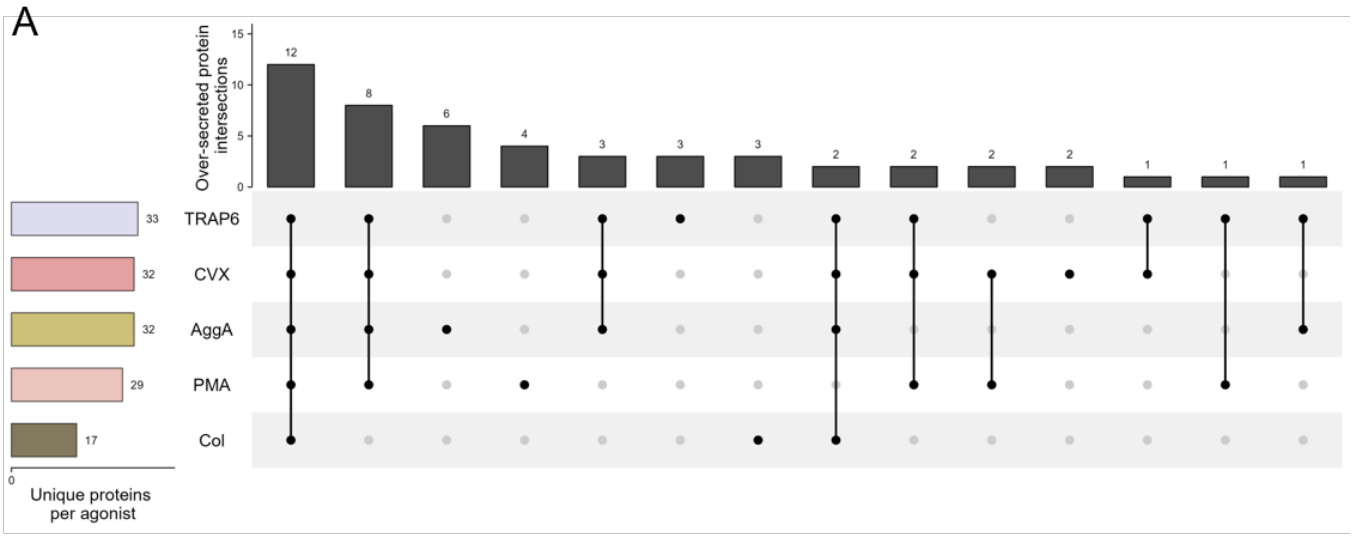
A
Over-secreted protein intersections
15
10
5
0
12
8
6
4
3
3
3
2
2
2
2
1
1
1
33
32
32
29
17
TRAP6
CVX
AggA
PMA
Col
0
Unique proteins per agonist

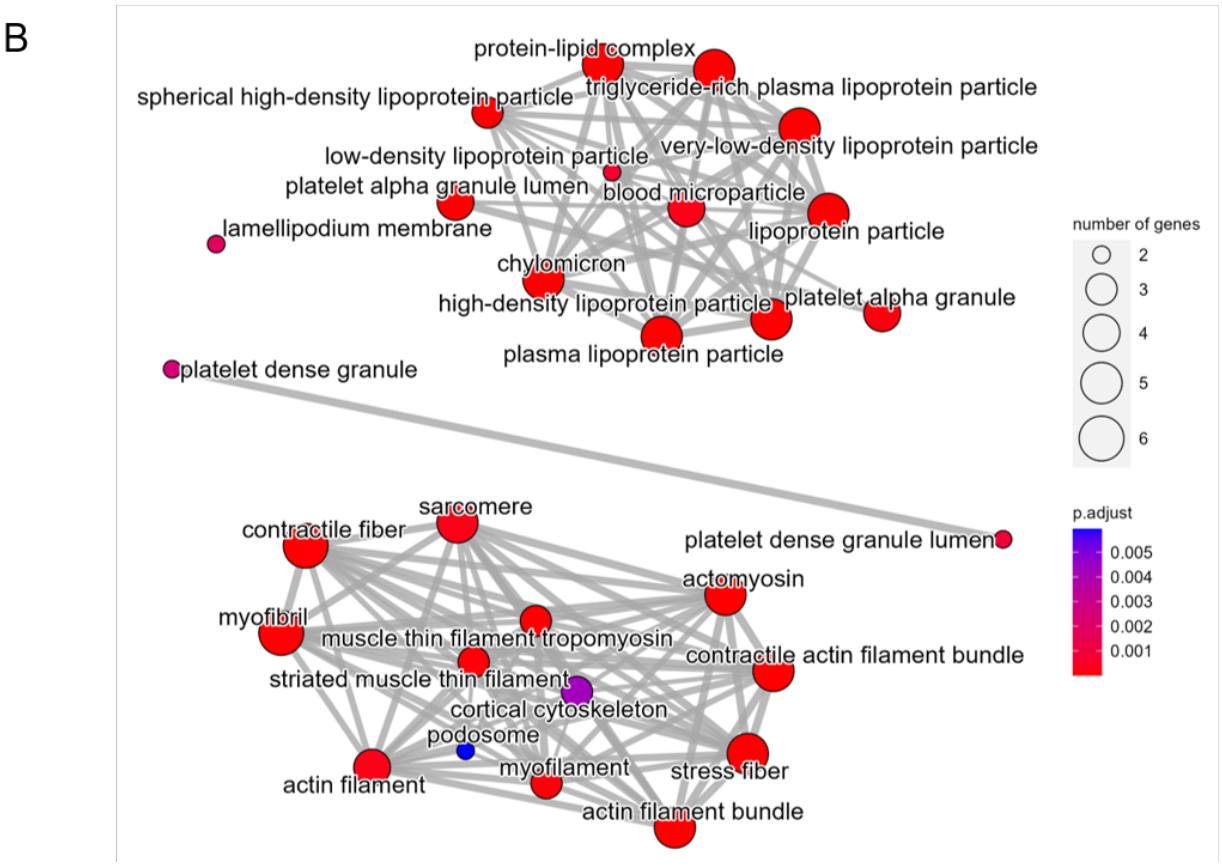
B
protein-lipid complex
triglyceride-rich plasma lipoprotein particle
spherical high-density lipoprotein particle
very-low-density lipoprotein particle
low-density lipoprotein particle
platelet alpha granule lumen
blood microparticle
lamellipodium membrane
lipoprotein particle
chylomicron
high-density lipoprotein particle
platelet alpha granule
plasma lipoprotein particle
platelet dense granule
number of genes
2
3
4
5
6
sarcomere
contractile fiber
platelet dense granule lumen
actomyosin
myofibril
muscle thin filament tropomyosin
contractile actin filament bundle
striated muscle thin filament
cortical cytoskeleton
podosome
myofilament
stress fiber
actin filament
actin filament bundle
p.adjust
0.005
0.004
0.003
0.002
0.001

Chapter IV

Figure S1. The aggregation response after single receptor stimulation, across all cohorts. Boxplots of the percentage of maximum aggregation rate (MAR, left) and area under the curve (AUC, right), for all agonists and cohorts. MDD: major depressive disorder, SA: suicidal attempt.

Figure S2. Gating strategy for the *in vitro* cultures. Dotplots displaying the markers and populations used in the gating strategy. Starting from the top left, the blue gate represents the fraction of nucleated cells in the culture, which is further divided in three different compartments, based on the expression of CD31 (PECAM-1): $CD31^{high}$ (red), $CD31^{mid}$ (orange), $CD31^{-}$ (grey). The bottom row depicts the gating strategy, starting from the $CD31^{high}$ and $CD31^{mid}$ populations, of the megakaryocyte fraction, using the CD42a (GPIX subunit of the vWF receptor), and the CD71 and Lin^{-} markers, respectively. The two contour plots on the right display the position of the selected populations on side (internal complexity) and forward (size) scatter parameters.

Figure S3. Gene ontology enrichment interrogation of the differentially expressed proteins in each cohort. Enrichment maps are shown for both the up- (left) and down-regulated (right) proteins, for the major depressive disorder (MDD), concurrent with (top) or without (middle) suicidal attempt (SA), and diabetes (bottom) cohorts.

Figure S4. Gene ontology enrichment interrogation of the differentially expressed proteins in each cohort. Enrichment maps are shown for both the up- (left) and down-regulated (right) proteins, for the psoriasis (top) and atopic dermatitis (bottom) cohorts.

Supplementary materials

Figure S1

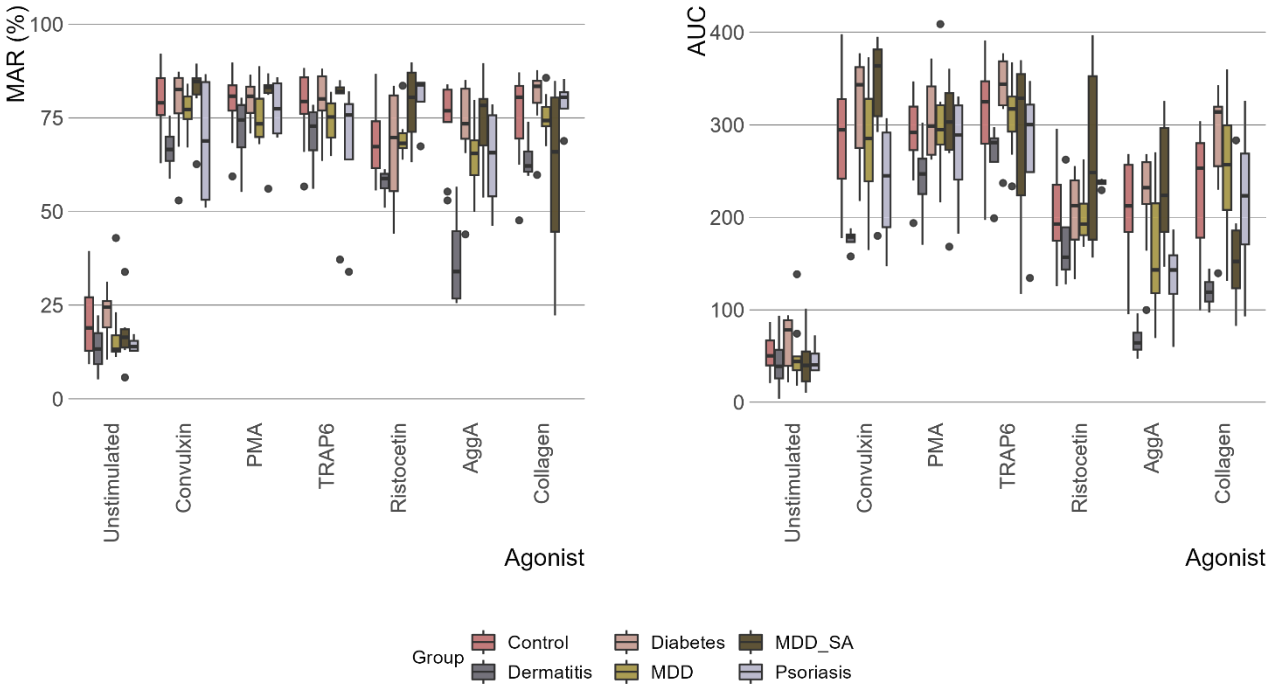

Figure S2

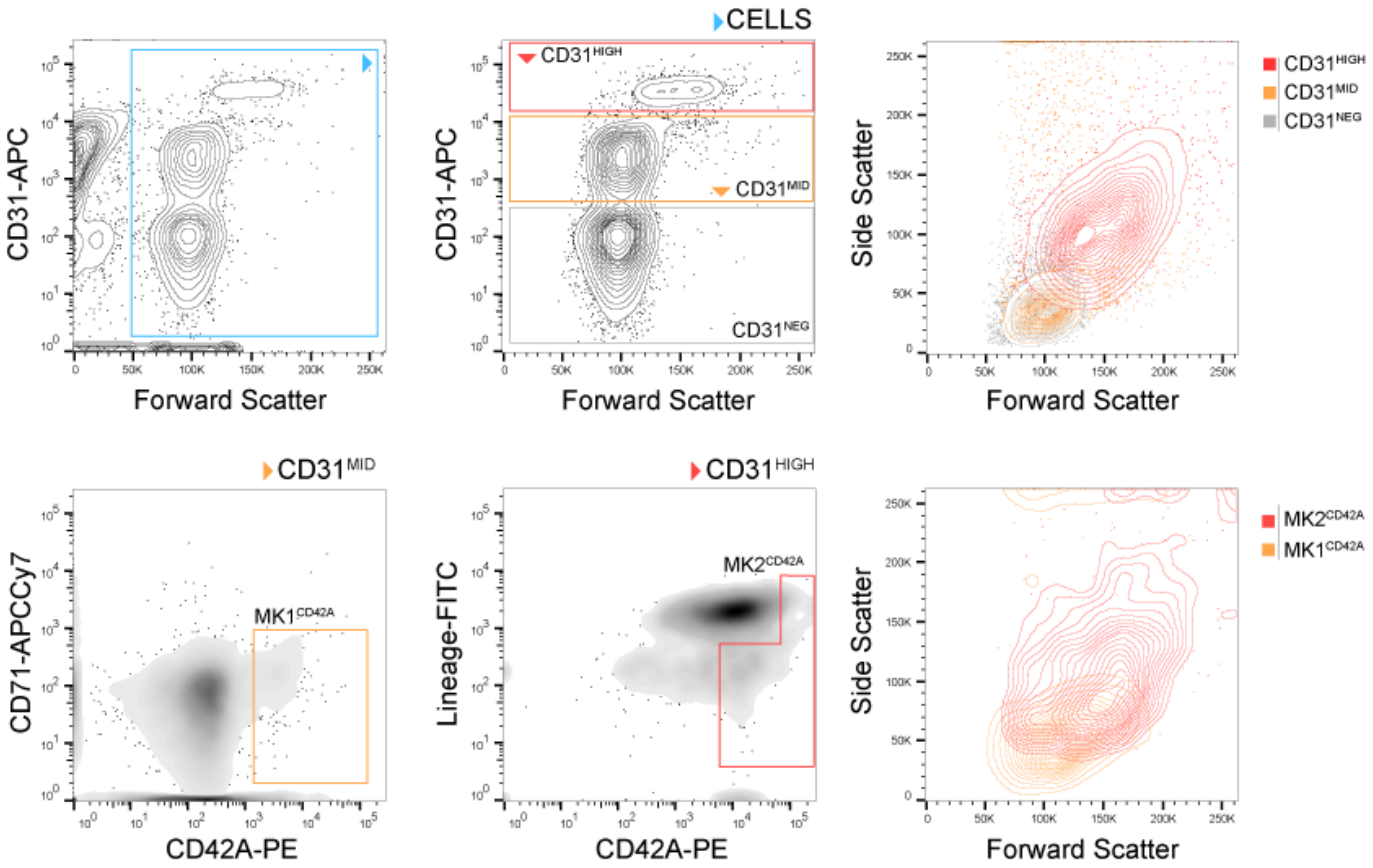
CELLS
CD31-APC
Forward Scatter
CD31HIGH
CD31MID
CD31NEG
Side Scatter
CD31HIGH
CD31MID
CD31NEG
CD31MID
CD71-APCCy7
CD42A-PE
MK1CD42A
CD31HIGH
Lineage-FITC
MK2CD42A
MK2CD42A
MK1CD42A

Figure S3

MDD SA Up Down

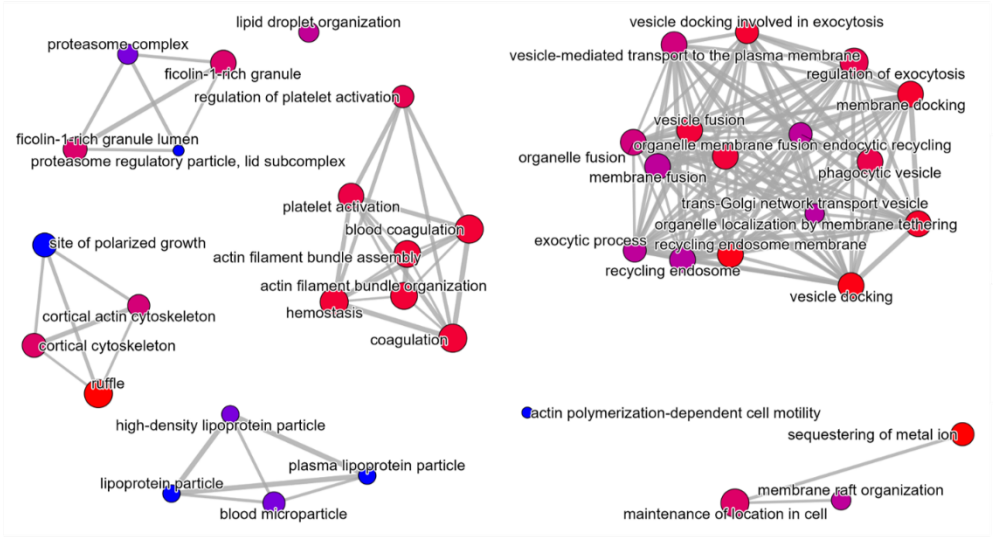

MDD Up Down

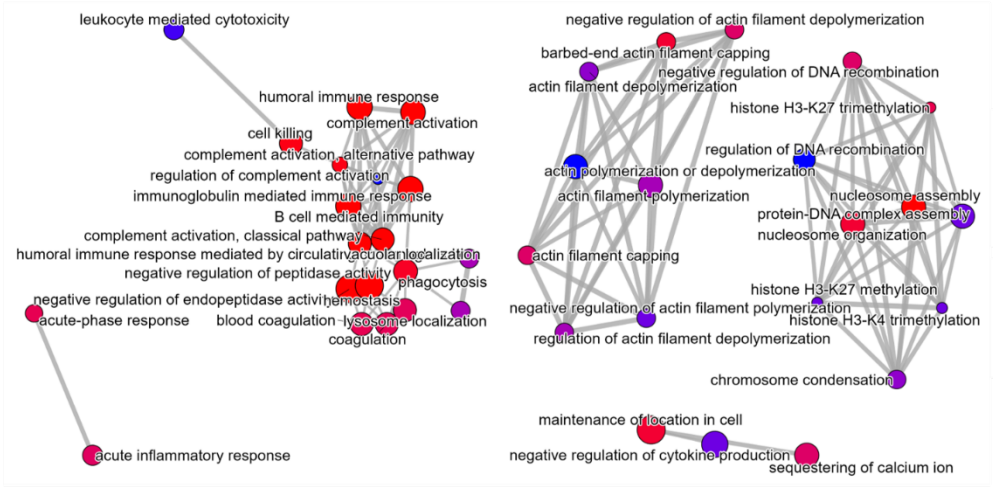

Diabetes Up Down

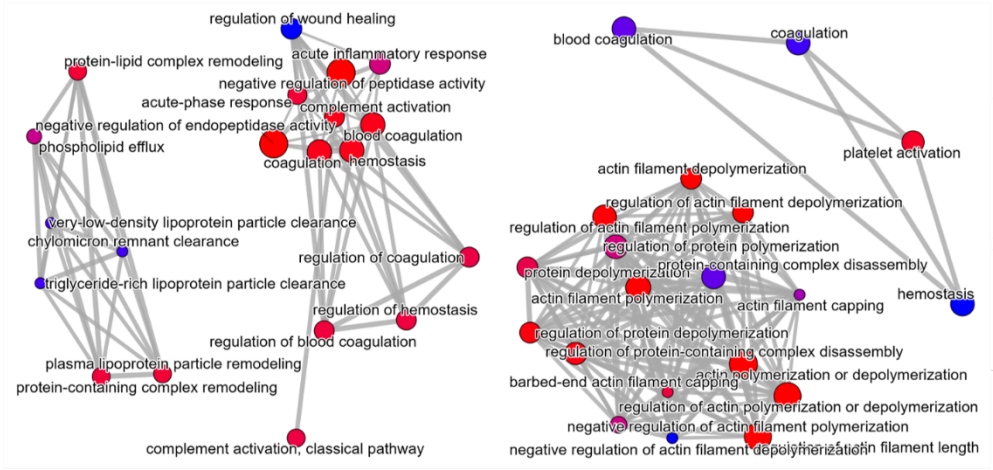

Figure S4

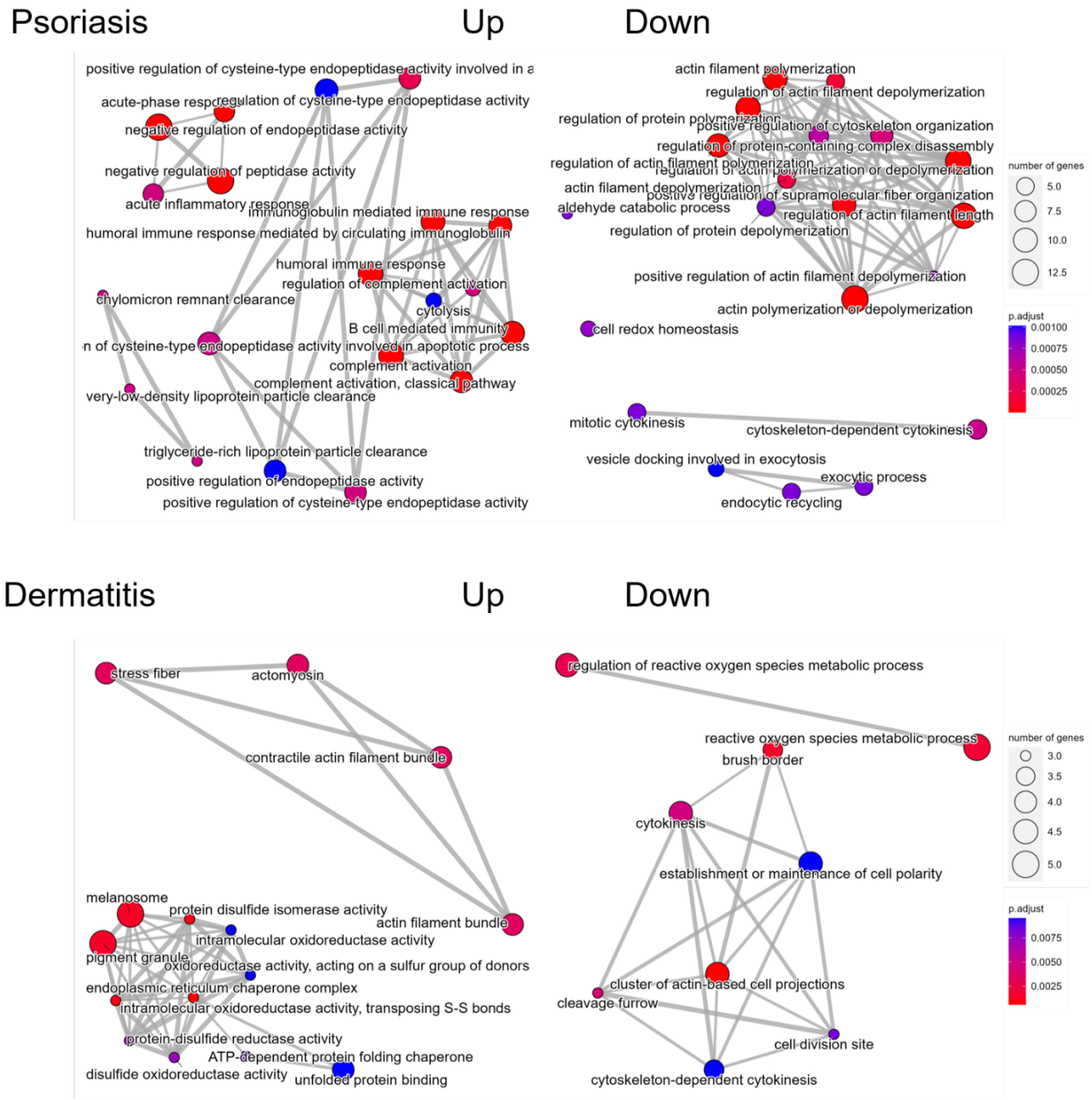
Psoriasis
Up
Down
positive regulation of cysteine-type endopeptidase activity involved in a
acute-phase respregulation of cysteine-type endopeptidase activity
negative regulation of endopeptidase activity
negative regulation of peptidase activity
acute inflammatory response
immunoglobulin mediated immune response
humoral immune response mediated by circulating immunoglobulin
humoral immune response
regulation of complement activation
chylomicron remnant clearance
cytolysis
B cell mediated immunity
n of cysteine-type endopeptidase activity involved in apoptotic process
complement activation
complement activation, classical pathway
very-low-density lipoprotein particle clearance
triglyceride-rich lipoprotein particle clearance
positive regulation of endopeptidase activity
positive regulation of cysteine-type endopeptidase activity
actin filament polymerization
regulation of actin filament depolymerization
regulation of protein polymerization
positive regulation of cytoskeleton organization
regulation of protein-containing complex disassembly
regulation of actin filament polymerization
regulation of actin polymerization or depolymerization
actin filament depolymerization
positive regulation of supramolecular fiber organization
aldehyde catabolic process
regulation of actin filament length
regulation of protein depolymerization
positive regulation of actin filament depolymerization
actin polymerization or depolymerization
cell redox homeostasis
mitotic cytokinesis
cytoskeleton-dependent cytokinesis
vesicle docking involved in exocytosis
exocytic process
endocytic recycling
number of genes
5.0
7.5
10.0
12.5
p.adjust
0.00100
0.00075
0.00050
0.00025
Dermatitis
Up
Down
stress fiber
actomyosin
contractile actin filament bundle
melanosome
protein disulfide isomerase activity
actin filament bundle
intramolecular oxidoreductase activity
pigment granule
oxidoreductase activity, acting on a sulfur group of donors
endoplasmic reticulum chaperone complex
intramolecular oxidoreductase activity, transposing S-S bonds
protein-disulfide reductase activity
ATP-dependent protein folding chaperone
disulfide oxidoreductase activity
unfolded protein binding
regulation of reactive oxygen species metabolic process
reactive oxygen species metabolic process
brush border
cytokinesis
establishment or maintenance of cell polarity
cluster of actin-based cell projections
cleavage furrow
cell division site
cytoskeleton-dependent cytokinesis
number of genes
3.0
3.5
4.0
4.5
5.0
p.adjust
0.0075
0.0050
0.0025

Publications

List of scientific publications related to the Thesis

This section lists the scientific publications contributed to by the author during the doctoral thesis period (the author's name is **highlighted**, and * implies equal contribution).

As chapters in this Thesis:

- **Martínez-Botía P**, Meinders M, De Cuyper IM, Eble JA, Semple JW, Gutiérrez L. Dissecting platelet proteomics to understand the pathophysiology of immune thrombocytopenia: studies in mouse models. *Blood Advances*. 2022;6(11):3529-3534.
- **Martínez-Botía P**, Villar P, Carbajo-Argüelles G, et al. Proteomics-wise, how similar are mouse and human platelets? *Platelets*. 2023. In press.

Directly related, but not used in this Thesis:

- **Martínez-Botía P***, Velasco A*, Rolle V, et al. Sex-dependent grades of haematopoietic modulation in patients with major depressive episodes are associated with suicide attempts. *European Neuropsychopharmacology*. 2020;40:17-30.
- **Martínez-Botía P**, Acebes-Huerta A, Seghatchian J, Gutiérrez L. In vitro platelet production for transfusion purposes: Where are we now? *Transfusion and Apheresis Science*. 2020;59(4):102864.
- **Martínez-Botía P**, Acebes-Huerta A, Seghatchian J, Gutiérrez L. On the Quest for In Vitro Platelet Production by Re-Tailoring the Concepts of Megakaryocyte Differentiation. *Medicina (Kaunas)*. 2020;56(12):671. Acebes-Huerta A,

- **Martínez-Botía P**, Martín Martín C, et al. Immunophenotyping and Cell Sorting of Human MKs from Human Primary Sources or Differentiated In Vitro from Hematopoietic Progenitors. *Journal of Visual Experiments*. 2021;(174): e62569.
- Villa-Fajardo M, Palma MCY, Acebes-Huerta A, **Martínez-Botía P**, et al. Platelet number and function alterations in preclinical models of sterile inflammation and sepsis patients: implications in the pathophysiology and treatment of inflammation. *Transfusion and Apheresis Science*. 2022;61(2):103413.
- Paniagua G, González-Blanco L, Sáiz PA, Moya-Lacasa C, Gutiérrez L, **Martínez-Botía P**, et al. Platelet and white blood-cell-based ratios: Differential inflammatory markers of severe mental disorders? *Revista de Psiquiatria y Salud Mental*. 2023. In press.

In all manuscripts, my contribution involved analysis and interpretation of the data, making of figures, and writing of the manuscript.

Other papers published during the Thesis

- Scheenstra MR*, **Martínez-Botía P***, Acebes-Huerta A, et al. Comparison of the PU. 1 transcriptional regulome and interactome in human and mouse inflammatory dendritic cells. *Journal of Leukocyte Biology*. 2021;110(4): 735-751.
- **Martínez-Botía P***, Bernardo Á*, Acebes-Huerta A*, et al. Clinical Management of Hypertension, Inflammation and Thrombosis in Hospitalized COVID-19 Patients: Impact on Survival and Concerns. *Journal of Clinical Medicine*. 2021;10(5):1073.